7-19-2005

Multibeam Observations of Mine Scour and Burial near Clearwater, Florida, Including a Test of the VIMS 2D Mine Burial Model

Monica L. Wolfson
University of South Florida

Multibeam Observations of Mine Scour and Burial near Clearwater, Florida, Including a Test of the VIMS 2D Mine Burial Model

by

Monica L. Wolfson

A thesis submitted in partial fulfillment
of the requirements for the degree of
Master of Science
College of Marine Science
University of South Florida

Major Professor: David F. Naar, Ph.D.
Peter A. Howd, Ph.D.
Stanley D. Locker, Ph.D.
Carl T. Friedrichs, Ph.D.

Date of Approval:
July 19, 2005

Keywords: multibeam bathymetry, sea level datum

Acknowledgements

Funding for this research was provided by the Office of Naval Research Mine Burial Program, under the management of Drs. Dawn Lavoie, Jill Karsten, Roy H. Wilkens, and Thomas Drake. I thank my committee: Drs. David Naar, Peter Howd, Stanley Locker, and Carl Friedrichs for their guidance and patience over the last couple of years. A special thanks goes out to Dr. Art Trembanis for all of his help with the model and for providing invaluable advice. Drs. Mike Richardson and Thomas Wever provided data and assistance. I would like to specifically recognize Dr. Gary Mitchum, Kate Ciembronowicz, Michelle McIntyre, Kara Sedwick, and Sage Lichtenwaler, without whom I would still be trying to figure out ArcMap and Matlab. I would also like to thank Brian Donahue for showing me how to collect and process multibeam data and for taking all my questions in stride. Most importantly, I would like to thank my family for their love and support.

Table of Contents

List of Tables

List of Figures

Multibeam Observations of Mine Scour and Burial near Clearwater, Florida, Including a Test of the VIMS 2D Mine Burial Model

Monica L. Wolfson

ABSTRACT

The ability to detect buried mines on the seafloor remains one of the most important tasks in mine countermeasures. As such, there is a vested interest in the development of predictive models of mine burial. This research was conducted in support of the Office of Naval Research Program in Mine Burial Prediction. Repeat high-resolution multibeam bathymetry data were collected over the Indian Rocks Beach (IRB) mine burial experiment site during January through March of 2003, in order to observe in situ scour and burial of instrumented inert mines and mine-like cylinders. These data were also used to test the validity of the VIMS 2D mine burial model.

A set of six high-resolution multibeam surveys were collected over the IRB experiment site. Three study sites within the IRB site were chosen: two fine sand sites, a shallow one located in ~ 13 meters of water depth and a deep site located in ~ 14 meters of water depth; and a coarse sand site in ~ 13 meters. Results from these surveys indicate that mines deployed in fine sand are upwards of 74.5% buried within two months of deployment. Mines deployed in the coarse sand showed a lesser amount of scour, burying until they presented roughly the same hydrodynamic roughness of the surrounding rippled bedforms. In general, scour around the mines formed pits ~ 0.30 meters deep, with the most pronounced scour occurring at the ends of the mine.

The multibeam data were also used to test the VIMS 2D mine burial model, which estimates percent burial of cylindrical mines based on predictions of wave-induced scour. The model proved valid for use in areas of fine sand, sufficiently predicting burial over the course of the experiment. In the area of coarse sand, the model greatly over-predicted the amount of burial. This is believed to be due to the presence of ripples around the mines, which affect local bottom morphodynamics and are not accounted for in the model. This issue is currently being addressed by modelers.

Chapter 1

Introduction

Mine countermeasures are some of the most pressing issues being addressed by the Navy today. Current methods of mine hunting involve the use of side-scan sonars, which are dependent on the mine casting a shadow for detection. If the mine scours into the seabed and/or becomes buried by sediment, mine hunting techniques may be severely compromised. The Office of Naval Research Program in Mine Burial Prediction was established to study the how, when, and why of mine burial and develop mine burial probability models. Three locations were selected as experiments sites for this program: Corpus Christi, Texas (2001 and 2002); Martha's Vineyard, Massachusetts (2003); and Indian Rocks Beach offshore of Clearwater, Florida (2003).

As part of the Indian Rocks Beach (IRB) experiment, repeat high-resolution multibeam surveys were made over the study site in order to observe in situ scour and burial of inert mines and mine-like cylinders. These data were used to perform temporal and spatial analyses of mine scour and burial and to test the validity of one of the probability models. This thesis represents the culmination of that research.

The second chapter of this thesis is a manuscript submitted April 15th, 2005 to a special issue of the Journal of Ocean Engineering focused on mine burial and scour (Wolfson et al., 2005). This chapter provides a detailed analysis of the surveys over an instrumented mine deployed in a fine sand site and one deployed in a coarse sand site.

Chapter three of this thesis includes the analyses and model comparisons for the remaining mines deployed as part of the IRB experiment. A more detailed analysis of the morphology of the scour formed around the mines is included in chapter four. Chapter five discusses the results and their significance. Chapter six summarizes the principle findings and conclusions of this thesis. Appendix A is a brief discussion on the method of determining changes in ambient seafloor elevation observed around the mines. Appendix B provides descriptions of the equations used to calculate the phase and amplitude lag of the tide record, as well the equations used to calculate beam width and spacing of the multibeam sonar.

Chapter 2

Multibeam Observations and Model Comparison for Two Mines in Fine and Coarse Sand

Abstract

High-resolution multibeam bathymetry data collected offshore of Clearwater, Florida, are compared to predictions of mine burial by the VIMS 2D model for wave-induced scour. This paper focuses specifically on two instrumented but inert mines: an acoustic mine located in fine sands; and an optical instrumented mine located in coarse sands. Temporal analyses of the observed scour and burial of the mines and a method for obtaining a vertical frame of reference (MLLW) from pressure sensor data are presented. In the fine sand case, the model initially predicts a greater amount of burial than observed in the multibeam data; however, the values show a convergence during the course of the experiment. When the ± 5-centimeter vertical uncertainty (RMS error) of the multibeam sonar is considered, the predicted estimates of mine burial fall within the observable range. Correcting for the tilt of the mine (using a pitch sensor within the mine) can reduce the discrepancy between the observed and predicted percent burial. In the coarse sand case, the model does not work as well. Initially the predictions are within the range of the multibeam measurement uncertainty but then they overestimate the amount of observed burial over the rest of the experiment. Rippled bedforms appear to be influencing the mine scour and burial and should be included in future modeling efforts.

Introduction

The ability to detect buried mines on the seafloor remains one of the most difficult tasks in mine countermeasures. Morphodynamics of the seafloor are often responsible for the burial of heavy objects, including, but not limited to, pipelines, breakwaters, concrete, debris, and mines (Richardson et al., 2001). Mines are readily buried on impact and by secondary processes such as scour and fill, liquefaction, and changes in seafloor morphology. While mine-hunting techniques successfully locate mines resting on the seafloor, a partially buried mine can avoid sonar detection and requires either mine sweeping or complete area avoidance (Richardson and Briggs, 2000). It is therefore necessary to develop methods of predicting mine burial under different environmental conditions and temporal scales. The ability to predict how quickly scour will form around a mine and how quickly the mine will become buried under different energy and geological conditions is important in designing search strategies.

High-resolution multibeam bathymetry data can be used to test current mine burial models by providing direct estimates of the scour and burial of a mine. Herein, the term mine actually refers to inert mine-like cylinders. Repeated passes of a multibeam sonar over a mine will document the amount of scour and percent burial over time, which can then be compared to the model predictions. This will test the validity of mine burial models. We define percent mine burial as percent of mine subsidence with respect to the ambient seafloor (Equation 1).

$$\% \text{ burial} = \left(\frac{D_m - \left(d_s - d_m \right)}{D_m} \right) x100 \qquad (1)$$

D_m = diameter of mine
d_s = depth of ambient seafloor
d_m = depth of top of mine

The Experiment

Mine burial experiments sponsored by the Office of Naval Research (ONR) were conducted off the coast of Clearwater, West-Central Florida between January 8th and March 12th, 2003 (Fig. 1). The study area was selected using side-scan, seismic, and multibeam data, as well as sediment cores. Two main sites were selected roughly 20 kilometers west of Indian Rocks Beach: a fine sand site and a coarse sand site, both located in water depth ~ 13 meters relative to mean low low water (MLLW) (Fig. 2). Four acoustic and six optical instrumented and inert mine-like cylinders were deployed in early January. In order to monitor current and wave interactions with the mines and the seafloor, and their subsequent effect, three instrumented quadpods and five tripods (spiders) were deployed in the vicinity of the mines. Each quadpod was fitted with a 1.5 MHz pulse coherent boundary layer profiler (SonTek PC-ADP), a 5 MHz acoustic Doppler point current meter (SonTek Hydra), an in situ grain size sensor (LISST-100), a conductivity/temperature sensor (SeaBird Microcat C-T), and an optical backscatter sensor (Downing OBS). Each spider was equipped with a 1.5 MHz bottom mounted acoustic Doppler profiler with wave directional capabilities (SonTek ADP).

All multibeam data were collected aboard the R/V Suncoaster on six cruises throughout the experiment: January 8th – 11th, when the mines were deployed; January 12th – 13th; January 16th – 17th, when the quadpods and spiders were deployed; January 19th – 20th; February 5th – 6th; and March 12th – 13th, when all deployed equipment was retrieved. During each cruise, multiple passes with the multibeam system were conducted over the mines. Once the multibeam data were post-processed, direct measurement of mine scour and burial was performed. We focus specifically on the acoustic instrumented mine number

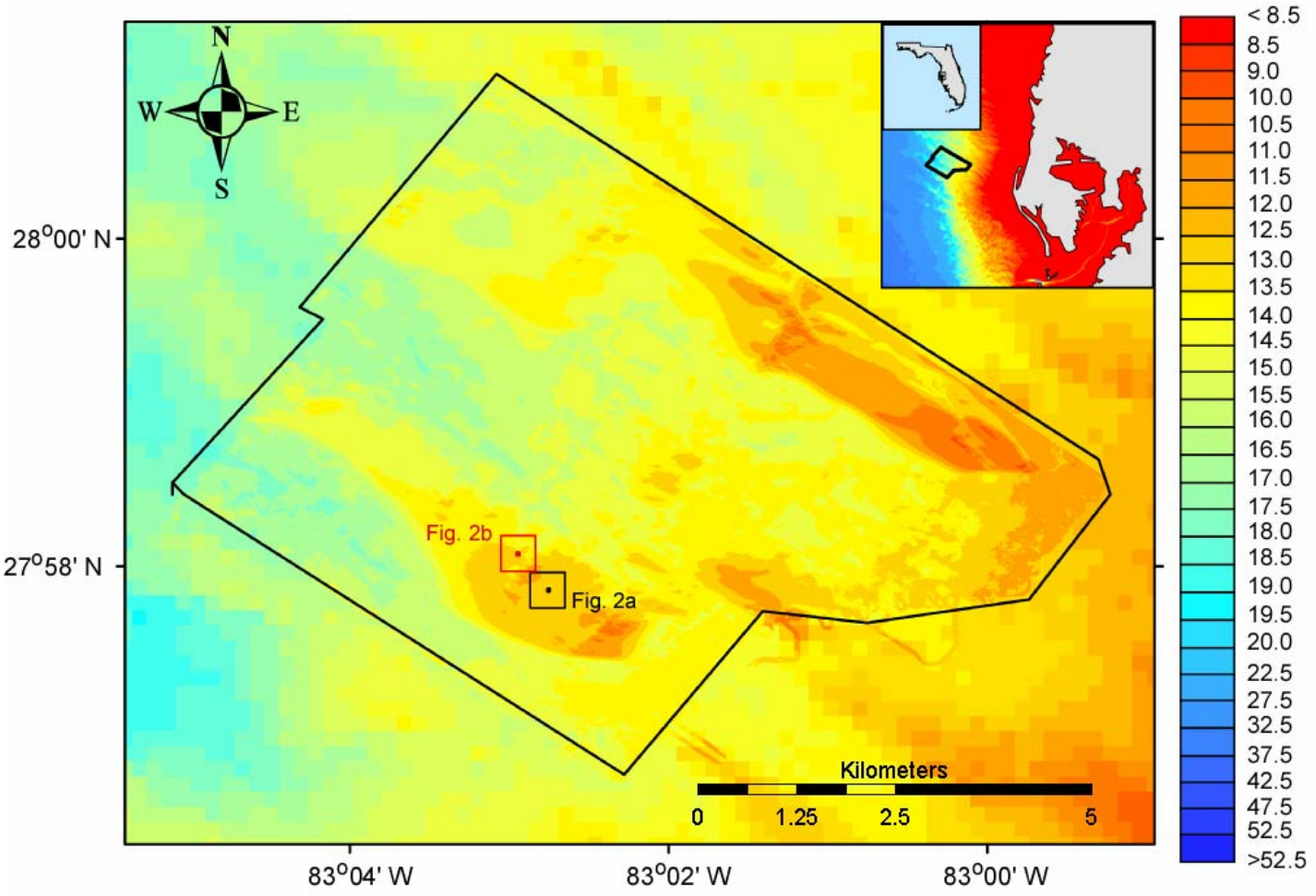

Figure 1. Location of the experiment site off Indian Rocks Beach, Florida. All depths are referenced to mean low low water (MLLW). The area outlined with a thin black line represents the data obtained in April 2002 during the site survey. The black dot in the middle of the black square and the red dot in the middle of the red square indicate the location of the fine sand site and coarse sand site respectively. Detailed images of these areas can be seen in Figure 2. Additional digital data provided by the USGS (Gelfenbaum and Guy, 2000) and NOAA (courtesy of D. Scharff, 2004). Figure modified from Naar and Donahue (2002).

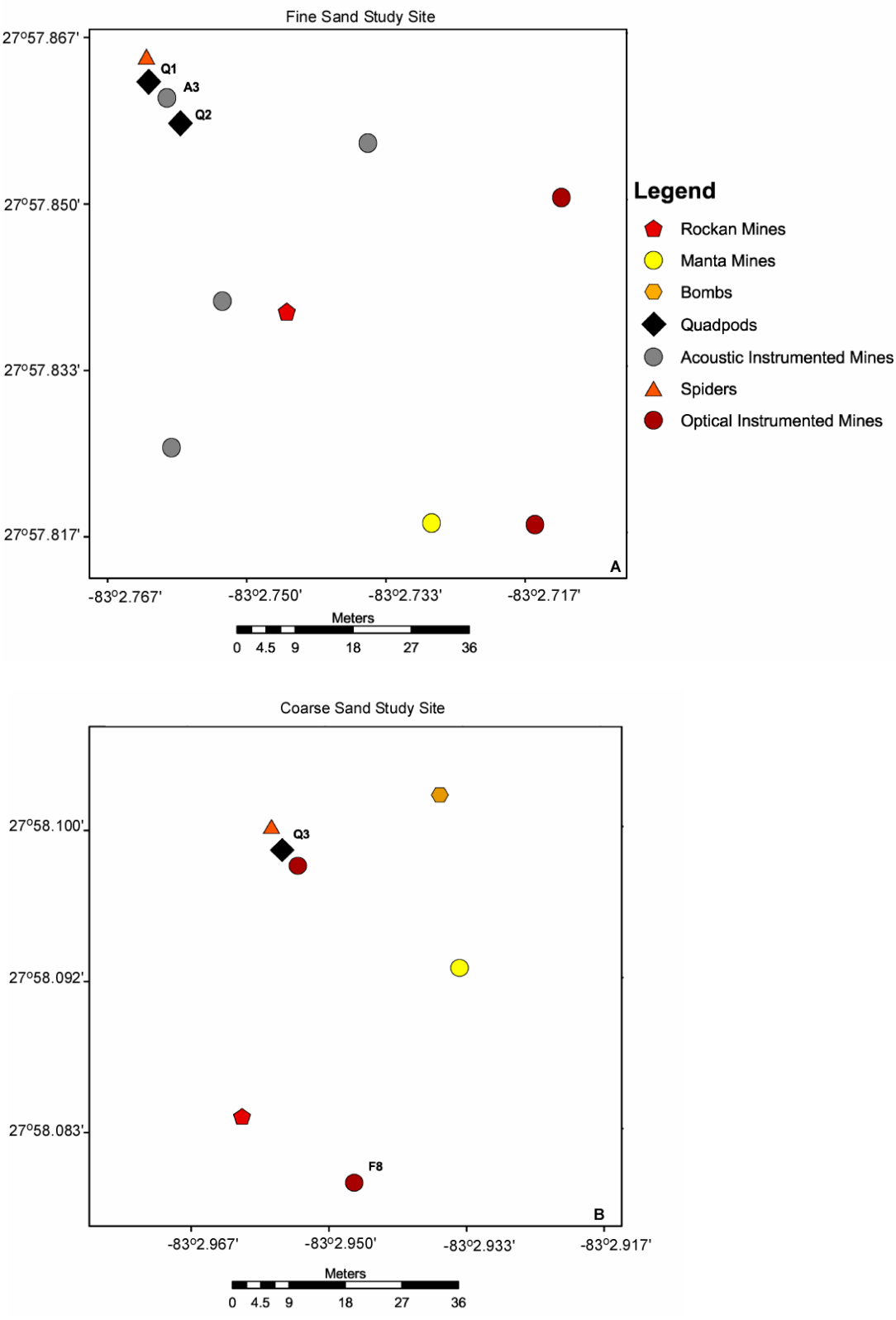

Figure 2. Location of the deployed equipment for the fine sand (2A) and coarse sand (2B) study sites. The fine sand study site also included an inert bomb, which has yet to be located in the multibeam data.

3 (A3) which was located in the fine sand site, and on the optical instrumented mine number 8 (F8) located in the coarse sand site.

Multibeam Data

The use of multibeam sonars as tools for both bathymetric mapping and backscatter imaging is well-established (Pohner, 1990; Clarke, 1998; Collins and Preston, 2002; Collins and Galloway, 1998; Gardner et al., 1998; and references therein). For our experiment, we used a Kongsberg Simrad EM 3000, a 300 kHz multibeam swath sonar with 127 overlapping 1.5° x 1.5° beams, producing a 130-degree swath transverse to ship heading. Vertical uncertainty (RMS error) of the EM 3000 is ± 5 to 10 centimeters depending on depth. Given that the sonar is usually mounted to a ship, its positioning accuracy is greater than that of towed side-scan sonars and ROV mounted devices. Therefore, multiple passes over the same stationary object should result in the same georeferenced position. Our tests suggest less than ± 1-meter accuracy in position of seafloor objects in multibeam compared with ± 10 meters for side-scan data (Locker et al., 2002). The high frequency of the multibeam soundings allows it to operate at faster boat speeds than side-scan sonars, which due to the towfish hydrodynamics have a wider swath and a slower ping rate.

Mine Burial and Scour Models

One of the main goals of the ONR Mine Burial Prediction Program is the development of accurate models to estimate the percent scour and burial as a function of energy, geological conditions, and time. The models must have a known and acceptable

degree of accuracy in areas of interest. Friedrichs (2001) conducted a review of five mine burial models, describing the main processes and discussing the validity of each model. Four of the five models (WISSP, NBURY, DRAMBUIE and Vortex Lattice) each model mine burial on the basis of scour. The fifth model, Mulhearn, models mine burial as a consequence of bedform migration. These models are only applicable in non-cohesive sediments and do not allow for a distribution of grain sizes.

It is clear from the review of these models that a new two-dimensional mine scour and burial model was needed, which Friedrichs and Trembanis developed at the Virginia Institute of Marine Science, (Trembanis et al., 2005). This model has been used to forecast and hindcast mine burial for the Clearwater, FL and Martha's Vineyard, MA ONR mine burial experiments. Data from instrumented mines measured percent burial of some mines; however, to properly measure the scour development over time around all the mines and their subsequent burial required systematic repeat multibeam mapping over a larger area.

Obtaining a Vertical Reference Frame

Converting depths from pressure sensor data to a chart datum such as mean low low water (MLLW) is required to make temporal comparisons as well as model versus data comparisons. These "pressure sensor" depths do not take into account the height of the pressure sensor above the bed. In this study, a Sontek PC-ADP (with internal quartz pressure sensor) was used to measure the height of the pressure sensor above the seabed (Fig. 3). The data show three distinct shifts (near Julian day 19, 25, and 54). It is necessary to distinguish shifts caused by the quadpod (and subsequently the pressure sensor) settling into the seabed versus changes in seabed elevation due to erosion, accretion, or bedform

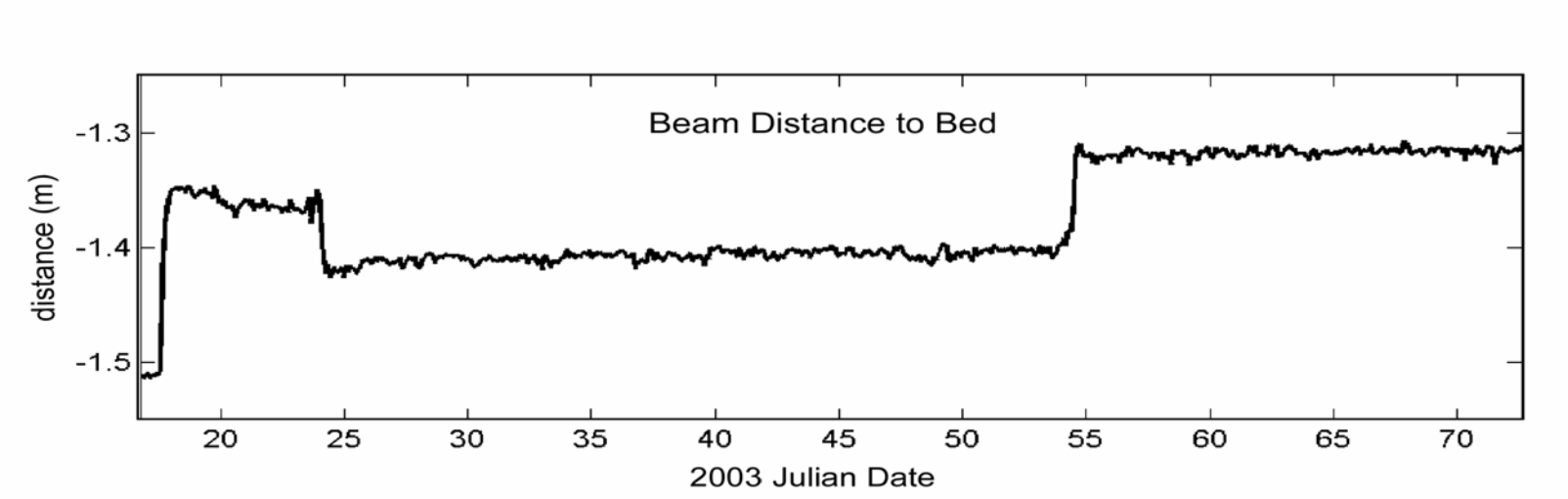

Figure 3. Beam distances to the bed for the fine sand site. Distances were obtained from a SonTek PC-ADP on quadpod 1 in order to measure height of the integrated pressure sensor off the bed. Profile shown is an average of usable data from the sensors on the PC-ADP. Note the three data shifts near day 19, 25, and 54.

migration while the quadpod remains stationary. Figure 4 shows a simplified cartoon schematic of the Sontek data through time along the horizontal axis and depth on the vertical axis. D_T represents the total depth, which is equal to the depth of the sensor below MLLW (D_S) plus the height of the sensor above the bed (H_S) plus the local tides. If the apparent change in water depth is simply a function of sensor settling, then ($D_S + H_S$) will remain constant, as illustrated by the first and second cases. If the apparent change is due to erosion or accretion of sediment, e.g., between the second and third cases, or the third and fourth cases, then ($D_S + H_S$) will not remain constant. In order to determine which the case is, the tide component must be isolated and subtracted from the pressure sensor depths.

Hourly tide data referenced to MLLW were obtained from NOAA station 8726724 in Clearwater, located at the seaward end of Big Pier 60, approximately 21 kilometers east of quadpod 1. The water depths obtained from the pressure sensor were shifted to overlay the NOAA tide heights by subtracting mean levels (de-meaned), and the two were directly compared. Figure 5 shows the NOAA tides minus the de-meaned pressure sensor data in the top diagram, and beam distances to the bed in the bottom diagram. If the two tides match then the difference between the tides should be zero. The cyclic pattern of the line indicates the difference in amplitude and phase between the two locations, changes due to seafloor elevation, as well as any noise in the pressure sensor data. The two solid arrows on the top diagram represent significant data shifts in one of the locations. We make the reasonable assumption that the NOAA station did not change height because there are no "tears" in the NOAA tide record. Thus, we can be confident that these two shifts occurred at the quadpod location. The open arrow on the bottom diagram indicates a significant shift in sensor height from the seabed but does not show up in the tide record. This means that

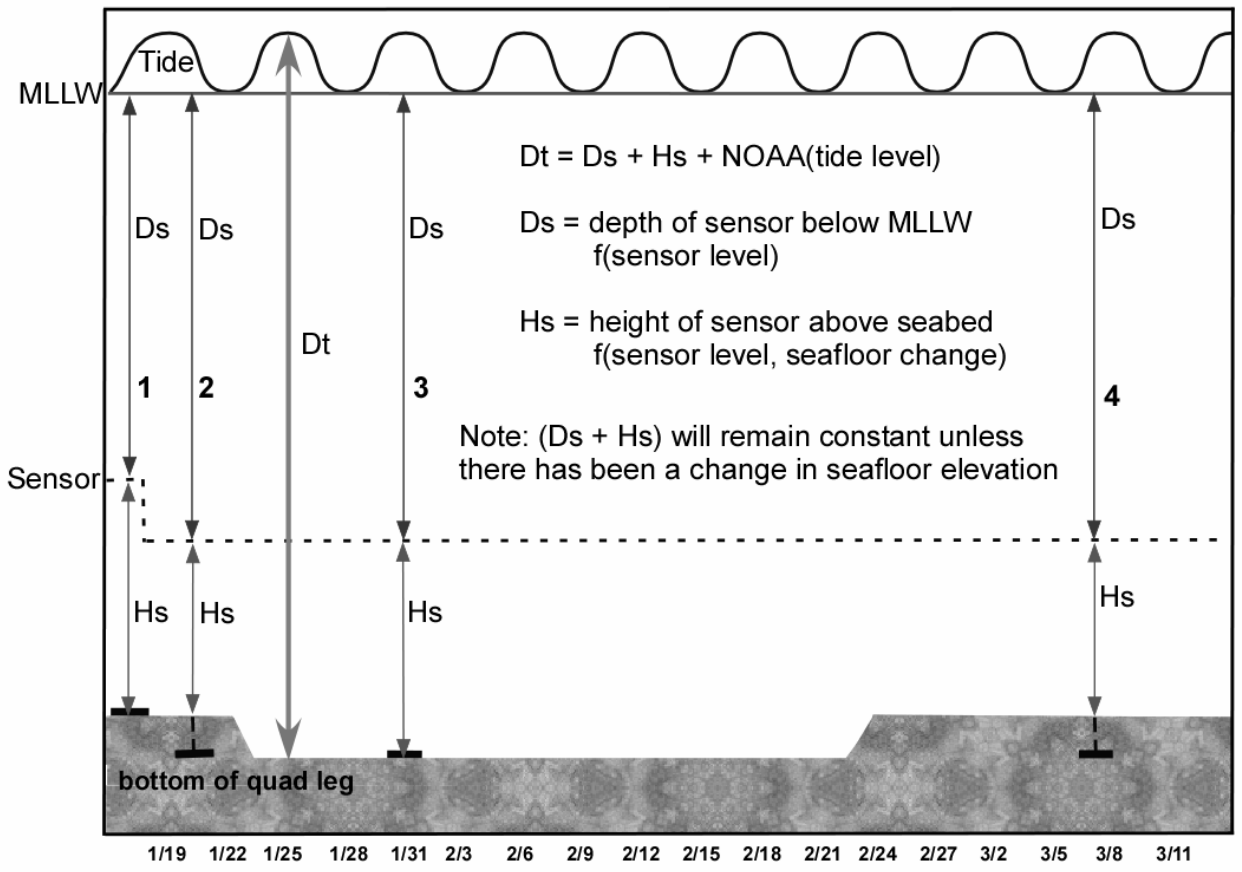

Figure 4. Schematic representation of the SonTek data. Time during the experiment is along the horizontal axis and depth is along the vertical axis.

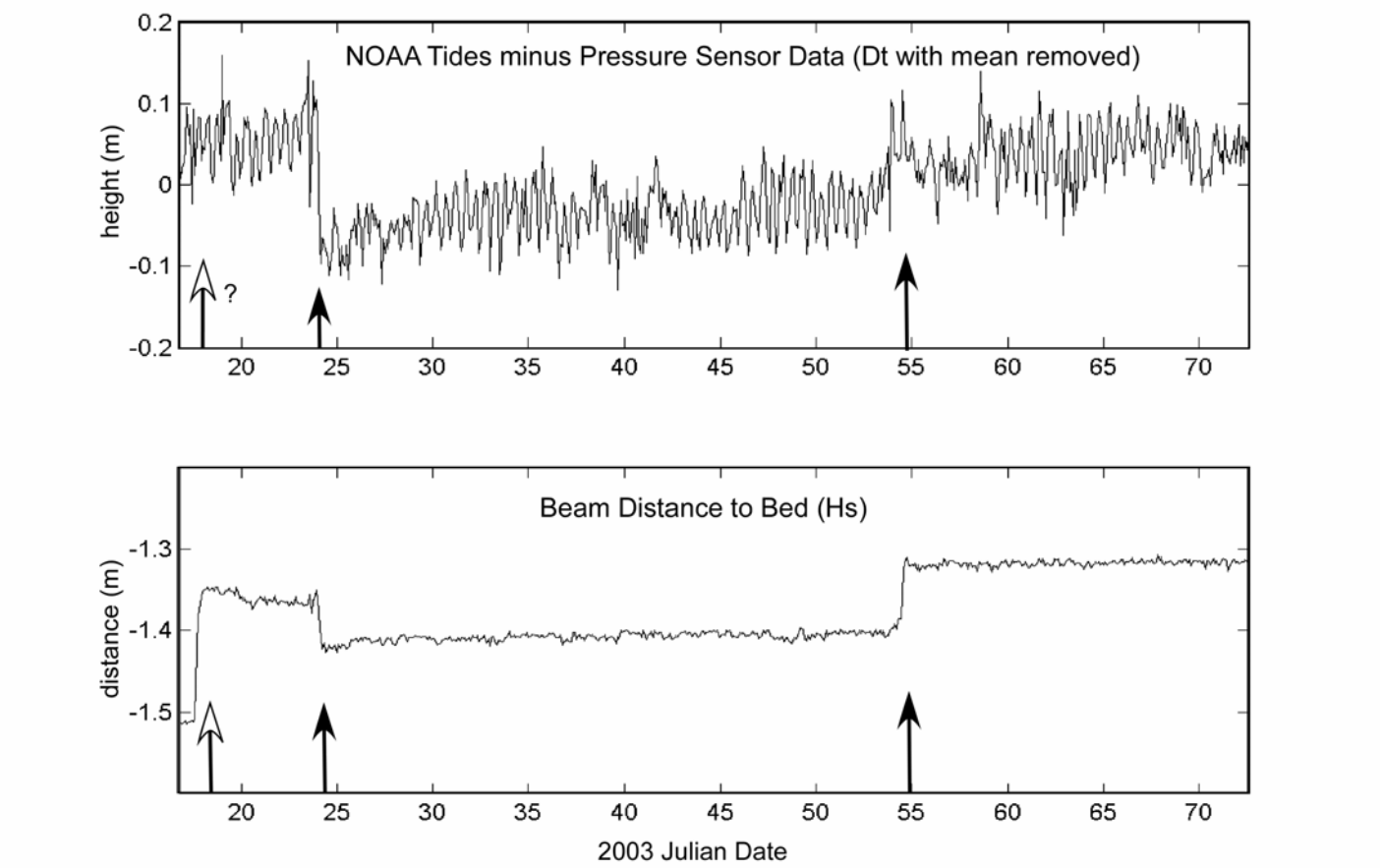

Figure 5. De-meaned pressure sensor data. Top graph shows the NOAA hourly tides minus the de-meaned Pressure sensor 1 data (equivalent of Dt shown in Figure 4 with the mean subtracted). The bottom graph shows the data from one of the SonTek PC-ADP measuring distances to the bed. The two solid arrows represent data shifts visible in both graphs. The open arrow represents a data shift in the bottom graph that is absent in the top.

($D_S + H_S$) remained constant and indicates the quadpod sank into the sediments. The two shifts denoted by a solid arrow, however, show up on both the graph of the beam distances to the bed and the NOAA tides minus the pressure sensor tides. This means that both H_S and D_S changed and the sum ($D_S + H_S$) did not remain constant, indicating a change in seafloor elevation.

In order to extract the changes in seafloor elevation from the data, the time series of the NOAA tides minus the pressure sensor data needs to be filtered. A lowpass Butterworth filter was applied to the data using a 36 hr period. The low frequency signal obtained represents changes in seafloor elevation and can subsequently be removed from the de-meaned pressure sensor data, leaving only the tidal component (Fig. 6). The phase lag between the pressure sensor tide record and the NOAA tide record was calculated to be approximately 4 minutes (see Appendix B for a description of the equations used). The amplitude of the pressure sensor tide record is off by a factor of 1.06 when compared to the NOAA record, corresponding to a maximum offset of 4.5 centimeters.

When the seafloor elevation under quadpod 1 is plotted, there are two significant shifts punctuated by smaller changes (Fig. 7). The inflection point of the first shift in seafloor elevation lines up with the first shift in our initial tide record, peak significant wave height, and peak wind speed. Maximum erosion, however, does not occur until 16 hours later. At the second shift, the tide shift and wind speed peak line up with the inflection point of the seabed elevation change; however, the significant wave height does not peak until 18 hours later at the time of maximum accretion. The reason for this discrepancy is not clear.

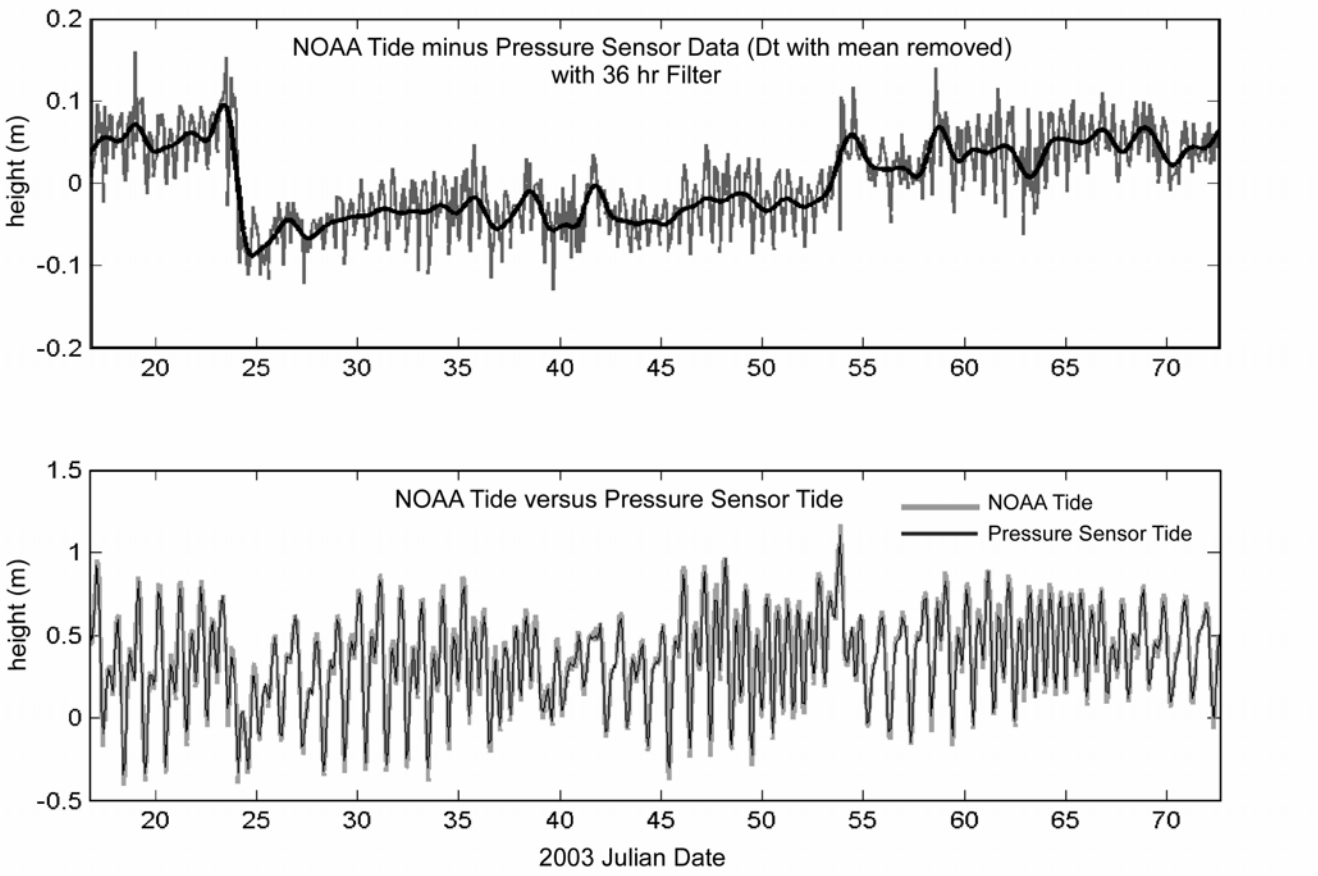

Figure 6. Filtered pressure sensor data. The top graph shows the NOAA tides minus the de-meaned pressure sensor data with the 36 hr filter. The bottom graph shows the NOAA tide versus the tide extrapolated from the pressure sensor data.

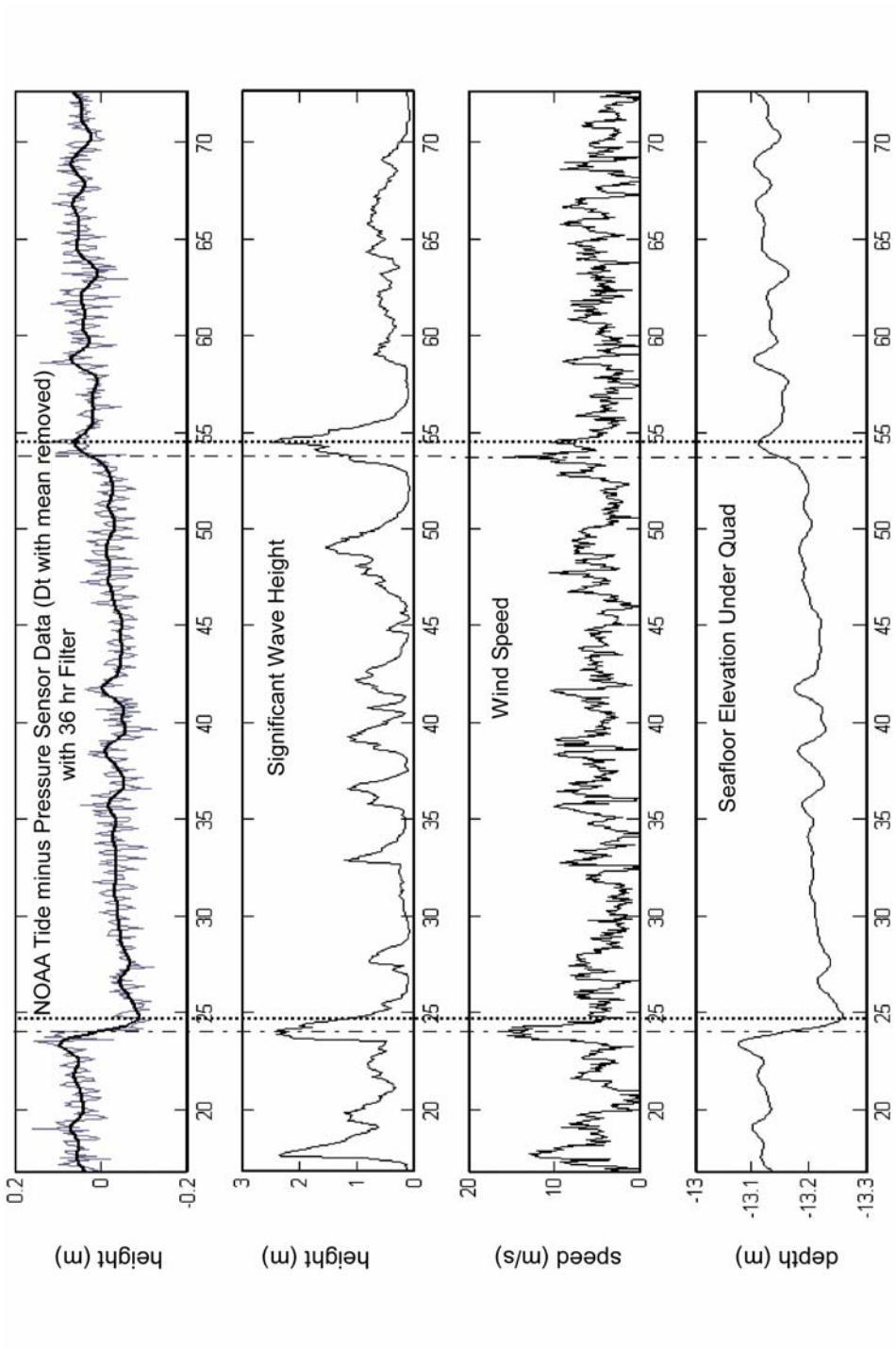

Figure 7. Seafloor elevation change. The top graph shows the NOAA tides minus the de-meaned pressure sensor data with the 36 hr Butterworth filter. The second graph shows significant wave height obtained from the ADCP, and the third shows wind speed in meters per second obtained from the NOAA buoy. The bottom graph shows calculated seafloor depth based off the pressure sensor data and the isolated tide record. The dashed lines cut through the inflection points of the two significant changes in seafloor elevation, while the dotted line cuts through the maximum change.

Temporal Analysis of Mine Burial

The rate at which mines subside relative to the ambient seafloor and become buried is extremely important to mine countermeasures. Current methods of mine hunting involve the use of side-scan sonars, which rely on shadow casting for detection. Once scour has formed around a mine and it subsides below ambient seafloor depth, it becomes more difficult for an acoustic shadow to form, thereby making detection with side-scan difficult if not impossible. Multibeam sonars do not have a nadir blind zone, are not towed deeply, and thus are more able to image the object as they pass directly over it. This has made it possible to image mines in different stages of scour and burial and observe the temporal scales of such processes, until they are fully covered by sediments. Six multibeam surveys of the fine study site were used in the analysis of the A3 mine: January 10th, 13th, 17th, and 20th, February 6th, and March 13th, 2003. The same surveys were used in the analysis of the F8 mine, with the exception of the January 10th survey since the mine was not deployed until January 11th. Each individual pass of the multibeam over the mines can be used to estimate the amount of scour and burial at that time. These passes were then used to monitor discrete changes in scour and burial during the experiment.

All multibeam data were cleaned and processed using CARIS HIPS and SIPS 5.3. All speed jumps greater than 1 knot and all time jumps greater than 1 second between consecutive pings were removed using a linear interpolation. Once the data were cleaned, a tide correction was applied. The multibeam data from surveys before the quadpods were deployed on January 16th were tide-corrected with data from NOAA station 8726724. Two tide records were obtained from pressure sensors mounted on quadpods deployed near the

mines using the previously discussed method, and used to tide-correct survey data subsequent to the 16th. The two tide records, one from quadpod 1 deployed near the A3 mine in the fine sand site and one from quadpod 3 deployed near the F8 mine in the coarse sand site, were found to be nearly identical. A multiplier of 0.94 was applied to the NOAA tide record to account for the difference in amplitude between the NOAA tide and the tide records obtained from the pressure sensors.

After applying the tide correction, the multibeam data was gridded in CARIS using a weighted mean gridding algorithm. The weight that any given sounding contributes to the grid varies with range and grazing angle to the seabed. The range weight is inversely proportional to the distance from the grid node (i.e., the closer to the node, the greater the weight). The grazing angle weight is most important in grids containing adjacent or overlapping track lines. Higher weight is given to beam from the inner part of a swath. Beams with a grazing angle between 75 and 90 degrees are given a weight of 1.0. This weight linearly decreases to 0.01 as the grazing angle with the seabed decreases to 15 degrees.

For each survey, 18-by-18 meter grids centered on the mines were created; gridded at a 20-centimeter horizontal resolution and referenced to MLLW. In some instances, the 20-centimeter grid resolution was too small to provide full coverage in areas of sparse data (e.g., the outer beam of the swath). In these cases, the grids were interpolated in order to fill these data gaps. Interpolation was based on a 3 x 3 grid node area with a threshold level of 6 neighbors. For example, if a node in the grid does not contain a value, the interpolation is limited to the neighboring 9 nodes. In order for the interpolation to take place, a minimum of 6 of these neighboring nodes must contain a pixel value. This helps limit the amount of

interpolation and prevents it from expanding the gridded surface outward from the actual survey area. Final imaging, including 3D rendering and artificial sun illumination, was completed using IVS Fledermaus 6.0.

Depth of the mine was defined as the shallowest point on the mine surface. Ambient seafloor depth was defined as an average of 35 depths taken around the mine outside the influence of any scour (see Appendix A for a more detailed analysis on ambient seafloor depth). Given that our study site is in shallow water (average depth ~ 13 meters) and we use a POS MV system with RTK for vessel positioning, we assume a vertical uncertainty of ± 5 centimeters. This decision was also made in an effort to avoid masking our signal with uncertainty; however, we realize that 5 centimeters may be optimistic and the actual uncertainty may be closer to 10 centimeters.

Temporal Changes in Scour and Burial over the A3 Mine

The A3 mine was situated over fine sand (median grain size .180 mm) at a water depth of 12.81 meters, and was closely surrounded by two quadpods and one spider (Fig. 8). The January 10th survey was the first to image the A3 mine after its January 8th deployment. The grid shows only the A3 mine, as the quadpods and spider were not deployed until January 16th (Fig. 9). In this image, as in all subsequent images, artificial sun illumination is from the northeast (045°) at an angle of 45 degrees above horizontal. The mine has only been deployed for approximately two days, and no scour is visible. The depth to the top of the mine is 12.32 meters, with the average depth of the seafloor around the mine at 12.81 meters. The difference, 0.49 meters, indicates that the mine is approximately 8% buried after two days. The beam mode of the multibeam during this

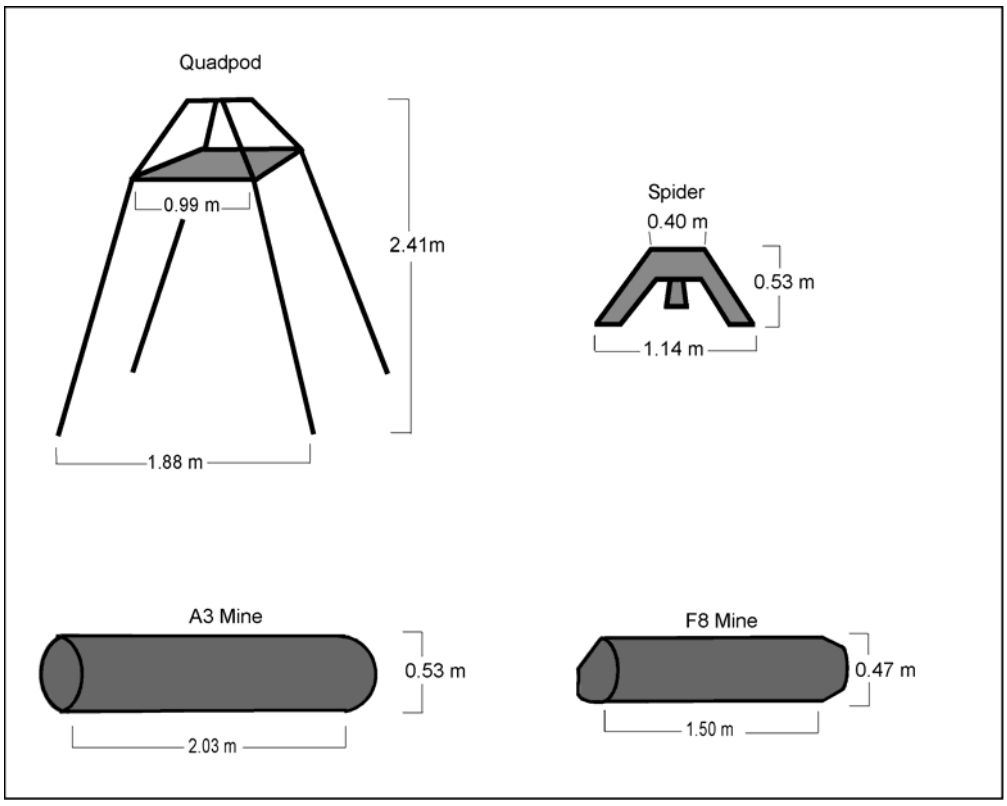

Figure 8. Dimensions of the quadpods, spiders, and mine-like cylinders visible in the multibeam images.

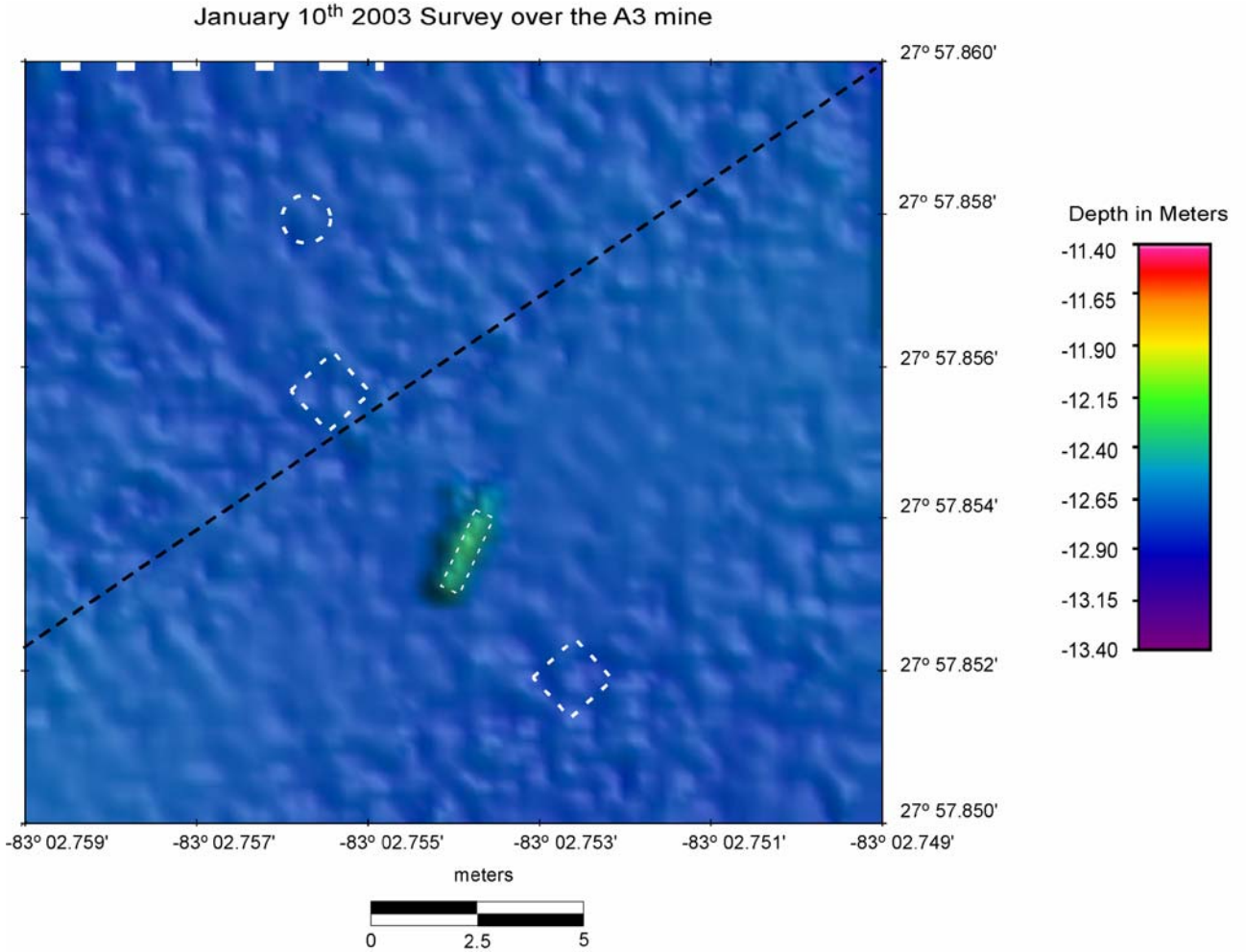

Figure 9. January 10th survey over the A3 mine. No scour is visible. The black dashed line indicates the ship's track line during the survey. The two white dashed boxes and the white dashed circle represent the future deployed locations of the two quadpods and one spider respectively. The mine itself is outlined with a faint white line. All outlines are scaled to the actual dimensions of the deployed equipment. The mine outline remains at the same scale and orientation throughout the rest of the images as a reference.

survey was set on target detection. It was discovered that this mode causes a widening of the beams (from 1.5° to 4.0°) in order to improve target detection capabilities, but it unfortunately blurs the mine and its orientation. Comparison with data from the heading sensor in the A3 mine itself indicates that the orientation should be north south (-5.7°), rather than the northeast southwest orientation apparent in the image. Orientation of the mine is in relation to magnetic north (declination: 0°19').

The January 13th survey is similar to that of January 10th, and there is no apparent scour around the mine (Fig. 10). The depth to the top of the mine is 12.42 meters, indicating a sinking of 0.10 meters since January 10th. The average depth of the seafloor around the mine is 12.88 meters, indicating a 13% burial of the mine. Again, the beam mode on the multibeam was set on target detection, explaining blurriness of the mine itself and the distortion of its orientation.

The survey of January 17th occurred just one day after the spiders and quadpods were deployed. The mine, quadpod 2, and the spider are all clearly visible, yet quadpod 1 does not show up (Fig. 11). It is unclear why the quadpod is not visible, though it is possible a bubble sweep occurred. A spike filter was also set on the multibeam at the time of this survey, though this filter is an unlikely cause of the quadpod's disappearance since the other quadpod shows up. There is still no visible scour at this time, although the average depth of the seafloor around the mine is 12.92 meters. The depth to the top of the mine is 12.48 meters, indicating the mine has now sunk 0.16 meters for a total burial of 17%. Target detection was not used during this or any subsequent survey, therefore the mine is less fuzzy and its orientation agrees with the orientation data from the mine itself.

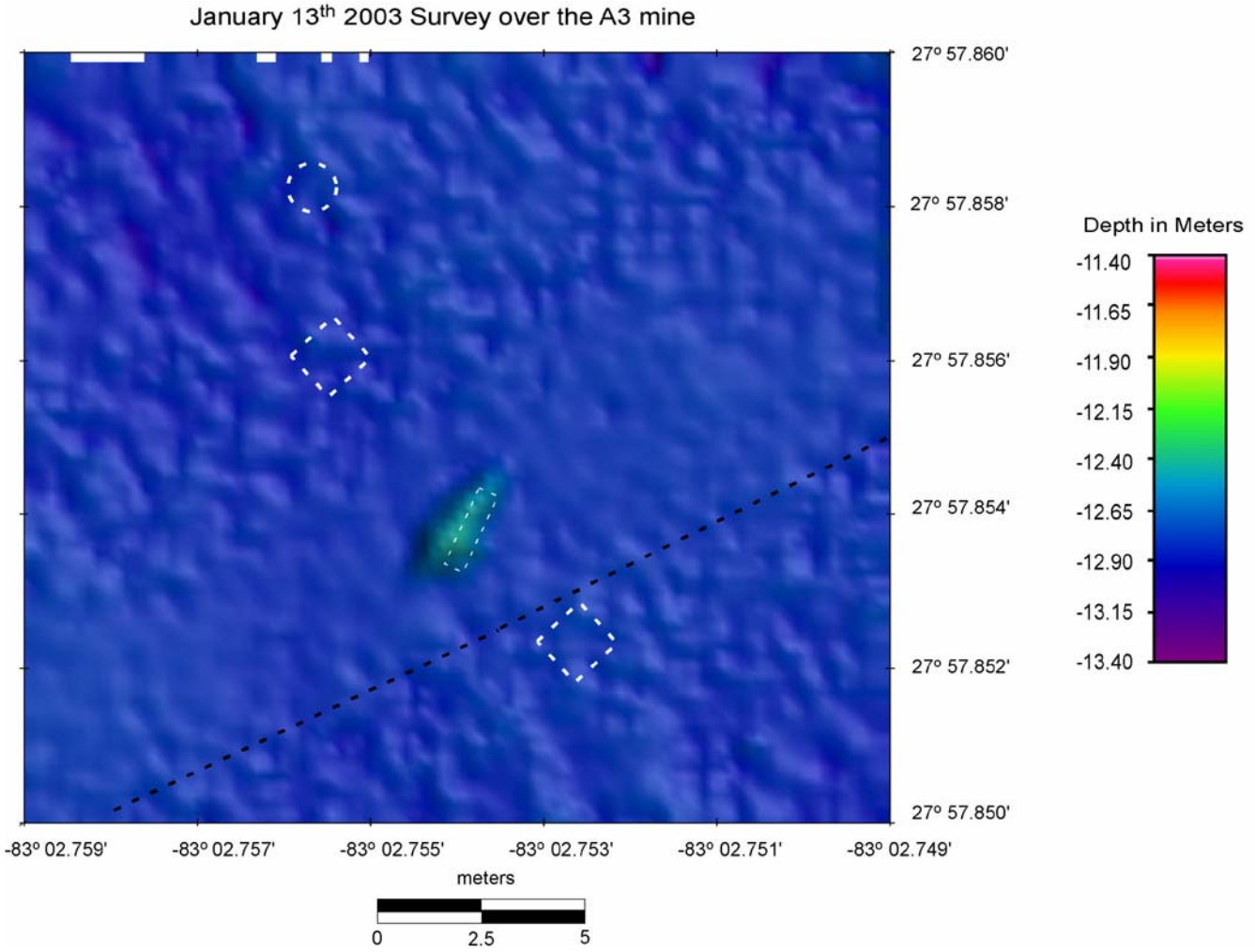

Figure 10. January 13th survey over the A3 mine. No scour is visible. The black dashed line indicates the ship's track line during the survey.

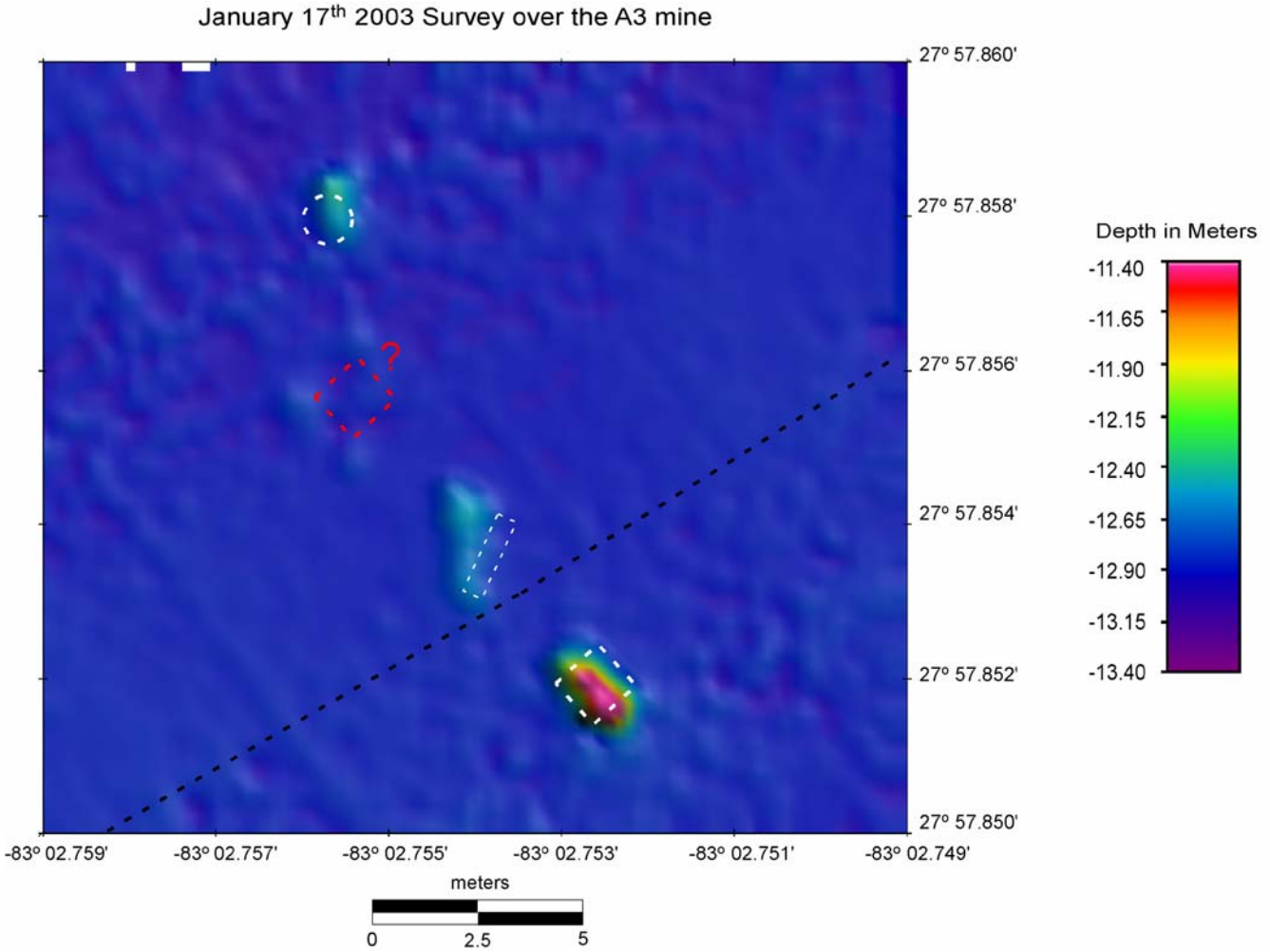

Figure 11. January 17th survey over the A3 mine. The quadpods and spiders have now been deployed and can be seen in the image, with the exception of quadpod 1. The red dashed box with the question mark denotes where quadpod 1 should be located.

In the January 20th survey, scour around the mine becomes evident (Fig. 12). It is also clear that the mine has sunk even further. The spider is not visible, although the scour pit that formed around the spider is. The cause of the spider not being detected is also unknown. The depth to the top of the mine is 12.62 meters, 0.30 meters deeper than that observed in the January 10th survey. The average depth of the seafloor around the mine is 12.82 meters, and the mine is now 62% buried. A scour pit has formed around the mine, with the deepest point measuring 13.04 meters.

The spider is visible in the February 6th image, and the scour has continued to develop around both the mine and the spider (Fig. 13). The depth to the top of the mine is 12.72 meters, indicating that the mine has sunk 0.40 meters since the initial survey on January 8th. The average depth of the seafloor around the mine is 12.81 meters, and burial of the mine is now up to 83%. The depth in the scour pit around the mine has increased to 13.18 meters.

The March 13th survey shows that the mine has become nearly flush with the ambient seafloor depth (Figs. 14 & 15). The mine is only visible due to the defining ring of scour around its periphery. The depth to the top of the mine is now 12.80 meters, indicating the mine has sunk a total of 0.48 meters since the start of observations. The average depth of the seafloor around the mine is 12.82 meters, and the mine is 96% buried. The spider has also scoured considerably and has sunk into the seafloor. Scour is also visible around the legs of both quadpods, though any sinking of the quadpods appears to be minimal, according to pressure sensor data on the quadpod and multibeam bathymetry data.

Overall, the total amount of scour over the course of the experiment formed a pit around the mine 0.40 meters deeper than the ambient seafloor and the mine sank 0.48

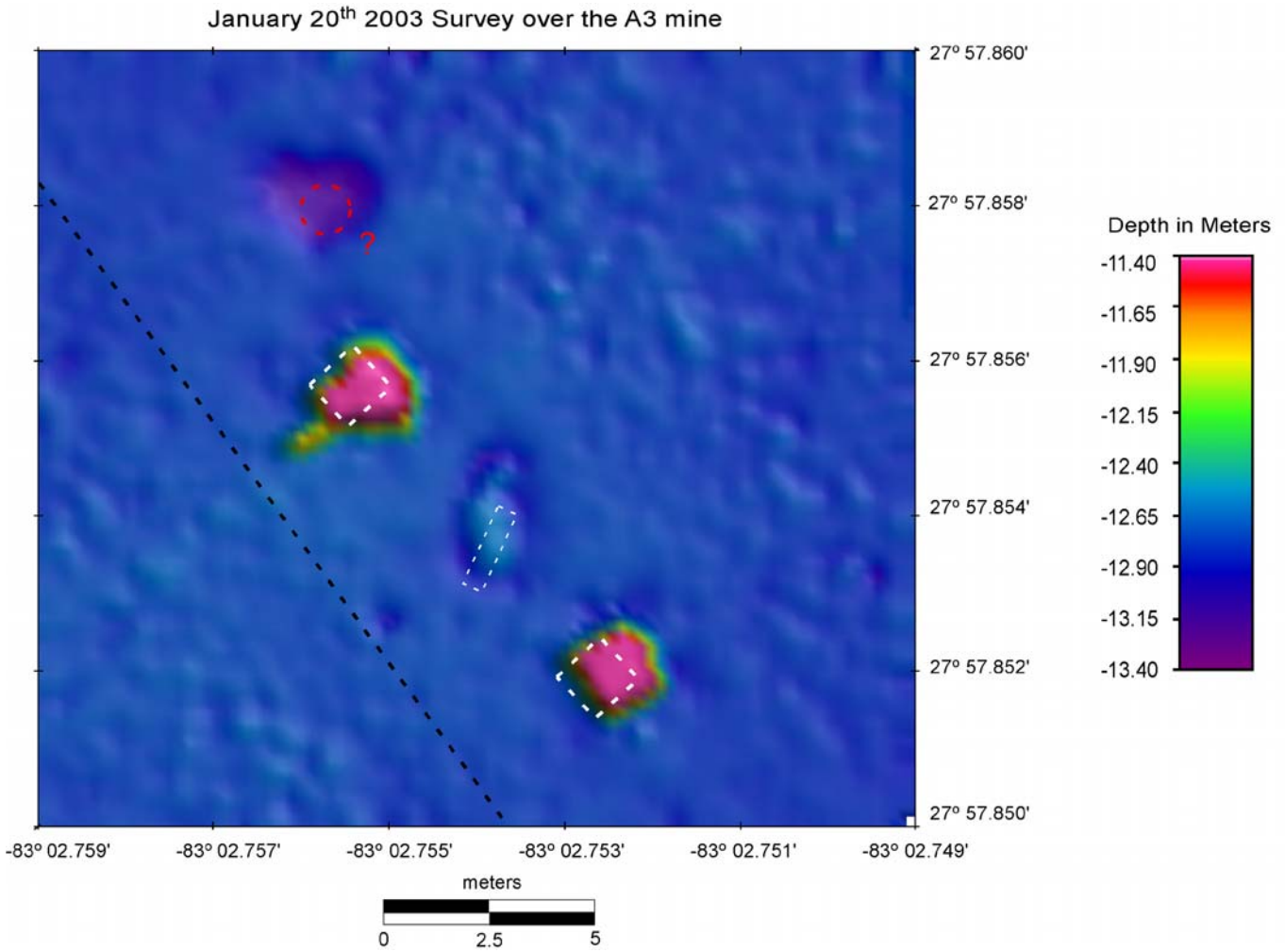

Figure 12. January 20th survey over the A3 mine. Note that both quadpods are now visible, although the spider is not. The red dashed circle with the question mark denotes where the spider should be located. A ring of scour can clearly be seen around the mine.

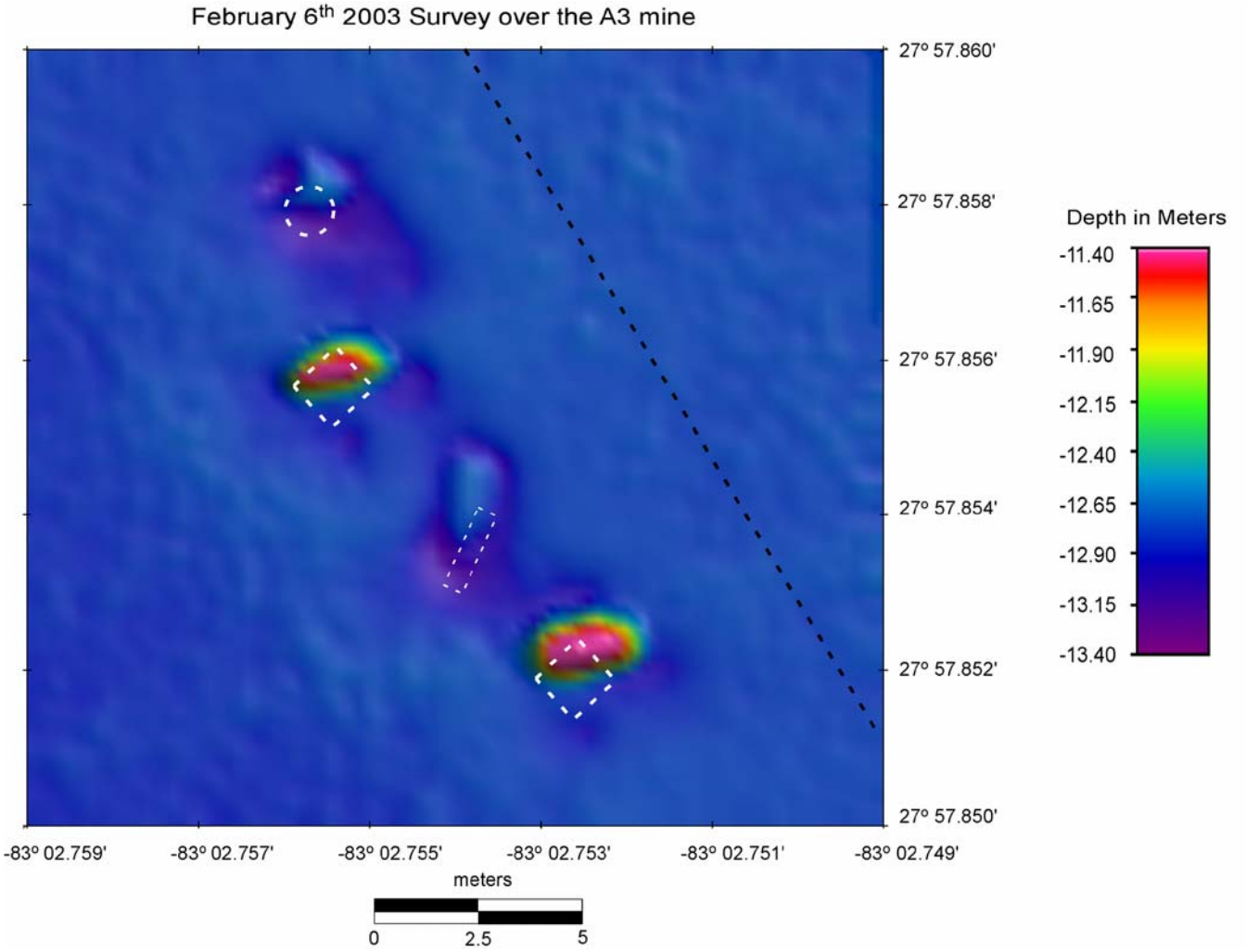

Figure 13. February 6th survey over the mine. The spider is once again visible. Scour pits can clearly be seen around the spider and the mine.

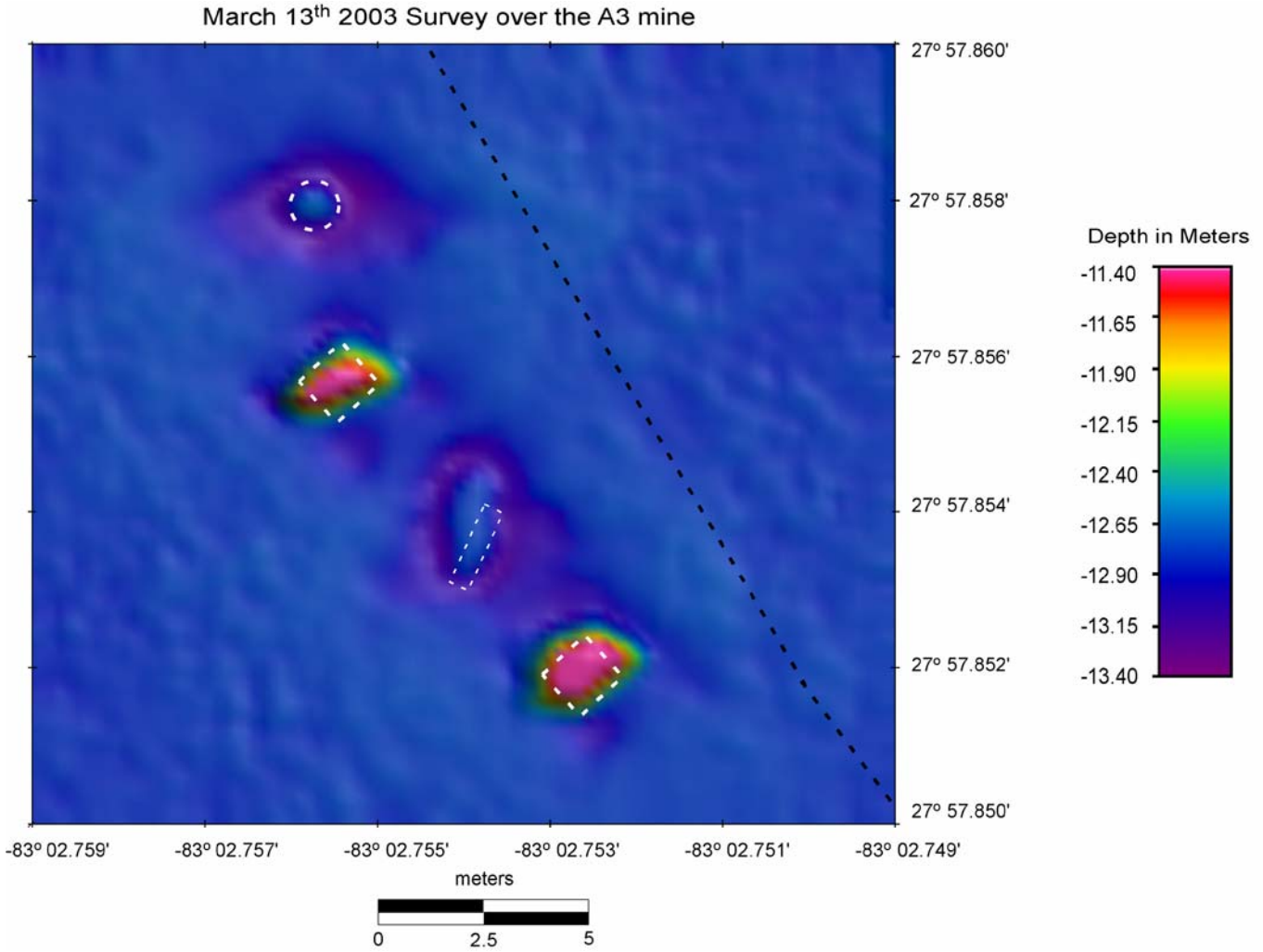

Figure 14. March 13th survey over the mine. Both quadpods and spiders are readily visible. The sharp ring of scour around the spider and the mine help set them off from the rest of the seafloor. Note the scour around the legs of the quadpods.

Figure 15. ROV video still image of the A3 mine on March 13, 2003. Camera is facing east-northeast showing a side view of the mine within the scour pit.

meters between January 10th and March 13th (Table 1; Fig. 16). The diameter of the mine is 0.53 meters, so a sinking of 0.48 meters would result in a 91% burial. Slight changes in the ambient seabed elevation over the course of the experiment, however, have resulted in the maximum amount of burial as observed in the multibeam images to be 96%.

Comparison of A3 Multibeam Observations to the VIMS 2D Burial Model

The model predicts percent burial of the mine given sediment size, bed stress, and mine diameter. NOAA WaveWatch3 monthly hindcast wave data were used to drive the model for wave-induced scour, by using linear wave theory to estimate near bed wave orbital velocity. The percent burial was then predicted by comparing the depth of the scour to the diameter of the mine. The percent burial as observed in the multibeam images was directly compared to the model predictions (Table 1).

The model was initialized with a local water depth of 12.81 meters (obtained from the January 10th survey over the mine) and 0% burial. There is no multibeam survey over the A3 mine on the day of deployment; however, SCUBA divers repositioned the mine shortly after deployment to ensure no impact burial. This makes certain that the model and the observed data are initialized with the same conditions. The model was run from the time of mine reposition, January 8th 2003 1600 GMT, to the time of the last multibeam survey over the mine, March 13th 2003 at 0200 GMT.

The first direct comparison between the observed and predicted burial occurs for the January 10th survey (Figs. 16 & 17). Observed data show the mine to be 7.5% buried; however, the model predicts a burial of 14.9%. This difference of 7.4% is the largest discrepancy between the predicted and observed data throughout the experiment. The

	Jan. 8	Jan. 10	Jan. 13	Jan. 17	Jan. 20	Feb. 6	Mar. 13
Depth of Mine	_____	12.32	12.42	12.48	12.62	12.72	12.80
Cumulative Amount of Change	_____	_____	0.10	0.16	0.30	0.40	0.48
Average Depth of Seafloor	_____	12.81	12.88	12.92	12.82	12.81	12.82
Cumulative Amount of Change	_____	_____	0.07	0.11	0.01	0.00	0.01
Scour Visible / Depth of Scour	_____	no	no	no	yes 13.04	yes 13.18	yes 13.22
% Mine Burial from Multibeam (± 9.4% due to 5 cm uncertainty of sonar)	0	7.5	13.2	17.0	62.3	83.0	96.2
% Mine Burial from Model	0	14.9	17.8	17.8	60.1	81.2	97.7
Mine Heading (degrees)	-5.7	-6.9	-6.6	-6.6	-1.0	3.37	7.1
Mine Pitch (degrees)	-0.7	-0.3	-0.4	-0.4	-0.8	-0.9	0.6
Mine Roll (degrees)	-0.4	7.8	7.4	7.4	14.1	25.6	33.1

Table 1. Data table for the A3 mine. All numbers are in meters except where noted. There is no multibeam survey on January 8th.

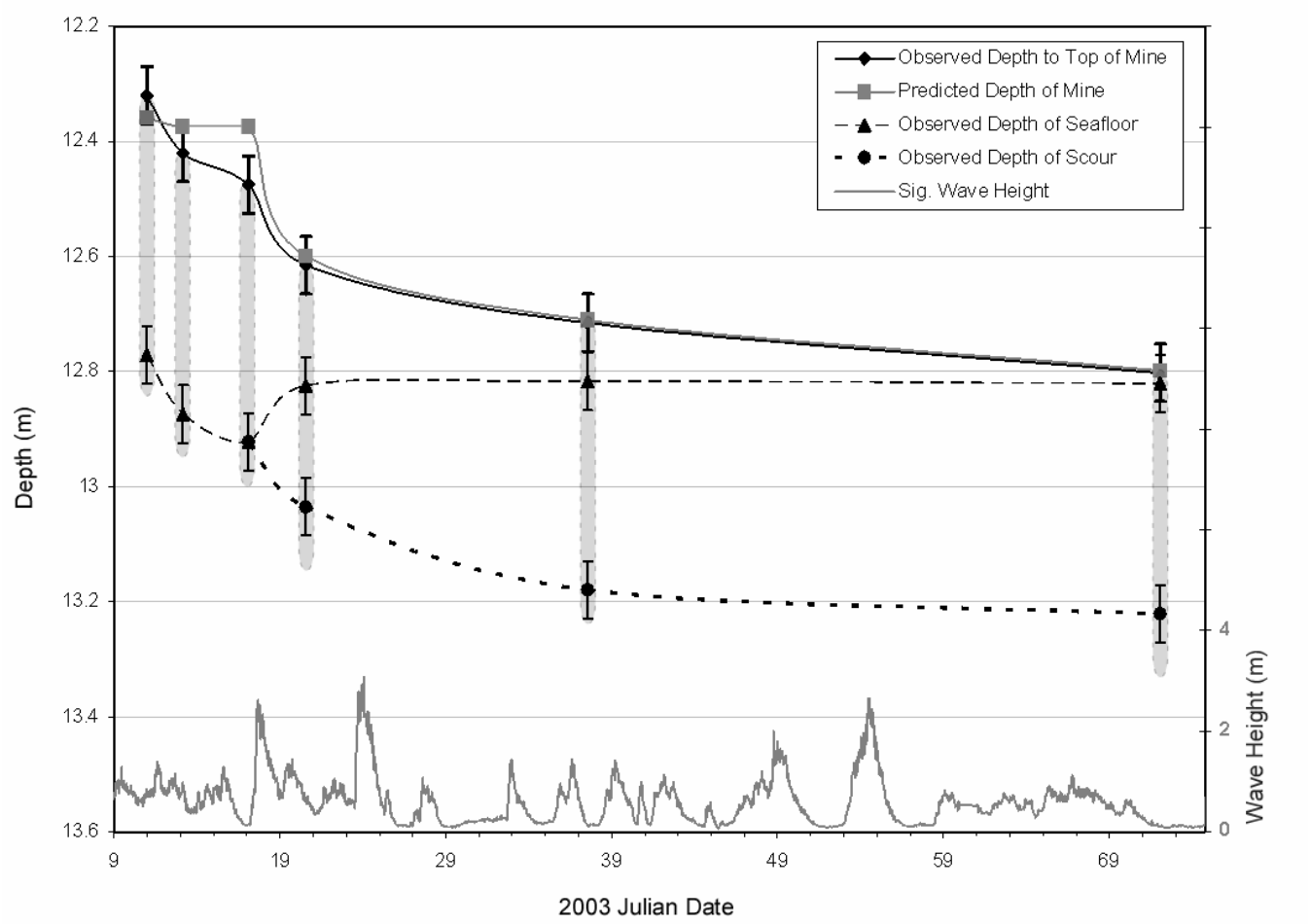

Figure 16. Comparison of multibeam observed (black) and predicted (gray) mine depth for the A3 mine over the course of the experiment. Predicted percent burial of the mine was converted to predicted depth of the mine using the 12.81-meter water depth used to initialize the model. Observed depth of seafloor and depth of scour from the multibeam are plotted as well. Significant wave height is plotted on the right y-axis. Error bars represent the 5-centimeter uncertainty inherent in the multibeam system. The light gray oval represents the A3 mine, and is scaled to the actual dimensions of the mine (length ~ 0.53 m, the diameter of the mine).

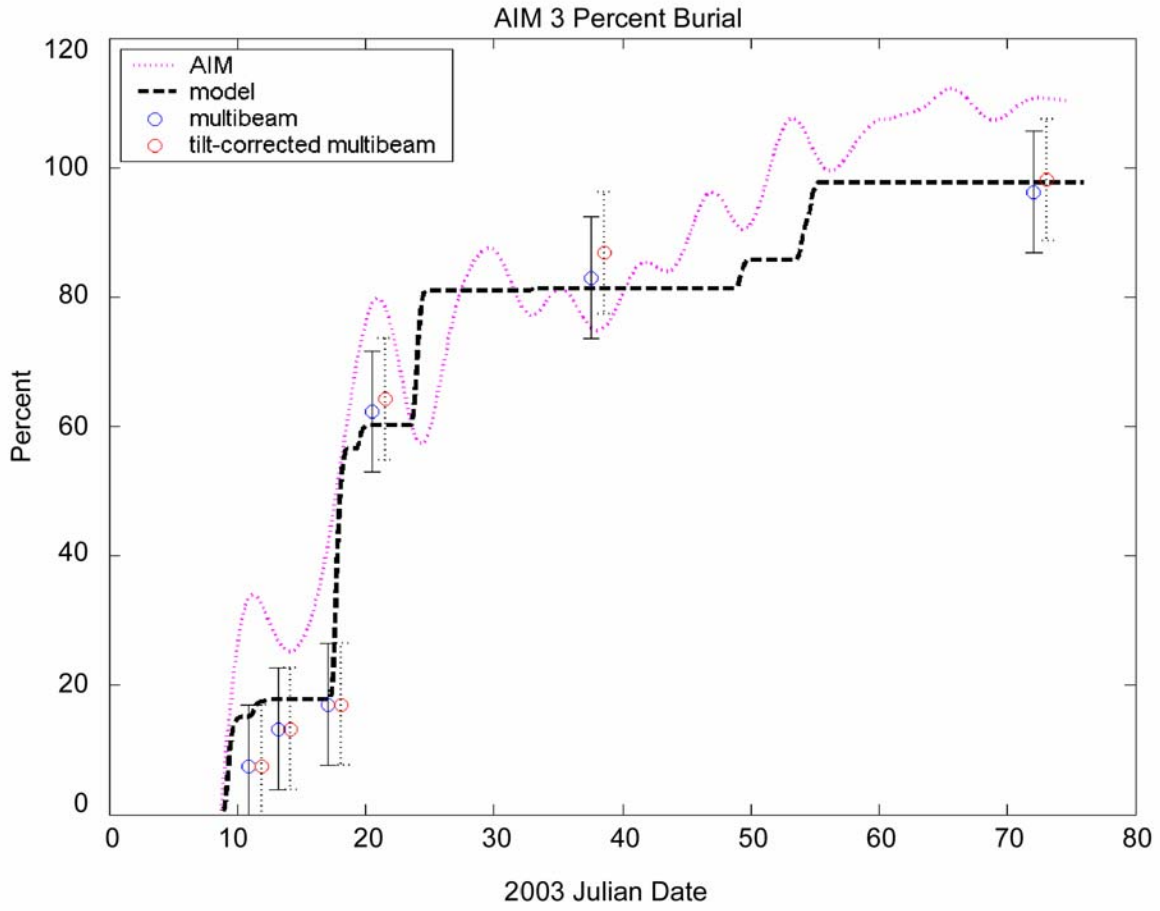

Figure 17. Comparison of the mine (magenta), predicted (dashed), observed (blue), and tilt-corrected observed (red) percent burial for the A3 mine over the course of the experiment. Tilt-corrected values have been horizontally offset for clarity. Error bars represent the 5-centimeter uncertainty inherent in the multibeam system.

multibeam sonar has an inherent uncertainty of ± 5 centimeters in its vertical accuracy, which corresponds to a percent burial of 9.4. Therefore, the model prediction falls within the range of multibeam values. The observed percent burial in the multibeam data is based off the shallowest point on the top surface of the mine, which could underestimate true burial of the mine due to pitch (tilting of the long axis of the cylinder). The predicted percent burial is based on the depth of the predicted scour in relation to the mine diameter, and therefore assumes a direct sinking of the mine with no concern for pitch. Sensors within the A3 mine measured roll, pitch, and heading throughout the experiment. The degree of pitch can be used to calculate how much deeper the center point on the top surface of the mine is from the shallowest point observed in the multibeam images. A correction can then be applied to the observed values for percent burial. Reviewing the data from the pitch sensor (Table 1) reveals a -0.3° pitch during the time of this survey; however, this only corresponds to ~ 6 millimeters and is beyond the multibeam resolution.

The January 13th comparison shows a discrepancy of 4.6%, with an observed burial of 13.2% compared to a predicted burial of 17.8%.This falls within the accuracy of the multibeam (Figs. 16 & 17). The mine shows a tilt of -0.4° at the time of this survey, which corresponds to a change of ~ 7 millimeters. The differences between the predicted and observed data begin to narrow in margin around the January 17th survey, with an observed burial of 17.0% and a predicted burial of 17.8%, a discrepancy of only 0.8%. Applying the tilt correction of 0.4° only alters the amount of burial by ~ 7 millimeters as well.

The January 20th and February 6th predictions fall within the multibeam uncertainty, even without the tilt correction (Fig. 16 & 17). The January 20th survey has an observed

and predicted burial of 62.3% and 60.1% respectively, a discrepancy of 2.2%. The measured degree of tilt during this survey is -0.8°, which corresponds to ~ 1 centimeter of burial and increases the discrepancy to 4.1%. The February 6th survey shows an observed burial of 83.0% and has a predicted burial of 81.2%, a discrepancy of 1.8%. The measured tilt during the survey of February 6th is -0.9°, which also adds a centimeter's worth of burial and would increase the discrepancy to 3.7%.

The comparison from the final survey on March 13th, 2003 shows a small discrepancy of 1.5% with an observed burial of 96.2% and a predicted burial of 97.7% (Figs. 16 & 17). This discrepancy decreases to a mere 0.4% when the tilt correction of 0.6°, corresponding to a change of 1 centimeter, is applied. The predicted value falls within the accuracy of the multibeam, even without the tilt correction.

Discussion of the A3 Comparisons

The VIMS 2D Burial Model is compared to six repeat high-resolution multibeam surveys over the A3 mine. The mine subsides and becomes partially buried throughout the experiment, but surrounding scour is not observed until the January 20th survey, twelve days after deployment. Direct comparison between these observations and the VIMS 2D Burial Model shows a good agreement (Fig. 17). The model was initialized with a 0% burial. Impact burial for the observed data was assumed to be 0% as well, based on limited SCUBA observations, thus allowing the initial conditions to be the same between the predicted and observed data. The overall trend throughout the experiment shows the modeled predictions are consistently within the measurement uncertainty of the multibeam data. A tilt correction can be applied to the observed values of mine burial in order to

calculate a direct sinking of the mine. This correction, however, only adds a centimeter of burial at most, corresponding to an increase 1.9% in observed burial and was not necessary. In field applications, tilt of cylindrical mines will not be available, but fortunately, their potential effect on true depth of burial is minimal.

Temporal Changes in Scour and Burial over the F8 Mine

The F8 mine was situated within a rippled scour depression (RSD) over coarse-sand (median grain size 0.840 mm) at a water depth of 13.20 meters. The January 13th survey was the first to image the F8 mine after its January 11th deployment (Fig. 18). The mine has only been in the environment for approximately two days, and no scour is visible. The observed depth to the top of the mine is 12.72 meters, with the average depth of the ambient seafloor at 13.20 meters, resulting in an observed burial of zero percent. The difference of 0.48 meters between the top of the mine and the seafloor is actually one centimeter greater than the diameter of the mine itself (0.47 meters). Pitch measurements recorded from orientation sensors within the mine show a zero degree tilt at the time of this survey, however, the discrepancy of 1-centimeter falls within the 5-centimeter measurement uncertainty of the multibeam. It is also possible that the mine is sitting on a mound of sand slightly shallower than the surrounding seabed. It is important to keep in mind that the ambient seafloor depth is also an approximate regional estimate. A north-south trending ripple field can be seen in the lower left of the image. Maximum height of the ripples is ~ 20 centimeters with a maximum wavelength of a ~ 1.25 meters. The ripple field is no longer apparent in the multibeam image from the January 17th survey (Fig. 19). The depth to the top of the mine is 12.80 meters, indicating a sinking of 0.08 meters since

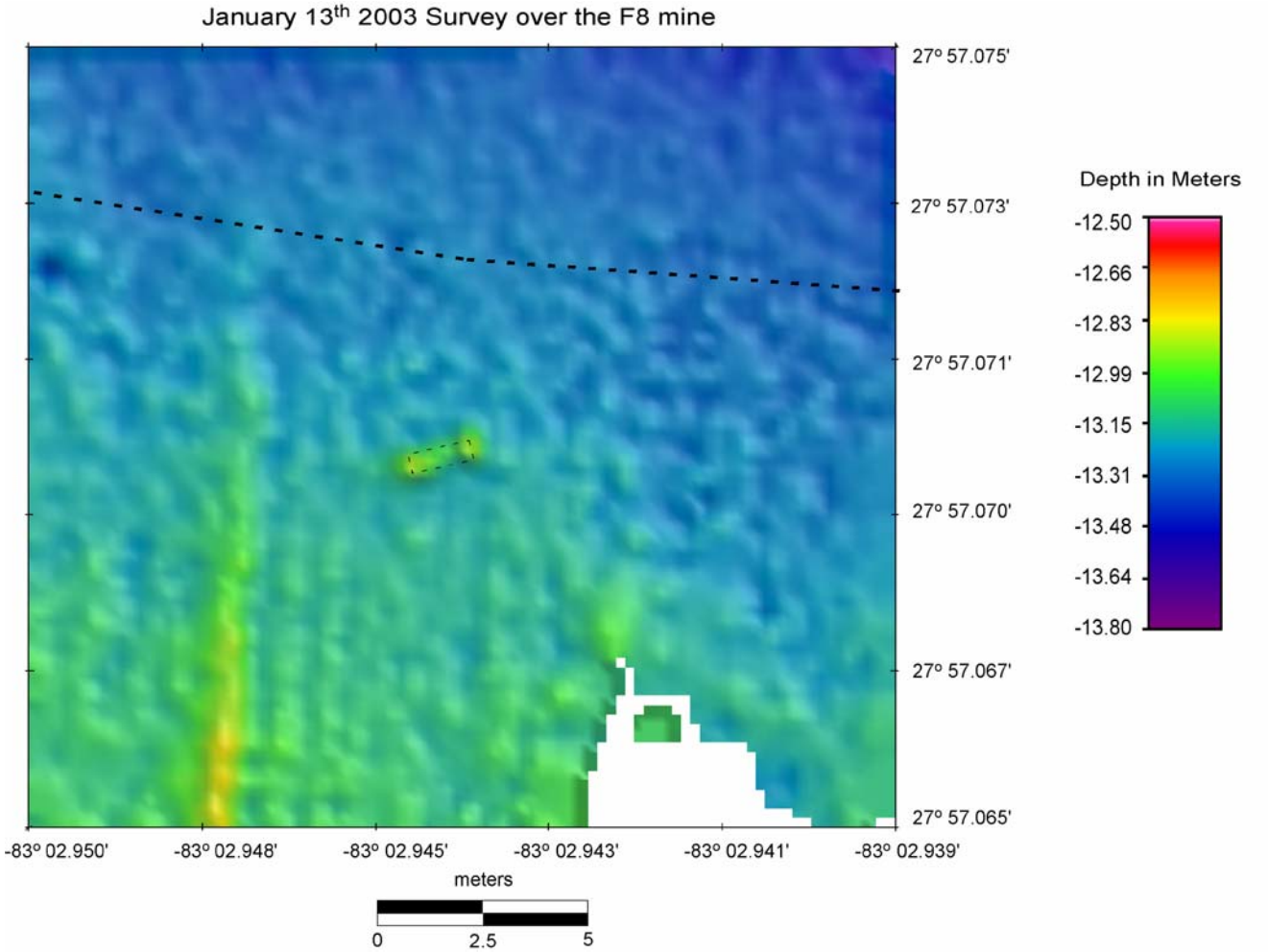

Figure 18. January 13th survey over the F8 mine. No scour is visible. The thick black dashed line indicates the ship's track line during the survey. The mine itself is outlined with a faint black dashed line scaled to the actual dimensions of the F8 mine. The mine outline remains at the same scale and orientation throughout the rest of the images as a reference.

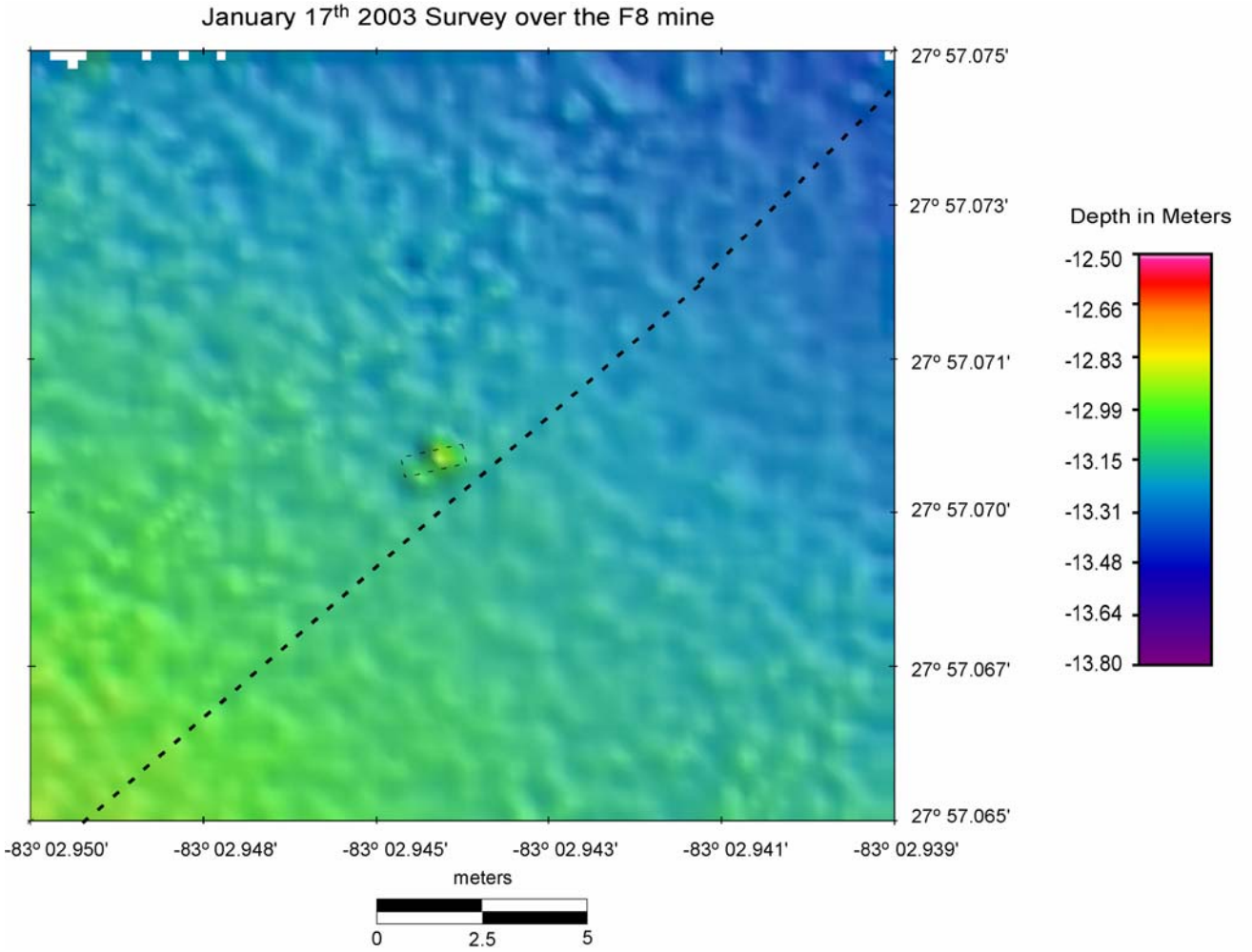

Figure 19. January 17th survey over the F8 mine. No scour is visible.

January 13th. The average depth of the seafloor around the mine is 13.17 meters, resulting in an observed burial of 21.3%. There is no scour visible around the mine at the time of this survey; however, it does become evident in the survey of January 20th (Fig. 20). Maximum depth in the scour pit that has formed at the southwest end of the mine is 13.27 meters. In the lower left of the image, ripples are again visible, although they are smaller than those observed in the January 13th survey. Ripple height is on the order of 10 centimeters and the wavelength is approximately 50 centimeters. The mine has sunk 6 centimeters more to a depth of 12.86 meters. Depth of the ambient seafloor is 13.15 meters, resulting in a percent burial of 38.3%.

The ripples are still visible in the survey of February 6th; however, they do not appear to be as well defined as in the previous survey (Fig. 21). The apparent wavelength of the ripples has increased to ~ 75 centimeters, though ripple height has appeared to remain the same. The scour pit at the southwest end of the mine has grown deeper, with a maximum depth of 13.32 meters. Depth to the top of the mine is 12.84 meters, 2 centimeters shallower than in the previous survey. The degree of tilt has not changed between this survey and the last; however, the 2-centimeter difference is within the uncertainty of the multibeam. Depth of the surrounding seafloor is 13.11 meters, resulting in a percent burial of 42.6%. The mine appears to the south of its original position indicated by the black dashed oval in the center of the image. Data from the orientation sensors within the mine do not indicate that the mine has rolled into its new position, as the roll has only changed by one degree since the last survey. The orientation sensors do not measure cumulative roll, however, so if the mine makes a full rotation the sensor will record no change. The maximum offset between the mine's current and original position is ~ 1.5

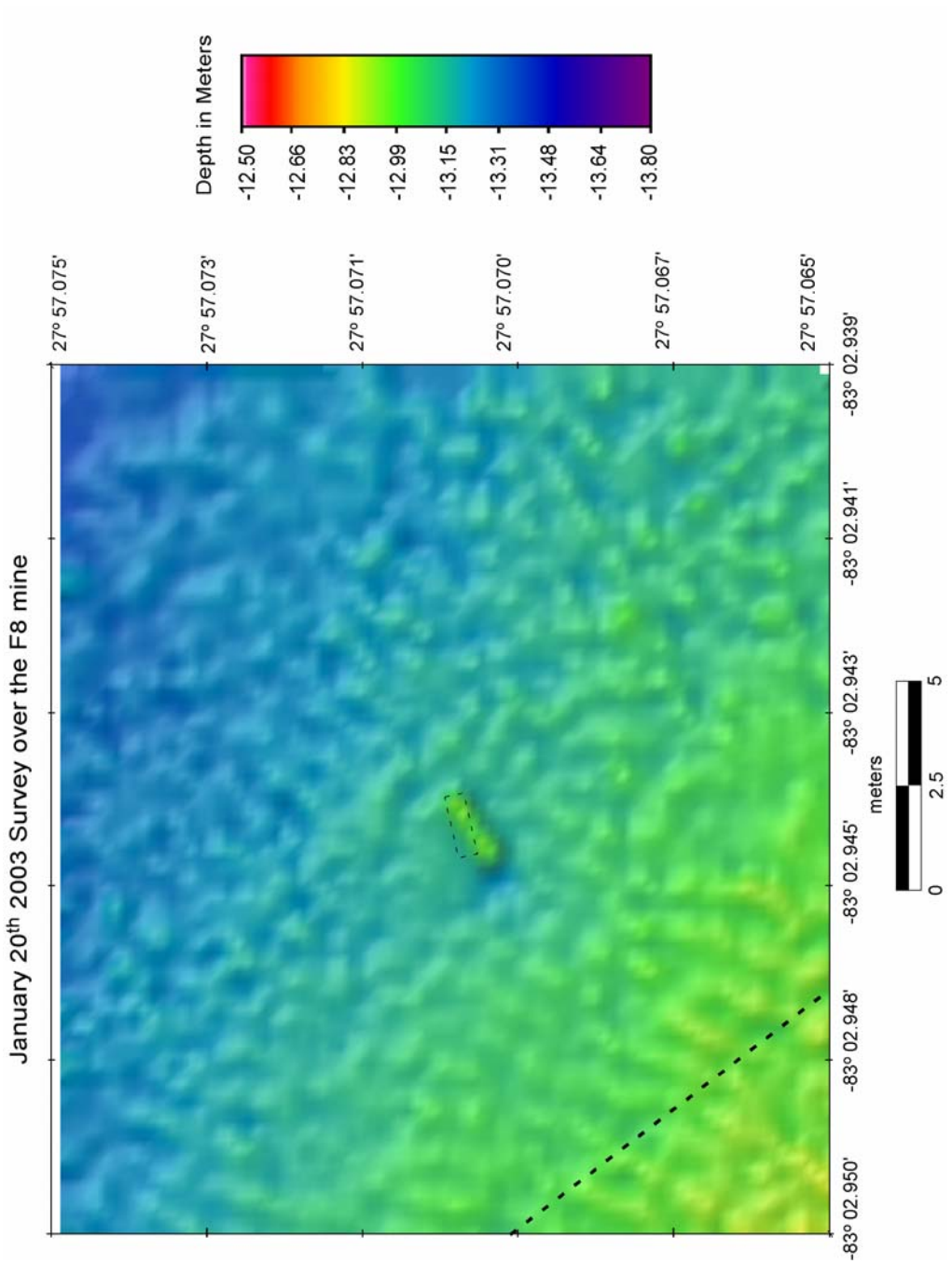

Figure 20. January 20th survey over the F8 mine. Scour is visible at the southwest end of the mine.

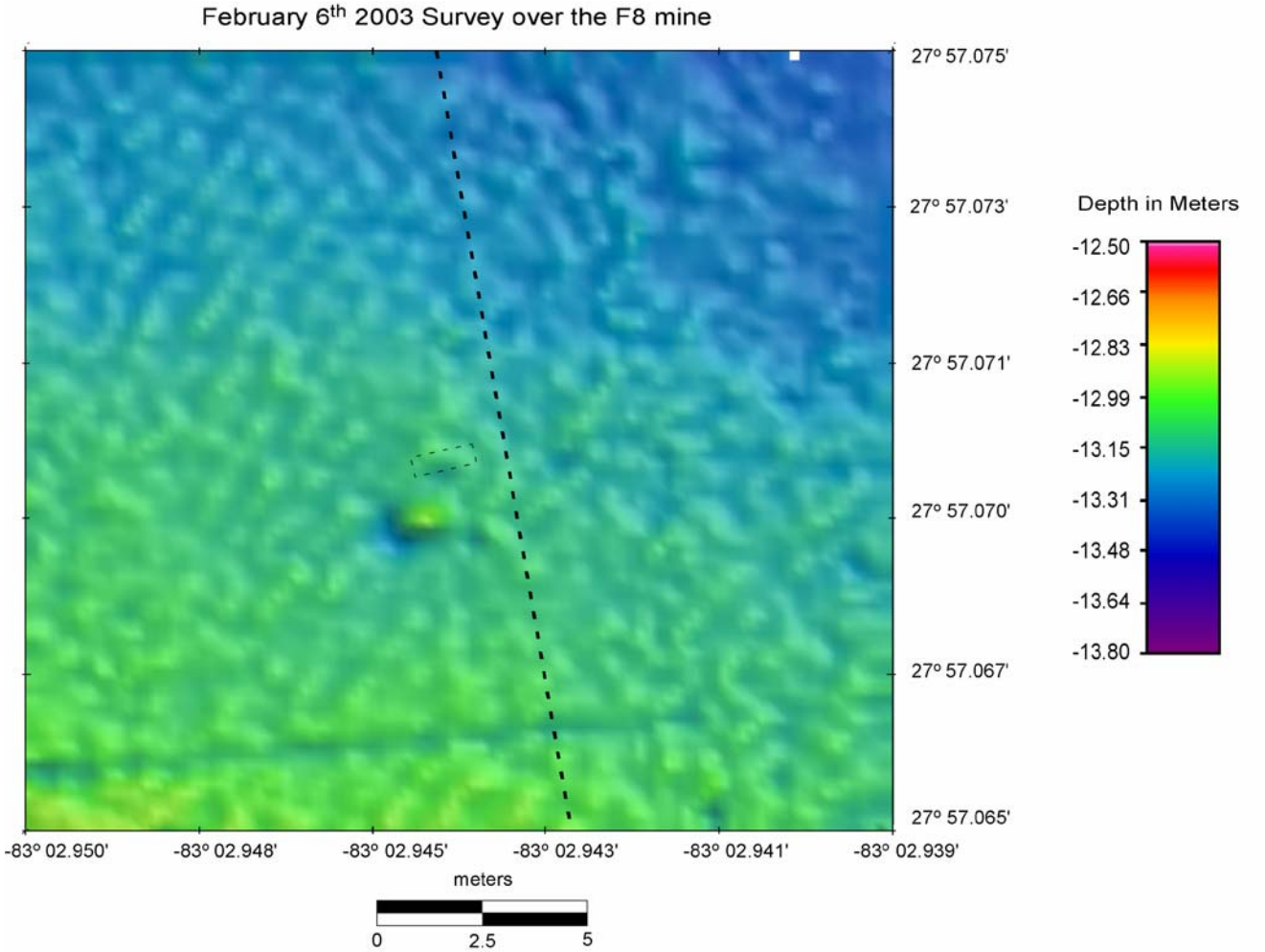

Figure 21. February 6th survey over the F8 mine. The scour pit has developed at the southwest end of the mine. The mine now appears slightly south of its original position as indicated by the faint black dashed oval.

meters; a complete roll of the mine would account for 1.4 meters. Roll measurements within the mine were made every 15 minutes, so if the roll were rapid the sensors would not record it. A storm event moved through the area causing elevated wave heights on January 24th 2003. It is therefore possible that the mine made a rapid and complete rotation at this time. The ability to measure cumulative roll is recommended for future inert mine development in order to record true roll. The multibeam system has a horizontal accuracy of ± 1-meter; however, there are no other offsets observed for the other mines during the same survey, suggesting that a 1-meter offset is likely to be a true southward displacement by some mechanism.

The March 13th survey again shows the mine to the south of its original position by 1.6 meters. This offset is within 10 centimeters of the offset observed in the February 6th image, and strongly supports the notion that this change is unlikely the source of system error and most likely a result of actual change. The mine is nearly flush with the surrounding ripples (Figs. 22 & 23). The ripples appear very well defined, with a wavelength of ~ 1.2 meters and a height of 12 centimeters. The depth to the top of the mine is 12.72 meters with a surrounding seafloor depth of 13.00 meters, resulting in an observed burial of 40.4%. The data seem to suggest an anomalous shallowing of the mine and ambient seafloor depth by 12 centimeters that we do not understand and cannot readily explain. The degree of tilt of the mine has decreased since the February 6th survey, indicating that tilt can not be used to explain part of this anomaly. The combined vertical uncertainty of the multibeam system for both the February 6th and March 13th surveys can account for 10 centimeters of this discrepancy; the remaining 2 centimeters is negligible. Other likely scenarios for the 12-centimeter discrepancy include error in the sound velocity

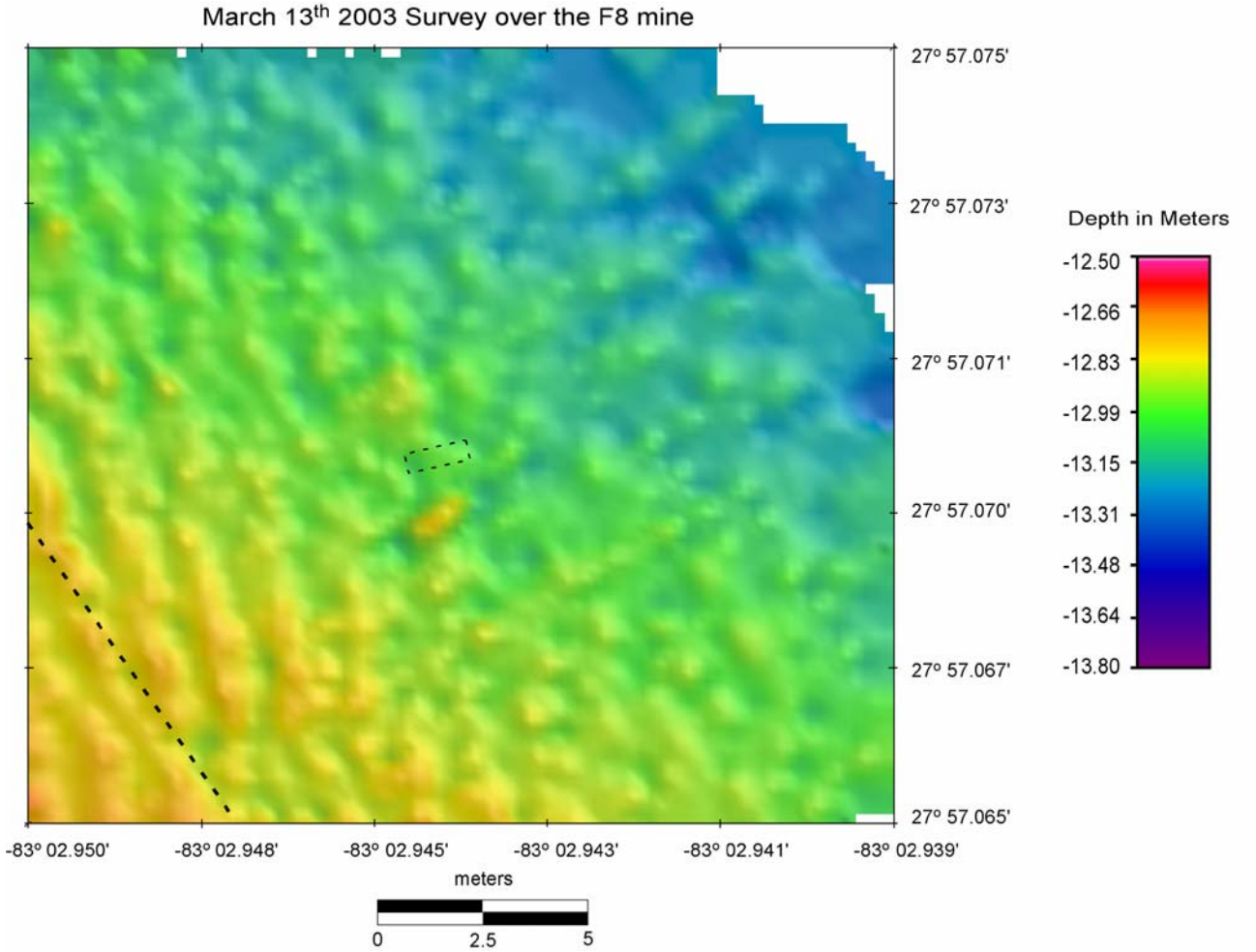

Figure 22. March 13th survey over the F8 mine. Scour is visible at both ends of the mine. There is a clear ripple field trending north-northwest/south-southeast. As in the last image, the mine appears south of its original position.

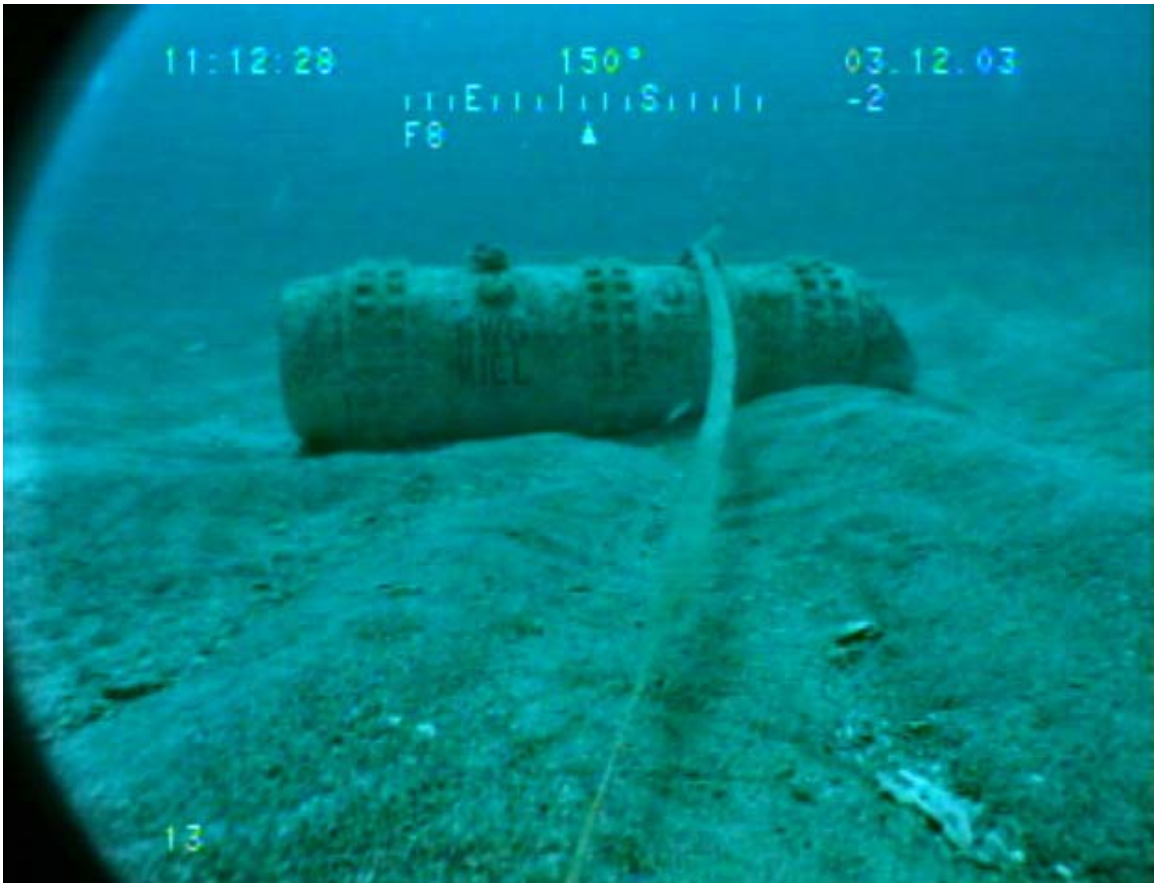

Figure 23. ROV video still image of the F8 mine on March 13, 2003. Camera is facing south-southeast showing a side view of the mine in the ripple field.

profile used by the multibeam system to calculate depth during the survey. The average sound velocity during this survey is 1520.90 meters/second; therefore, it would only take an error of 14.02 meters/second to account for 12 centimeters. It is also possible that an error exists in the tide record used to correct the data during processing, or that there is a greater vertical uncertainty in the multibeam system. Of these possibilities, we suspect that changes in the sound velocity profile is the most likely reason for error, because the tide record and multibeam system have worked quite well elsewhere, and it is common to have changes in sound velocity in coastal settings.

Between the January 13th survey and the survey of February 6th, the mine sank a total of 12 centimeters and became 42.6% buried (Table 2; Fig. 24). An anomalous shallowing during the March 13th survey resulted in the mine having the same depth at both the beginning and end of the experiment. The average depth of the seafloor decreased by 0.20 meters over the course of the experiment indicating localized deposition in the area. As a result of this deposition, there was an observed burial for the March 13th survey of 40.4%.

Comparison of F8 Multibeam Observations to the VIMS 2D Burial Model

The model was initialized with a local water depth of 13.20 meters (obtained from the January 13th survey) and a 0% burial for comparison with the F8 mine observations. SCUBA divers sent down shortly after deployment checked the status of the mine, but they did not reposition it. The model start time was set at January 11th, 2003 at 2300 GMT, the time of mine deployment, and was run until March 13th, 2003 at 1000 GMT, the time of the last multibeam survey over the mine (Table 2).

	Jan. 11	Jan. 13	Jan. 17	Jan. 20	Feb. 6	Mar. 13
Depth of Mine	———	12.72	12.80	12.86	12.84	12.72
Cumulative Amount of Change	———	———	0.08	0.14	0.12	0.00
Average Depth of Seafloor	———	13.20	13.17	13.15	13.11	13.00
Cumulative Amount of Change	———	———	-0.03	-0.05	-0.09	-0.20
Scour Visible / Depth of Scour	———	no	no	yes 13.27	yes 13.32	yes 13.11
% Mine Burial from Multibeam (± 10.6% due to 5 cm uncertainty of sonar)	0	0	21.3	38.3	42.6	40.4
% Mine Burial from Model	0	0	0	47.4	75.5	92.5
Mine Pitch (degrees)	0	0	0	-2	-2	-1
Mine Roll (degrees)	-12	-11	-8	-1	0	0

Table 2. Data table for the F8 mine. All numbers are in meters except where noted. There is no multibeam survey on January 11th.

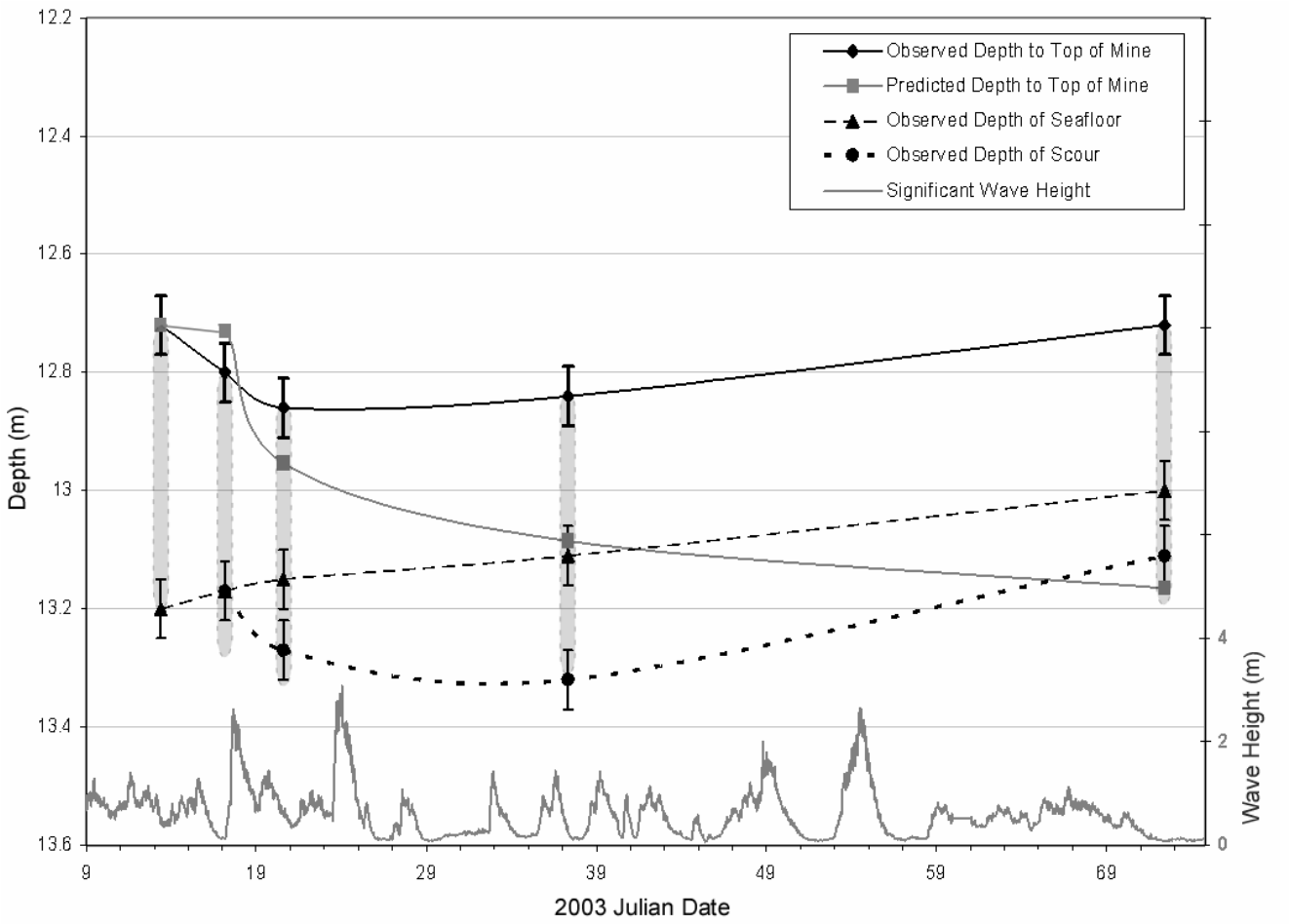

Figure 16. Comparison of multibeam observed (black) and predicted (gray) mine depth for the F8 mine over the course of the experiment. Predicted percent burial of the mine was converted to predicted depth of the mine using the 13.20-meter water depth used to initialize the model. Observed depth of seafloor and depth of scour from the multibeam are plotted as well. Significant wave height is plotted on the right y-axis. Error bars represent the 5-centimeter uncertainty inherent in the multibeam system. The light gray oval represents the F8 mine, and is scaled to the actual dimensions of the mine (length ~ 0.47 m, the diameter of the mine).

The first comparison between the model and the observed data occurs on January 13th (Figs. 24 & 25). Both the model and the observed data show a 0% burial of the mine. There is no tilt of the mine at the time of this survey, indicating that the mine is sitting completely flat on the seafloor. The model continues to predict a 0% burial for the January 17th comparison, resulting in a discrepancy of 21.3% with the observed burial. The degree of tilt is still zero at this time, so no correction factor can be applied to the observed values. The 5-centimeter vertical uncertainty of the multibeam equates to 10.6% burial of the F8 mine; however, this still leaves a discrepancy of 10.7%.

The January 20th comparison shows an observed burial of 38.3% versus a predicted burial of 47.4% (Figs. 24 & 25). The discrepancy of 9.1% falls within the measurement uncertainty of the multibeam. The mine has a -2° tilt at the time of this survey; applying a correction factor to the observed value of mine burial adds 3 centimeters of burial, resulting in a 43.9% total burial. This reduces the discrepancy between the predicted and observed values to 3.5%.

The model predicts a 75.5% burial of the mine for February 6th, but the observed value is only 42.6%, an offset of 32.9% (Figs. 24 & 25). The mine continues to have a 2° tilt at this time; however, this can only account for 3.5% of the difference. The greatest discrepancy between the model and the observations occurs during the March 13th comparison. The observed data show a 40.4% burial of the mine compared with a predicted value of 92.5%, resulting in a 52.1% offset. There is -1° tilt of the mine at this time, which would add 1 centimeter of burial and decrease the offset to 50%. The 5- centimeter vertical uncertainty of the multibeam system can further reduce this discrepancy by another 10.4%.

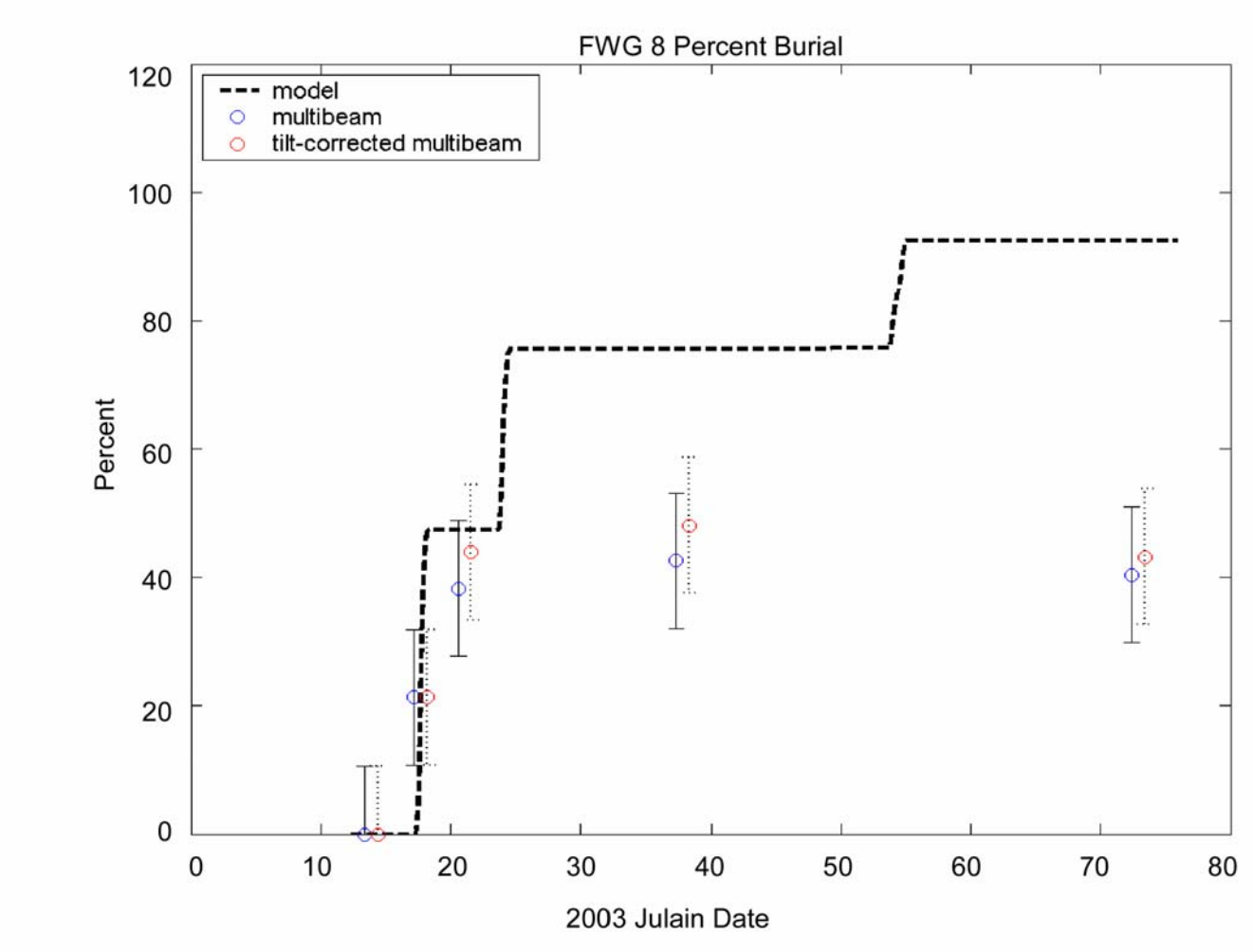

Figure 25. Comparison of the predicted (dashed), observed (blue), and tilt-corrected observed (red) percent burial for the F8 mine over the course of the experiment. Tilt-corrected values have been horizontally offset for clarity. Error bars represent the 5-centimeter uncertainty inherent in the multibeam system.

The anomalous 12-centimeter shallowing of the mine apparent at the time of this survey would account for another 25.5%. Combining these corrections still leaves a discrepancy of 14.5% between the predicted and observed values of mine burial.

Discussion of the F8 Comparisons

The VIMS 2D Burial Model is compared with five repeat high-resolution multibeam observations over the F8 mine. Over the course of the experiment, the mine becomes ~ 40.4% buried. Direct comparison between these observations and the VIMS 2D Burial Model indicates the model does not work well in areas of coarse sand (Fig. 25). The trend throughout the experiment shows the modeled predictions are consistently higher than the actual observed values. Applying a tilt correction and taking the uncertainty of the multibeam into consideration cannot account for the discrepancies. This indicates that some other factor must be affecting mine burial that is not accounted for in the model, such as the presence of rippled bedforms near the mine. This is issue is currently being addressed by the modelers (Trembanis et al., 2005).

Conclusions

High-resolution multibeam bathymetry data are useful to successfully document burial of inert mines over time at both a fine sand and a coarse sand site off Clearwater, Florida. While the amount of observed burial by subsidence was significant in the fine sand site (96.2 %), the mine remained uncovered by sediment. This has been shown to actually increase the likelihood of detection using side-scan sonars as a result of the larger scour pit that forms around the mine. The VIMS 2D burial model was compared with in situ

multibeam observations of mine burial at both sites. The model works well in the fine-sand case, staying consistently within the measurement uncertainty of the multibeam system. It does not work so well in the coarse sand analysis, where initial comparisons are good but quickly diverge throughout the rest of the experiment. Possible sources of error are that the model uses one water depth. This assumes the local water depth does not change over the course of the experiment; however, localized erosion and accretion has been observed at both study sites. The presence of rippled bedforms at the coarse sand site is also observed during the experiment. These ripples directly affect morphodynamics of the seafloor and thus can affect rates of mine burial. Currently, the addition of a bedform correction to the model is being explored by the modelers.

Chapter 3

Multibeam Observations and Model Comparison of the Remaining Mines

Introduction

The following mine analyses were completed using the same methodology as described in the previous chapter. There were five remaining mines in the shallow fine sand site, one in the coarse sand site, and two mines in a deep fine sand site (~ 14 meters relative to MLLW) (Figs. 26 & 27). As described in the previous chapter, all multibeam data were cleaned and processed using CARIS HIPS and SIPS 5.3 (see chapter 2 for a detailed description on). All images are 18-by-18 meter grids centered on the mine at a horizontal resolution of 0.20 meters and referenced to MLLW. Final imaging, including 3D rendering and artificial sun illumination, was completed using IVS Fledermaus 6.0. Artificial sun illumination is from the northeast (045°) and at an angle of 45 degrees above horizontal. Since the analyses of the A3 and F8 mines showed that tilt correction made little difference in mine burial, and given that tilt of the mine will not be available during actual field applications, it was not included in the following analyses.

The A1 Mine

Temporal Analysis of Scour and Burial

The acoustic instrumented mine 1 (A1) was deployed on January 8th, 2003 in the shallow fine sand site at a water depth of 12.77 meters, and was oriented north-south. The

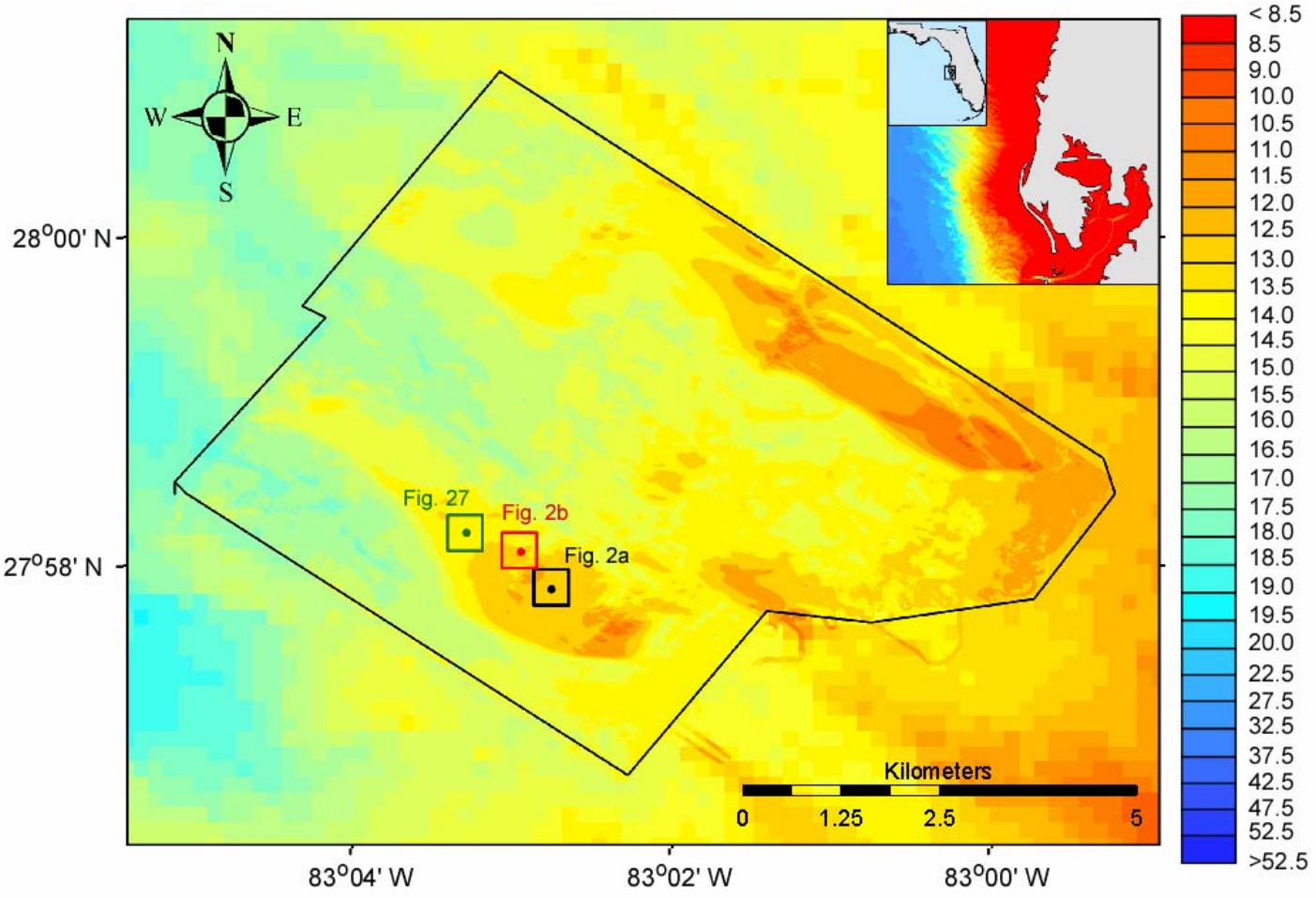

Figure 26. Location of the deep fine sand study site. Study site is represented by the green dot in the middle of the green square. All depths are referenced to MLLW.

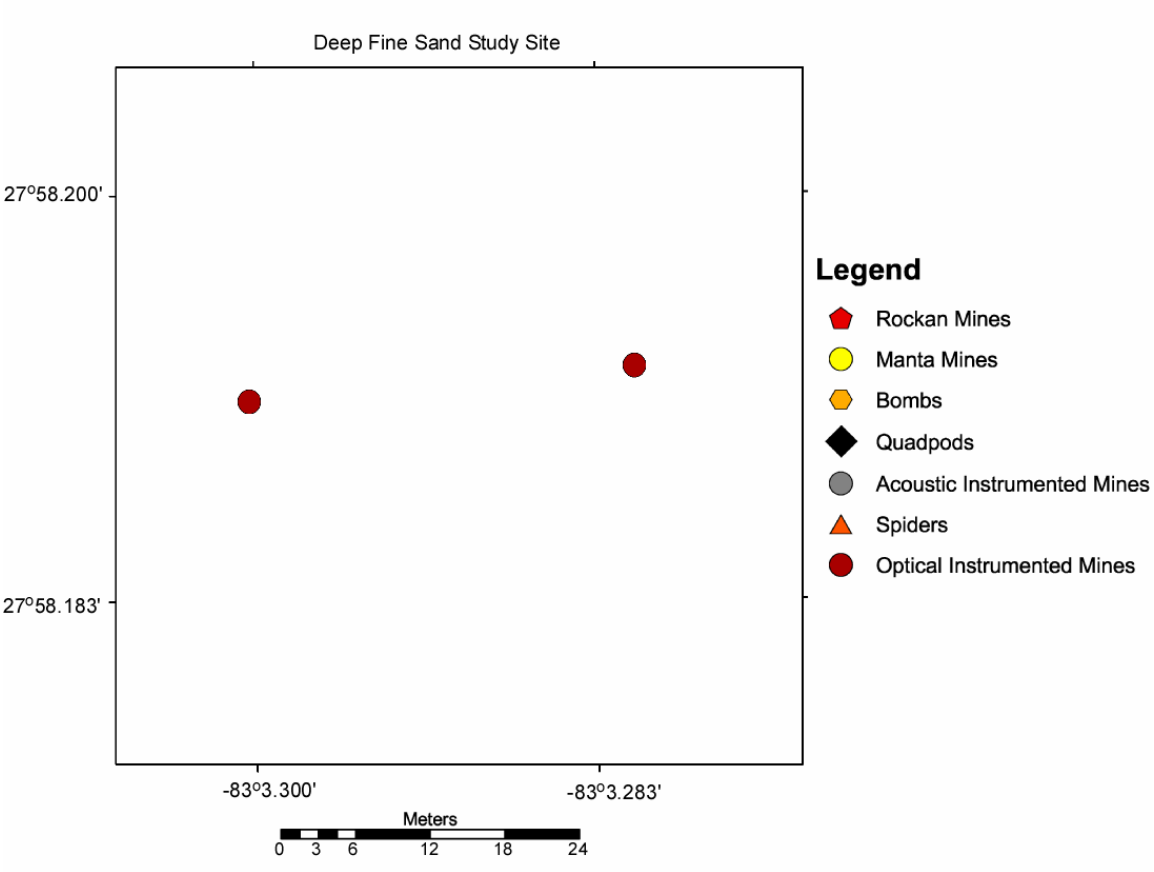

Figure 27. Location of deployed equipment in the deep fine sand site.

survey on January 10th was the first to image the mine after its deployment (Fig. 28). The depth of the mine is 12.20 meters with an ambient seafloor depth of 12.77 meters. This implies that the mine is just resting on the seafloor and scour has not yet begun to form. The mine appears to have a northwest-southeast orientation; however, data from the mine itself indicates more straight north-south orientation (-2.9°). The multibeam system was set on target detection during this survey and may explain the discrepancy in orientation.

The mine orientation appears more north-south in the January 13th survey, although the mine itself is somewhat blurred (Fig. 29). Target detection was still on during this survey as well, which may account for this. The mine has sunk 0.19 meters, to a depth of 12.39 meters, since January 10th. Localized erosion around the mine has caused the ambient seafloor depth to drop to 12.91 meters, resulting in a 1.8% burial. There is no scour evident around the mine.

The ambient seafloor depth stays relatively constant between the survey of January 13th and that of January 17th, 12.90 meters and 12.91 meters respectively, and no scour is evident. The mine does not show up well in this survey, and appears as two separate bumps in the image (Fig. 30). It is possible that a bubble sweep occurred causing interference with the beams. The depth to the top of the mine is now 12.52 meters, 0.13 meters deeper than in the previous survey, resulting in an observed burial of 28.3%.

During the time between the January 17th and January 20th surveys, two distinct scour pits have formed at the north and south ends of the mine, despite an overall localized deposition around the mine of 0.12 meters (Fig. 31). The maximum depth measured in the scour pits is 13.15 meters, and the ambient seafloor depth is now 12.82

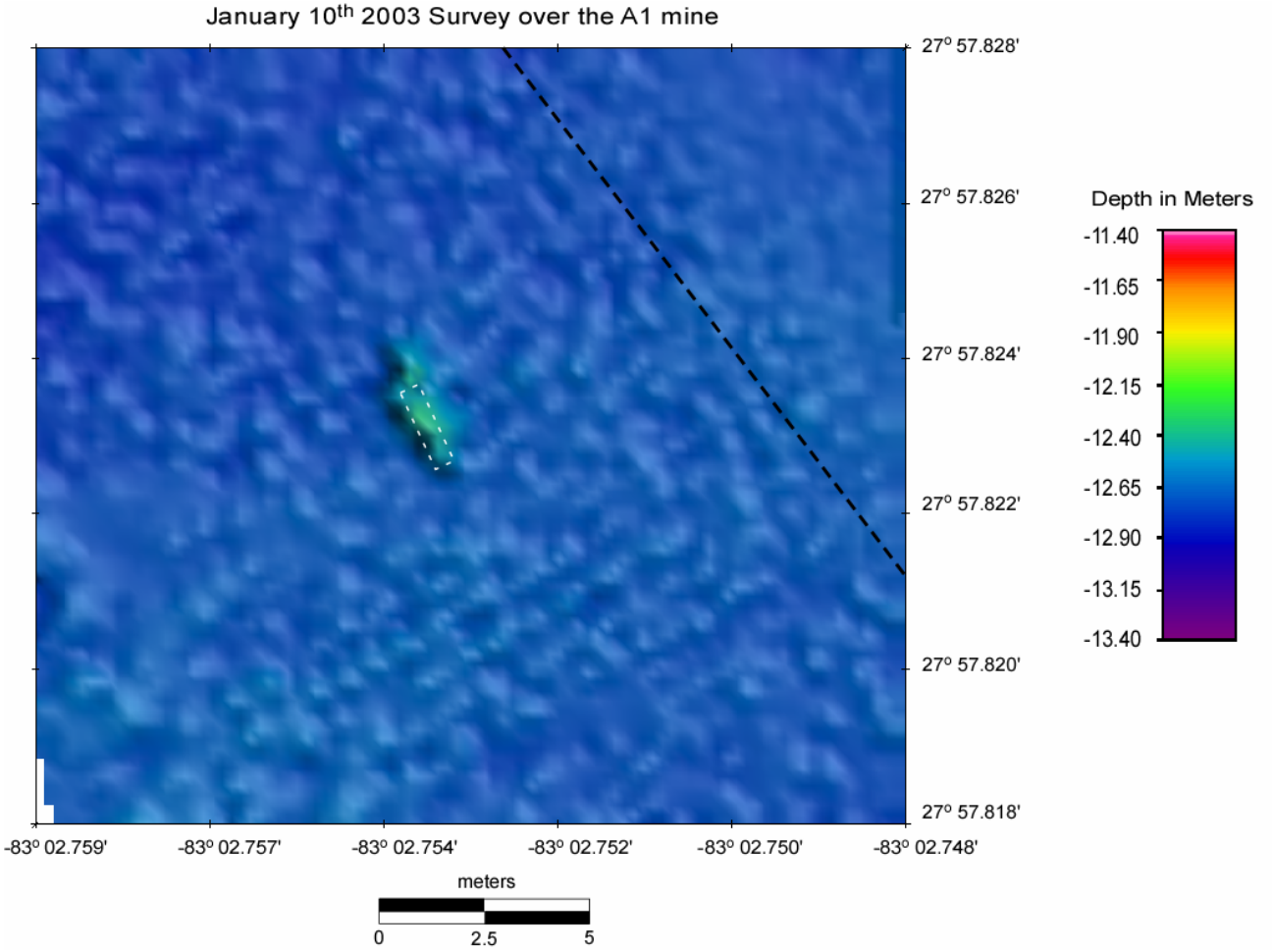

Figure 28. January 10th survey over the A1 mine. In all multibeam images, the black dashed line represents the ship's track line during the survey. The mine is outlined with a faint white line scaled to the mine's actual dimensions. The mine outline remains at the same orientation throughout the A1 multibeam images as a reference.

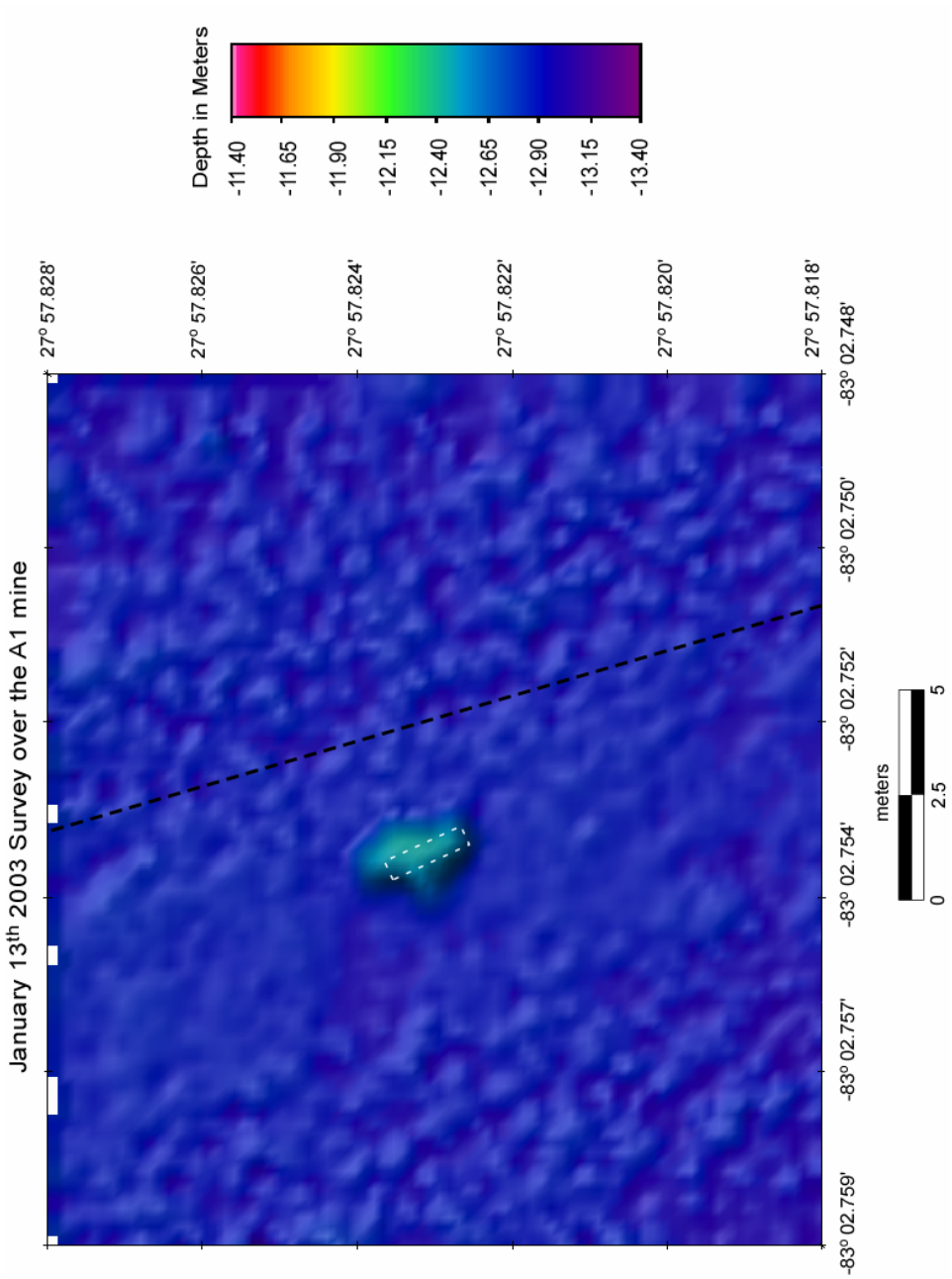

Figure 29. January 13th survey over the A1 mine.

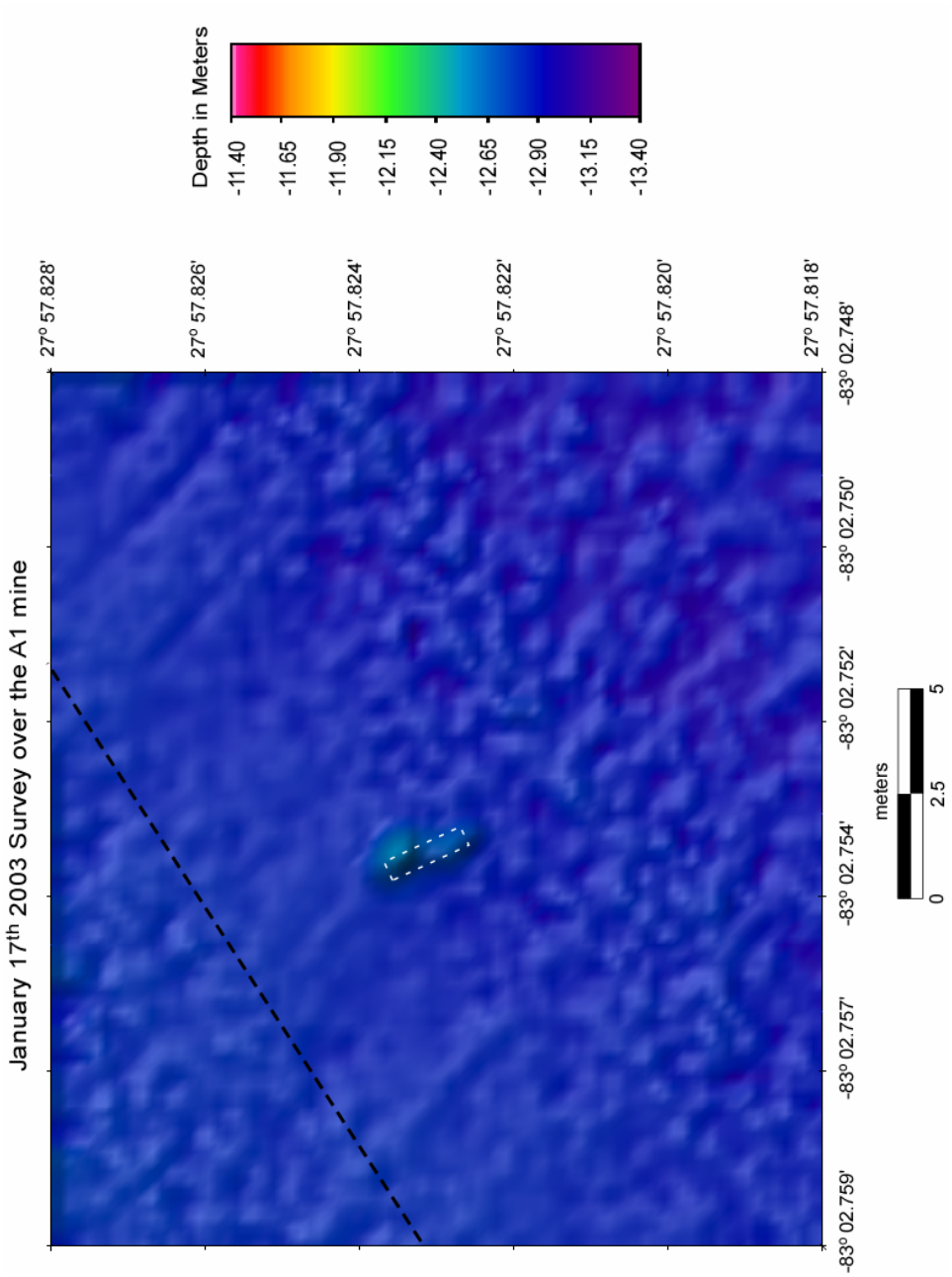

Figure 30. January 17th survey over the A1 mine.

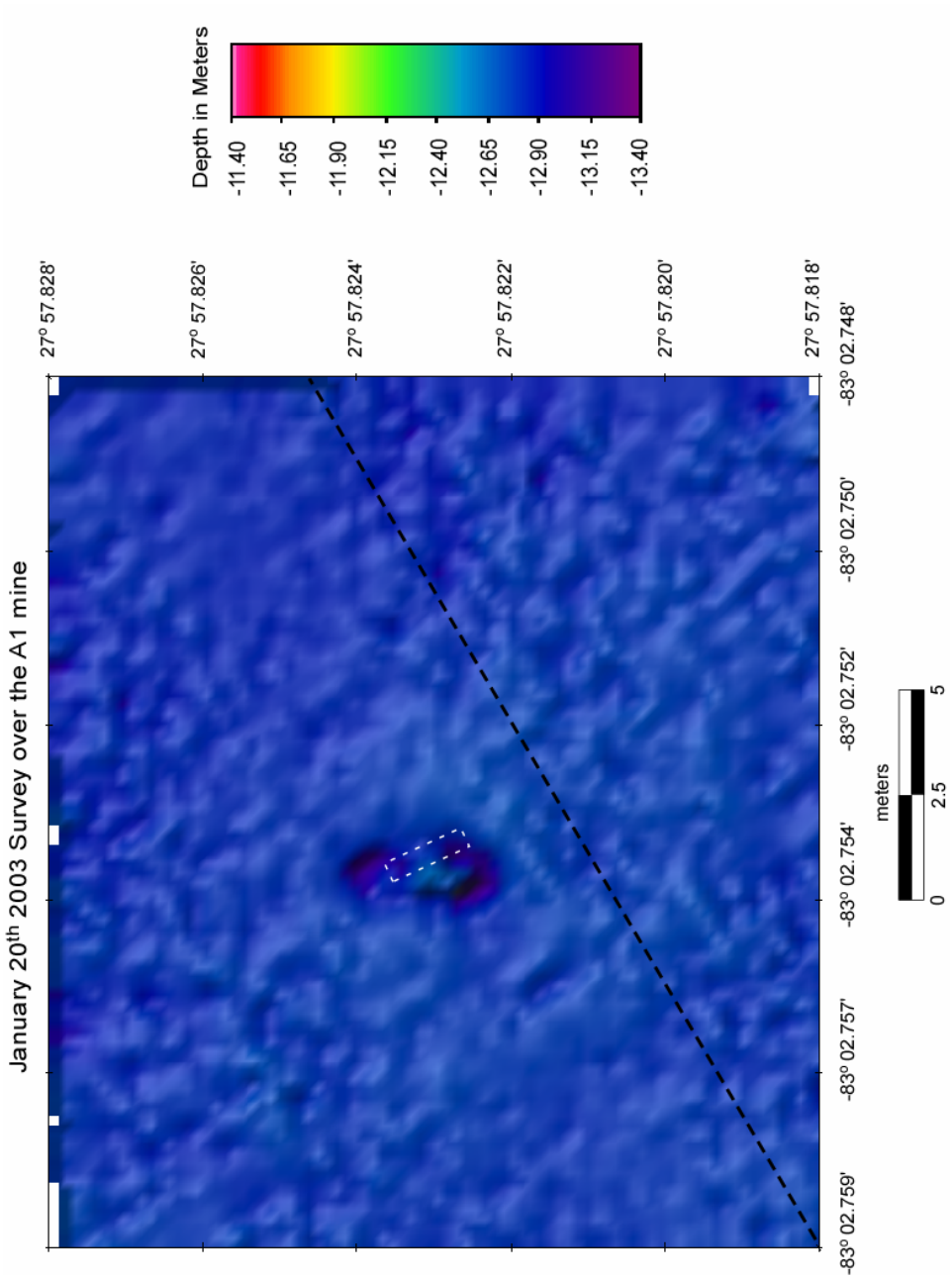

Figure 31. January 20th survey over the A1 mine.

meters. A storm event passing through the area on January 17th caused increased wave heights (peaking at ~ 2.34 meters at 4 pm GMT) and can account for the rapid scour development. The mine is at a depth of 12.65 meters, a sinking of 0.13 meters since the 13th, and is 67.9% buried. The observed orientation of the mine is north-south and agrees with the data from the sensor within the mine (-0.3°).

In the image from the February 6th survey, the mine is only visible due to the defining ring of scour (Fig. 32). The depth to the top of the mine and the depth of the surrounding seafloor are 12.88 and 12.90 meters respectively, a difference of only 0.02 meters resulting in a 96.2% burial. The greatest amount of scour occurs at the southern end of the mine, where the maximum depth within the pit reaches 13.33 meters.

During the March 13th survey, the mine lays just within the inner beams of the multibeam swath (Fig.33). The wavy pattern to the west of the mine is caused by the outer beams of the sonar hitting the seafloor at greater grazing angles. Data interpolation in CARIS was used to patch data holes. The mine depth is 12.80 meters, 0.08 meters shallower than the February 6th survey. This discrepancy can be accounted for by the vertical uncertainty of the multibeam system for both the February 6th and March 13th surveys, which combines to 0.10 centimeters. Other possible explanations include possible changes in the sound velocity profile in the water column versus that used by the multibeam system during data collection to calculate depth. For a more detailed discussion of these possibilities, please refer to the discussion of the temporal observations of scour and burial of the F8 mine in chapter 2 of this thesis. The depth of the ambient seafloor during this survey is 12.81 meters, 0.09 meters shallower than in the previous survey. It is not clear whether this difference is related to the shallowing of the

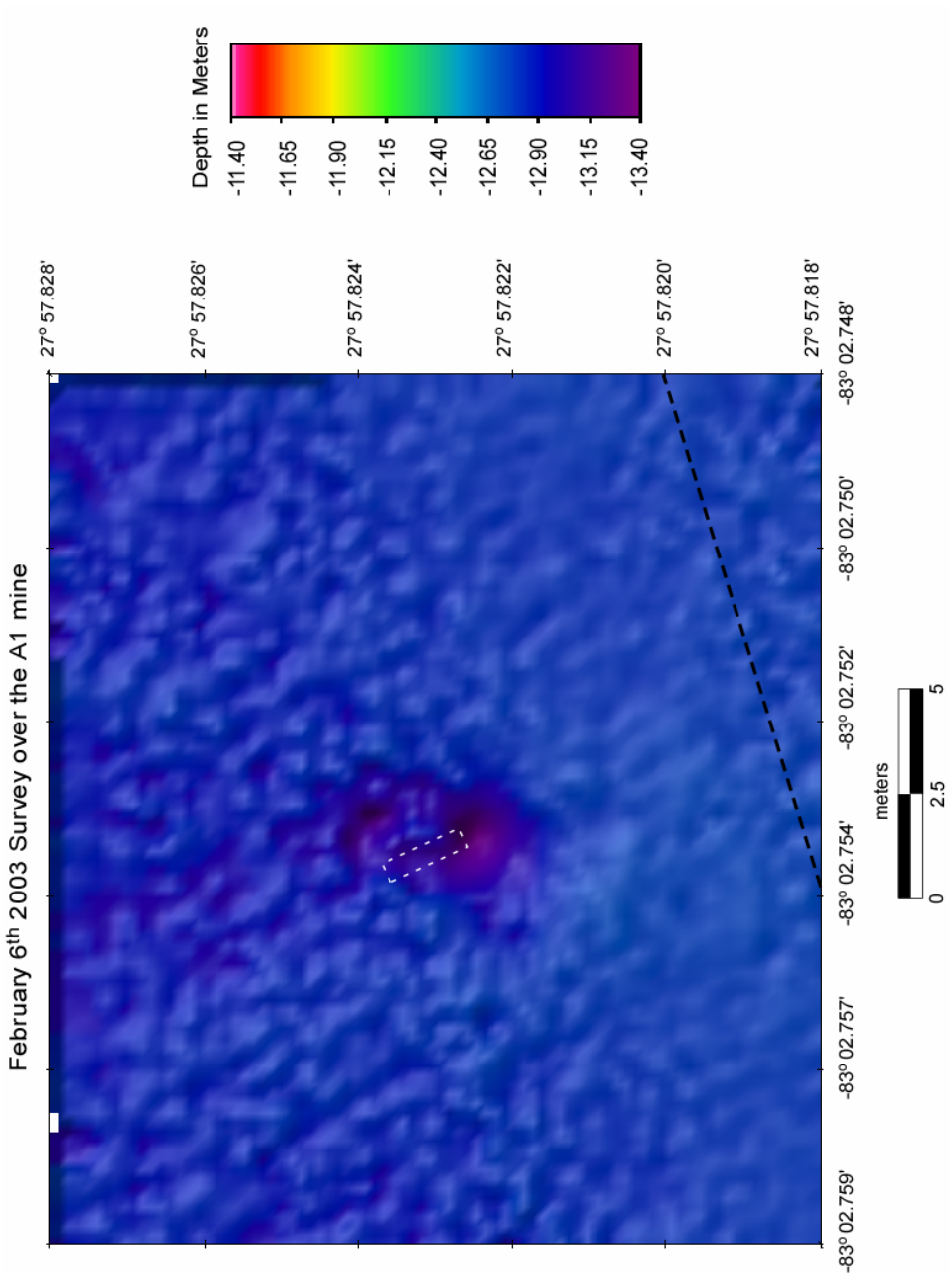

Figure 32. February 6th survey over the A1 mine.

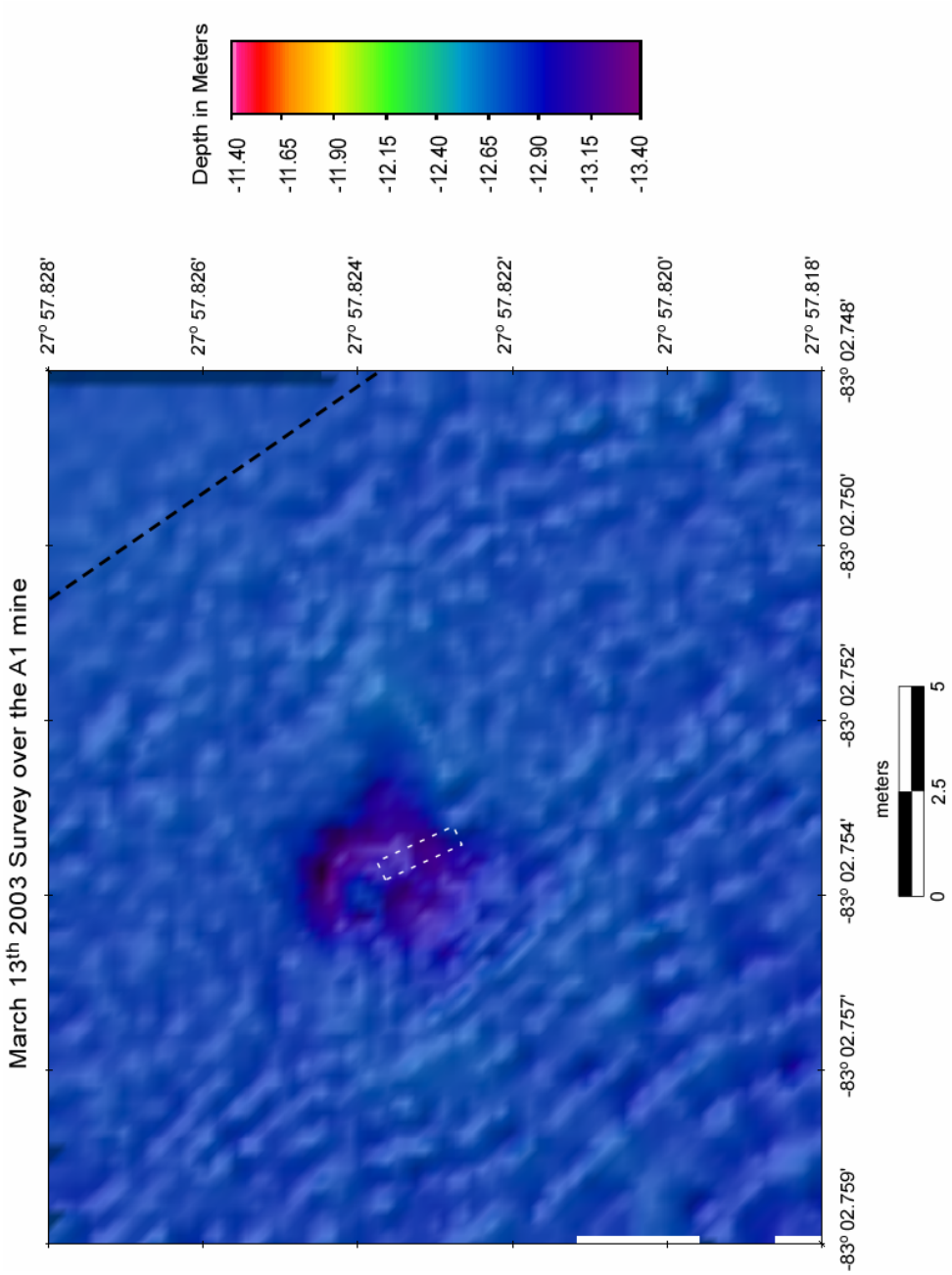

Figure 33. March 13th survey over the A1 mine.

mine, or whether it represents actual localized deposition around the mine. The observed burial of the A1 mine based off a mine depth of 12.80 meters and an ambient seafloor depth of 12.81 meters is 98.1% (Fig. 34).

In total, the mine sank 0.68 meters between the January 10th and February 6th surveys (Table 3; Fig. 35). An apparent shallowing of the mine in the March 13th survey reduced this total to 0.60 meters. Over the course of the experiment the average depth of the seafloor surrounding the mine increased by a total of 0.04 meters. Scour became evident around the mine during the January 20th survey and developed into a pit 0.59 meters deeper than the ambient seabed by March 13th. The final observed burial for the A1 mine was 98.1%.

Comparison of A1 Multibeam Observations to the VIMS 2D Burial Model

The VIMS 2D burial model was initialized with a local water depth of 12.77 meters (obtained from the January 10th survey over the mine) and 0% burial. The model was run from the time of mine reposition, January 8th 2003 1600 GMT, to the time of the last multibeam survey over the mine, March 13th 2003 at 0300 GMT. The first direct comparison between the observed and predicted burial occurs for the January 10th survey (Figs. 35 & 36). The multibeam data indicate the mine is resting on the seabed and is not buried at all. The model; however, predicts a burial of 15.3% at this time. The multibeam sonar has an inherent uncertainty of ± 5 centimeters in its vertical accuracy, which corresponds to a percent burial of 9.4. The discrepancy is 15.3% between the model and the multibeam observations, so the model does not fall within the range of multibeam values.

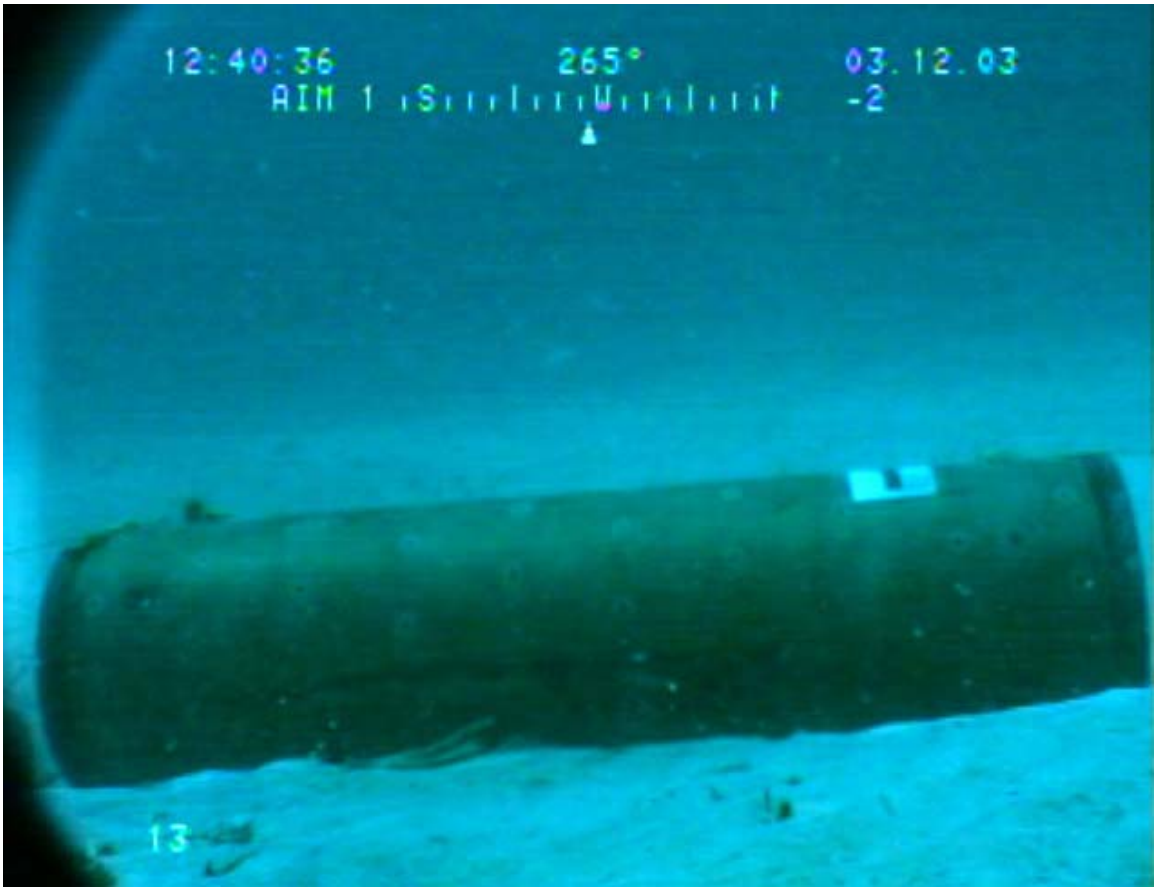

Figure 34. ROV video still image of the A1 mine on March 13, 2003.

	Jan. 8*	Jan. 10	Jan. 13	Jan. 17	Jan. 20	Feb. 6	Mar. 13
Depth of Mine	_____	12.20	12.39	12.52	12.65	12.88	12.80
Cumulative Amount of Change	_____	_____	0.19	0.32	0.45	0.68	0.60
Average Depth of Seafloor	_____	12.77	12.91	12.90	12.82	12.90	12.81
Cumulative Amount of Change	_____	_____	0.14	0.13	0.05	0.13	0.04
Scour Visible / Depth of Scour	_____	no	no	no	yes 13.15	yes 13.33	yes 13.39
% Mine Burial from Multibeam (± 9.4% due to 5 cm uncertainty of sonar)	0	0	1.8	28.3	67.9	96.2	98.1
% Mine Burial from Model	0	15.3	18.1	18.1	60.5	81.6	98.0
Mine Heading (degrees)	-2.9	-2.1	-1.9	-1.8	-0.3	0.7	1.1
Mine Pitch (degrees)	-0.2	-0.3	1.0	0.7	0.6	0.6	0.8
Mine Roll (degrees)	4.8	1.3	-1.3	-1.3	-5.8	-23.4	-32.5

Table 3. Data table for the A1 mine. All numbers are in meters except where noted. There is no multibeam survey on January 8th.

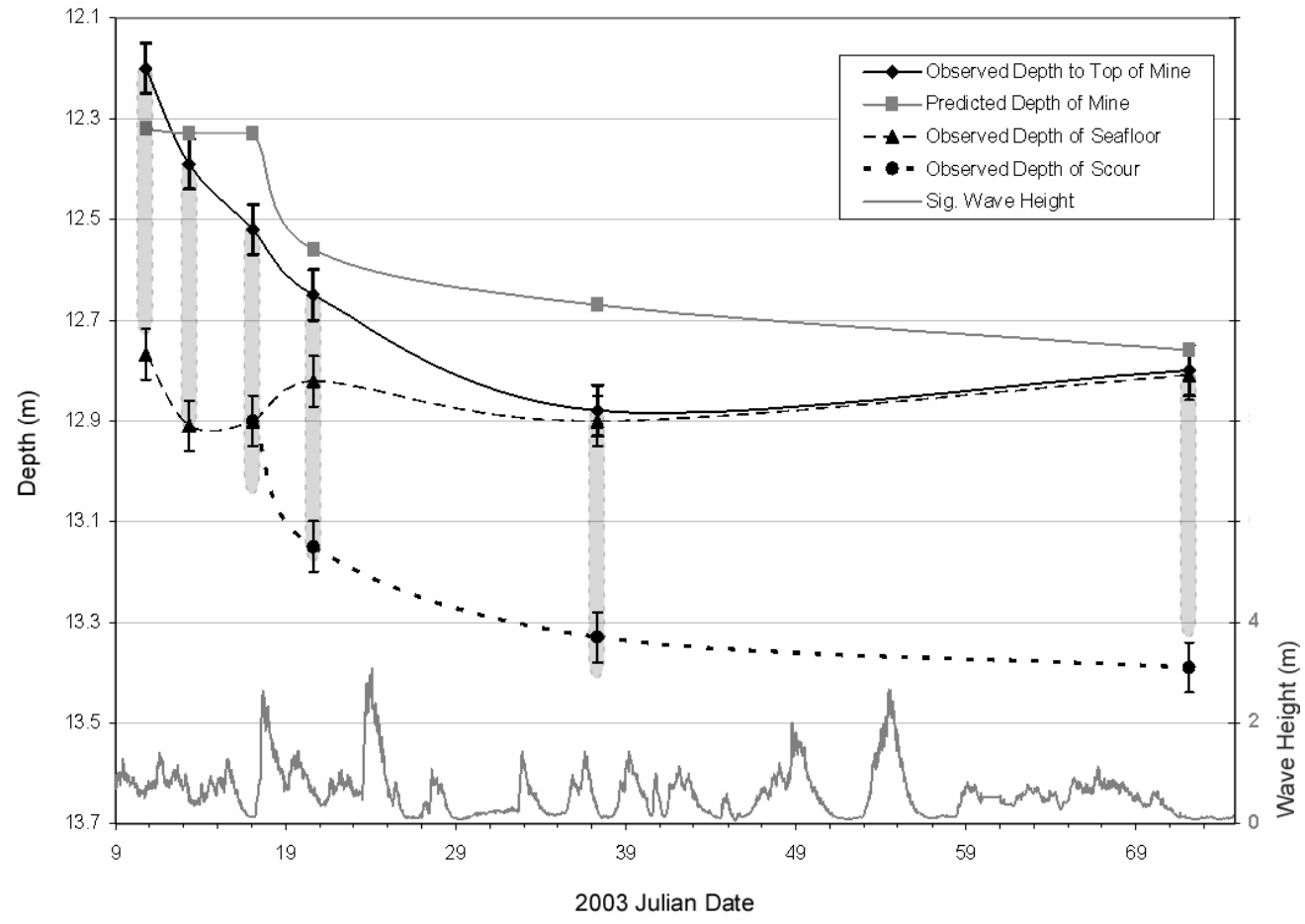

Figure 35. Comparison of multibeam observed (black) and predicted (gray) mine depth for the A1 mine over the course of the experiment. Predicted percent burial of the mine was converted to predicted depth of the mine using the 12.77-meter water depth used to initialize the model. Observed depth of seafloor and depth of scour from the multibeam are plotted as well. Significant wave height is plotted on the right y-axis. Error bars represent the 5-centimeter uncertainty inherent in the multibeam system. The light gray oval represents the A1 mine, and is scaled to the actual dimensions of the mine (length ~ 0.53 m, the diameter of the mine).

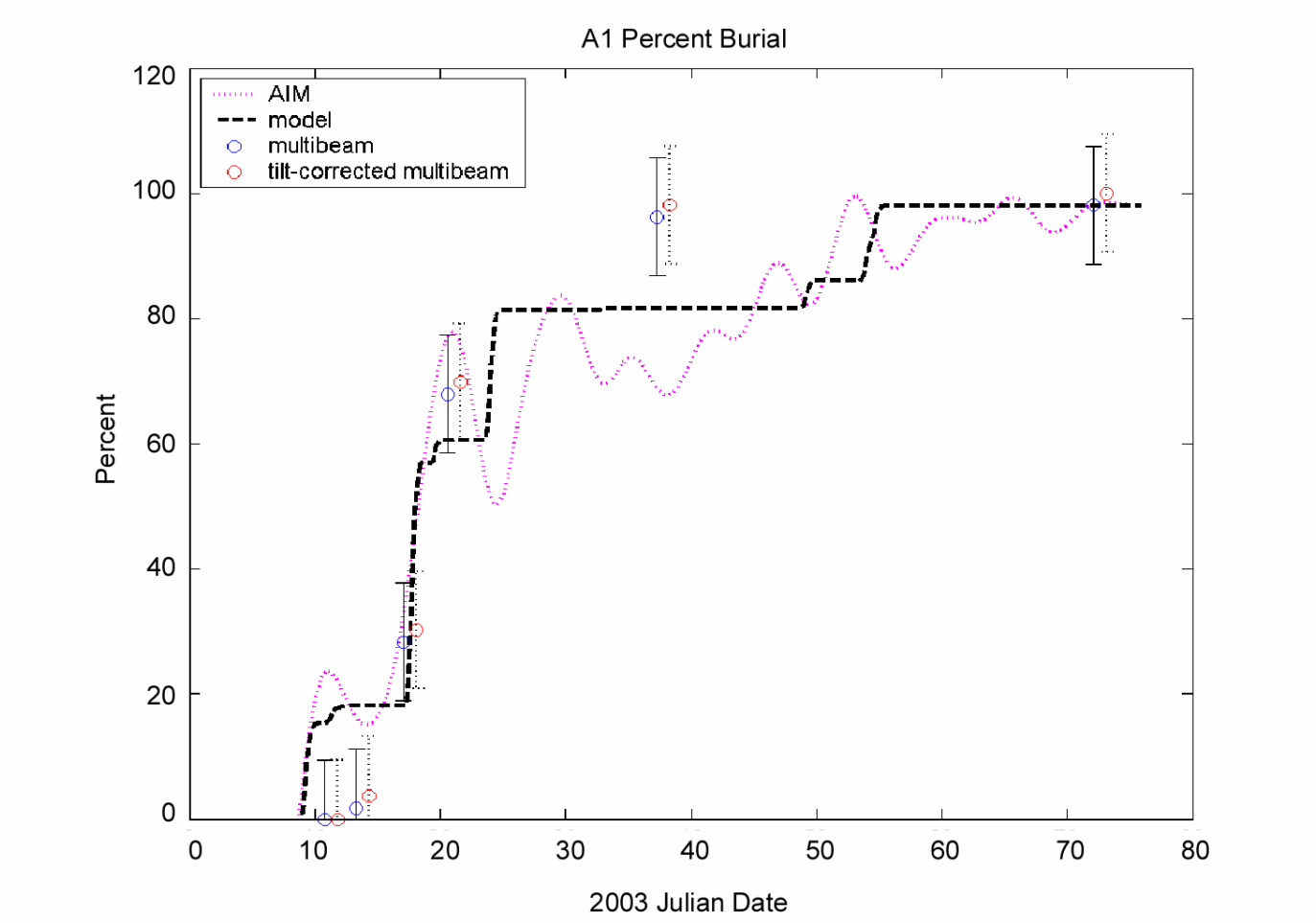

Figure 36. Comparison of the mine (magenta), predicted (dashed), observed (blue), and tilt-corrected observed (red) percent burial for the A1 mine over the course of the experiment. Tilt-corrected values have been horizontally offset for clarity. Error bars represent the 5-centimeter uncertainty inherent in the multibeam system.

The model predictions from January 13th and January 17th do not fall with the range of the multibeam data either (Figs. 35 & 36). The predicted value of mine burial for both the January 13th and January 20th comparisons is 18.1%, whereas the observed burial for both surveys is 1.8% and 28.3%, respectively. The model performs better during the January 20th evaluation, predicting a burial of 60.5% compared to an observed value of 67.9%, and falls within the range of multibeam values.

The model underestimates the amount of burial during the February 6th comparison, and is once again outside the range of multibeam values (Figs. 35 & 36). Observed burial during this survey is 96.2%; however, the predicted burial is only 81.6%, a difference of 14.6%. The March 13th comparison is the final test of the model for the A1 mine. The model prediction and observed value are nearly identical, with a predicted burial of 98.0% and an observed value of 98.1%.

The A2 Mine

Temporal Analysis of Scour and Burial

The acoustic instrumented mine 2 (A2) was deployed in the shallow fine sand site on January 8th, 2003 at a water depth of 12.87 meters in an east-west orientation. The observed depth of mine during the first survey on January 10th is 12.40 meters (Fig. 37). The depth of the ambient seafloor is 12.87 meters, resulting in an observed burial of 11.3%. The mine appears quite blurred in this image, presumably, because the beam mode was set to target detection on the multibeam system (which later was discovered to widen the beams and blur the image). The orientation of the mine appears to be east-west in the image, although this is difficult to determine due to the distortion of the mine. The

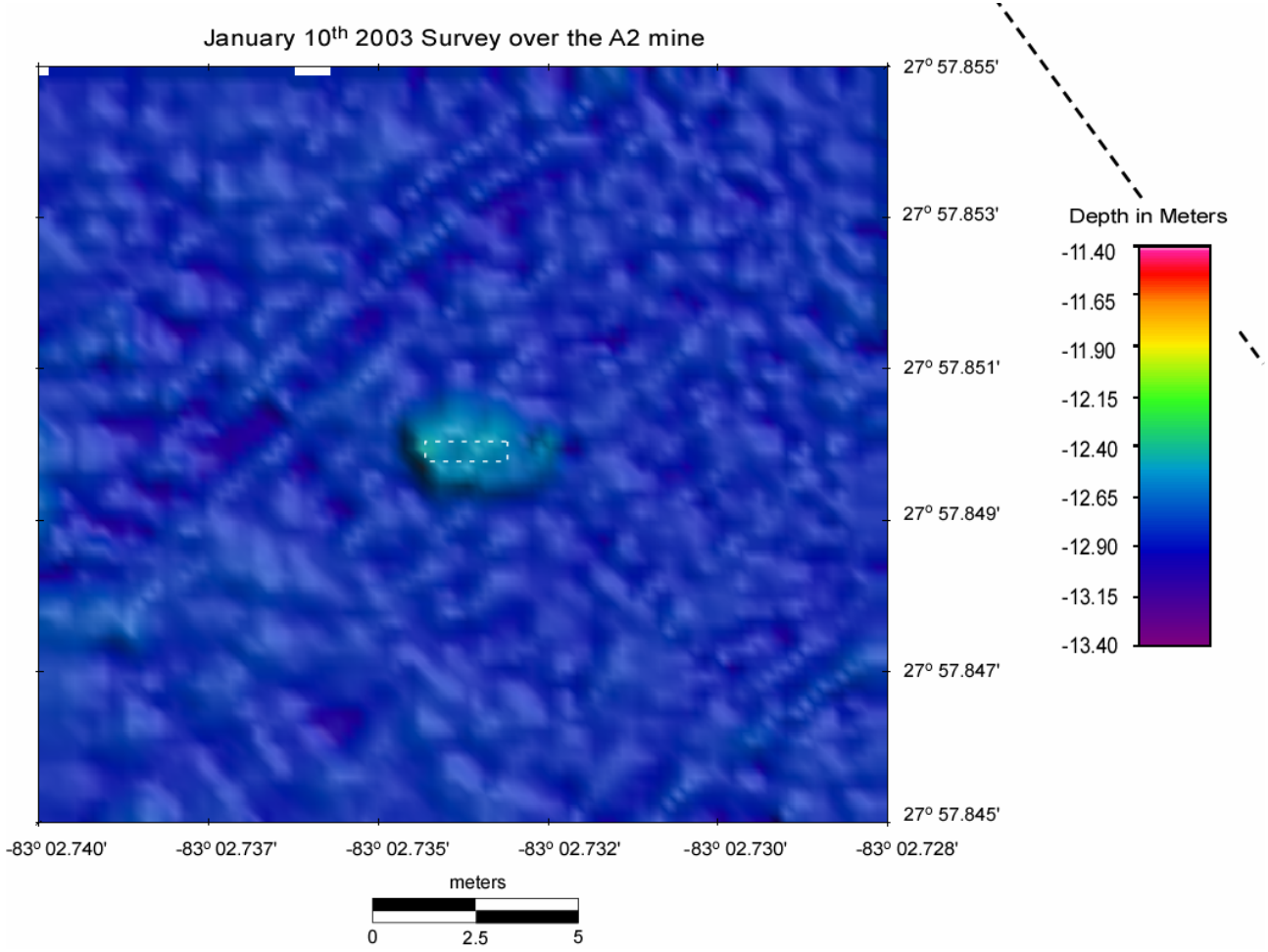

Figure 37. January 10th survey over the A2 mine. In all multibeam images, the black dashed line represents the ship's track line during the survey. In this image, the track line is outside of the gridded area. The mine is outlined with a faint white line scaled to the mine's actual dimensions. The mine outline remains at the same orientation throughout the A2 multibeam images as a reference.

orientation sensor within the mine indicates that the mine should have a more eastnortheast-westsouthwest trend (~ 70°).

The mine appears less distorted in the January 13th image, though target detection was still on (Fig. 38). The mine depth has remained constant at 12.40 meters, while the surrounding seafloor depth has decreased to 12.92 meters, reducing the observed burial to 1.8%. The mine may have provided protection to the underlying sand while the surrounding sand was locally eroded by currents.

Target detection mode remained on during the January 17th survey, explaining why the mine still appears quite distorted in the image (Fig. 39). Although the mine has clearly sunk into the seabed, no scour is evident extending around the mine. The depth of the mine is 12.53 meters with a surrounding seafloor depth of 12.98 meters. The observed burial during this survey is 15.0%.

Scour becomes evident around the mine during the January 20th survey (Fig. 40). There is a small pit of scour developing at eastern end of the mine, but the majority of development appears at the western end where the maximum depth reaches 13.27 meters. The mine has sunk a further 0.06 meters since the 17th and is now at a depth 12.59 meters. The ambient seafloor is 12.89 meters, indicating a localized deposition of 0.09 meters and resulting in an observed burial of 43.4%.

The scour has continued to develop and surrounds the mine during the February 6th survey, although the depth within the pit remains constant at 13.27 meters (Fig. 41). The depth to the top of the mine is 12.82 meters, 0.23 meters deeper than in the previous survey. The ambient seafloor is 12.86 meters and the observed burial is 92.5%. The observed burial increases to 96.2% during the March 13th survey, with a mine depth of

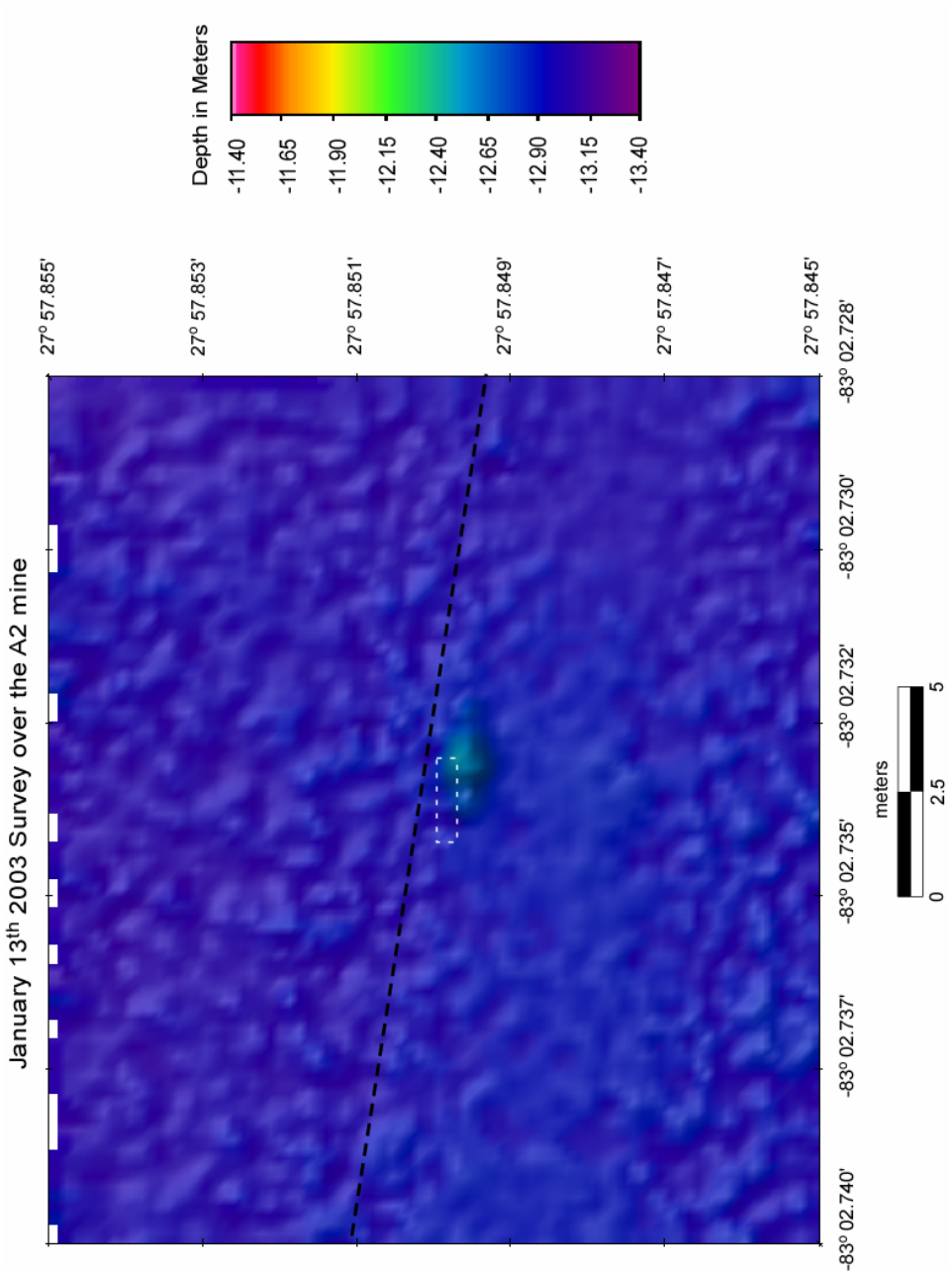

Figure 38. January 13th survey over the A2 mine.

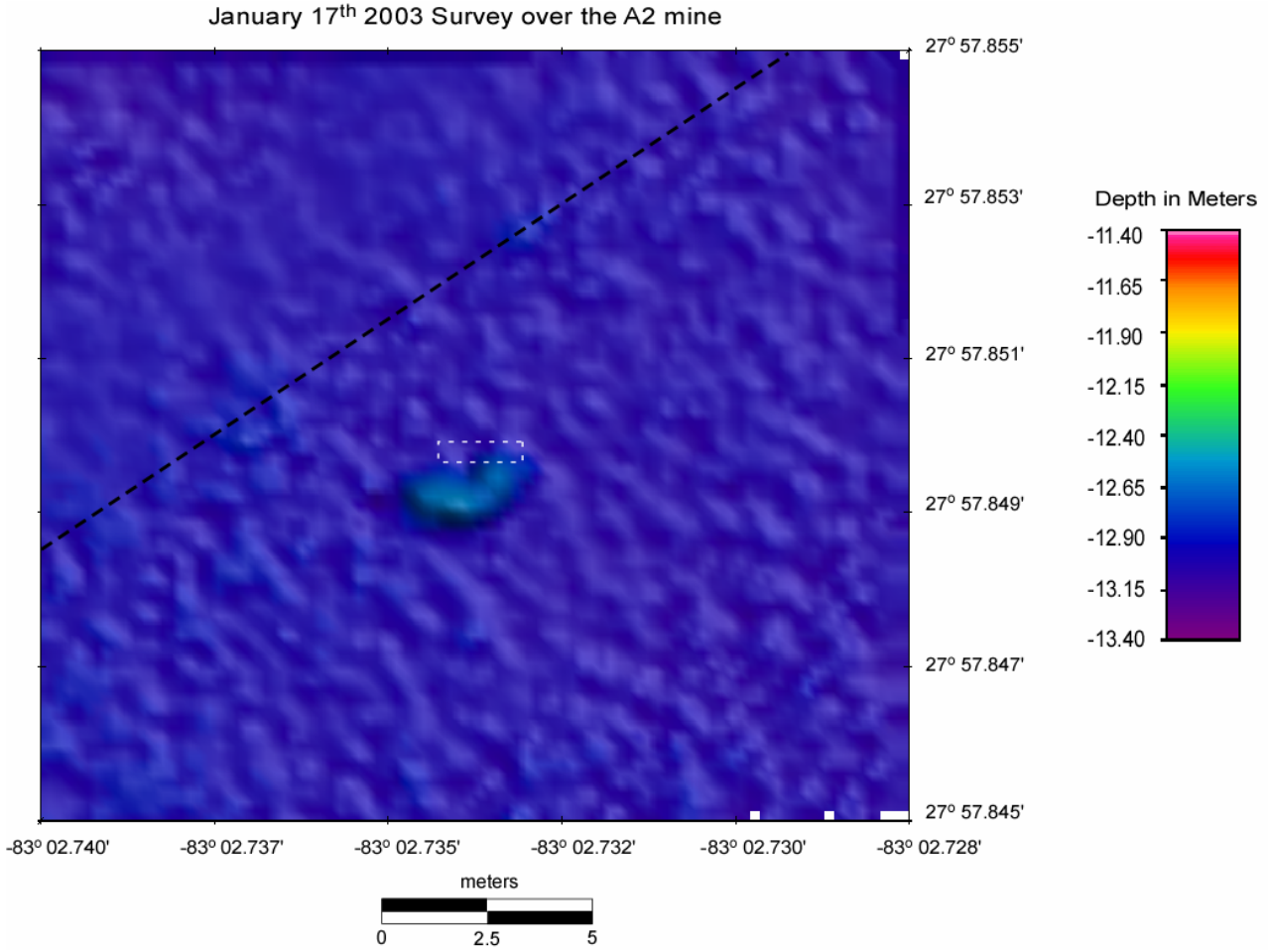

Figure 39. January 17th survey over the A2 mine.

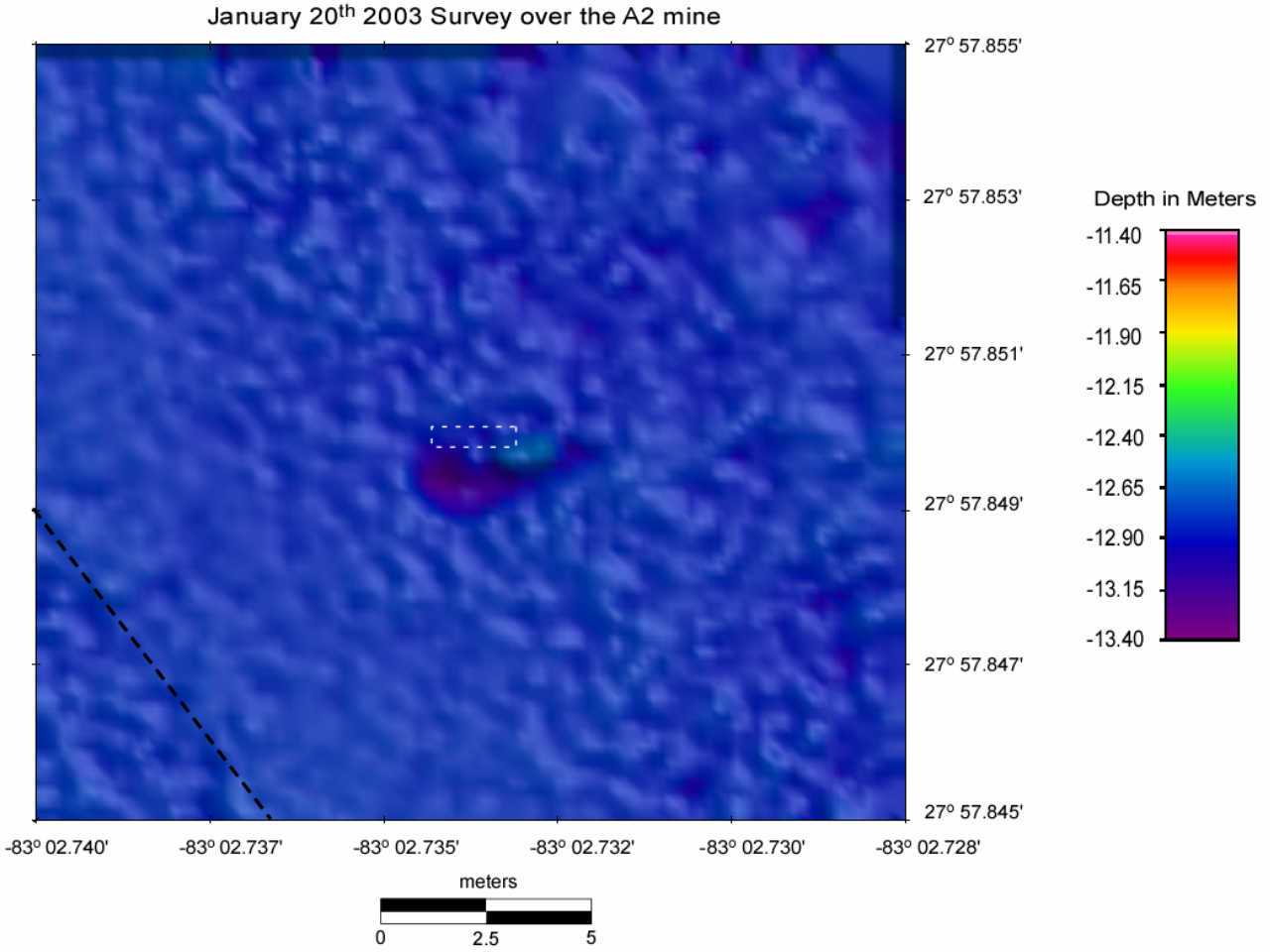

Figure 40. January 20th survey over the A2 mine.

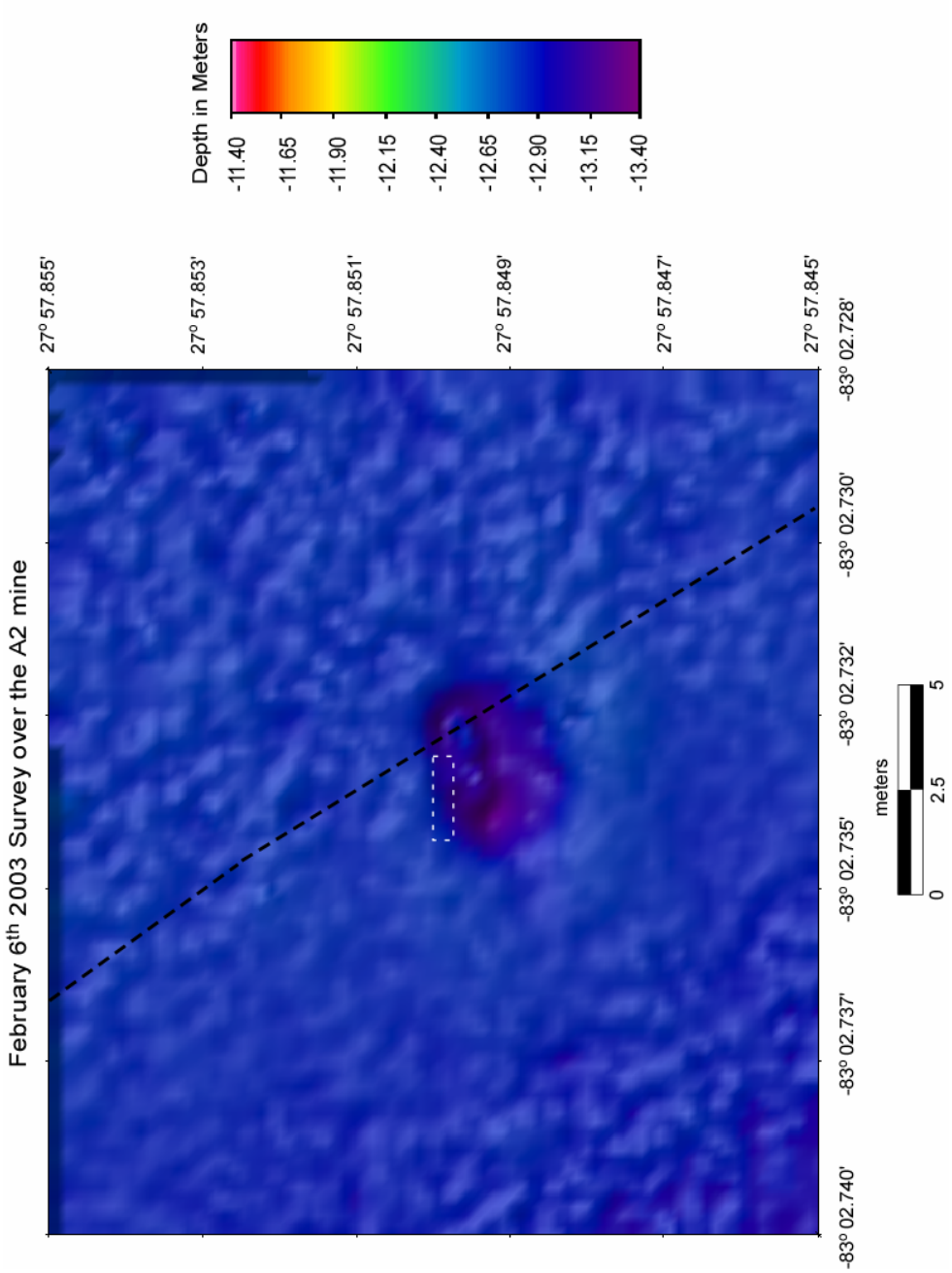

Figure 41. February 6th survey over the A2 mine.

12.88 meters and an ambient seafloor depth of 12.90 meters (Figs. 42 & 43). The scour has continued to expand out from the around the mine, and maximum depth within the pit is 13.25 meters.

Overall, the A2 mine sank a total of 0.48 meters and became 96.2% buried (Table 4; Fig. 44). Scour around the mine formed a pit 0.35 meters deeper than the surrounding seafloor. The ambient seafloor became a total of 0.03 meters deeper over the course of the experiment.

Comparison of A2 Multibeam Observations to the VIMS 2D Burial Model

The VIMS 2D burial model was initialized with a local water depth of 12.87 meters (obtained from the January 10th survey over the mine) and 0% burial. The model was run from the time of mine reposition, January 8th 2003 1600 GMT, to the time of the last multibeam survey over the mine, March 13th 2003 at 0200 GMT. The first direct comparison between the observed and predicted burial occurs for the January 10th survey (Figs. 44 & 45). The observed percent burial at this time is 11.3% compared to a predicted value of 14.7%. The difference is only 3.4%, and the predicted burial falls within the range of multibeam values.

The January 13th comparison shows a discrepancy of 15.6% with a predicted percent burial of 17.4% and an observed value of 1.8% (Figs. 44 & 45). This discrepancy is most likely due to the fact that the mine did not sink between the January 10th and January 13th surveys. The predicted burial for the January 17th comparison is also 17.4%. There is an observed burial of 15.4% at this time, resulting in a discrepancy of 2% that is well within the ± 9.4% uncertainty range.

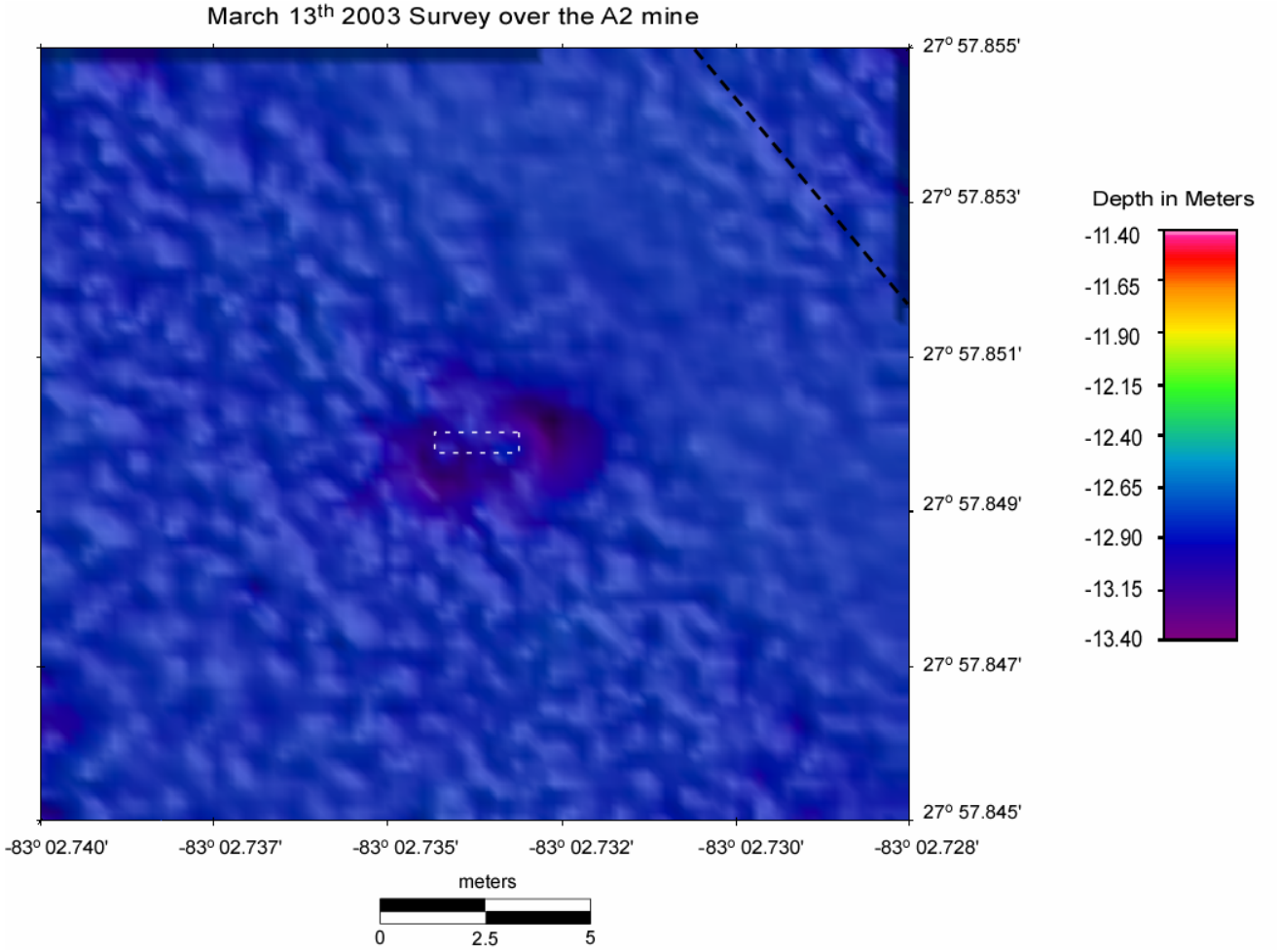

Figure 42. March 13th survey over the A2 mine.

Figure 43. ROV video still image of the A2 mine on March 13, 2003.

	Jan. 8*	Jan. 10	Jan. 13	Jan. 17	Jan. 20	Feb. 6	Mar. 13
Depth of Mine	_____	12.40	12.40	12.53	12.59	12.82	12.88
Cumulative Amount of Change	_____	_____	0.00	0.13	0.19	0.42	0.48
Average Depth of Seafloor	_____	12.87	12.92	12.98	12.89	12.86	12.90
Cumulative Amount of Change	_____	_____	0.05	0.11	0.02	-0.01	0.03
Scour Visible / Depth of Scour	_____	no	no	no	yes 13.27	yes 13.27	yes 13.25
% Mine Burial from Multibeam (± 9.4% due to 5 cm uncertainty of sonar)	0	11.3	1.8	15.0	43.4	92.5	96.2
% Mine Burial from Model	0	14.7	17.4	17.4	59.5	80.7	97.3
Mine Heading (degrees)	71.2	69.9	69.8	69.0	64.4	62.7	62.9
Mine Pitch (degrees)	0.2	0.1	0.0	0.6	-0.1	-0.9	-0.9
Mine Roll (degrees)	1.4	5.7	5.6	4.6	8.6	21.6	21.5

Table 4. Data table for the A2 mine. All numbers are in meters except where noted. There is no multibeam survey on January 8th.

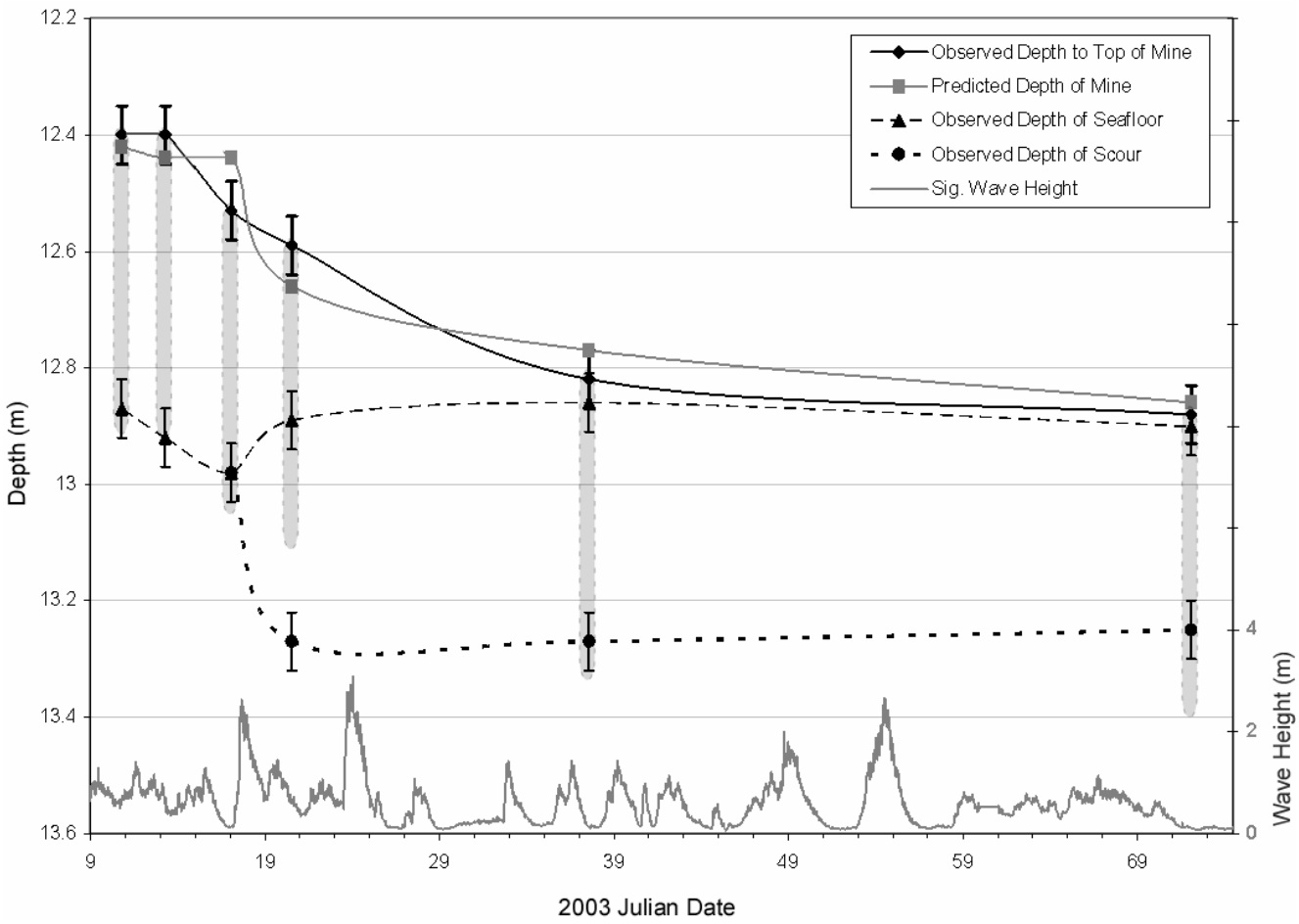

Figure 44. Comparison of multibeam observed (black) and predicted (gray) mine depth for the A2 mine over the course of the experiment. Predicted percent burial of the mine was converted to predicted depth of the mine using the 12.87-meter water depth used to initialize the model. Observed depth of seafloor and depth of scour from the multibeam are plotted as well. Significant wave height is plotted on the right y-axis. Error bars represent the 5-centimeter uncertainty inherent in the multibeam system. The light gray oval represents the A2 mine, and is scaled to the actual dimensions of the mine (length ~ 0.53 m, the diameter of the mine).

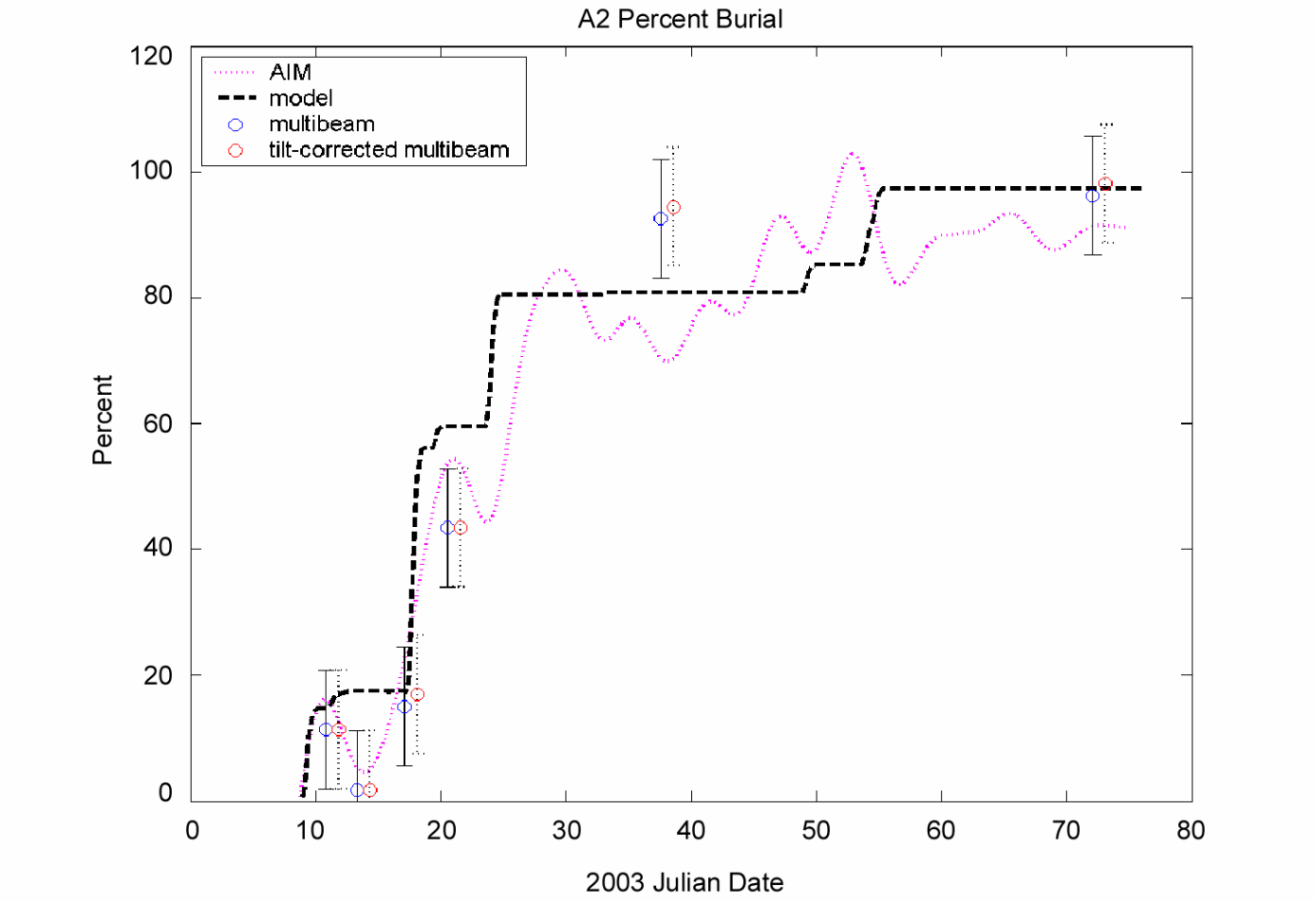

Figure 45. Comparison of the mine (magenta), predicted (dashed), observed (blue), and tilt-corrected observed (red) percent burial for the A2 mine over the course of the experiment. Tilt-corrected values have been horizontally offset for clarity. Error bars represent the 5-centimeter uncertainty inherent in the multibeam system.

The model overestimates the amount of burial during the January 20th comparison, with a predicted burial of 59.5% and an observed burial of 43.4% (Figs. 44 & 45). The 16.1% offset is outside the range of the multibeam values. The offset from the February 6th comparison is also outside the acceptable range, with a predicted and observed burial of 80.7% and 92.5%, respectively. The comparison from March 13th shows the predicted value falls well within the ± 9.4% uncertainty range, with a predicted burial of 97.3% and an observed burial of 96.2%.

The A4 Mine

Temporal Analysis of Scour and Burial

The acoustic instrumented mine 4 (A4) was deployed on January 8th, 2003 in the shallow fine sand site. It was positioned in an east-west orientation (79.3°) at a water depth of 12.77 meters. The January 10th survey over the mine shows a 1.8% observed burial with a mine depth of 12.25 meters and an ambient seafloor depth of 12.77 meters (Fig. 46). There is no scour evident around the mine at this time. The observed orientation appears in agreement with the data from the orientation sensor within the mine itself. The slight blurriness of the mine can be attributed the target detection mode of the multibeam.

There is no scour evident in the January 13th survey either, though the mine has sunk 0.18 meters for a depth of 12.43 meters (Fig. 47). The seafloor depth around the mine is 12.90 meters, giving an observed burial of 11.3%. The ends of the mine appear blurry in this image; this is also likely due to the multibeam beam mode being set to target detection. Interestingly, the mine appears even more blurry and distorted in the

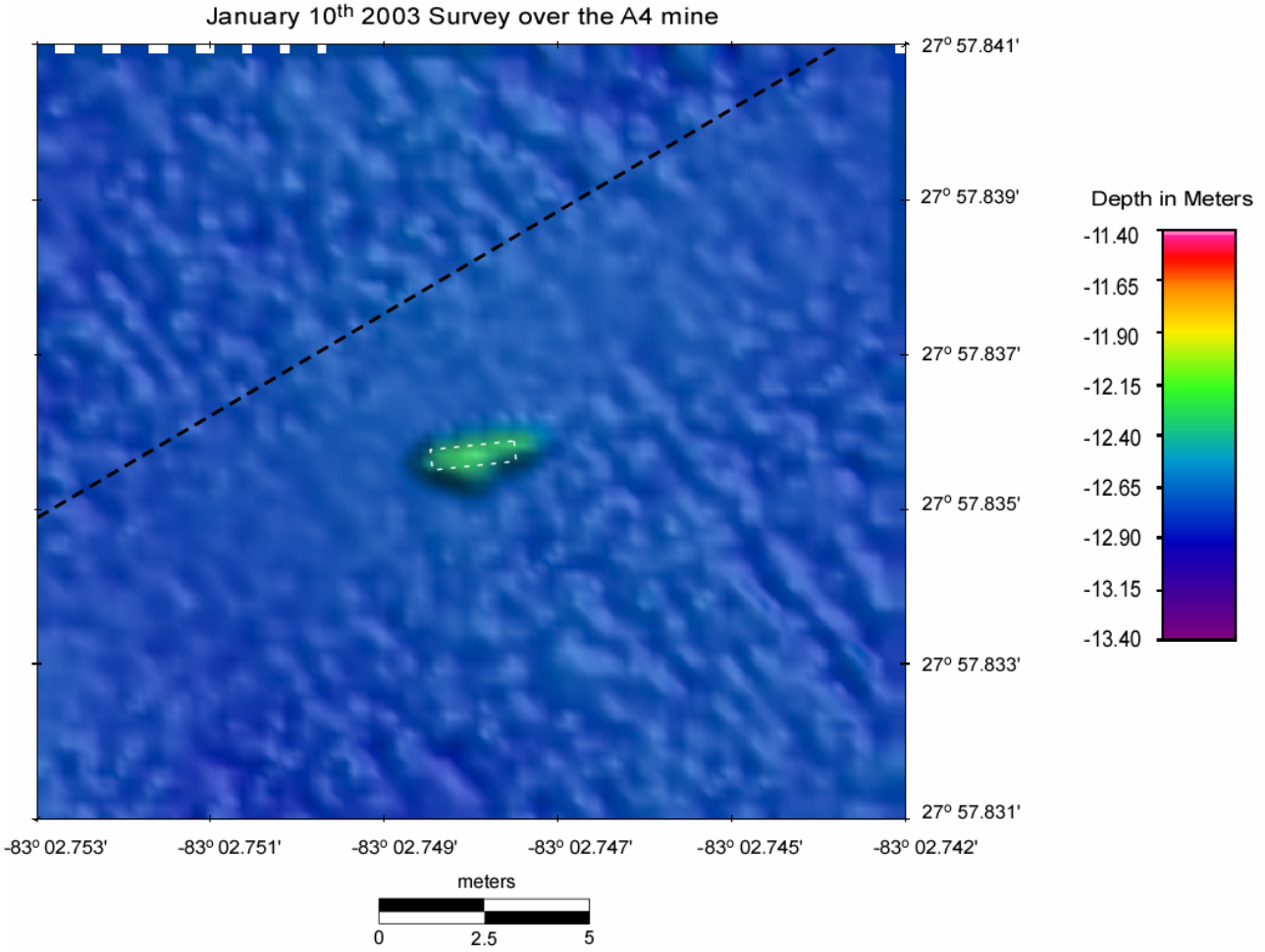

Figure 46. January 10th survey over the A4 mine. In all multibeam images, the black dashed line represents the ship's track line during the survey. The mine is outlined with a faint white line scaled to the mine's actual dimensions. The mine outline remains at the same orientation throughout the A4 multibeam images as a reference.

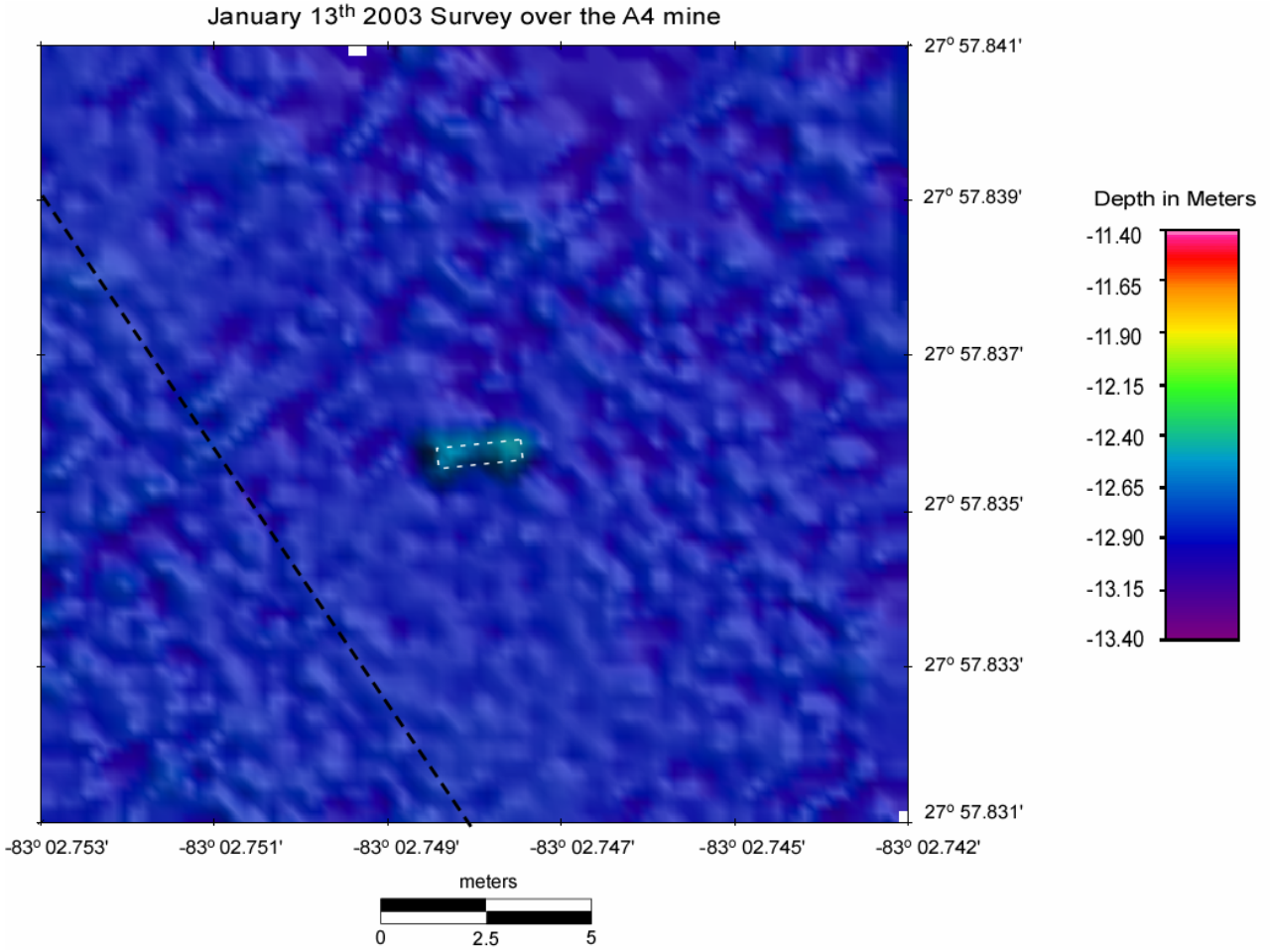

Figure 47. January 13th survey over the A4 mine.

image from the January 17th survey even though target detection was turned off at this time (Fig.48). The same phenomenon can be see in the A2 multibeam observations. Again, it is unclear what is causing this. The depth to the top of the mine is 12.40 meters, an apparent shallowing of 0.03 meters since January 13th; however, this is within the ± 5-centimeter uncertainty of the multibeam. The ambient seafloor depth remains essentially the same at a depth of 12.91 meters, resulting in an observed burial of 3.7%.

On January 20th, three days later, the seafloor depth around the mine still appears unchanged at a depth of 12.90 meters, despite the fact that the mine has sunk 0.22 meters and now resting at a depth of 12.62 meters (Fig. 49). The observed burial of the A4 mine at this time is 47.2%. The mine does not appear distorted in this image, and, in fact, does not, itself, actually show up very well. However, it is visible in this image because of the defining pit of scour wrapping around from the south side of the mine around to the east. The maximum depth measured within the scour pit is 13.22 meters.

The mine images quite well during the February 6th image and is surrounded by a ring of scour measuring 13.28 meters at its deepest point (Fig. 50). The mine appears to have rolled 0.42 meters northwest from its original position into the scour pit. The maximum amount of recorded roll up to February 6th is -17.9°, which only equates to .08 meters. Orientation sensors within the mine recorded data approximately every 38 minutes and do not record cumulative roll, so it is possible that the mine made a complete roll that was not recorded. A complete roll of the mine would shift its position 1.67 meters (the mine perimeter). If the mine rolled into a pit formed by scour; however, it would roll without shifting its actual position the full 1.67 meters. The depth of the mine

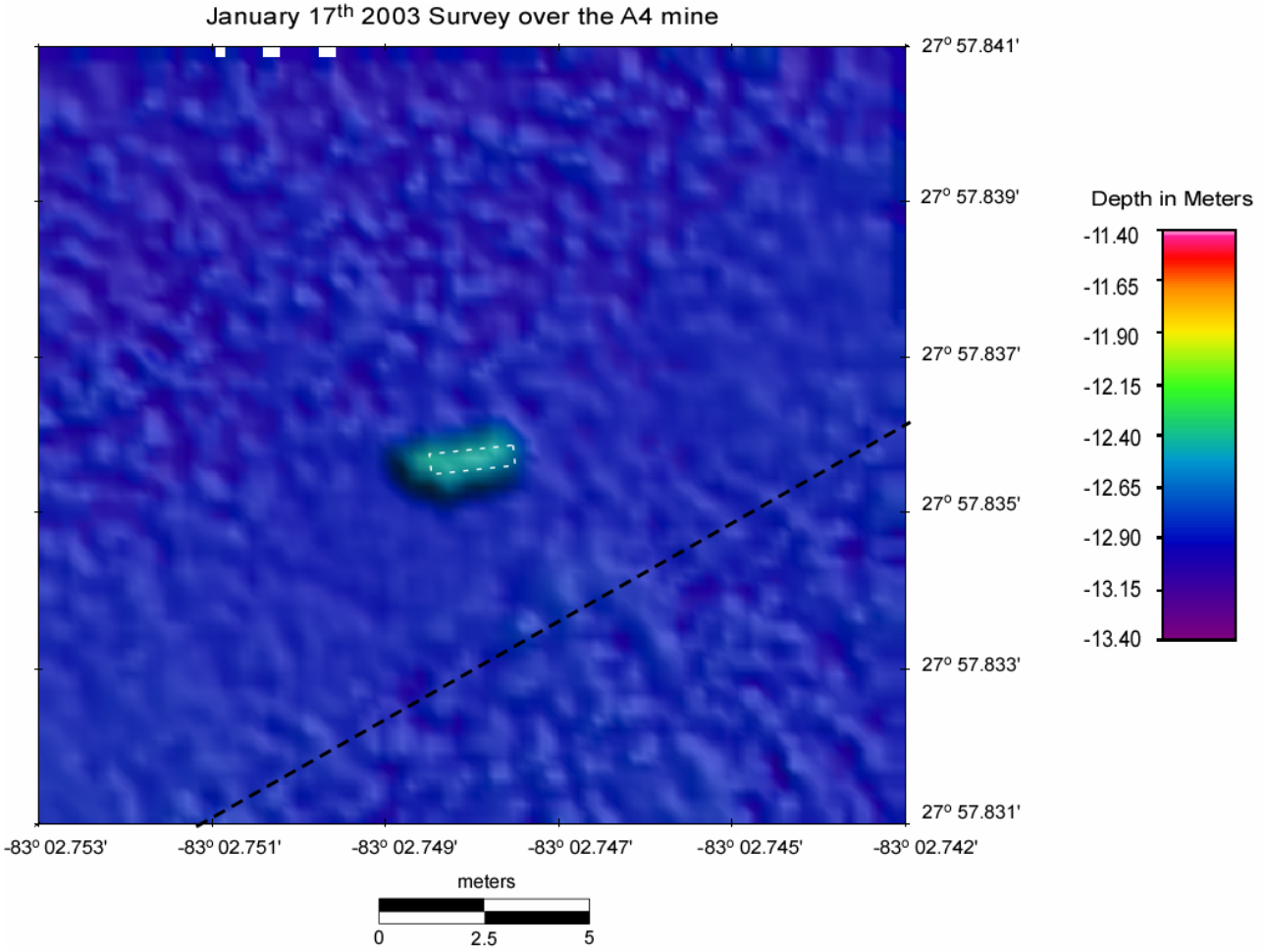

Figure 48. January 17th survey over the A4 mine.

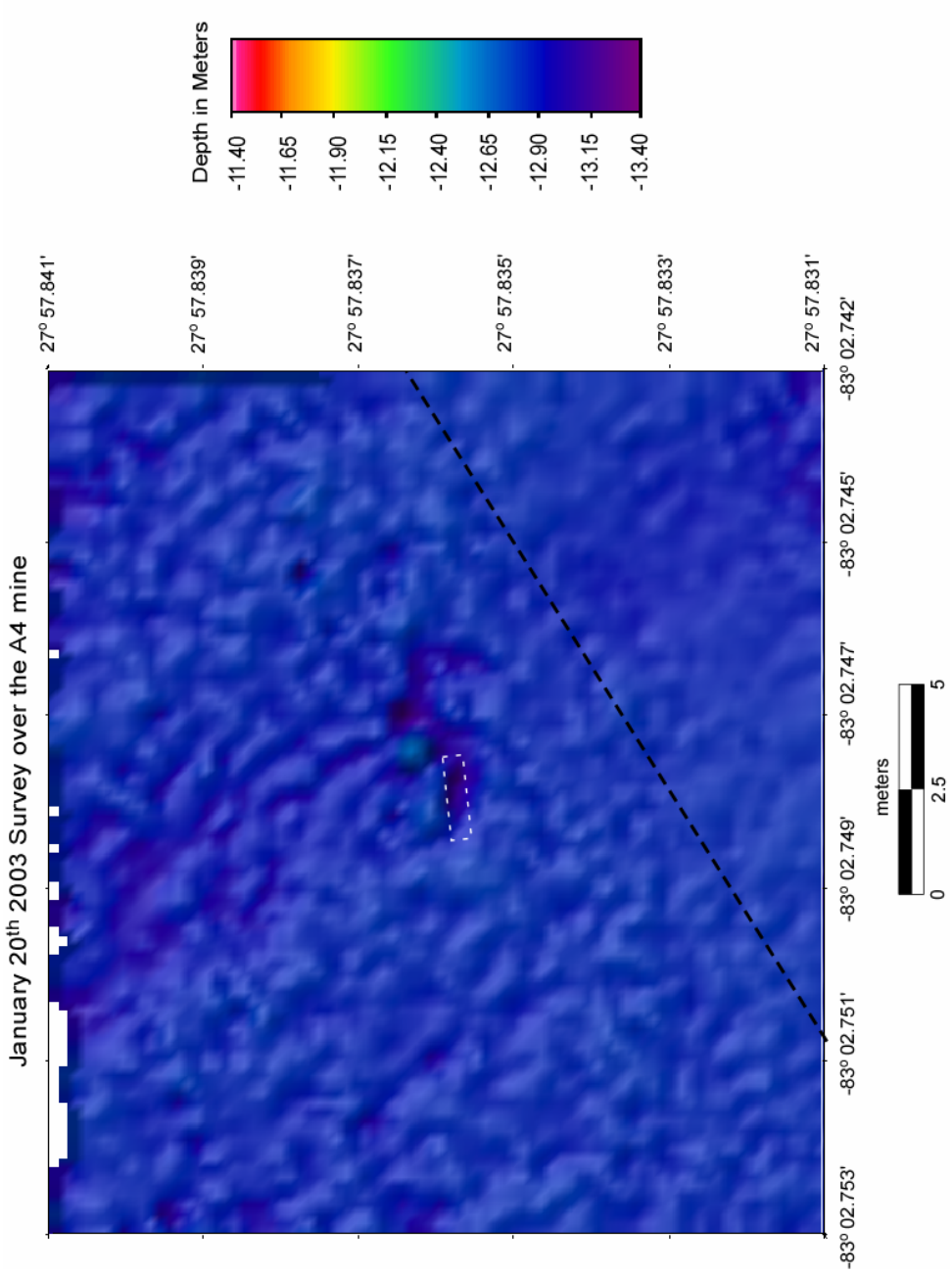

Figure 49. January 20th survey over the A4 mine.

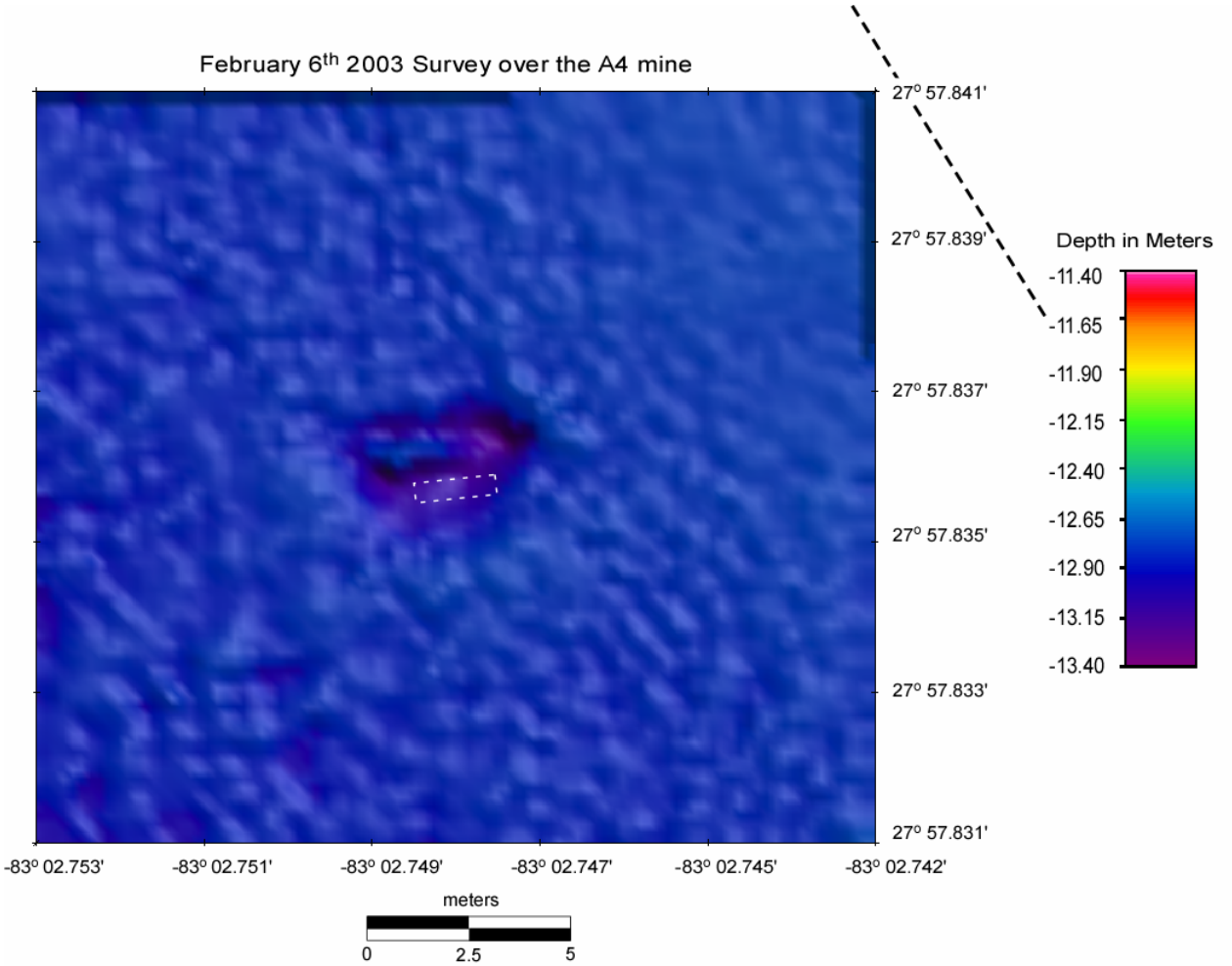

Figure 50. February 6th survey over the A4 mine. In this image, the track line is outside of the gridded area.

during this survey is 12.77 meters and the ambient seafloor depth is 12.86 meters, indicating an observed burial of 83.0%.

The mine appears back in its original position during the March 13th survey, indicating that the shift in position in the February 6th image may be due to the positional accuracy of the multibeam (± 1 meter) rather than actual change (Figs. 51 & 52). Once again, there is an apparent shallowing of the mine in this image. The depth to the top of the mine is 12.68 meters, .09 meters shallower than in the previous image. The depth of the ambient seafloor is 12.81 meters, indicating localized deposition around the mine. There also appears to be some infilling of the scour pit as the maximum depth has decreased to 13.11, a change of 0.17 meters. The observed burial for the March 13th survey over the A4 mine is 75.5%.

Overall, the A4 mine sank a total of 0.43 meters and became 75.5% buried (Table 5; Fig. 53). Scour around the mine formed a pit 0.30 meters deeper than the surrounding seafloor. The ambient seafloor became a total of 0.04 meters deeper over the course of the experiment.

Comparison of A4 Multibeam Observations to the VIMS 2D Burial Model

The comparison of the VIMS 2D burial model with the A4 mine represents the last of the model tests using the acoustic instrumented mines. The model was initialized with a local water depth of 12.77 meters (obtained from the January 10th survey over the mine) and 0% burial, and was run from the time of mine reposition, January 8th 2003 1600 GMT, to the time of the last multibeam survey over the mine, March 13th 2003 at 0300 GMT. The first direct comparison between the observed and predicted burial occurs

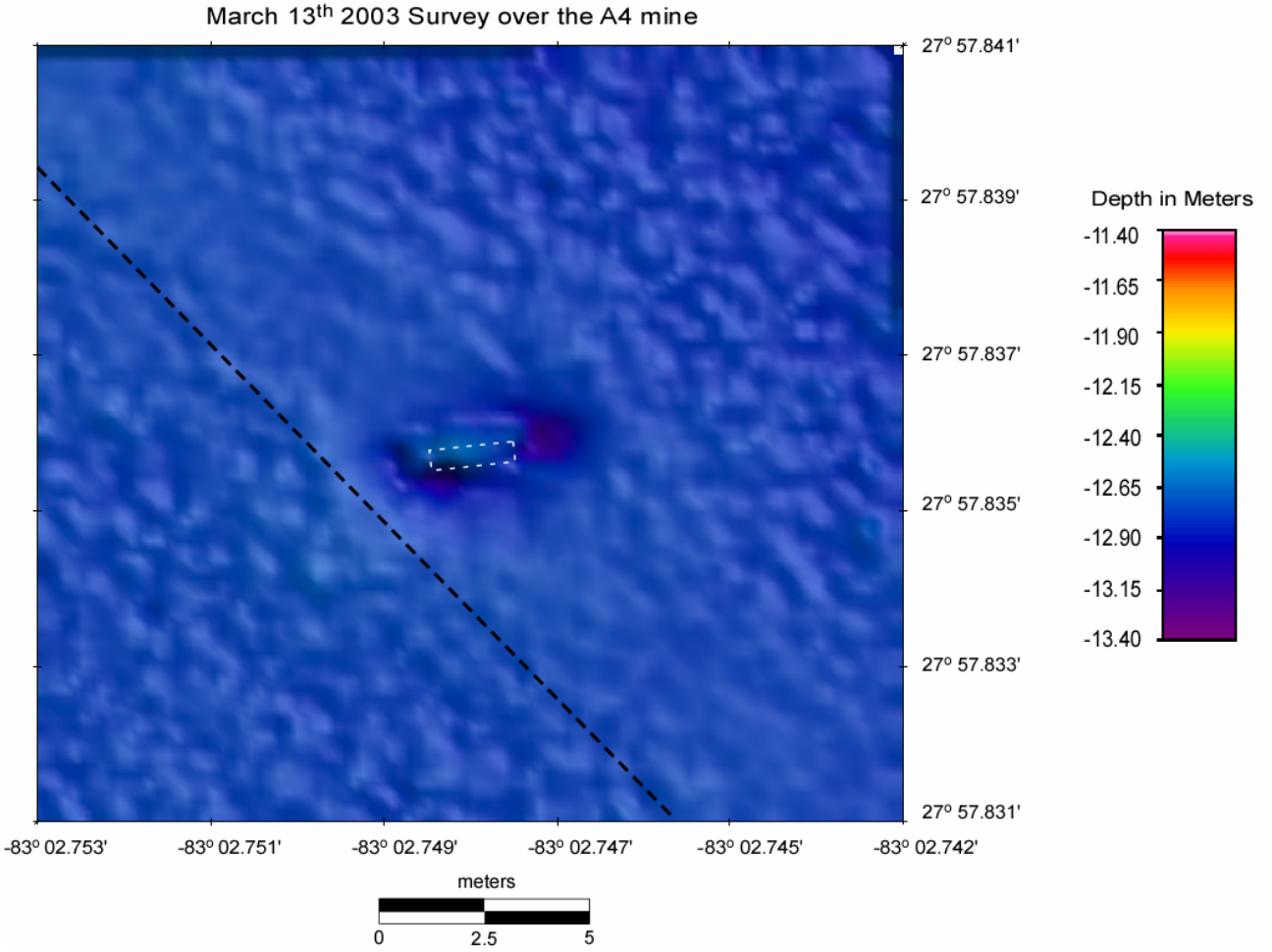

Figure 51. March 13th survey over the A4 mine.

Figure 52. ROV video still image of the A4 mine on March 13, 2003.

	Jan. 8*	Jan. 10	Jan. 13	Jan. 17	Jan. 20	Feb. 6	Mar. 13
Depth of Mine	_____	12.25	12.43	12.40	12.62	12.77	12.68
Cumulative Amount of Change	_____	_____	0.18	0.15	0.37	0.52	0.43
Average Depth of Seafloor	_____	12.77	12.90	12.91	12.90	12.86	12.81
Cumulative Amount of Change	_____	_____	0.13	0.14	0.13	0.09	0.04
Scour Visible / Depth of Scour	_____	no	no	no	yes 13.22	yes 13.28	yes 13.11
% Mine Burial from Multibeam (± 9.4% due to 5 cm uncertainty of sonar)	0	1.8	11.3	3.7	47.2	83.0	75.5
% Mine Burial from Model	0	15.4	18.1	18.1	60.5	81.6	98.0
Mine Heading (degrees)	79.3	78.4	78.4	77.98	73.2	69.3	69.4
Mine Pitch (degrees)	-0.2	-0.2	-0.2	1.1	-0.1	-0.5	-0.6
Mine Roll (degrees)	2.1	4.0	4.0	2.0	-5.1	-9.9	-9.8

Table 5. Data table for the A4 mine. All numbers are in meters except where noted. There is no multibeam survey on January 8th.

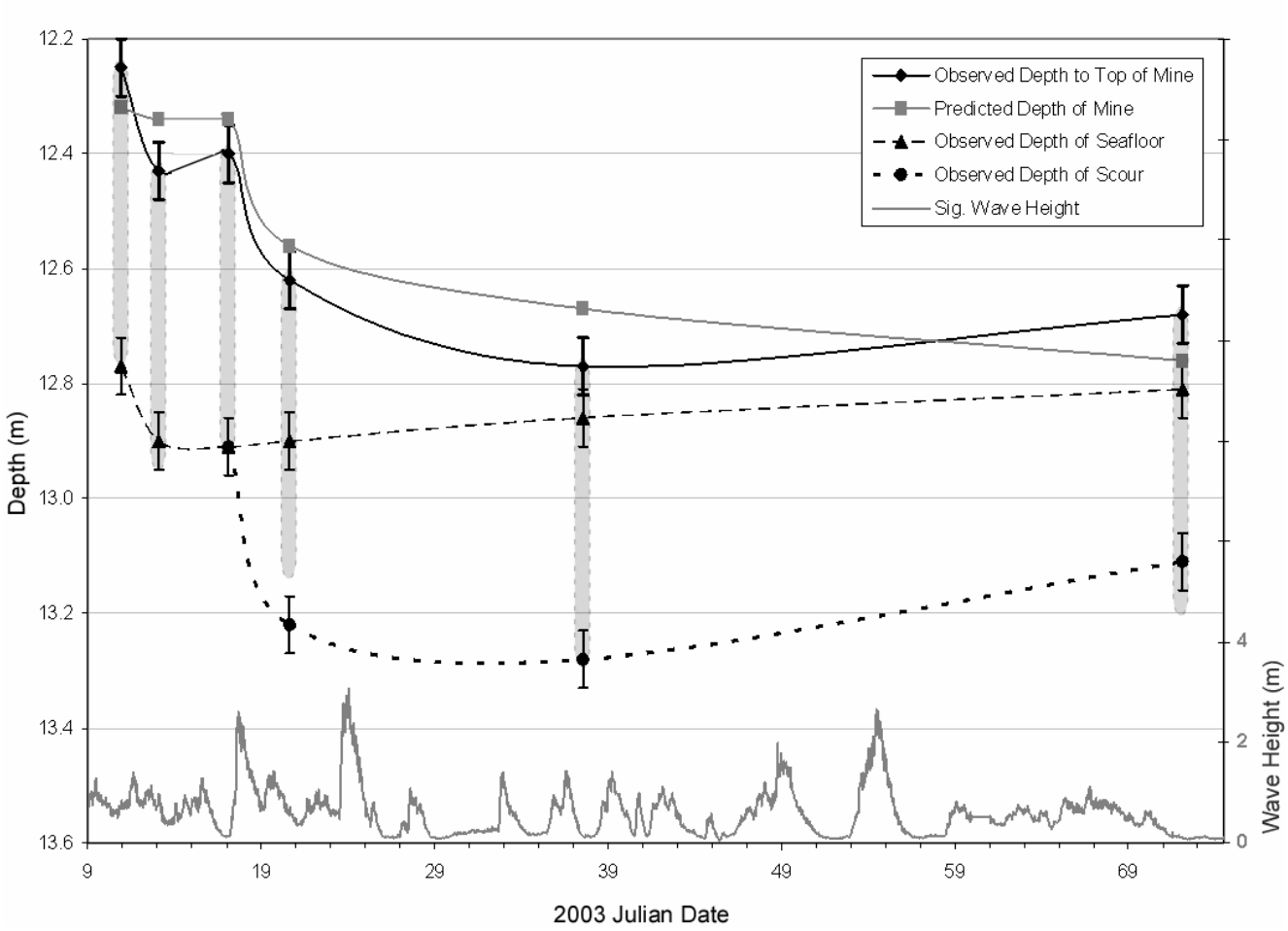

Figure 53. Comparison of multibeam observed (black) and predicted (gray) mine depth for the A4 mine over the course of the experiment. Predicted percent burial of the mine was converted to predicted depth of the mine using the 12.77-meter water depth used to initialize the model. Observed depth of seafloor and depth of scour from the multibeam are plotted as well. Significant wave height is plotted on the right y-axis. Error bars represent the 5-centimeter uncertainty inherent in the multibeam system. The light gray oval represents the A4 mine, and is scaled to the actual dimensions of the mine (length ~ 0.53 m, the diameter of the mine).

for the January 10th survey (Figs. 53 & 54). The observed percent burial at this time is 1.8% compared to a predicted value of 15.4%, a discrepancy of 13.6%. The observed values have a range of ± 9.4% due to the vertical uncertainty of the multibeam system; however, the prediction for this comparison falls outside this range.

The January 13th comparison shows a discrepancy of 6.8%, with an observed burial of 11.3% and a predicted burial of 18.1%, which falls within the range of multibeam values (Figs. 53 & 54). The predicted burial for the January 17th comparison is 18.1% as well; however, the observed burial is only 3.7% due to the 0.03 meter shallowing of the mine. The predicted value, therefore, lies outside the multibeam range. This holds true for the comparison for January 20th as well. The model estimates that the mine should be 60.5% buried at this time; however, the multibeam data only indicate a burial of 47.2%, leaving a discrepancy of 13.3%.

On February 6th, the model and the observed values are in agreement, with a predicted value for burial of 81.6% and an observed value of 83.0% (Figs. 53 & 54). The discrepancy of 1.4% falls well within the acceptable range. The same is not true of the final comparison on March 13th. The apparent shallowing of the mine has resulted in an observed burial of only 75.5%, while the model predicts a burial of 98.0%.

The F5 Mine

Temporal Analysis of Scour and Burial

The F5 mine was one of two optical instrumented mine located in the shallow fine sand site during the 2003 IRB mine burial experiment. It was deployed on January 12th, 2003 in 12.96 meters of water and oriented northeast-southwest. The optical mines have

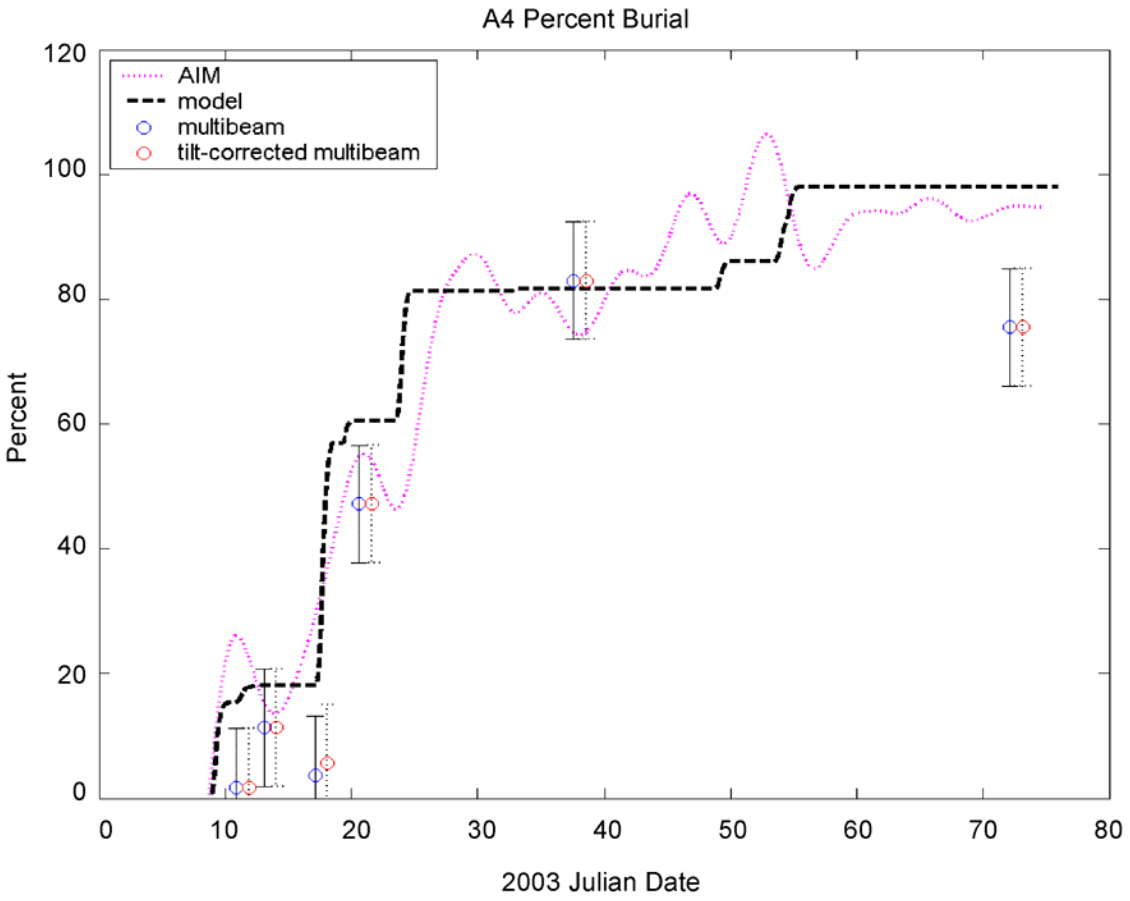

Figure 54. Comparison of the mine (magenta), predicted (dashed), observed (blue), and tilt-corrected observed (red) percent burial for the A4 mine over the course of the experiment. Tilt-corrected values have been horizontally offset for clarity. Error bars represent the 5-centimeter uncertainty inherent in the multibeam system.

steel casings and do not include compasses in their suite of instrumentation; therefore, the apparent orientation cannot be checked against the mine itself.

The January 13th survey was the first to pass over the F5 mine after its deployment (Fig. 55). The depth to the top of the mine is 12.52 meters and the depth of the surrounding seafloor is 12.96 meters. The amount of observed burial at this time is 6.4%. The mine does not image very well during this survey and the seafloor appears quite mottled. The reason for the poor appearance of the mine is not clear. The appearance of the seafloor may be in part due to actual bed morphology at the time of the seafloor and in part due to noise in the data.

The seafloor appears to have smoothed out in the image from the January 17th survey (Fig. 56). The mine shows up quite clearly in this image, though it appears somewhat blurry and distorted. The depth to the top of the mine is 12.61 meters with a surrounding seafloor depth of 13.00 meters. The observed burial in this image is 17.0% and there is no evident scour around the mine. The mine does not appear to show up at all in the image from the January 20th survey (Fig. 57). A scour pit can clearly be seen in the image, with a maximum depth of 13.19 meters and a slight rise in the middle. The rise appears as two separate bumps within the scour pit and cannot be attributed to the mine with any certainty. The shallowest depth of this rise is 12.89 meters, which sets it vertically flush with the surrounding seafloor. If this was indeed, the mine, conditions would indicate a 100% burial. Due to the combined facts that the mine is not fully buried in subsequent images, the rise appears as two separate bumps in this image, and that the F6 mine does not show up during the January 20th survey either (to be discussed), it was decided to not treat the rise as the mine.

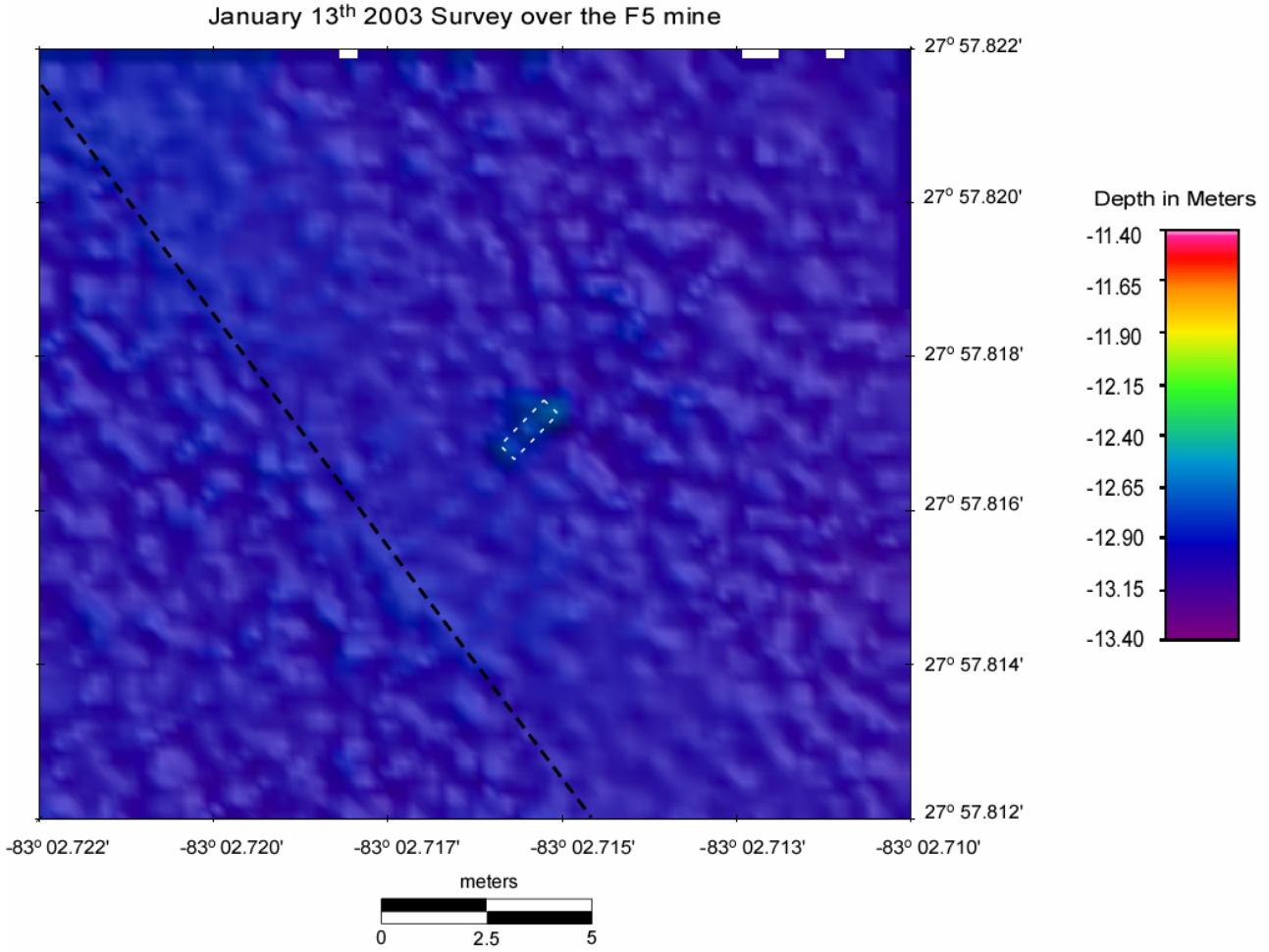

Figure 55. January 13th survey over the F5 mine. The black dashed line indicates the ship's track line during the survey. The mine itself is outlined with a faint white dashed line scaled to the actual dimensions of the mine. The mine outline remains at the same scale and orientation throughout the rest of the F5 multibeam images as a reference.

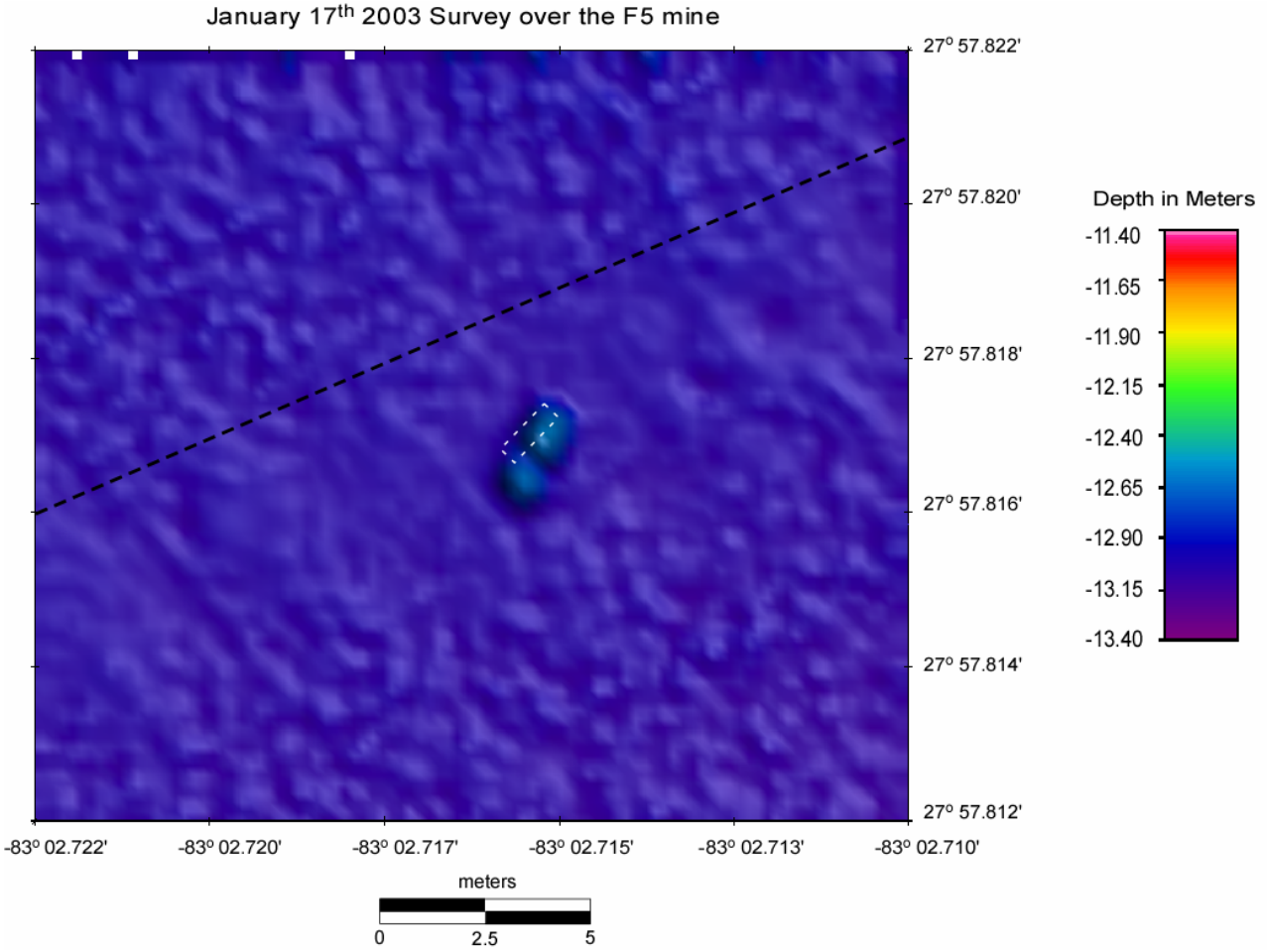

Figure 56. January 17th survey over the F5 mine.

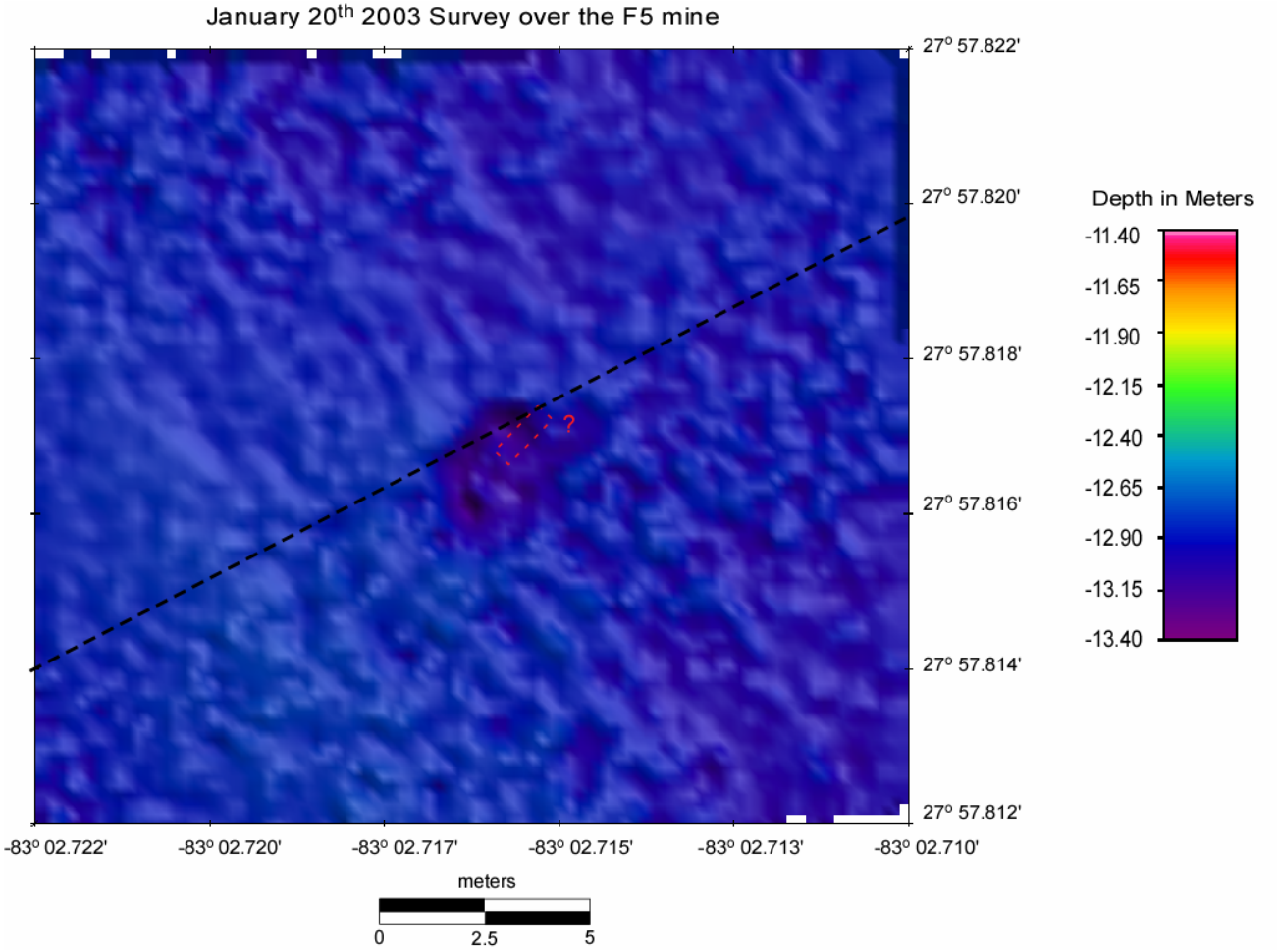

Figure 57. January 20th survey over the F5 mine. The mine is not evident in this image, though a well-defined scour pit can be clearly seen.

The mine is clearly visible in the image from the February 6th survey, resting at a depth of 12.77 meters and is surrounded by a ring of scour that expands out to the southeast of the mine (Fig. 58). The depth of the ambient seafloor is 12.87 meters and the observed amount of burial is 78.7%. Maximum depth within the surrounding scour is 13.22 meters. The mine continues to show up quite well in the March 13th image (Figs. 59 & 60). It has sunk a further .09 meters, for a total depth of 12.86 meters. The depth of the ambient seafloor and depth within the scour pit has remained unchanged, resulting in an observed burial of 97.9%.

Over the course of the experiment, the F5 mine sank a total of 0.34 meters and the surrounding seafloor showed a localized deposition of 0.09 meters (Table 6; Figs. 61). Final observed burial of the F5 mine was 97.9%. Scour around the mine formed a pit 0.35 meters deeper than the surrounding seafloor.

Comparison of F5 Multibeam Observations to the VIMS 2D Burial Model

For comparison with the F5 mine, the VIMS 2D burial model was initialized with a local water depth of 12.96 meters (obtained from the January 13th survey over the mine) and 0% burial. It was run from the time of mine deployment (there was no repositioning of the F5 mine by divers), January 12th 2003 0000 GMT, to the time of the last multibeam survey over the mine, March 13th 2003 at 0300 GMT. The first direct comparison between the observed and predicted burial occurs for the January 13th survey (Figs. 61 & 62). The predicted burial at this time is 3.9% and the observed burial is 6.4%. The observed values of burial have a range of ± 10.6% for the optical mines (0.47-meter diameter, see Fig. 8) due to the vertical uncertainty of the multibeam system.

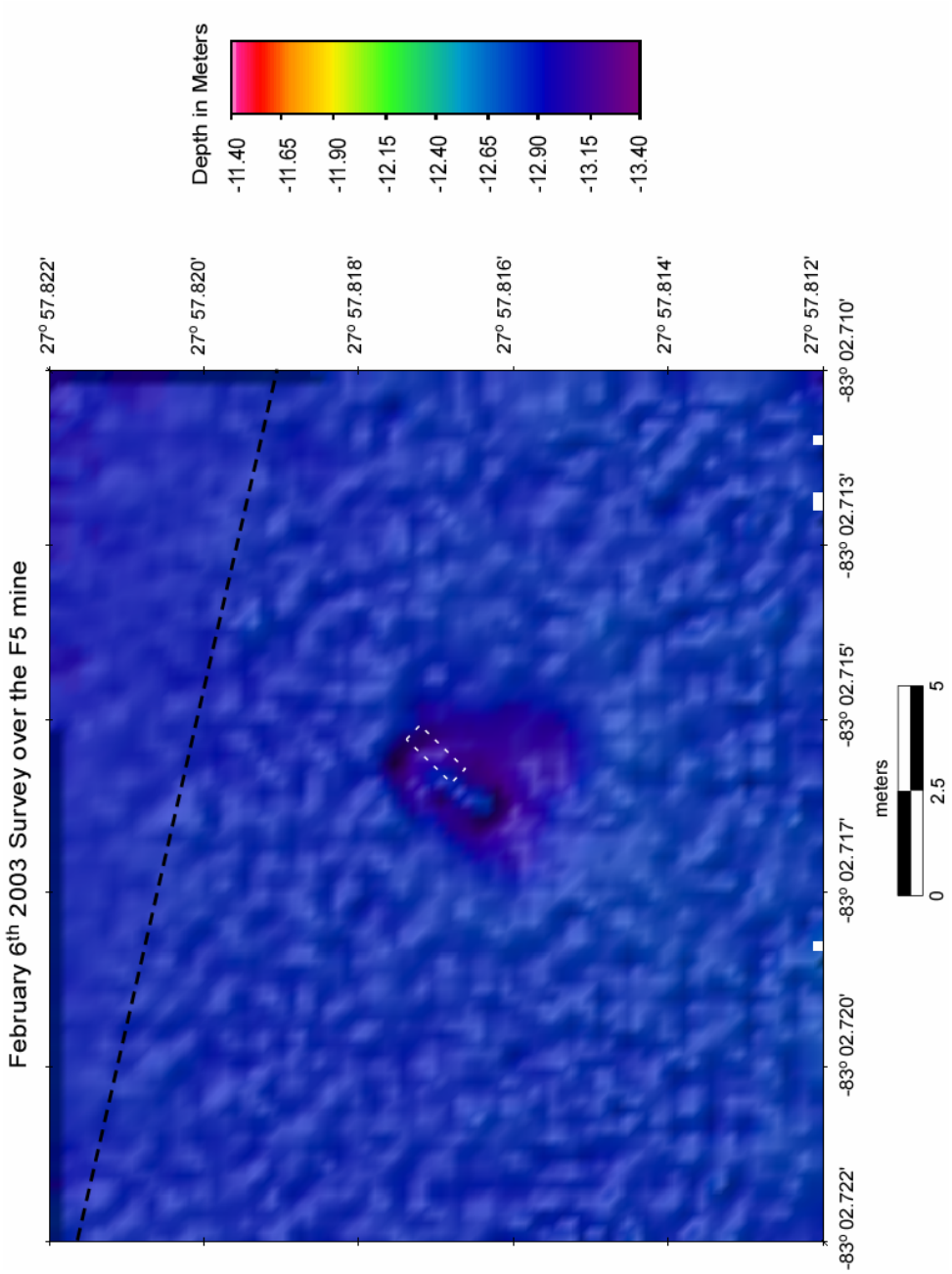

Figure 58. February 6th survey over the F5 mine.

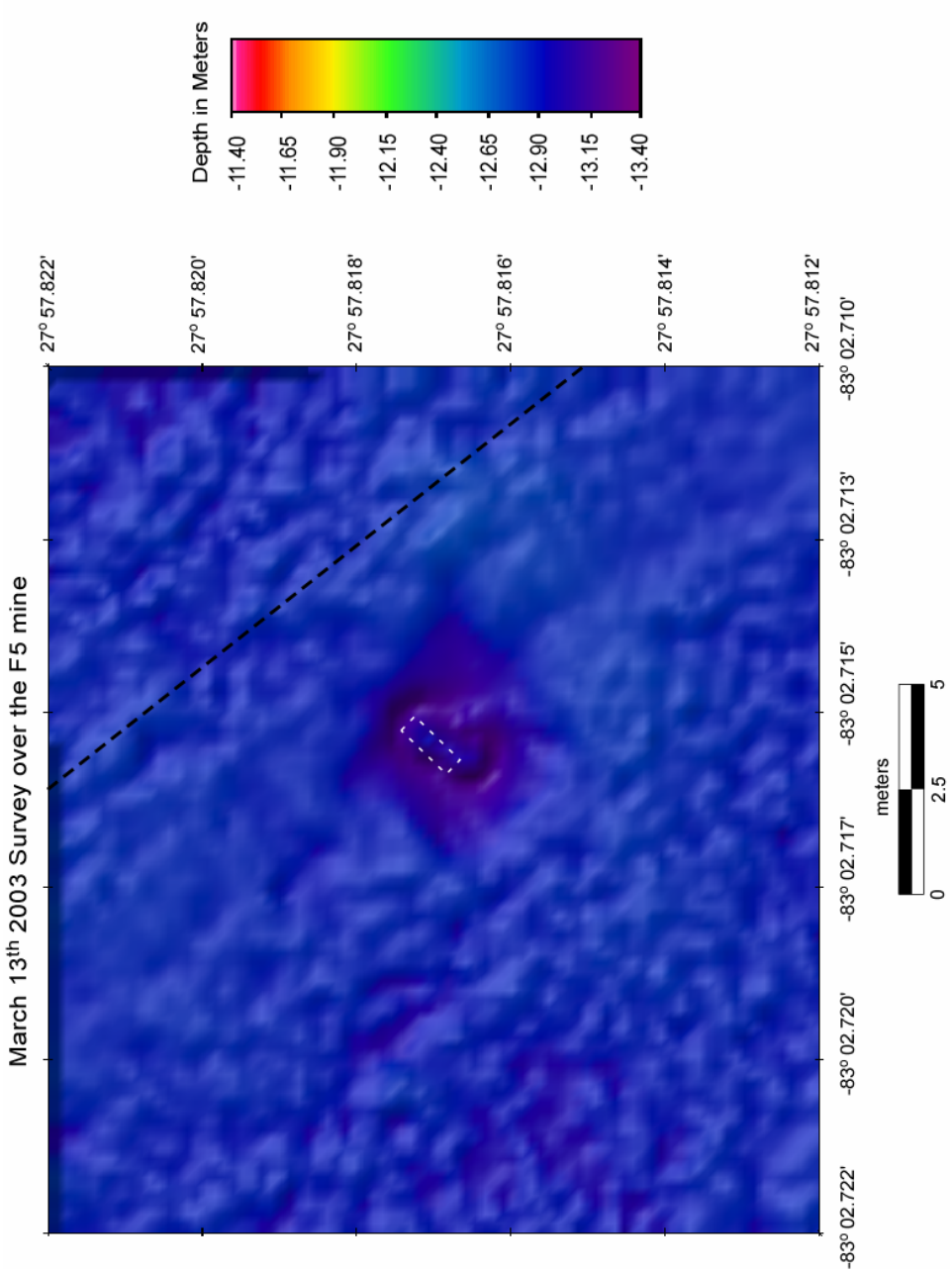

Figure 59. March 13th survey over the F5 mine.

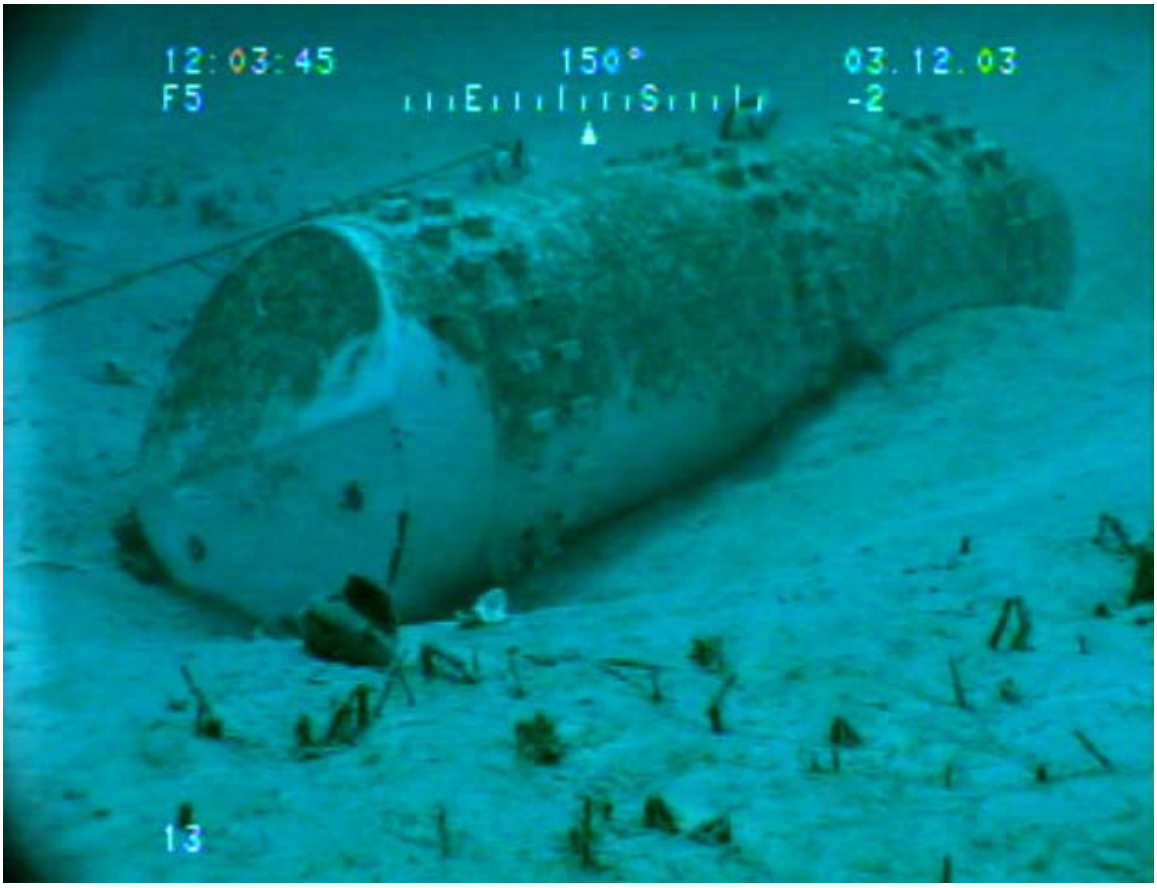

Figure 60. ROV video still image of the F5 mine on March 13, 2003.

	Jan. 11*	Jan. 13	Jan. 17	Jan. 20	Feb. 6	Mar. 13
Depth of Mine	_____	12.52	12.61	____	12.77	12.86
Cumulative Amount of Change	_____	_____	0.09	____	0.25	0.34
Average Depth of Seafloor	_____	12.96	13.00	12.89	12.87	12.87
Cumulative Amount of Change	_____	_____	0.04	-0.07	-0.09	-0.09
Scour Visible / Depth of Scour	_____	no	no	yes 13.19	yes 13.22	yes 13.22
% Mine Burial from Multibeam (± 10.6% due to 5 cm uncertainty of sonar)	0	6.4	17.0	____	78.7	97.9
% Mine Burial from Model	0	3.9	4.2	62.5	85.0	100.9
Mine Pitch (degrees)	2	1	2	2	1	2
Mine Roll (degrees)	20	3	5	8	16	17

Table 6. Data table for the F5 mine. All numbers are in meters except where noted. There is no multibeam survey on January 11th.

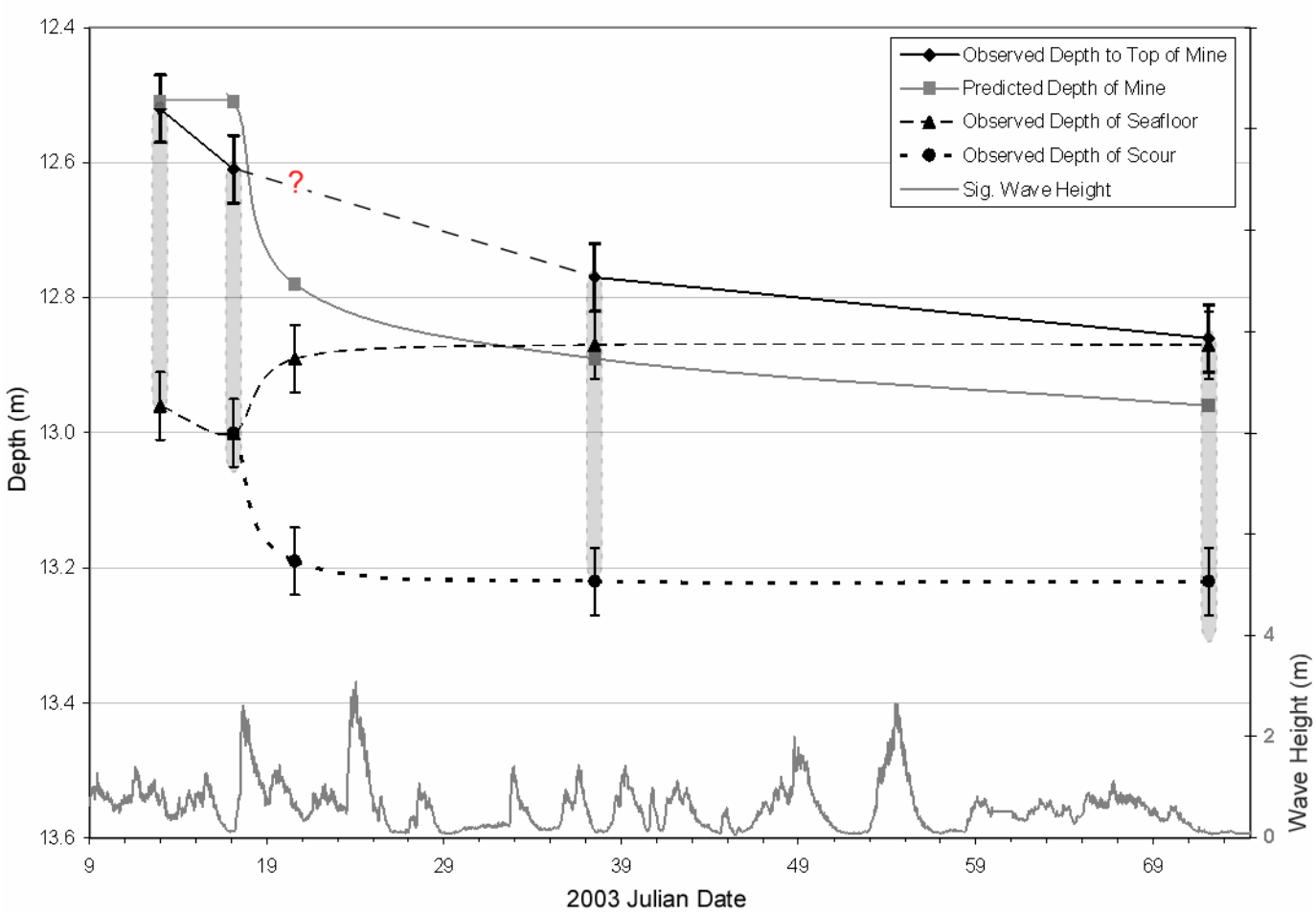

Figure 61. Comparison of multibeam observed (black) and predicted (gray) mine depth for the F5 mine over the course of the experiment. Predicted percent burial of the mine was converted to predicted depth of the mine using the 12.96-meter water depth used to initialize the model. Observed depth of seafloor and depth of scour from the multibeam are plotted as well. Significant wave height is plotted on the right y-axis. Error bars represent the 5-centimeter uncertainty inherent in the multibeam system. The light gray oval represents the F5 mine, and is scaled to the actual dimensions of the mine (length ~ 0.47 m, the diameter of the mine). The mine did not image on Julian day 20.

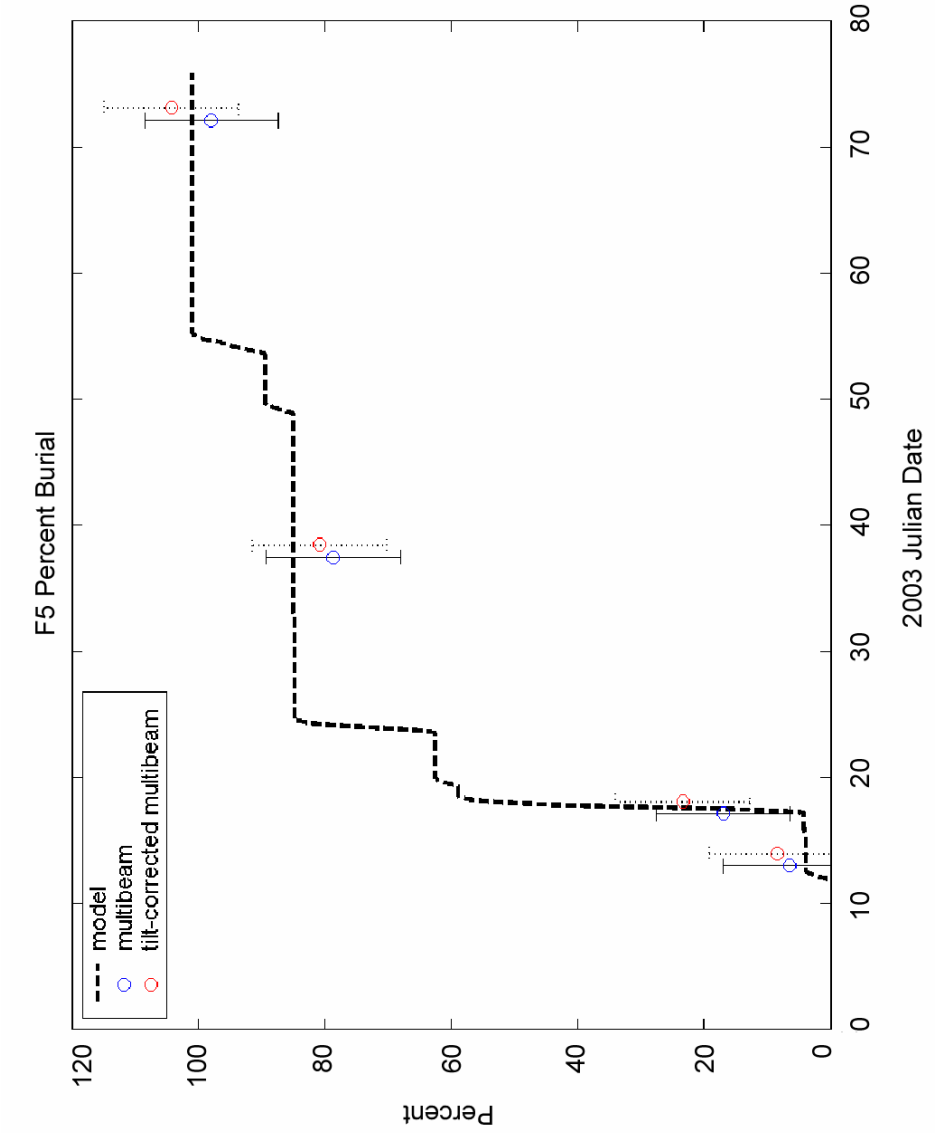

Figure 62. Comparison of the predicted (dashed), observed (blue), and tilt-corrected observed (red) percent burial for the F5 mine over the course of the experiment. Tilt-corrected values have been horizontally offset for clarity. Error bars represent the 5-centimeter uncertainty inherent in the multibeam system.

The January 17th comparison shows a discrepancy of 12.8%, which falls outside the range of multibeam values (Figs. 61 & 62). The observed burial for this comparison is 17.0% while the model predicts a burial of only 4.2%. There is no comparison for January 20th due to the fact that the mine cannot be distinguished in the multibeam image. The model prediction of percent burial at the time of the survey over the mine; however, is 62.5%.

On February 6th, the discrepancy between the model and the multibeam data is 6.3%, within the range of observable values (Figs. 61 & 62). The predicted amount of burial is 85.0%, while 78.7% is actually observed in the multibeam data. The discrepancy decreases to a mere 3% for the March 13th comparison, with a predicted burial of 100.9% and an observed burial of 97.9%.

The F6 Mine

Temporal Analysis of Scour and Burial

The optical instrumented mine number 6 (F6) was deployed in the shallow fine sand site on January 12th, 2003. It was situated in 13.00 meters of water depth in a northwest-southeast orientation. The first survey to image the mine after deployment was on January 13th (Fig. 63). The target detection mode on the multibeam sonar has caused the mine to appear blurry in the image. The depth to the top of the mine is 12.57 meters and the surrounding seafloor depth is 13.00 meters, giving an observed burial of 8.5%. Target detection was not set during the January 17th survey over the mine, although the mine still appears blurry. The blurriness may explain – along with the ± 5-centimeter vertical uncertainty of the multibeam for this survey – the apparent 6-centimeter

shallowing of the mine (Fig. 64). Furthermore, the combined vertical uncertainty of the multibeam for both the January 13th and January 17th surveys can explain the apparent discrepancy in mine depth between the two. Depth to the top of the mine is now 12.51 meters. The depth of the seafloor around the mine is 13.01, which indicates that the mine is resting 3 centimeters above the bed if the depth of the mine is accurate. The tilt of the mine has not changed since the January 13th survey, and therefore cannot be the reason for the offset between mine depth and seafloor depth. Consequently, the observed burial of the mine for the January 17th survey is zero. The early stages of scour pit development can be seen off the northeast and southwest sides of the mine. Maximum depth measured in the scour is 13.17 meters.

As in the case of the F5 mine, the F6 mine does not show up in the image from the January 20th survey (Fig. 65). The scour pit can be clearly seen, but there is no evidence of the mine. The reason for this is not clear, yet we have seen this elsewhere (e.g., Fig. 57), and it is not known if this phenomenon is related to the F5 case or if it is merely coincidence. The maximum depth of the scour pit is 13.18 meters and the average depth of the surrounding seafloor is 12.95 meters.

The image from the February 6th survey shows the mine quite clearly resting within a pit of scour at a depth of 12.75 meters (Fig. 66). The depth of the surrounding seafloor is 12.93 meters, giving an observed burial of 61.7%. The scour pit itself has remained relatively constant, with a maximum depth of 13.17 meters. The mine appears to have rolled to the northwest in the March 13th survey image (Figs. 67 & 68). Sensors within the mine recorded a 16° change in roll since the previous survey, which can only account for 0.06 meters of the 0.27-meter offset. This offset; however, is well within the

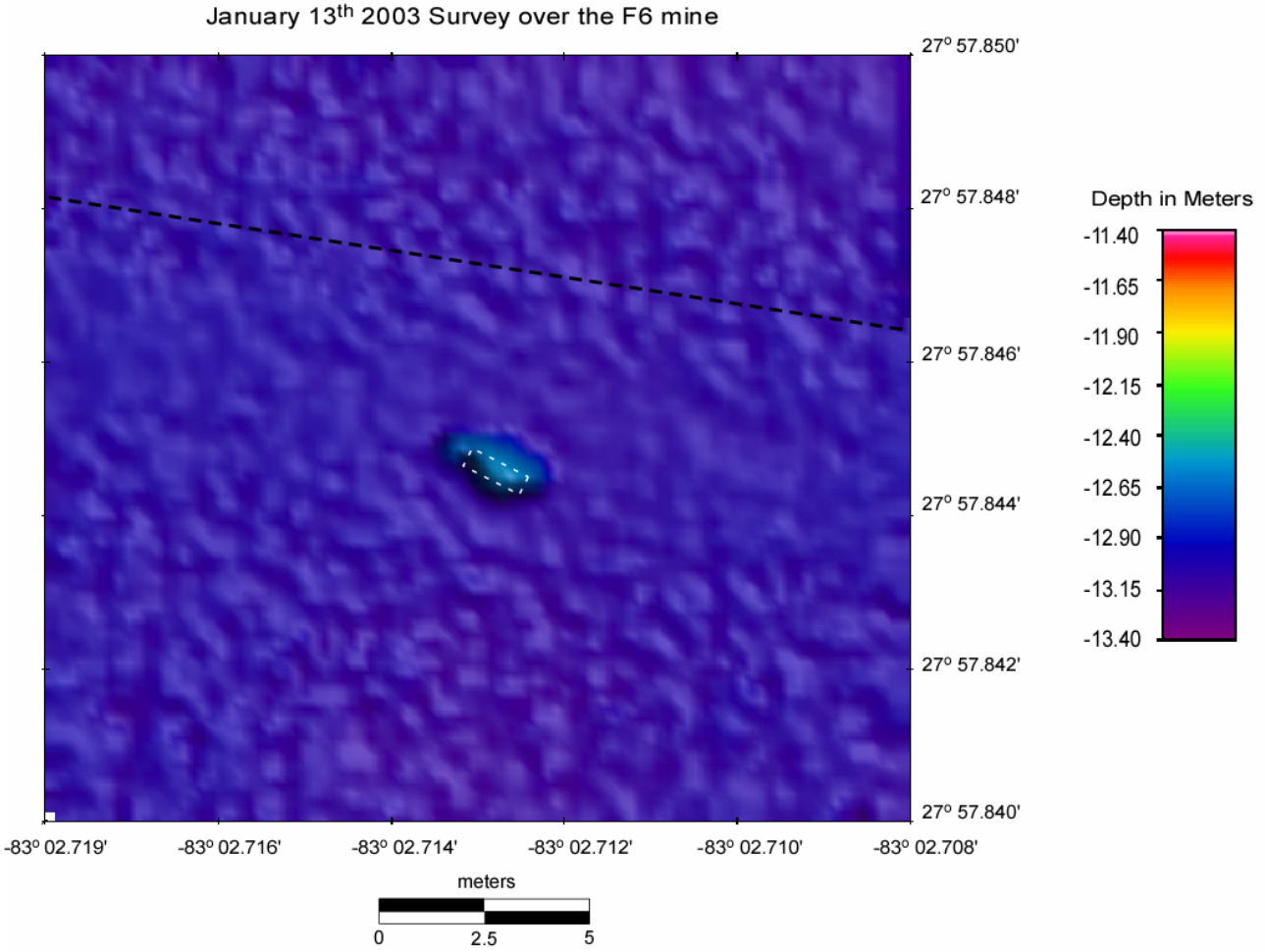

Figure 63. January 13th survey over the F6 mine. The black dashed line indicates the ship's track line during the survey. The mine itself is outlined with a faint white dashed line scaled to the actual dimensions of the mine. The mine outline remains at the same scale and orientation throughout the rest of the F6 multibeam images as a reference.

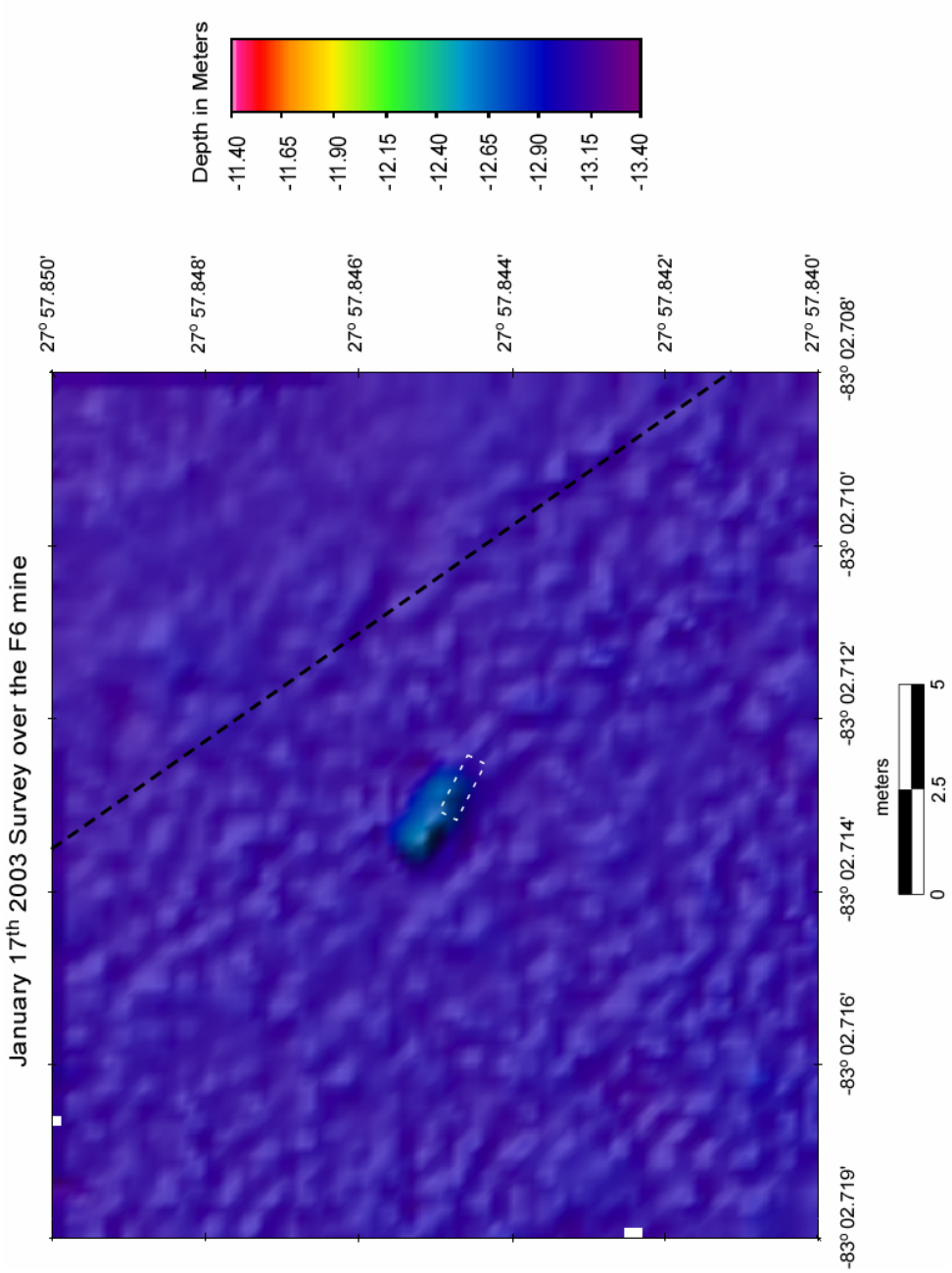

Figure 64. January 17th survey over the F6 mine.

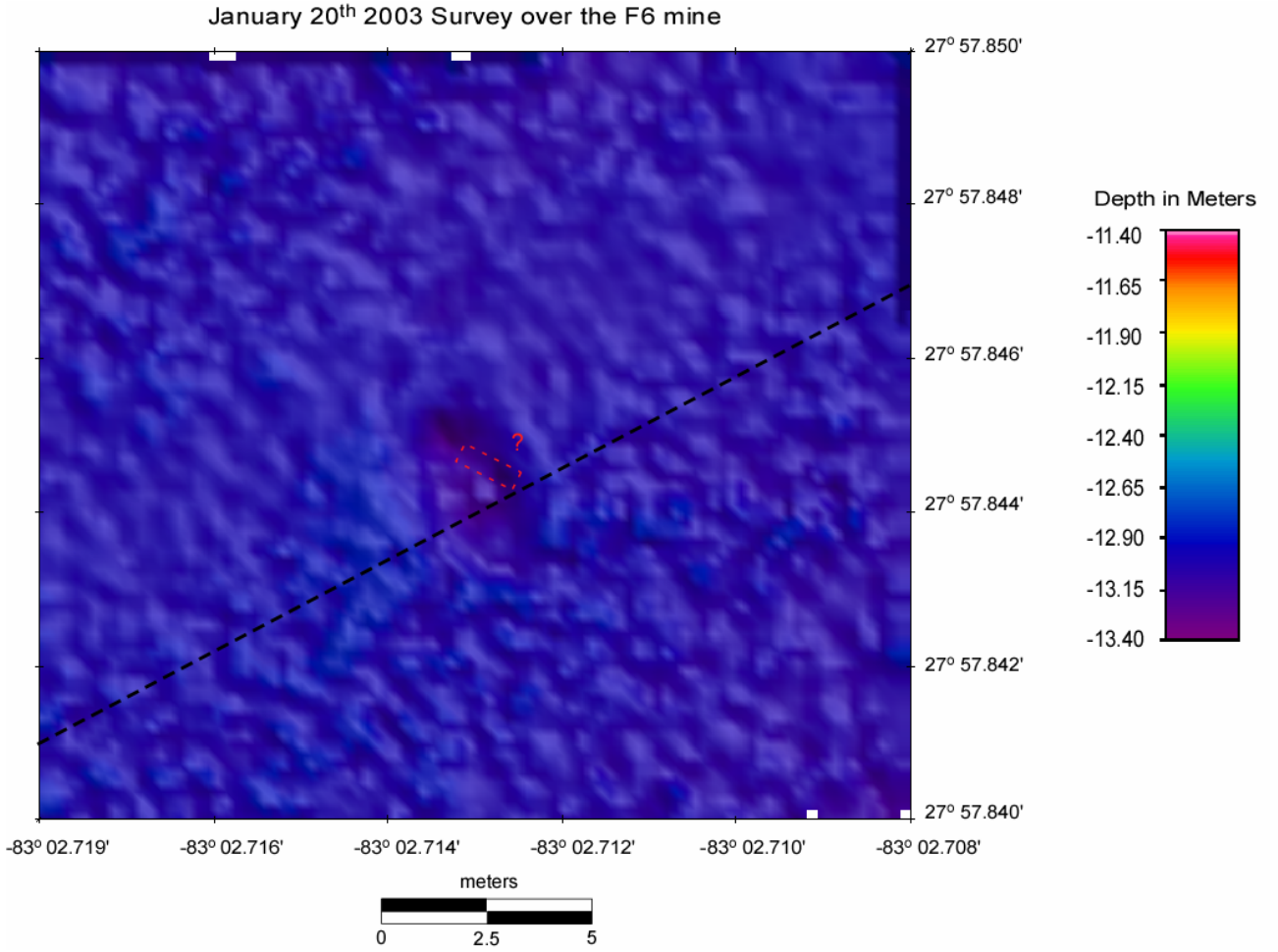

Figure 65. January 20th survey over the F6 mine. The mine is not evident in this image, though a well-defined scour pit can be clearly seen.

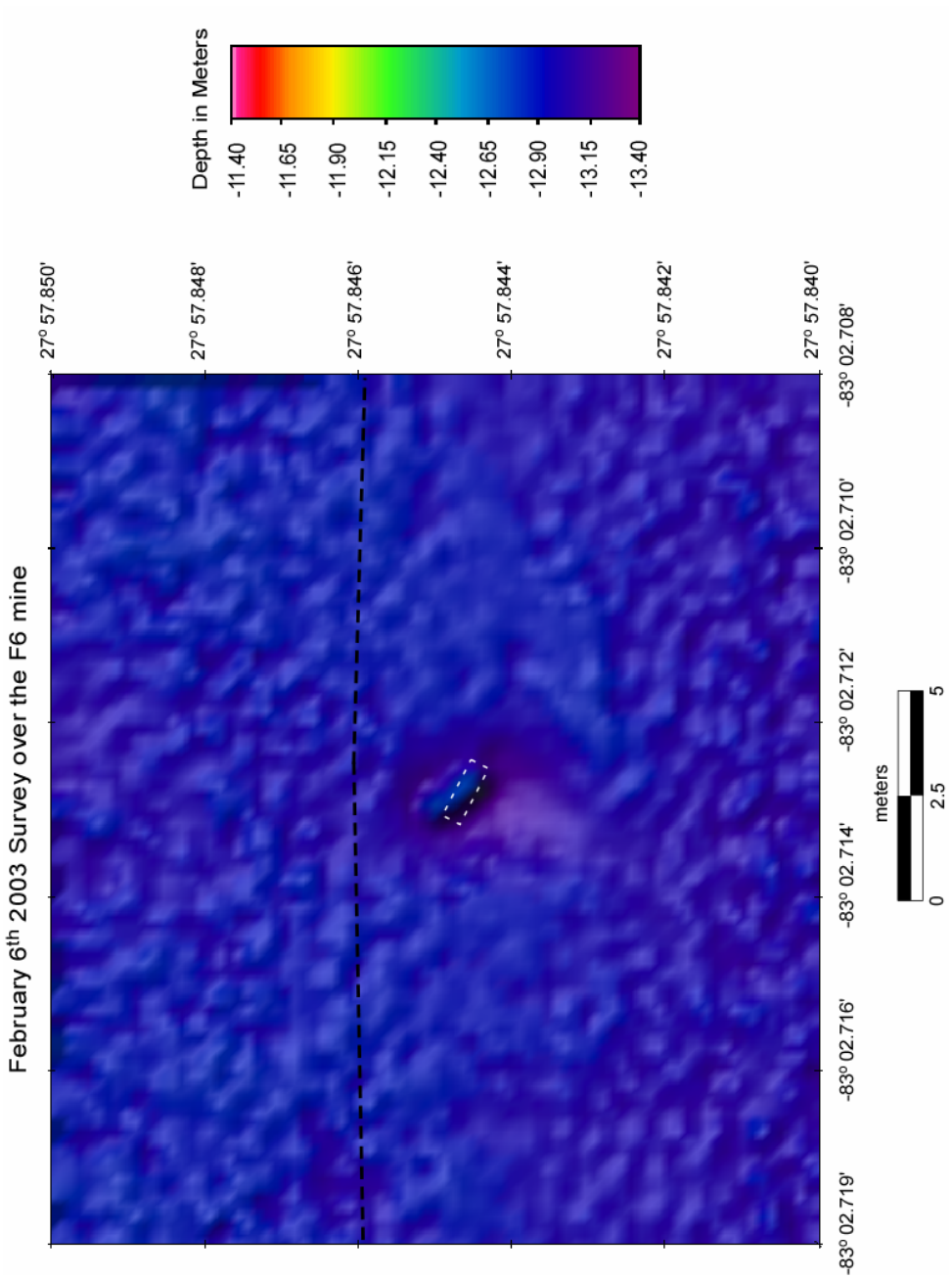

Figure 66. February 6th survey over the F6 mine.

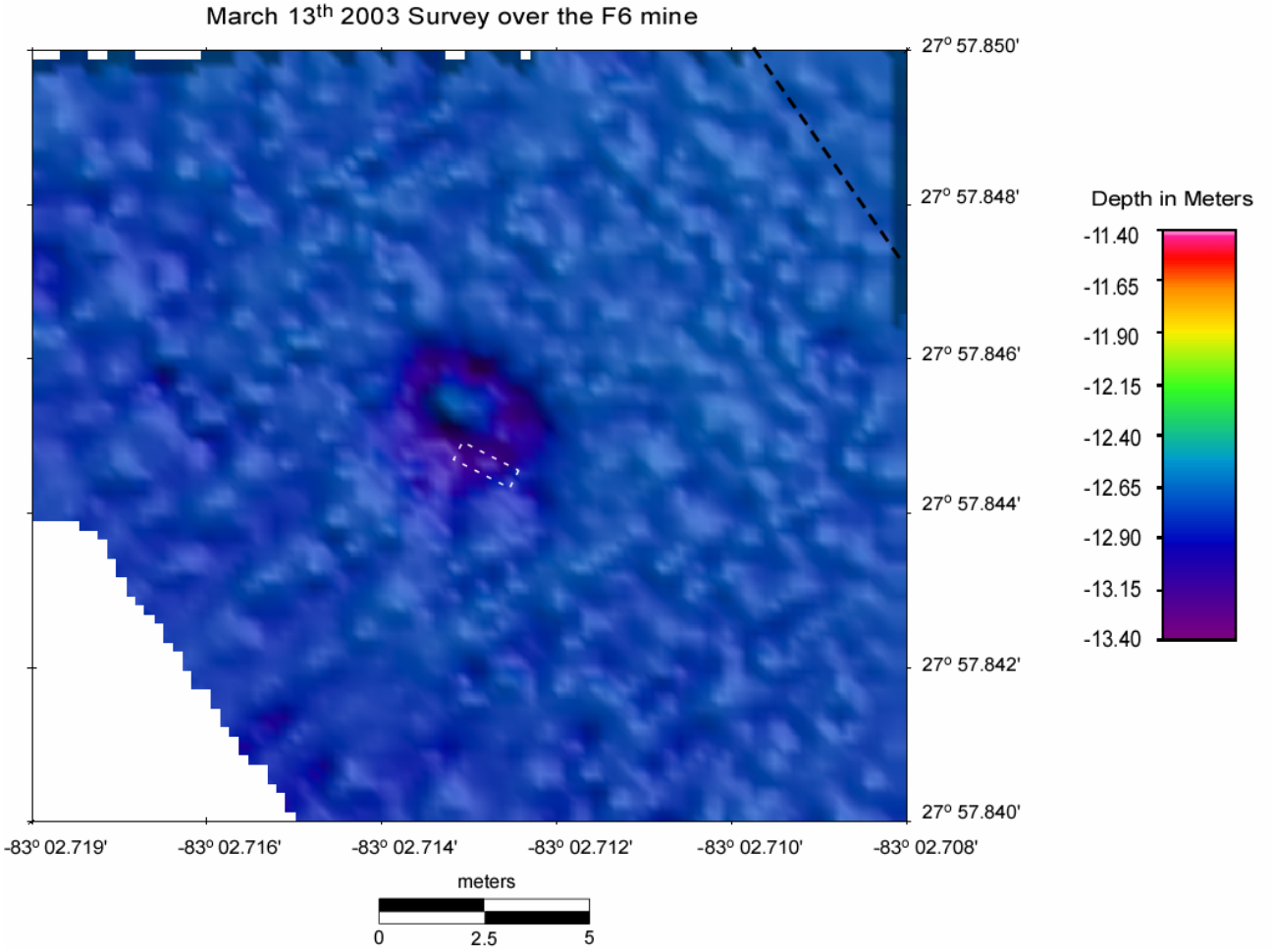

Figure 67. March 13th survey over the F6 mine.

Figure 68. ROV video still image of the F6 mine on March 13, 2003.

horizontal accuracy of the multibeam system. It is also possible that the mine has rolled back and forth within the scour pit, which would account for the sensors not recording the full amount of roll. The depth of the mine is 12.68 meters, indicating a shallowing of 7 centimeters since the survey of February 6th. The combined ± 5-centimeter vertical uncertainty of the multibeam for both the February 6th and March 13th surveys can be used to explain the apparent 7-centimeter offset of mine depth. For other possible explanations, refer to the discussion of the F8 mine. Maximum depth within the scour pit and depth of the ambient seafloor is 13.26 meters and 12.80 meters respectively, indicating a final observed burial of 74.5% for the F6 mine.

Overall, the F6 mine appears to have sunk a total of 0.11 meters (Table 7; Fig. 69). Final observed burial of the F6 mine is 74.5%. Scour around the mine formed a pit 0.46 meters deeper than the surrounding seafloor. The average depth of the seafloor around the mine shows a localized deposition of 0.20 meters over the course of the experiment.

Comparison of F6 Multibeam Observations to the VIMS 2D Burial Model

In order that the VIMS 2D burial model could be compared with observational data from the F6 mine, the model was initialized with a local water depth of 13.00 meters (obtained from the January 13th survey over the mine) and 0% burial. The model was run from the time of mine deployment on January 12th, 2003 at 0000 GMT to the time of the last survey over the mine, March 13th, 2003 at 0900 GMT.

The first comparison between the VIMS model and the multibeam observations occurs for the January 13th survey (Figs. 69 & 70). The observed data shows the mine to

	Jan. 11*	Jan. 13	Jan. 17	Jan. 20	Feb. 6	Mar. 13
Depth of Mine	———	12.57	12.51	____	12.75	12.68
Cumulative Amount of Change	———	———	-0.06	____	0.18	0.11
Average Depth of Seafloor	———	13.00	13.01	12.95	12.93	12.80
Cumulative Amount of Change	———	———	0.01	-0.05	-0.07	-0.20
Scour Visible / Depth of Scour	———	no	yes 13.17	yes 13.18	yes 13.17	yes 13.26
% Mine Burial from Multibeam (± 10.6% due to 5 cm uncertainty of sonar)	0	8.5	0	____	61.7	74.5
% Mine Burial from Model	0	3.8	4.0	62.1	84.6	100.7
Mine Pitch (degrees)	2	2	2	2	2	1
Mine Roll (degrees)	0	-19	-19	-13	-13	3

Table 7. Data table for the F6 mine. All numbers are in meters except where noted. There is no multibeam survey on January 11th.

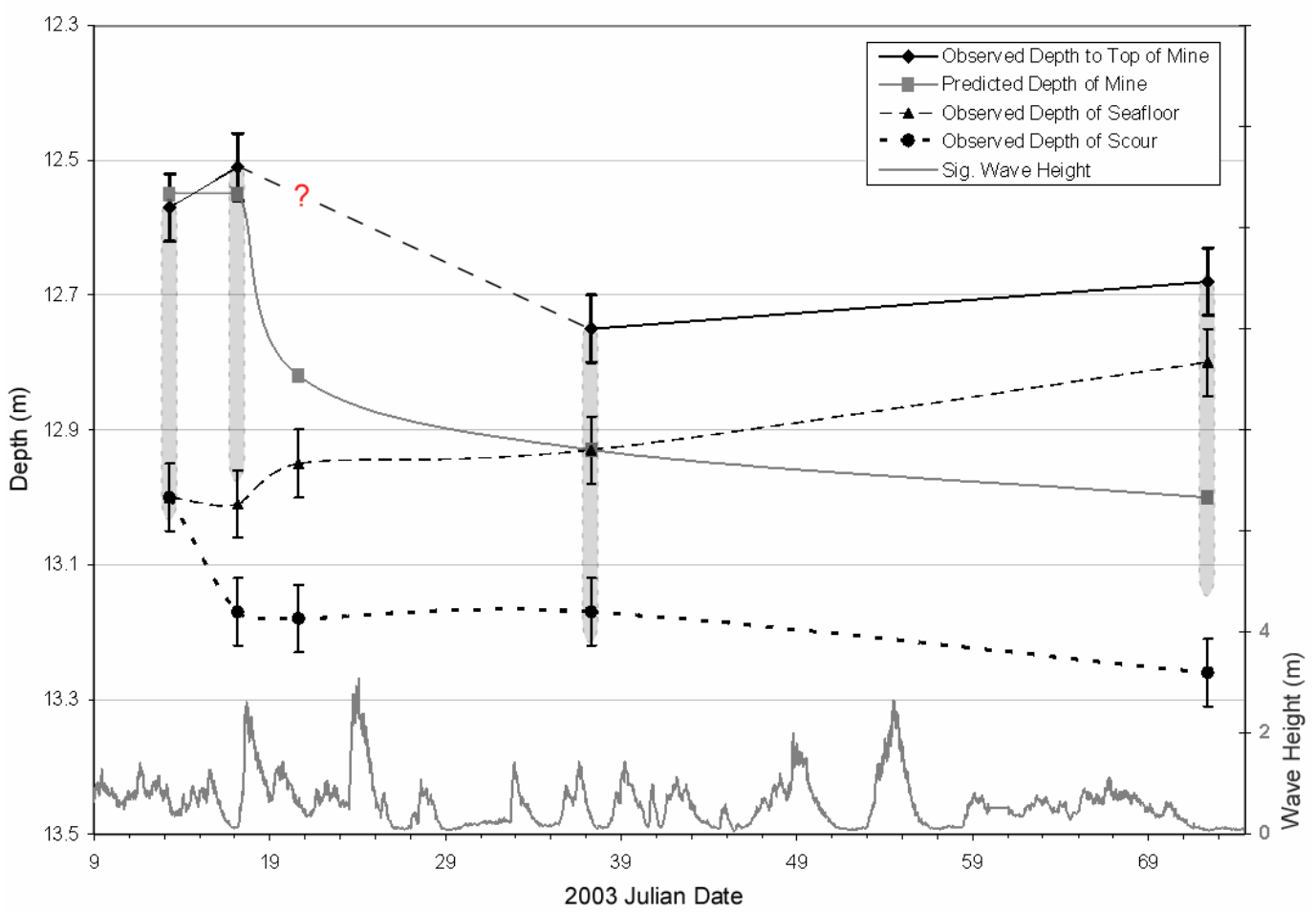

Figure 69. Comparison of multibeam observed (black) and predicted (gray) mine depth for the F6 mine over the course of the experiment. Predicted percent burial of the mine was converted to predicted depth of the mine using the 13.00-meter water depth used to initialize the model. Observed depth of seafloor and depth of scour from the multibeam are plotted as well. Significant wave height is plotted on the right y-axis. Error bars represent the 5-centimeter uncertainty inherent in the multibeam system. The light gray oval represents the F6 mine, and is scaled to the actual dimensions of the mine (length ~ 0.47 m, the diameter of the mine). The mine did not image on Julian day 20.

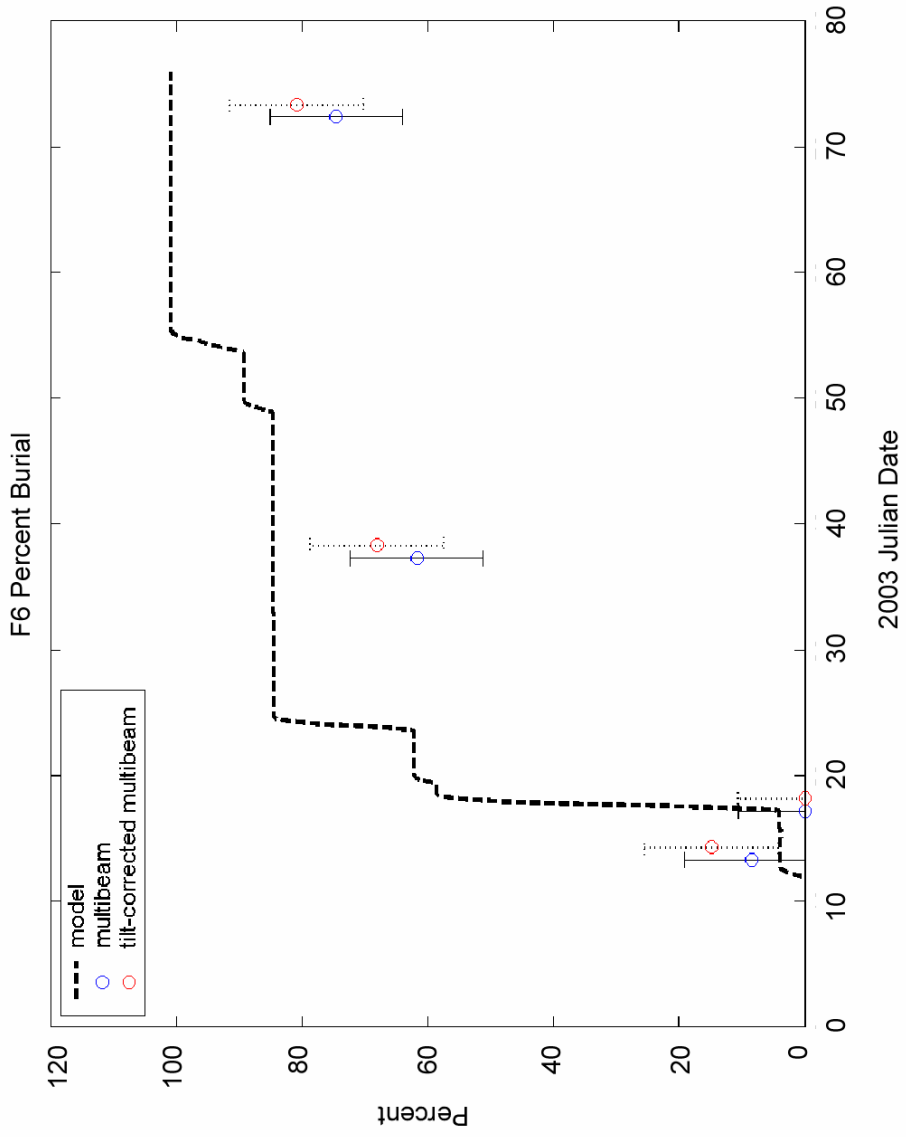

Figure 70. Comparison of the predicted (dashed), observed (blue), and tilt-corrected observed (red) percent burial for the F6 mine over the course of the experiment. Tilt-corrected values have been horizontally offset for clarity. Error bars represent the 5-centimeter uncertainty inherent in the multibeam system.

be 8.5% buried; however, the model only predicts a burial of 3.8%. The discrepancy of 4.7% falls within the ± 10.6% range of uncertainty of the observed multibeam values. The 6-centimeter shallowing of the mine that occurs in the January 17th survey results in an observed burial of zero percent. The model predicts a 4.0% burial for the 17th, and therefore remains within the acceptable range.

At the time of the January 20th survey, the model predicts a 62.1% burial, although no comparison can be made since the mine does not appear in the image (Figs. 69 & 70). The next comparison occurs for the February 6th survey and shows a discrepancy of 22.9%, which falls outside the acceptable ± 10.6% range. The observed burial at the time of this survey is 61.7%, while the model predicts a burial of 84.6%. The model prediction from March 13th of 100.7% falls well outside this range as well, when compared to the observed burial of 74.5%. This offset of 26.2% is the largest discrepancy between the model predictions and the observed data for the 6 mines located in the shallow fine sand site.

The F7 Mine

Temporal Analysis of Scour and Burial

The optical instrumented mine number 7 (F7) was located in the coarse sand site lying within a rippled scour depression. It was deployed on January 11th 2003, and repositioned by divers on January 12th, 2003 at ~ 2000 GMT. The January 13th survey was the first to pass over F7 after its deployment (Fig. 71). No ripples can be distinguished in the image, despite their presence around the F8 mine deployed in the same location. The observed orientation of the mine appears north northeast by south

southwest, and the depth to the top of the mine is 13.34 meters. The depth of the ambient seafloor around the mine is 13.83 meters, a difference of 0.49 meters. The diameter of the F7 mine is only 0.47 meters; however, the 2-centimeter discrepancy can be accounted for by the ± 5-centimeter uncertainty of the multibeam system. It is also possible that the mine is resting on a mound of sand slightly shallower than the surrounding seafloor. The observed percent burial for this survey is zero.

A quadpod and one spider were deployed in the coarse sand site near the F7 mine on January 16th, 2003 and should be visible in subsequent images. The mine does not image very well during the January 17th survey, despite the multibeam passing directly overhead (Fig. 72). The spider does not show up at all in this image, while the quadpod, on the other hand, is quite apparent. The spider has a relatively small profile (top surface area = 0.07 m^2), so it is possible that the sonar was unable to get enough hits off the surface in order to adequately image it. The depth to the top of the mine is 13.27 meters, 0.07 meters shallower than on January 13th. There has been no change in the degree of tilt for the F7 mine since January 13th; however, the combined vertical uncertainty of the multibeam from the January 13th and January 17th surveys can account for this offset. The depth of the seafloor around the mine has increased to 13.87 meters, a difference of 0.60 meters from the observed top of the mine. This offset is 13 centimeters greater than the diameter of the mine. Assuming the sonar's vertical uncertainty accounts for 5 centimeters, there is still a discrepancy of 8 centimeters that cannot be explained. Although uncertainty in the sound velocity profile is a possible explanation, the fact that a shallowing of the F8 mine did not occur during the same survey, makes it an unlikely cause. As mentioned in Chapter 1, the ± 5-centimeter vertical uncertainty of the sonar

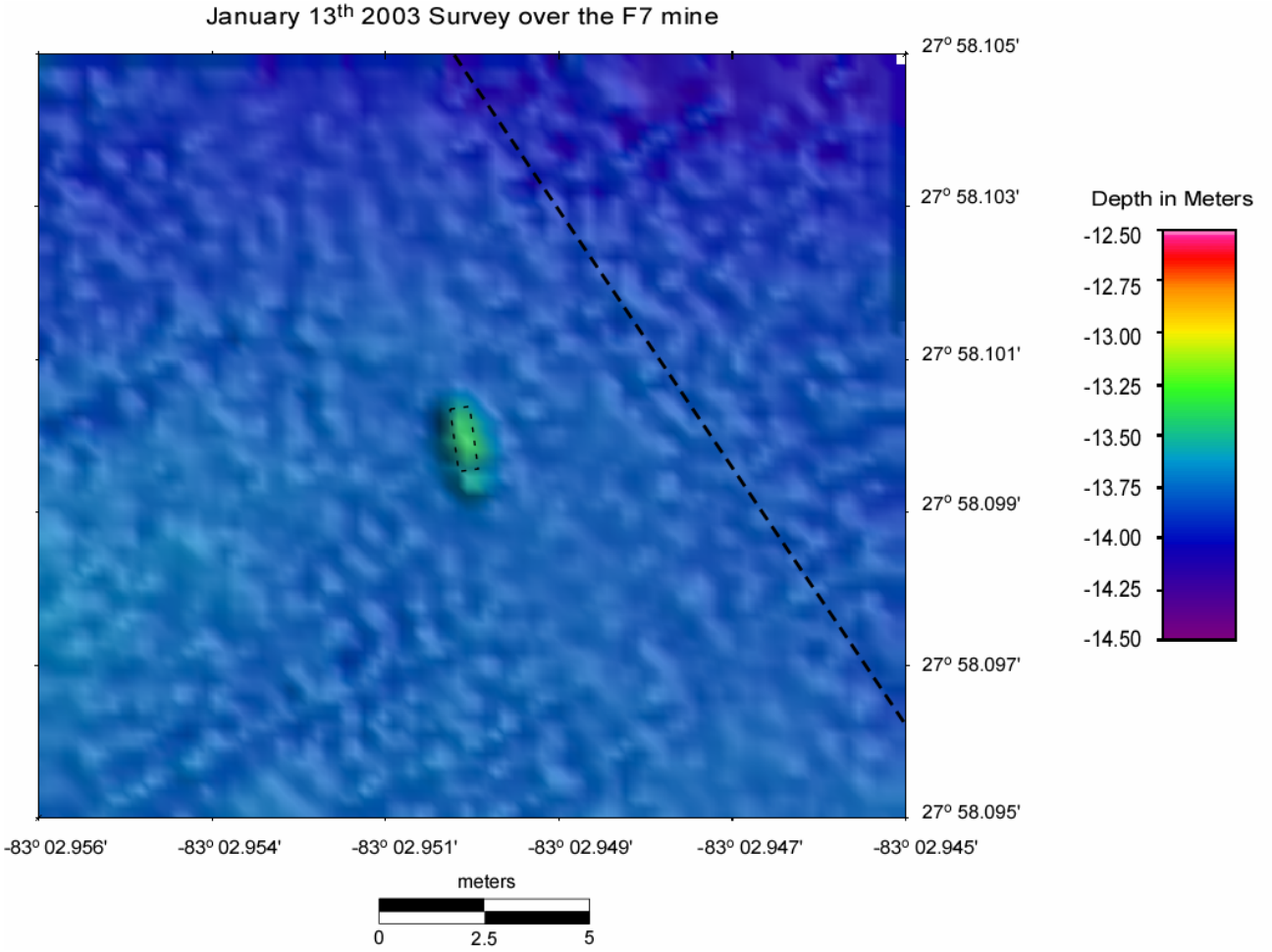

Figure 71. January 13th survey over the F7 mine. The black dashed line indicates the ship's track line during the survey. The mine itself is outlined with a faint black dashed line scaled to the actual dimensions of the mine. The mine outline remains at the same scale and orientation throughout the rest of the F7 multibeam images as a reference.

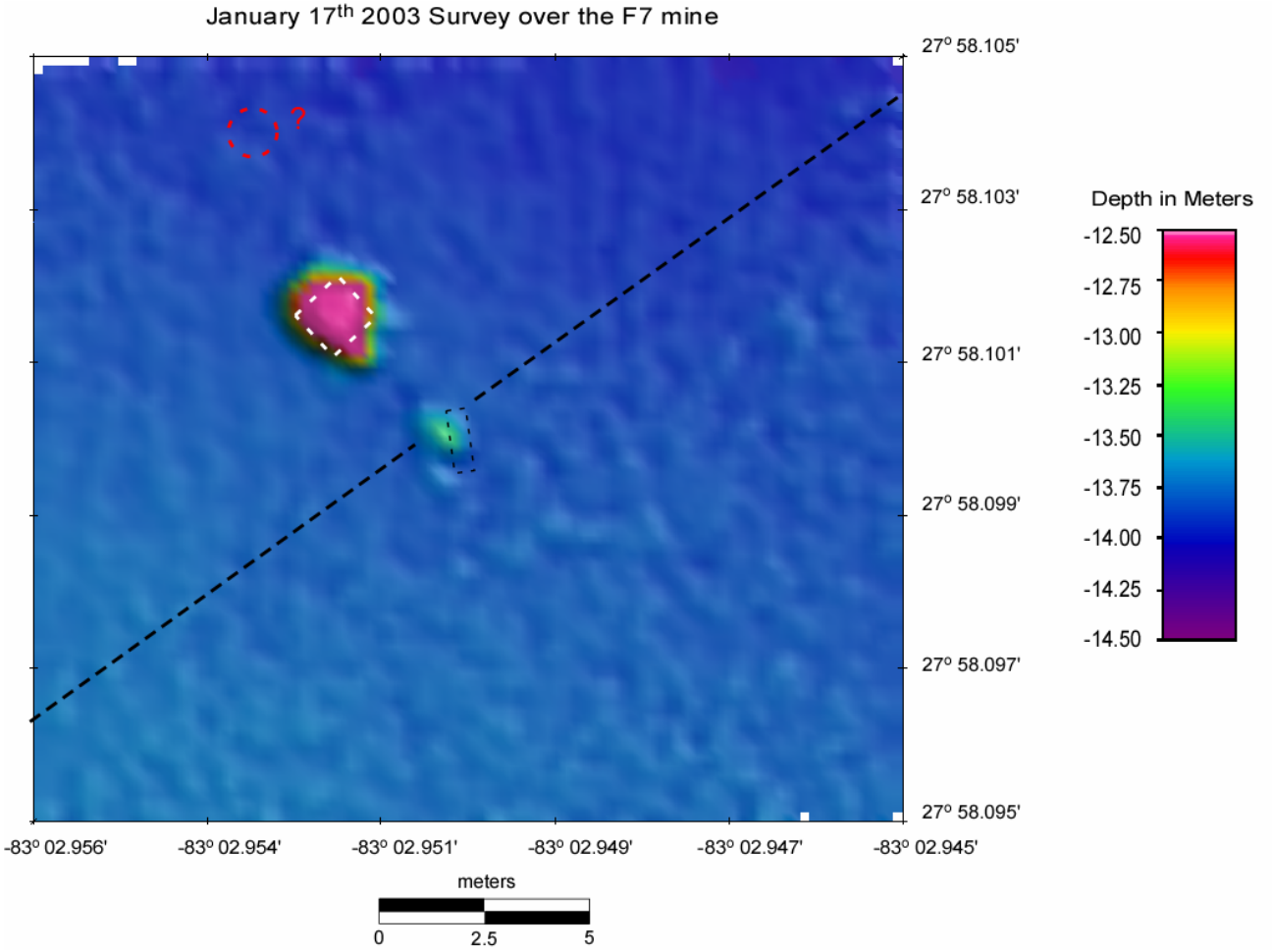

Figure 72. January 17th survey over the F7 mine. The quadpod images quite clearly, and is outlined with a white-dashed square scaled to the dimensions of the quadpod. The red dashed circle with a question marks denotes the position of the spider that did not image.

was estimated based on the shallow depth in which this study took place, and use of the POS MV positioning system equipped with RTK. This discrepancy may be an indicator that the actual vertical uncertainty of the multibeam system may be closer to 10 centimeters. Given this offset between the mine depth and the depth of the ambient seafloor, the amount of burial at the time of this survey is assumed to be zero. Faint ripples trending approximately north south are apparent in the image to the north of the track line. The ripples have an average wavelength of ~ 1.5 meters and a height of ~ 10 centimeters.

The mine has sunk 0.10 meters in the January 20th image, resulting in a depth of 13.35 meters (Fig. 73). The depth of the surrounding seafloor is 13.79 meters, giving a percent burial of 10.6. The ripple field is no longer visible at this time, and there is no scour evident. Neither the quadpod nor the spider show up during this survey or the subsequent one from February 6th (Fig. 74). The quadpod presents a greater profile than the spider; however, the legs of the quadpod are quite slim and come up over the quapod's top platform to form a t-junction (Fig. 8). It is possible that the beams of the sonar hit these legs and were reflected away rather than back to the sonar. It is also possible that a bubble sweep occurred causing interference at the time the sonar passed over these instruments. The depth to the top of the mine in the February 6th image is 13.35 meters. This apparent 2-centimeter decrease in depth can be accounted for by the vertical uncertainty of the multibeam. The depth of the seafloor is 13.81 meters, decreasing the amount of burial observed to 2.1%.

The March 13th survey over the F7 mine is the only one to image both the spider and the quadpod as well as the mine. A ripple field is clearly evident trending north

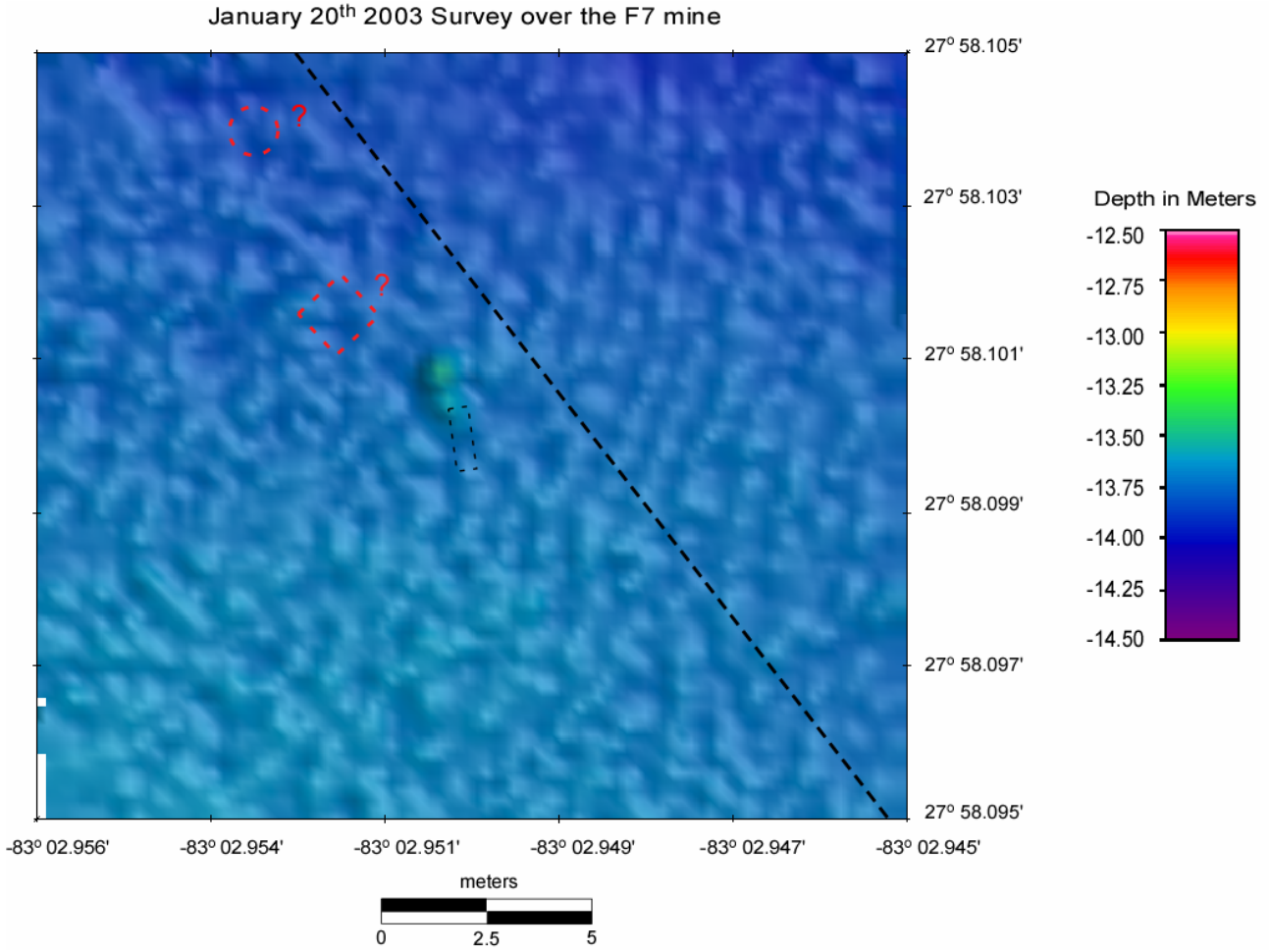

Figure 73. January 20th survey over the F7 mine. Neither the quadpod nor the spider are evident in this image. Their deployed locations are outlined with a dashed red line.

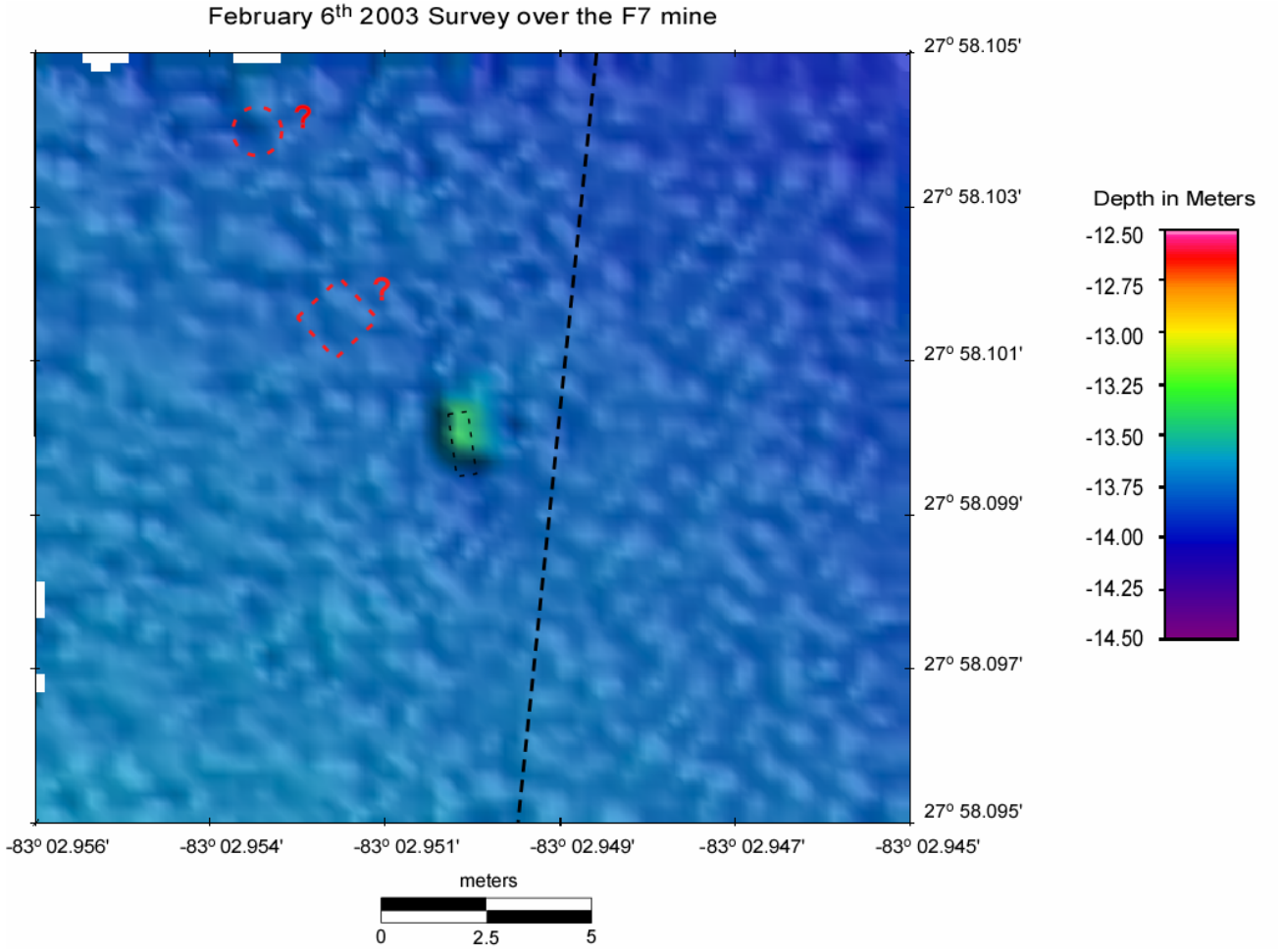

Figure 74. February 6th survey over the F7 mine. Again, neither the quad not the spider appear in this image.

northwest by south southeast across the image with an average wavelength of ~ 1.0 meters and a height of 15 centimeters (Figs. 75 & 76). The depth to the top of the mine has remained constant at 13.35 meters since the survey of February 6th. The average seafloor depth around the mine is 13.76 meters, giving an observed burial of 12.8%.

Between the January 13th and March 13th surveys, the F7 mine sunk a total of 1 centimeter (Table 8; Fig. 77). The average depth of the seafloor around the mine decreased 7 centimeters during this time, mainly due to the formation of rippled bedforms in the area. The final observed burial for the F7 mine was 12.8%.

Comparison of F7 Multibeam Observations to the VIMS 2D Burial Model

It has been shown that the VIMS 2D burial model does not work well for coarse sand sites where rippled bedforms are prevalent (see Chapter 2; Traykovski et al., 2005; Trembanis et al., 2005). . The same holds true for the comparisons with the F7 mine, which resides in a rippled scour depression. The model was initialized with a local water depth of 13.83 meters and 0% burial. It was run from the time the mine was redeployed by divers, January 12th, 2003 at 0000 GMT to the time of the last multibeam survey over the mine on March 13th, 2003 at 0500 GMT.

The first two comparisons between the model predictions and the observed data, January 13th and January 17th, are in agreement with a 0% burial in both cases (Figs. 77 & 78). The January 20th comparison; however, shows the model diverging from the multibeam data with a predicted burial of 39.0% and an observed burial of only 10.1%. The 28.4% discrepancy is well outside the ± 10.6% range of the multibeam. The model

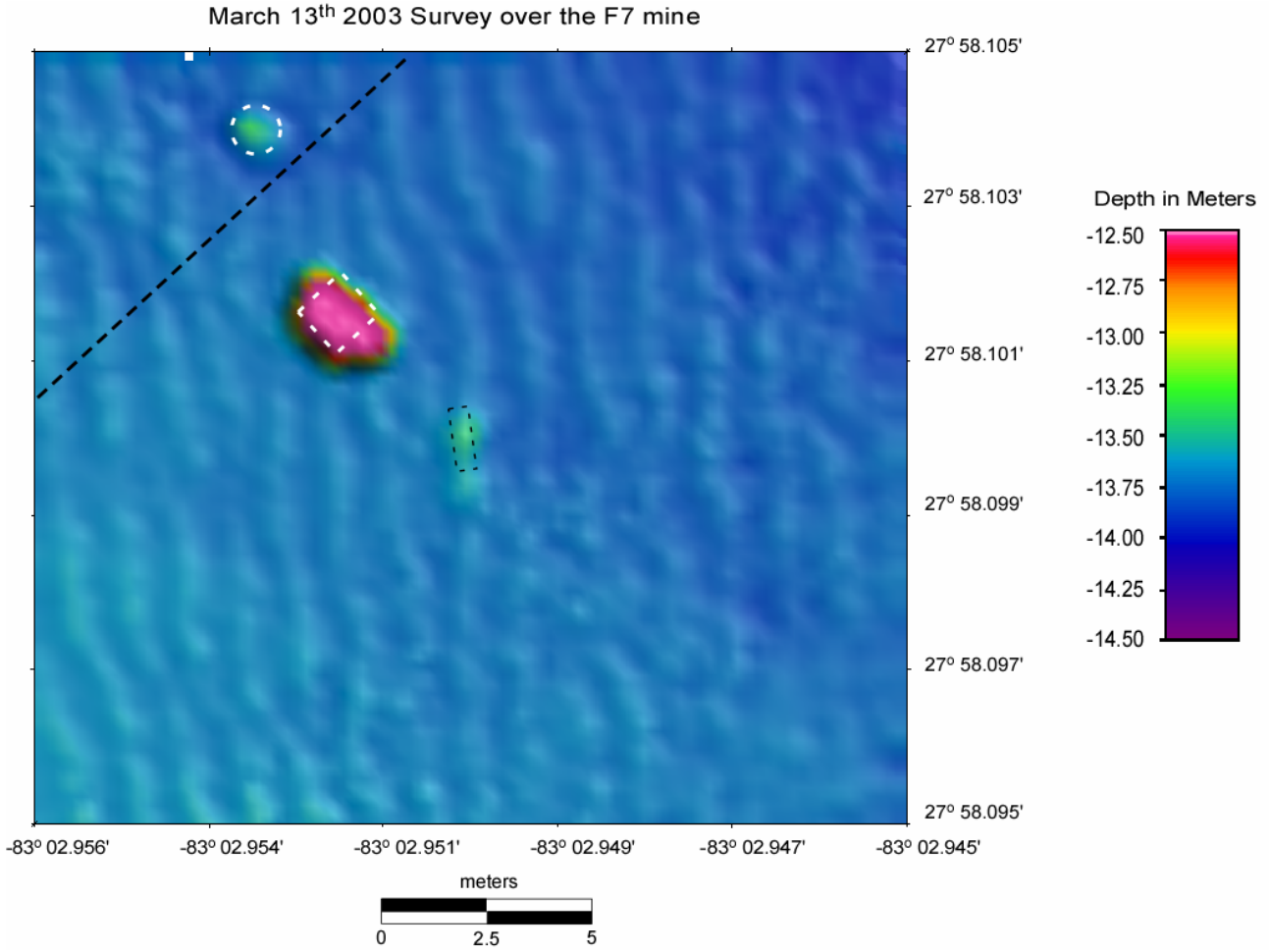

Figure 75. March 13th survey over the F7 mine. Note that both the spider and the quadpod are now evident.

Figure 76. ROV video still image of the F7 mine on March 13, 2003.

	Jan. 11*	Jan. 13	Jan. 17	Jan. 20	Feb. 6	Mar. 13
Depth of Mine	_____	13.34	13.27	13.37	13.35	13.35
Cumulative Amount of Change	_____	_____	-0.07	0.03	0.01	0.01
Average Depth of Seafloor	_____	13.83	13.87	13.79	13.81	13.76
Cumulative Amount of Change	_____	_____	0.04	-0.04	-0.02	-0.07
Scour Visible / Depth of Scour	_____	no	no	yes 13.86	yes 13.99	no
% Mine Burial from Multibeam (± 10.6% due to 5 cm uncertainty of sonar)	0	0	0	10.6	2.1	12.8
% Mine Burial from Model	0	0	0	39.0	68.4	85.1
Mine Pitch (degrees)	2	1	1	2	1	1
Mine Roll (degrees)	-5	-4	0	2	4	2

Table 8. Data table for the F7 mine. All numbers are in meters except where noted. There is no multibeam survey on January 11th.

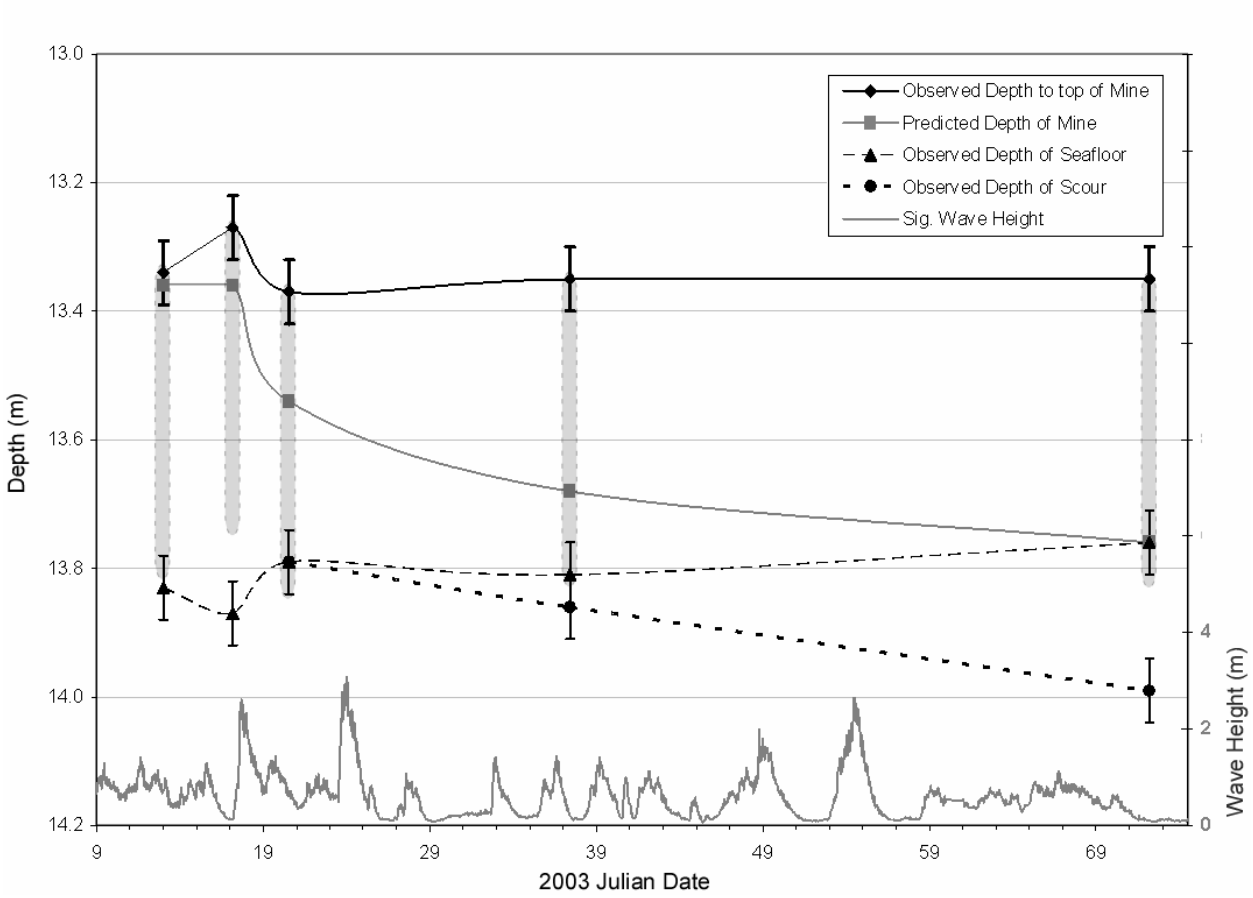

Figure 77. Comparison of multibeam observed (black) and predicted (gray) mine depth for the F7 mine over the course of the experiment. Predicted percent burial of the mine was converted to predicted depth of the mine using the 13.83-meter water depth used to initialize the model. Observed depth of seafloor and depth of scour from the multibeam are plotted as well. Significant wave height is plotted on the right y-axis. Error bars represent the 5-centimeter uncertainty inherent in the multibeam system. The light gray oval represents the F7 mine, and is scaled to the actual dimensions of the mine (length ~ 0.47 m, the diameter of the mine).

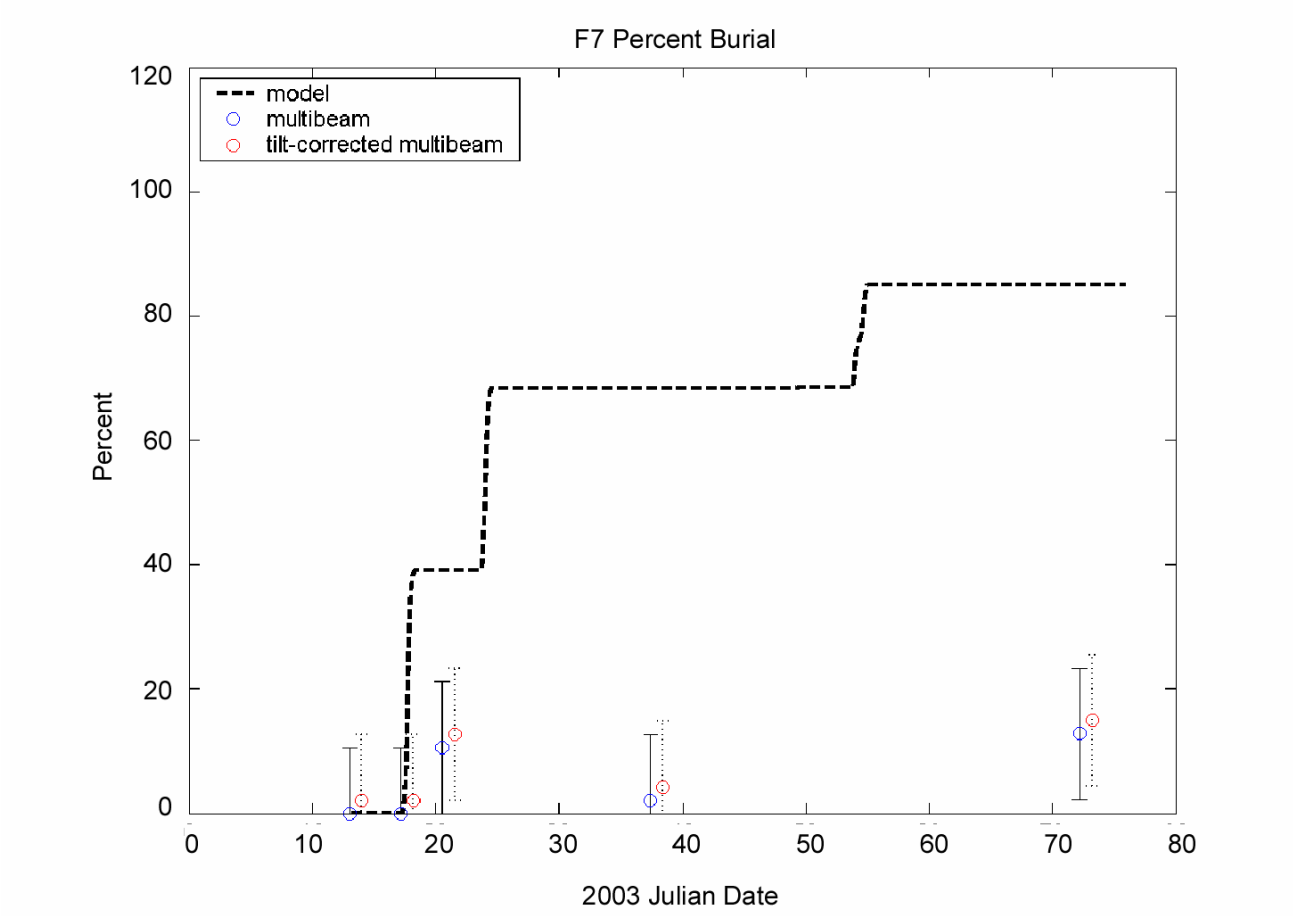

Figure 78. Comparison of the predicted (dashed), observed (blue), and tilt-corrected observed (red) percent burial for the F7 mine over the course of the experiment. Tilt-corrected values have been horizontally offset for clarity. Error bars represent the 5-centimeter uncertainty inherent in the multibeam system.

continues to significantly diverge from field observations for both the February 6th and March 13th comparisons. On February 6th, the model predicts a 68.4% burial of the F7 mine while the multibeam data only show a 2.1% burial, an offset of 66.3%. This offset increases to 72.3% for March 13th, with a predicted burial of 85.1% and an observed burial of only 12.8%. These discrepancies suggest that rippled bedforms cannot be ignored and should be included in future modeling efforts.

The F9 Mine

Temporal Analysis of Scour and Burial

The optical instrumented mine number 9 (F9) was one of two mines located in the deep fine sand site. F9 was deployed on January 11th, 2003 in a water depth of 13.88 meters and repositioned by divers on January 13th to lay in an east-west orientation. The first survey to image the mine after deployment was on January 13th (Fig. 79). The mine appears somewhat distorted in the image as a result of the target detection mode on the multibeam sonar. The depth to the top of the mine is 13.37 meters, and the surrounding seafloor has an average depth of 13.88 meters. The diameter of the mine is 0.47 meters, a discrepancy of 4 centimeters. This discrepancy could be a result of the vertical accuracy of the multibeam or of mine resting on a mound of sand slightly higher than the surrounding seabed. Pitch sensors in the mine recorded a 2° tilt at the time of this survey, which could account for up to 3 centimeters of the offset. The observed amount of burial for F9 during this survey is 0%.

The survey from January 17th did not pass over the deep fine sand site; therefore, the next observation occurs during the January 20th survey (Fig. 80). The depth to the top

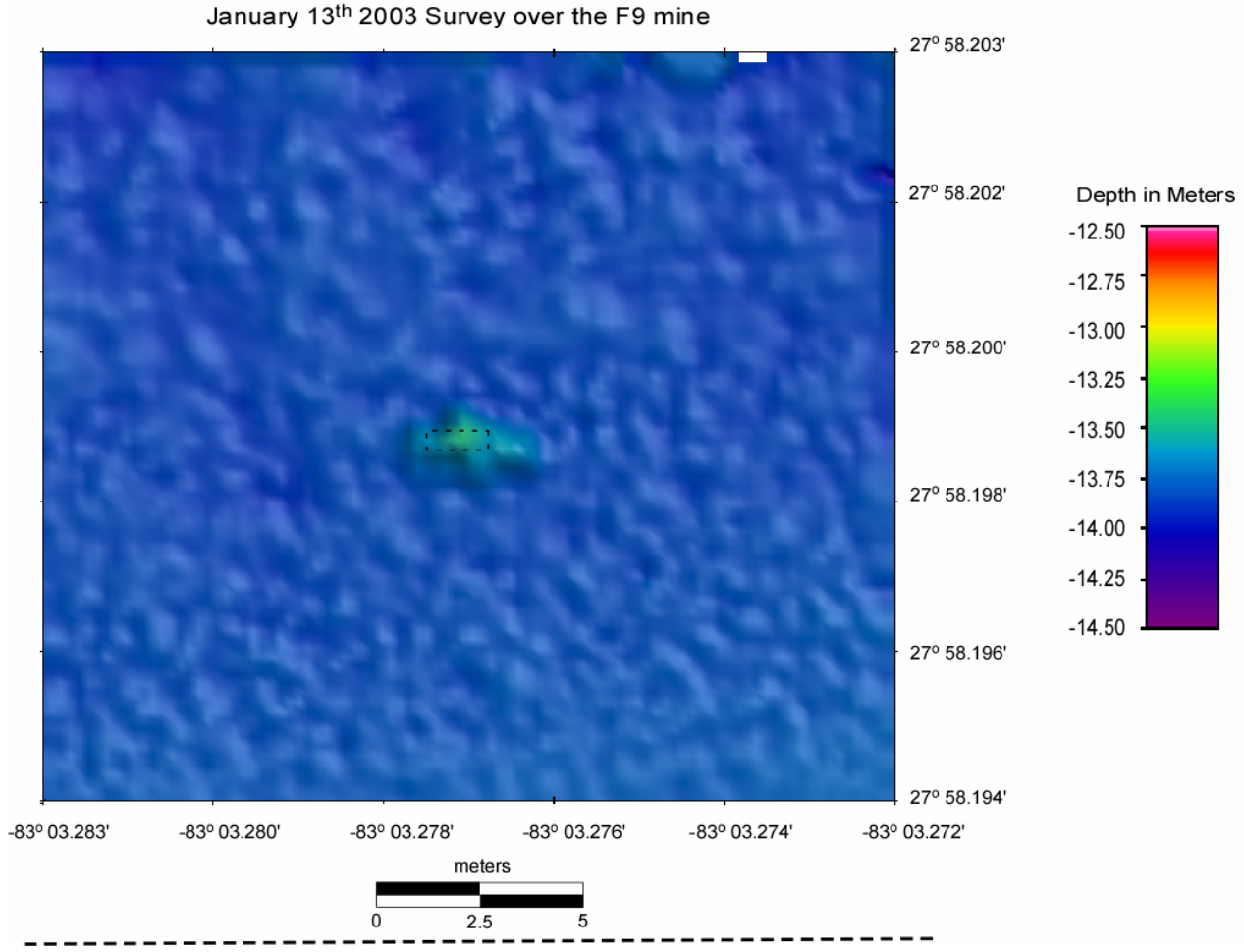

Figure 79. January 13th survey over the F9 mine. The black dashed line indicates the ship's track line during the survey. In this image, the track line falls outside the gridded area. The mine itself is outlined with a faint black dashed line scaled to the actual dimensions of the mine. The mine outline remains at the same scale and orientation throughout the rest of the F9 multibeam images as a reference.

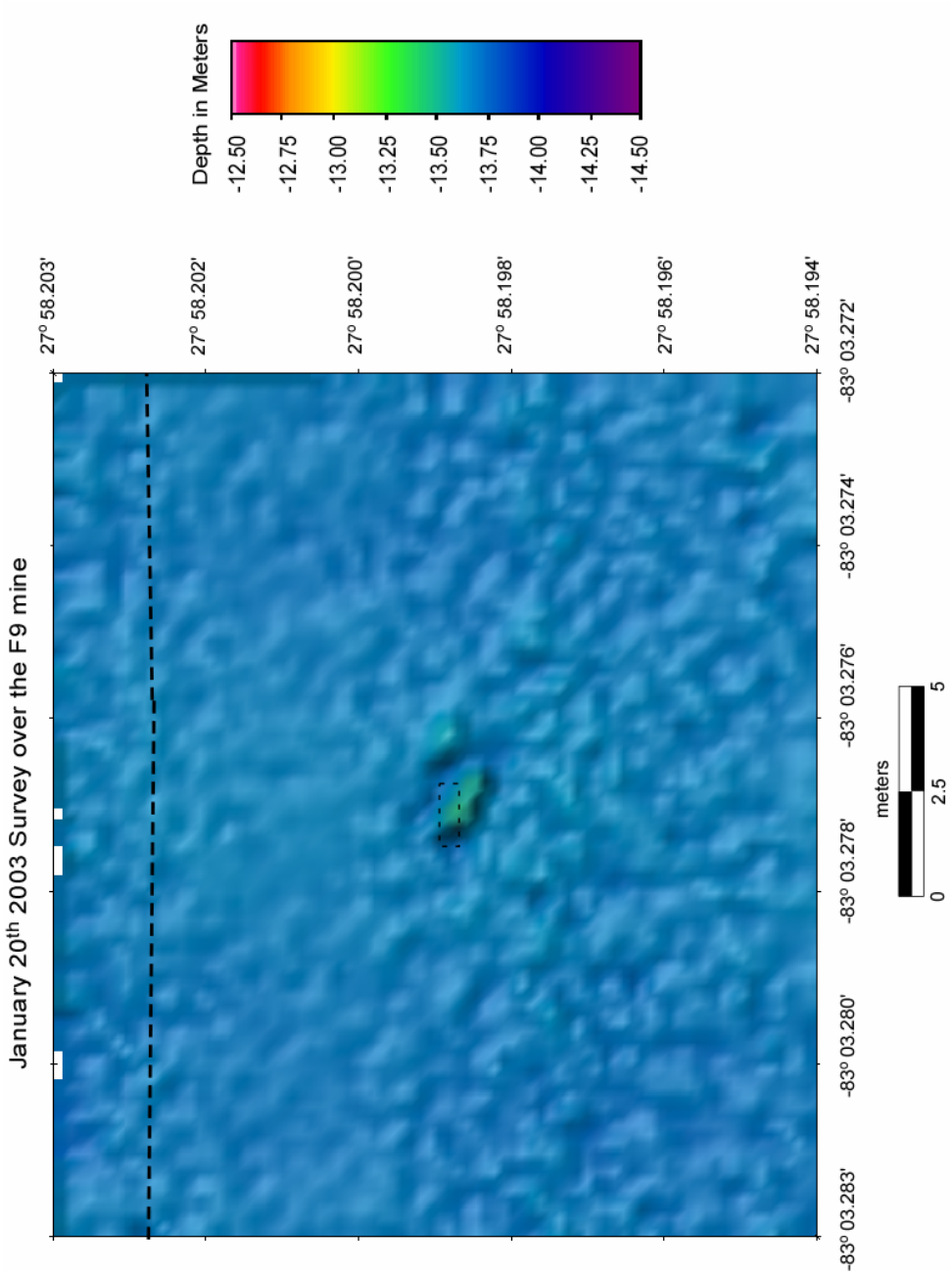

Figure 80. January 20th survey over the F9 mine.

of the mine is now 13.39 meters, 2 centimeters shallower than on the 13th. The ambient seafloor shows a localized deposition of 0.18 meters, depth is 13.70 meters, and results in an observed burial of 34.0%. Scour has started to develop around the mine with a maximum depth of 13.86 meters. By February 6th, the scour has extended to form a ring around the mine (Fig. 81). Maximum depth with the scour pit has increased to 13.94 meters. The seafloor depth around the mine is now 13.67 meters and the depth of mine itself is 13.45 meters, giving an observed burial of 53.2%. The mine appears distorted in this image despite the fact that the target detection mode on the multibeam was turned off.

The change in seafloor depth is obvious in the March 13th image; average depth of the seafloor around the mine is now 13.47 meters (Figs. 82 & 83). This sedimentation of 0.20 meters is not just observed around the scour pit, but occurs over the whole grid. The depth of the mine is 13.41 meters, a decrease of 4 centimeters since February 6th. The tilt of the mine has actually decreased since the last survey, indicating this discrepancy is most likely a result of the ± 5-centimeter vertical uncertainty of the multibeam rather than a tilt effect. Maximum depth in the scour pit has decreased to 13.85 meters. The mine appears to be 87.2% buried at this time.

The F9 mine has sunk a total of 0.04 meters over the course of the experiment, resulting in a final observed burial of 87.2% (Table 9; Fig. 84). The average seafloor depth has steadily shallowed since the first survey, for a total shallowing of 0.41 meters.

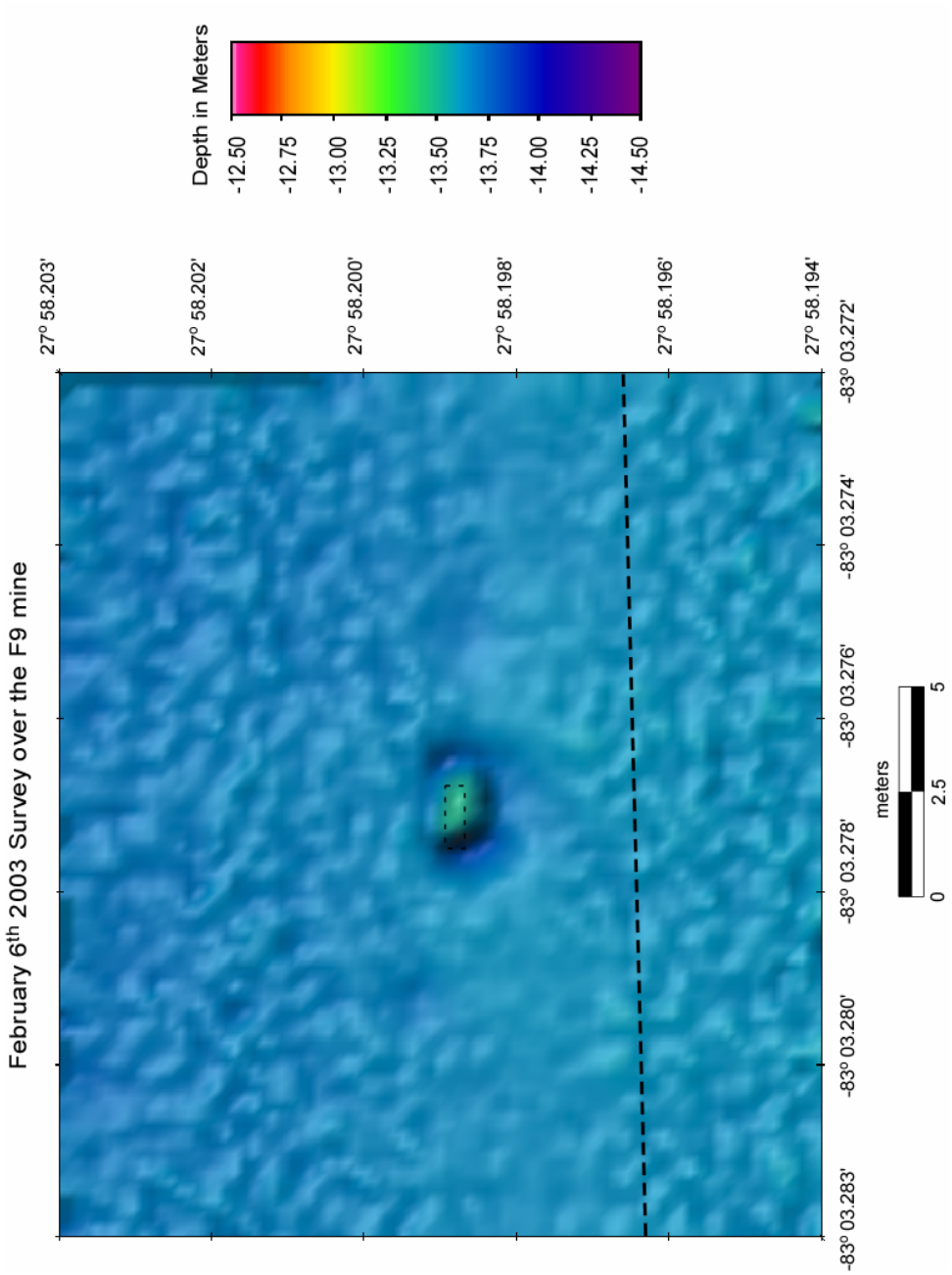

Figure 81. February 6th survey over the F9 mine.

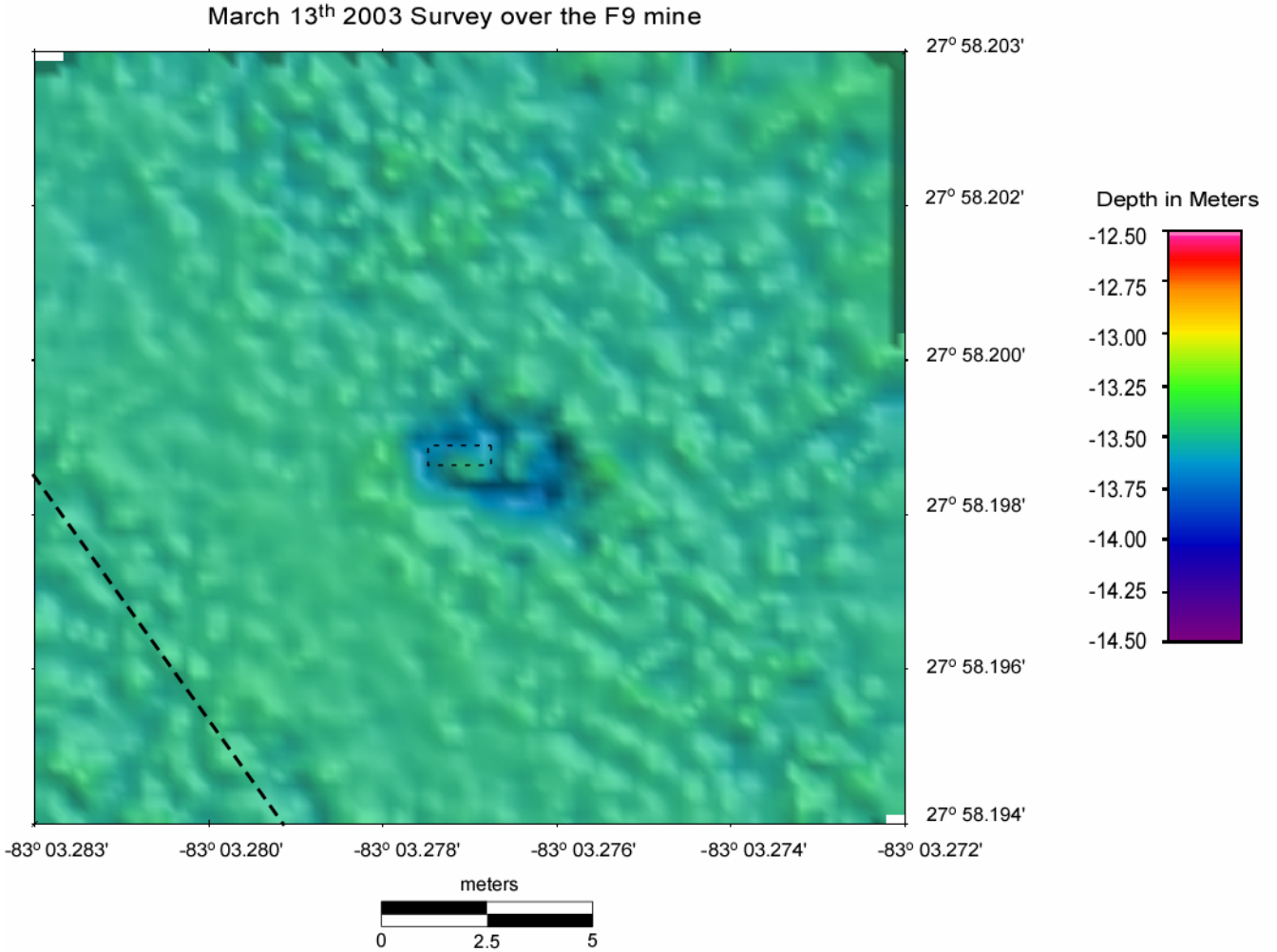

Figure 82. March 13th survey over the F9 mine.

Figure 83. ROV video still image of the F9 mine on March 13, 2003.

	Jan. 11*	Jan. 13	Jan. 17	Jan. 20	Feb. 6	Mar. 13
Depth of Mine	_____	13.37	No image	13.39	13.45	13.41
Cumulative Amount of Change	_____	_____	_____	0.02	0.08	0.04
Average Depth of Seafloor	_____	13.88	_____	13.70	13.67	13.47
Cumulative Amount of Change	_____	_____	_____	-0.18	-0.21	-0.41
Scour Visible / Depth of Scour	_____	no	_____	yes 13.86	yes 13.94	yes 13.85
% Mine Burial from Multibeam (± 10.6% due to 5 cm uncertainty of sonar)	0	0	_____	34.0	53.2	87.2
% Mine Burial from Model	0	0	_____	53.8	77.1	95.1
Mine Pitch (degrees)	2	2	_____	1	3	1
Mine Roll (degrees)	-4	1	_____	-2	-22	-18

Table 9. Data table for the F9 mine. All numbers are in meters except where noted. There is no multibeam survey on January 11th.

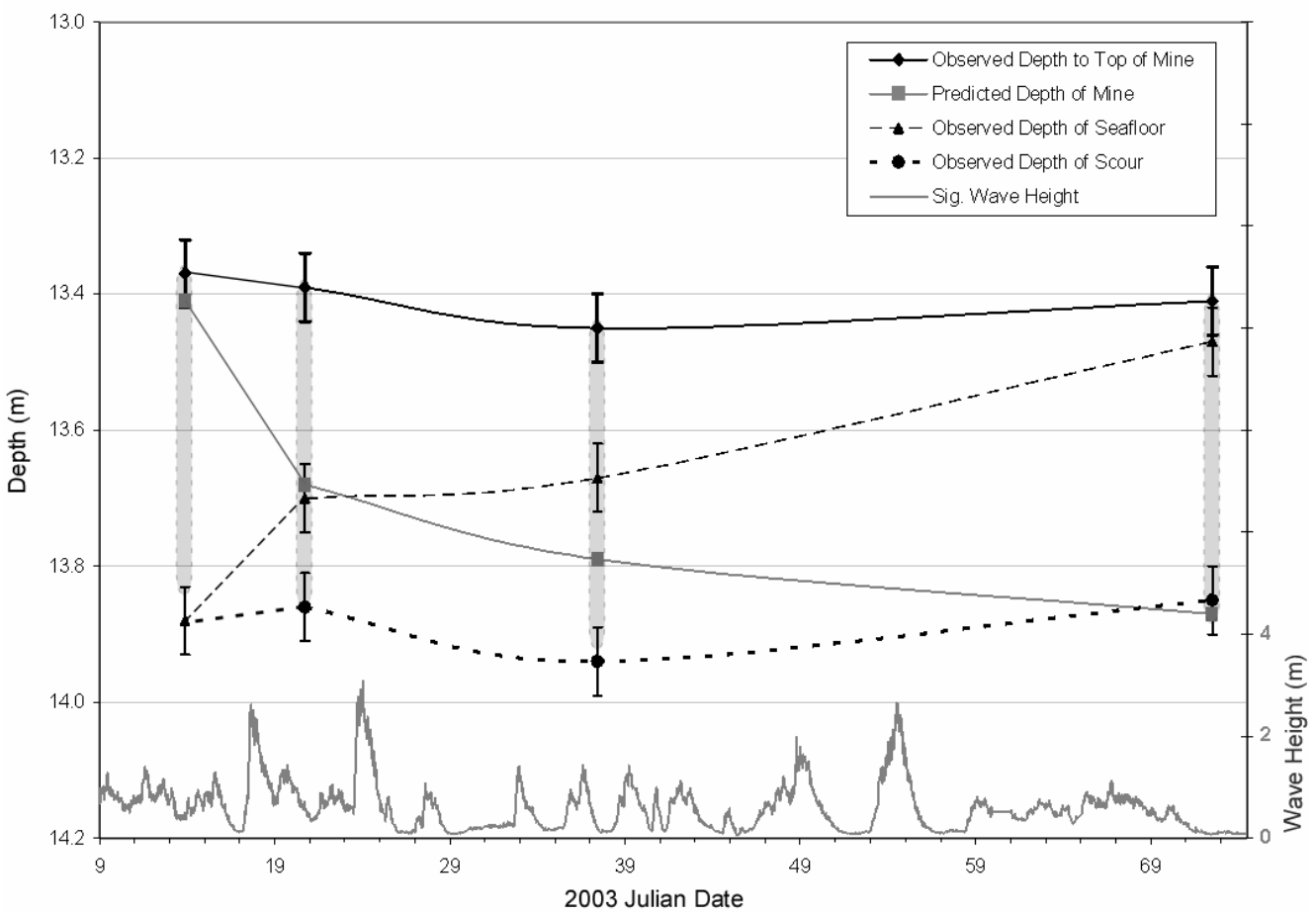

Figure 84. Comparison of multibeam observed (black) and predicted (gray) mine depth for the F9 mine over the course of the experiment. Predicted percent burial of the mine was converted to predicted depth of the mine using the 13.88-meter water depth used to initialize the model. Observed depth of seafloor and depth of scour from the multibeam are plotted as well. Significant wave height is plotted on the right y-axis. Error bars represent the 5-centimeter uncertainty inherent in the multibeam system. The light gray oval represents the F9 mine, and is scaled to the actual dimensions of the mine (length ~ 0.47 m, the diameter of the mine). There was no survey on Julian day 17.

Comparison of F9 Multibeam Observations to the VIMS 2D Burial Model

The VIMS 2D burial model was initialized with a local seafloor depth of 13.88 meters and 0% burial for comparison with the F9 multibeam observations. The model was run from January 13th, 2003 at 1500 GMT, the time that the divers repositioned the mine, to March 13th, 2003 at 1200 GMT, the time of the last survey over the mine.

The first comparison occurs for the January 13th survey over the mine; both the data and the model indicate a percent burial of zero at this time (Figs. 84 & 85). On January 20th, the data show an observed burial of 34.0%, while the model predicts a burial of 53.8%. The model overestimates the amount of burial by 19.8%, which is outside the ± 10.6% range of the multibeam data. The model continues to predict a greater amount of burial than what is actually observed for the February 6th survey as well. The multibeam data indicate a burial of 53.2% at this time; however, the model predicts a burial of 77.1%, a difference of 23.9%. It is not until the March 13th survey that the model predictions fall back within the acceptable range. The observed amount of burial for this survey is 87.2%. The model predicts a burial of 95.1% at this time, a discrepancy of only 7.9%.

The F10 Mine

Temporal Analysis of Scour and Burial

The optical instrumented mine number 10 (F10) was the last instrumented mine deployed as part of the mine burial experiments off Indian Rocks Beach. F10 was deployed on January 11th, 2003 in the deep fine sand site in a water depth of 13.90 meters. SCUBA divers repositioned the on January 13th to lay in a north-south

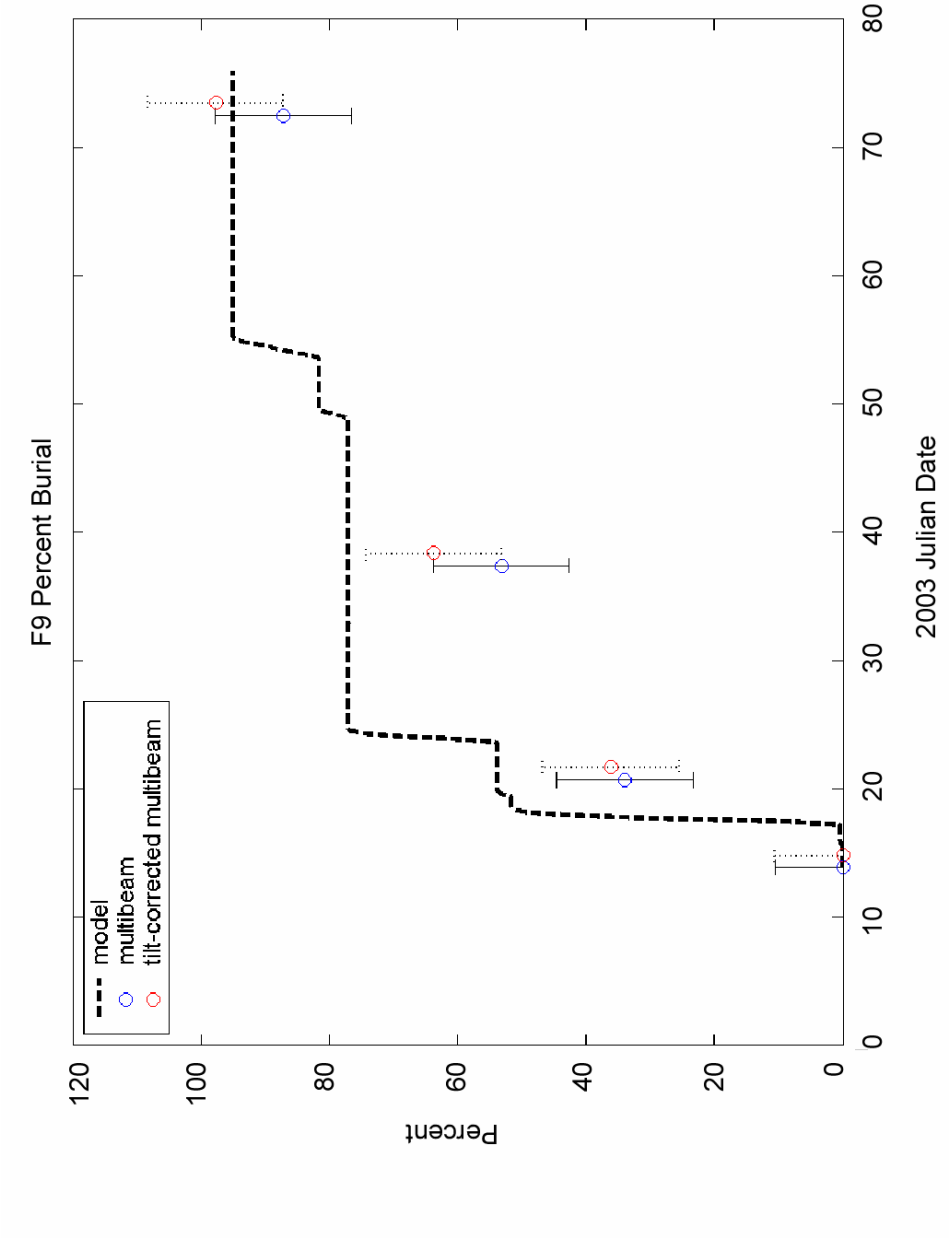

Figure 85. Comparison of the predicted (dashed), observed (blue), and tilt-corrected observed (red) percent burial for the F7 mine over the course of the experiment. Tilt-corrected values have been horizontally offset for clarity. Error bars represent the 5-centimeter uncertainty inherent in the multibeam system.

orientation. The first survey to image the mine after deployment was on January 13th (Fig. 86). The mine appears somewhat distorted in the image as a result of the target detection mode on the multibeam sonar. The top of the mine is at a depth of 13.42 meters, and the surrounding seafloor has an average depth of 13.90 meters. The difference, 0.58 meters, is 11 centimeters greater than the diameter of the F10 mine. The 2° tilt of the mine at this time can account for 3 centimeters, and the vertical uncertainty of the multibeam can account for another 5. There is no clear explanation for the remaining 3 centimeters; however, it is possible that the target detection mode has caused the mine to appear shallower than it actually is, or that the mine is resting on a mound of sand slightly shallower than the surrounding seabed. The observed amount of burial for F10 for the January 13th survey is 0%.

The next observation of the F10 mine does not occur until January 20th, because the January 17th survey did not pass over the deep fine sand site (Fig. 87). The depth to the top of the mine is now 13.60 meters, indicating a sinking of 0.18 meters since the 13th. The ambient seafloor depth is 13.73 meters, showing a deposition of 0.17 meters, which agrees with the 0.18-meter deposition seen around the F9 mine. The mine is 72.3% buried and is only evident in the image as a result of the ring of scour that has formed around it. The maximum observed depth within the scour is 14.07 meters.

On February 6th, the observed depth to the top of the mine is 13.59 meters (Fig. 88). The 1-centimeter difference between this observation and that of January 20th is well within the vertical accuracy of the multibeam sonar and is essentially negligible. The depth of the seafloor around the mine is 13.69 meters, resulting in a percent burial of 78.7%. The scour has continued to extend around the southern end of the mine, although

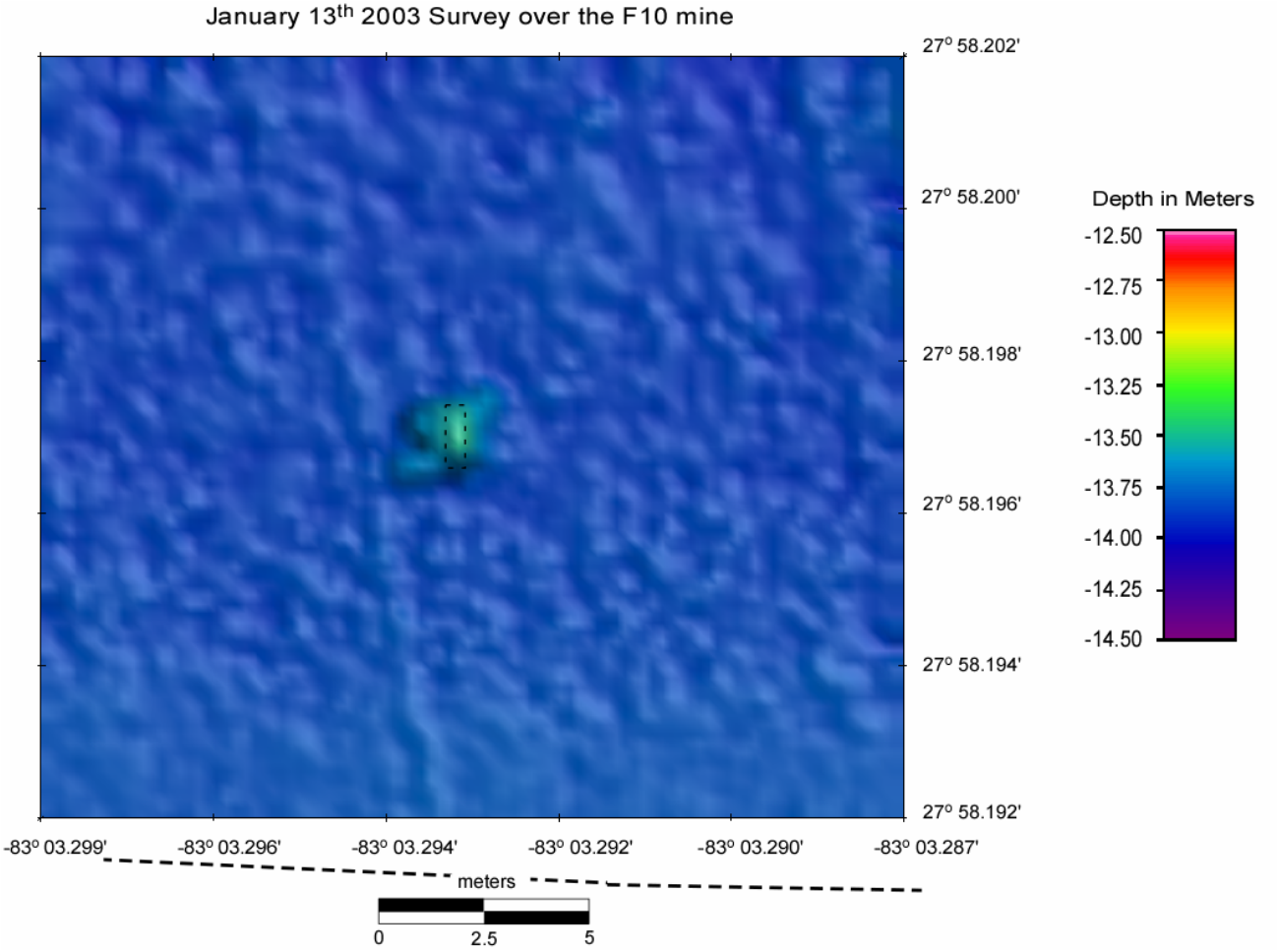

Figure 86. January 13th survey over the F10 mine. The black dashed line indicates the ship's track line during the survey. In this image, the track line falls outside the gridded area. The mine itself is outlined with a faint black dashed line scaled to the actual dimensions of the mine. The mine outline remains at the same scale and orientation throughout the rest of the F10 multibeam images as a reference.

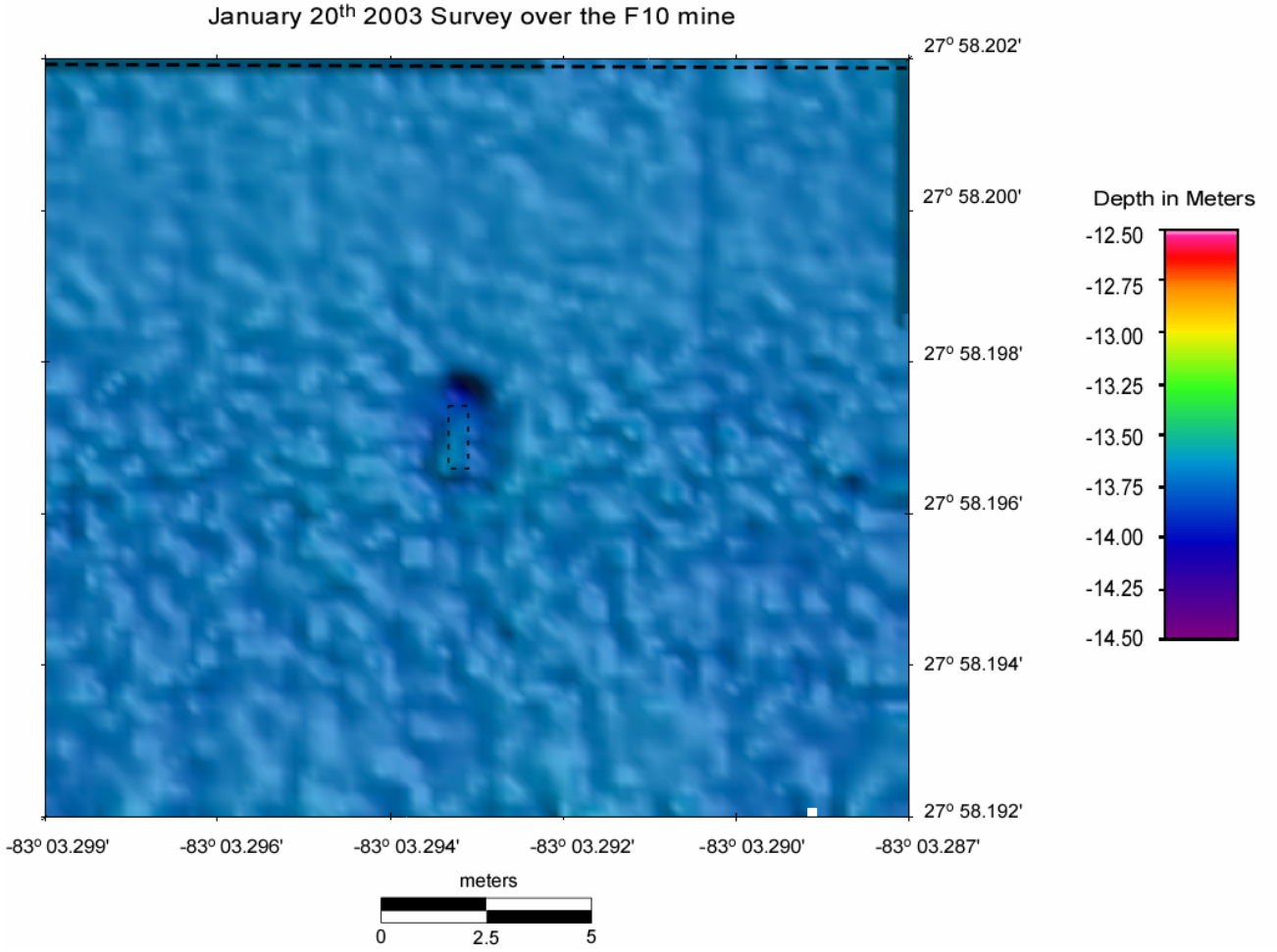

Figure 87. January 20th survey over the F10 mine. Track line runs just along the top of the grid.

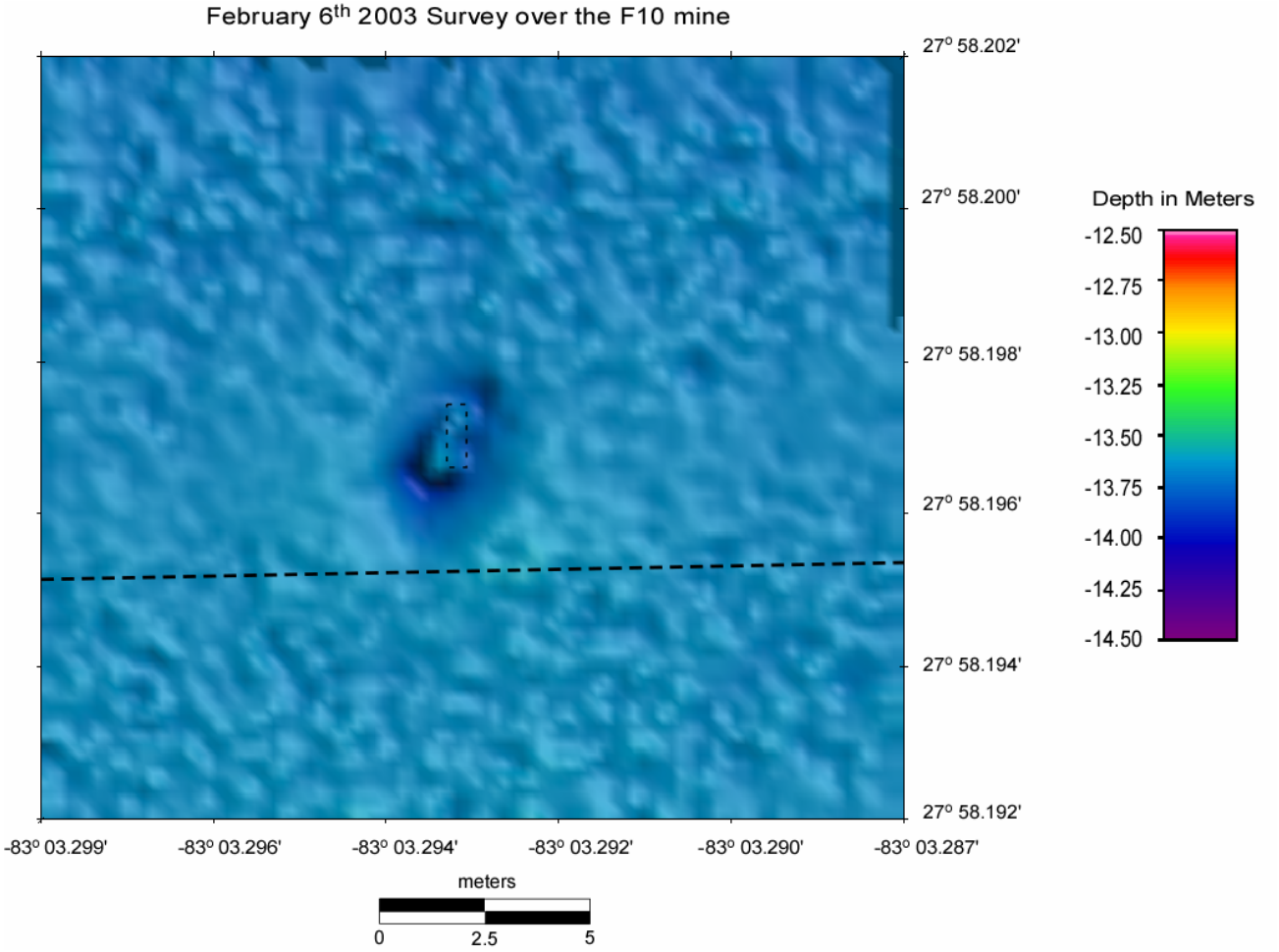

Figure 88. February 6th survey over the F10 mine.

the maximum depth within the pit has decreased to 14.05 meters.

The February 6th survey represents the last multibeam data over the mine. Although the survey from March 13th (Fig. 89) passed over the deep fine sand site, the F10 mine lay in the outer beams of the sonar swath and was not imaged. Between January 13th and February 6th, 2003, the F10 mine sank a total 0.17 meters and became 78.7% buried (Table 10; Fig. 90). The surrounding seafloor depth showed a localized deposition of 0.21 meters during this time, and a ring of scour with a maximum depth of 14.05 meters developed around the mine.

Comparison of F10 Multibeam Observations to the VIMS 2D Burial Model

The comparison of the VIMS 2D burial model with the F10 multibeam observations was the last test of the model for this project. The model was initialized with a local seafloor depth of 13.90 meters and 0% burial, and run from January 13th, 2003 at 1500 GMT, the time of mine reposition, to February 6th, 2003 at 1000 GMT, the time of the last survey over the mine. The first comparison takes place for the January 13th survey (Figs. 90 & 91). The model does not predict any burial at this time, and there is 0% observed in the multibeam data. On January 20th, the data show an observed burial of 72.3%, while the model predicts a burial of only 53.6%, a discrepancy of 18.7%, which is outside the uncertainty range of the multibeam system. The final comparison between the model and the F10 mine on February 6th shows that the two are agreement. A burial of 78.7% is observed in the data and the model predicts a burial of 76.9%, a discrepancy of only 1.8%.

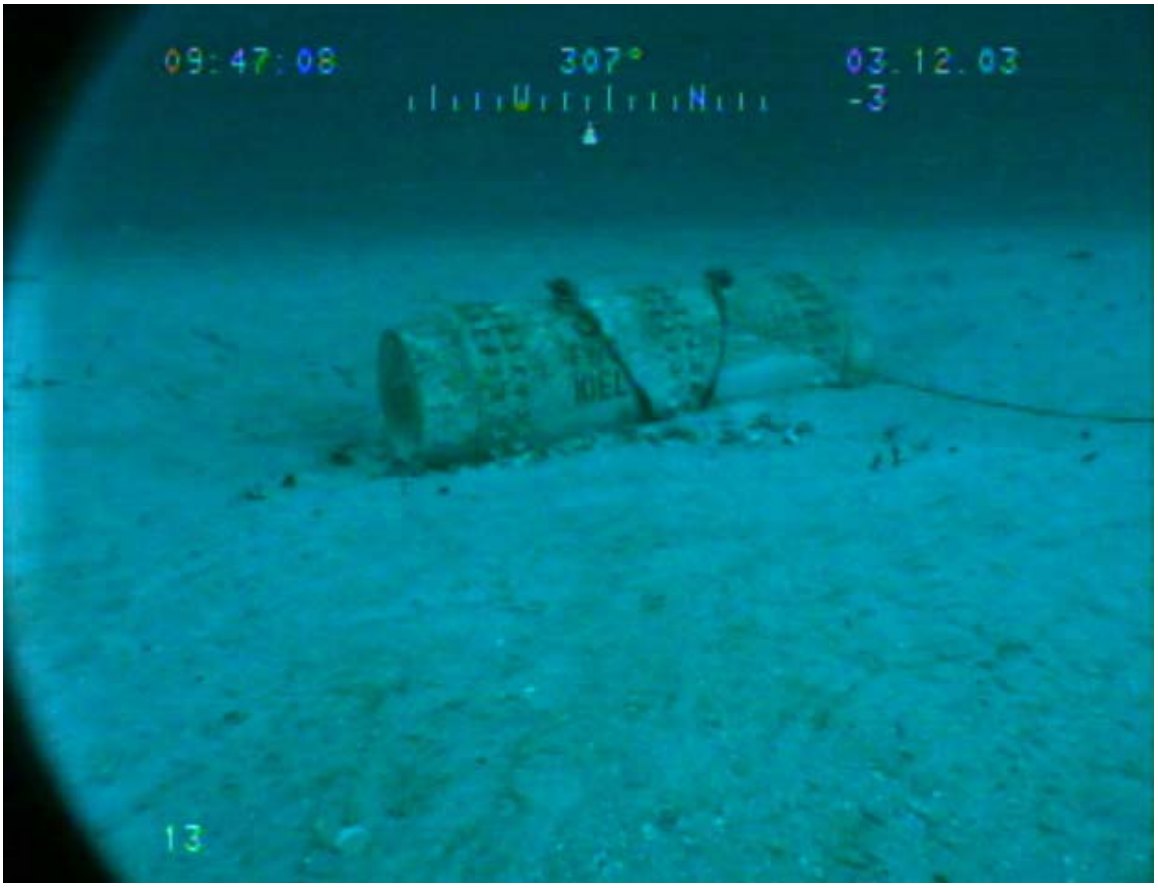

Figure 89. ROV video still image of the F10 mine on March 13, 2003. There is no ROV video still image from the Feb. 6, 2003 survey.

	Jan. 11*	Jan. 13	Jan. 17	Jan. 20	Feb. 6	Mar. 13
Depth of Mine	_____	13.42	No image	13.60	13.59	No image
Cumulative Amount of Change	_____	_____	_____	0.18	0.17	_____
Average Depth of Seafloor	_____	13.90	_____	13.73	13.69	_____
Cumulative Amount of Change	_____	_____	_____	-0.17	-0.21	_____
Scour Visible / Depth of Scour	_____	no	_____	yes 14.07	yes 14.05	_____
% Mine Burial from Multibeam (± 10.6% due to 5 cm uncertainty of sonar)	0	0	_____	72.3	78.7	_____
% Mine Burial from Model	0	0	_____	53.6	76.9	_____
Mine Pitch (degrees)	2	-1	_____	2	2	_____
Mine Roll (degrees)	-4	-2	_____	2	8	_____

Table 10. Data table for the F10 mine. All numbers are in meters except where noted. There is no multibeam survey on January 11th.

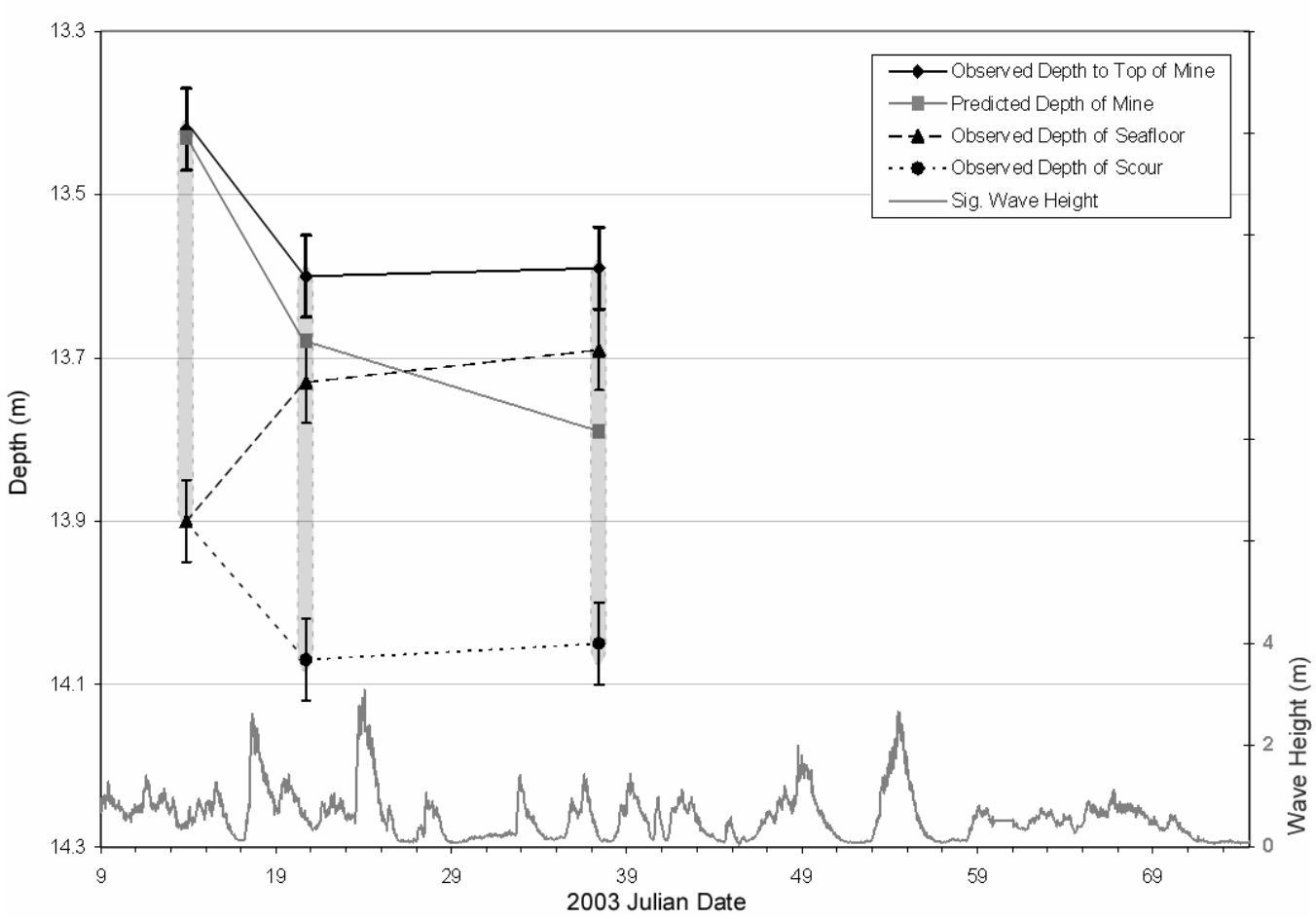

Figure 90. Comparison of multibeam observed (black) and predicted (gray) mine depth for the F10 mine over the course of the experiment. Predicted percent burial of the mine was converted to predicted depth of the mine using the 13.90-meter water depth used to initialize the model. Observed depth of seafloor and depth of scour from the multibeam are plotted as well. Significant wave height is plotted on the right y-axis. Error bars represent the 5-centimeter uncertainty inherent in the multibeam system. The light gray oval represents the F10 mine, and is scaled to the actual dimensions of the mine (length ~ 0.47 m, the diameter of the mine). There is no survey data on Julian days 17 and 72.

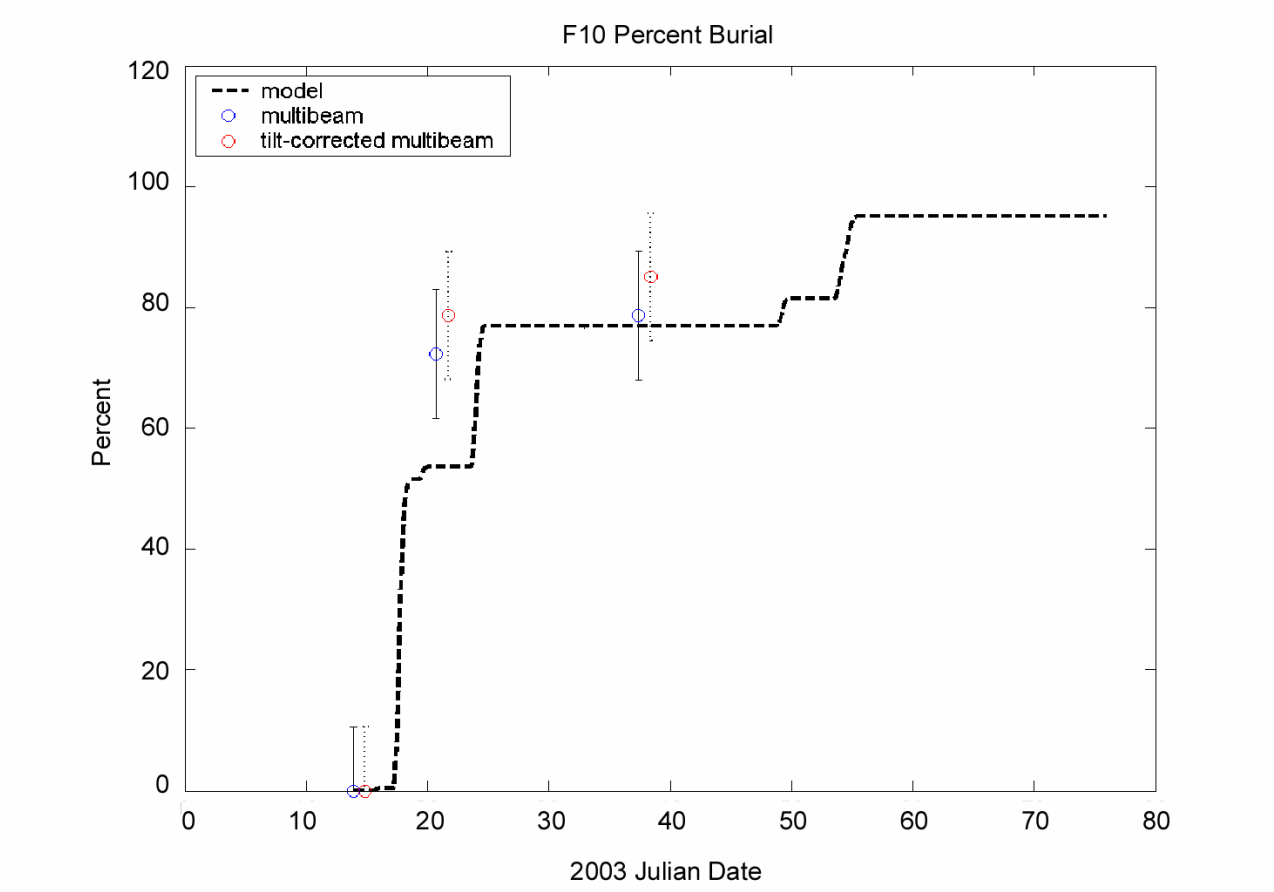

Figure 91. Comparison of the predicted (dashed), observed (blue), and tilt-corrected observed (red) percent burial for the F10 mine over the course of the experiment. Tilt-corrected values have been horizontally offset for clarity. Error bars represent the 5-centimeter uncertainty inherent in the multibeam system.

Summary of Results

High-resolution multibeam surveys were performed over the Indian Rocks Beach mine burial experiment site in order to observe in situ scour and burial of the mines. These data were then used to test the validity of the VIMS 2D burial model, which estimates the amount of burial for cylindrical mines by predicting scour formation based on the Whitehouse-Soulsby equation. The observational data show that for fine sands (mean grain size 0.18 mm), cylindrical mines were at least 74.5% buried within two months of deployment; with four of the eight mines showing a burial of 96% or greater. The two mines deployed in the coarse sand site were 12.8% (F7) and 40.4% (F8) buried within two months of deployment. Although the mines deployed in fine sand showed a significant amount of burial in terms of subsidence below the ambient seabed, there was very little infilling of the scour pits or covering of the mines with sand. As a result, the ability to detect these mines with side-scan sonar was actually enhanced. Despite the lesser degree of burial for the two coarse site mines, it is possible that they would not be detected in side-scan surveys due to the presence of rippled bedforms of nearly the same size commonly found in shallow water coarse sediments.

The VIMS 2D burial model developed by Carl Friedrichs and Art Trembanis at the Virginia Institute of Marine Science was tested using the multibeam surveys of the mines. The model performed well for the mines deployed in fine sands with the exception of the A4 and F6 mines. These two mines both showed an anomalous shallowing during the last multibeam survey of the experiment. Despite this, the performance of the model with the other mines illustrates that it sufficiently predicts burial in areas of fine sand. The anomalous shallowing is likely related to some other unknown source error because

it is difficult to imagine a process that would cause the mine to rise in an absolute sense with respect to the MLLW chart datum used.

In the case of coarse sands; however, the model did not perform nearly as well. For both of the mines deployed in the coarse sand site, the model significantly over-predicted the amount of burial. An anomalous 12-centimeter shallowing was observed for the F8 mine during the March 13th survey; however, this did not appear to be the cause of the model's inability to adequately predict burial in coarse sands. As is seen in the Marta's Vineyard mine burial study site (Traykovski et al., 2005), it is believed that the cause is the presence of rippled bedforms around the mines, which are not accounted for in the model. These ripples directly affect morphodynamics of the seafloor and thus can affect rates of mine burial. This issue is being addressed in current and future modeling efforts (Trembanis et al., 2005).

Other possible sources of error involve the ambient seafloor depth around the mine. The model assumes that the local seafloor remains constant throughout the model run; however, localized erosion and deposition over the course of the experiment were observed in the multibeam data. It is also important to keep in mind that the observed ambient seafloor depth around the mine was an approximation based on the average of 35 measurements from the multibeam data. All references to localized deposition and erosion refer to the area around the mine and just outside the scour pit. A discussion of how changes in seafloor elevation were calculated within the grids is included in Appendix A.

Chapter 4

Analysis of Mine Scour

Introduction

Scour formed around and under mines is the driving mechanism for mine burial in non-cohesive fine sand. The scour process is the basis of mine burial probability models. Therefore, an understanding of the temporal and spatial scales of mine scour is essential. This chapter is an analysis of the morphology and hypsometry of the scour that formed around the mines deployed in both the deep and shallow fine sand sites during the IRB mine burial experiment. The two mines deployed in the rippled scour depression showed little to no scour due to the coarse-sized grains and rippled morphology, and thus were not included in this analysis.

Methods

For the eight mines deployed in fine sands, bathymetric finite difference grids were created by subtracting the first survey over the mine from the final survey. This resulted in a difference grid showing areas of deposition (positive values) and erosion (negative values) between the two surveys. These grids have a vertical accuracy of ± 10 centimeters due to the combined ± 5-centimeter vertical accuracy of the multibeam surveys. Although difficult to estimate, the surface area accuracy is assumed to be ± 2 meters based on the combined 1-meter positional accuracy of the multibeam; however,

the number may be overly conservative. The 0-meter contour on each grid represents the level of zero change in seafloor elevation between the first and last surveys over the mine. The scour pit was then contoured in 10-centimeter intervals and the area within each contour was calculated. The first contour of the scour was defined as the shallowest contour that formed a closed polygon around the pit. Two cross-sections were taken across each scour pit, a long profile passing through the deepest points of the pit and a short profile cutting through the shallowest points. All analyses were done using ArcGIS 9. Hypsometry graphs based off the depth and area of each contour were made in EXCEL for each scour pit.

Scour Analysis

The A1, A2, A3, and A4 mines were deployed in the shallow fine sand site and were 2.03 meters long with a diameter of 0.53 meters. For these mines, the grid from the January 10th survey was subtracted from the March 13th survey grid. The scour around the A1 mine formed a pit with an approximate surface area of 20.03 meters^2 and volume of 3.67 meters^3 (Figs. 92 & 93). The pit was divided into 8 contour intervals ranging in depth from -0.08 meters to -0.88 meters. The actual maximum depth measured within the pit was -0.90 meters; however, the volume of the pit between the -0.88-meter contour and the -0.90 meter maximum depth was negligible (3.7×10^{-6}), so the maximum depth for purposes of this analysis was considered -0.88 meters. The shallowest contour of the scour pit was -0.08 meters, indicating an erosion of the seafloor between the January 10th and March 13th surveys that was not contained within the scour pit. The long cross-section (between points C and D on the grid) passes through the deepest point within the

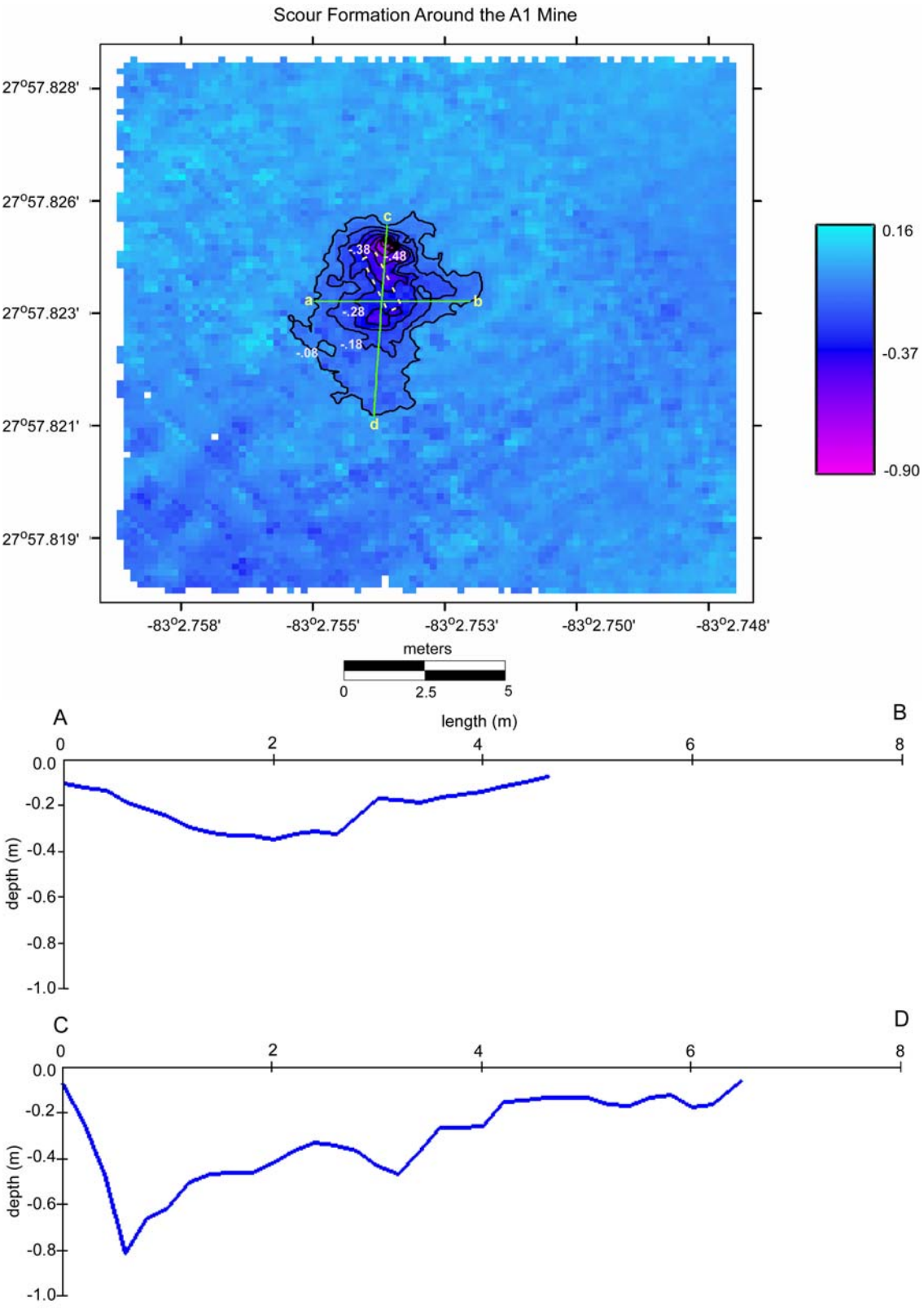

Figure 92. A1 scour pit. Contours are in 10-cm increments. Yellow outline denotes last position of mine as observed in the March 13th survey.

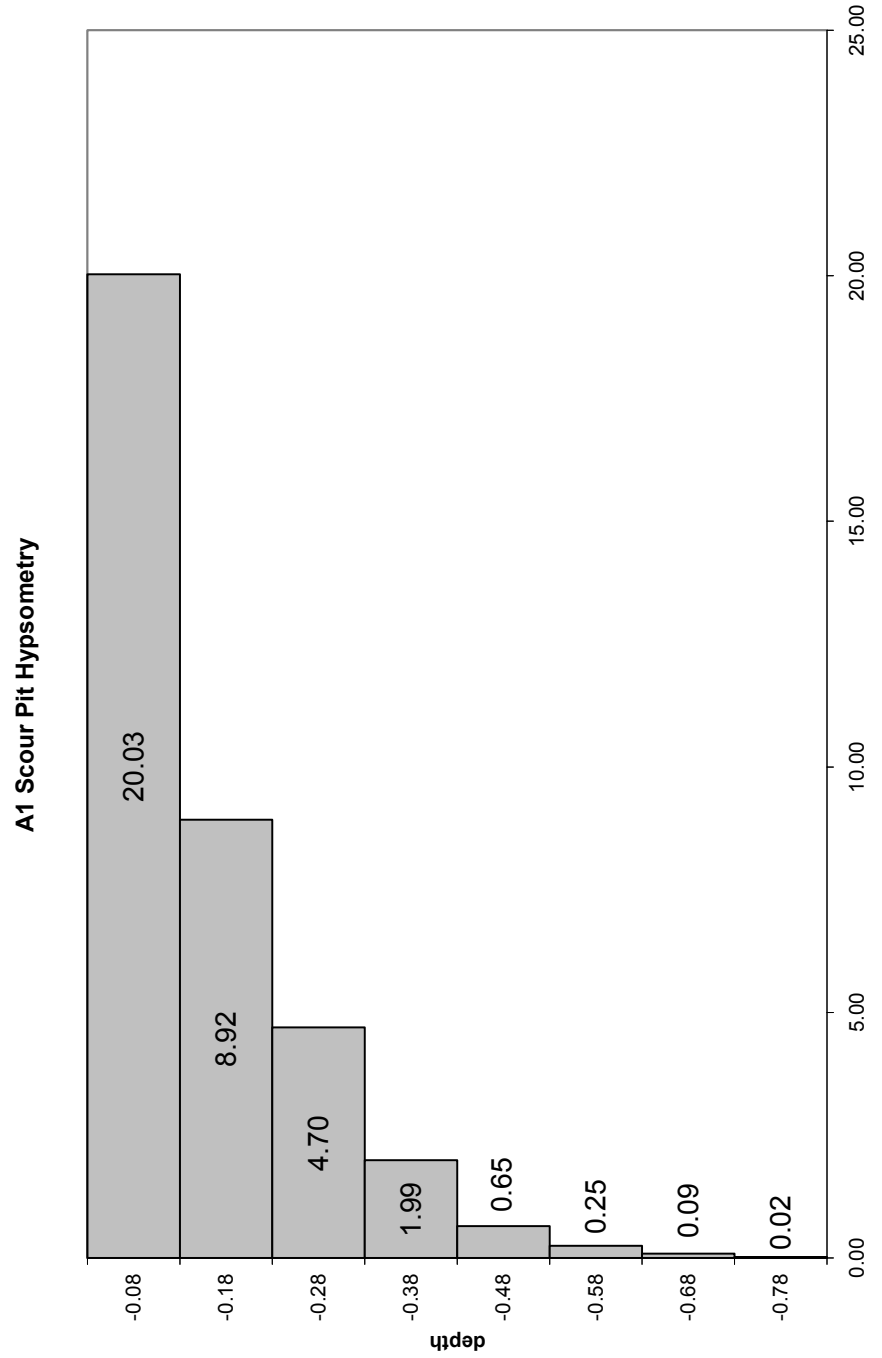

Figure 93. A1 scour pit hypsometry.

scour, ~ -0.88 meters, and was approximately 6.5 meters long. The short cross-section (between points A and B) is approximately 4.5 meters long and reached a depth of -0.36 meters.

A pit approximately 13.98 meters^2 in surface area and 1.91 meters^3 in volume was formed by the scour around the A2 mine (Figs. 94 & 95). The pit was divided into 3 contour intervals ranging in depth from -0.06 to -0.26 meters. Maximum depth measured within the pit was -0.35 meters. The shallowest contour of the scour pit has a negative value, -0.06, indicating that there was regional erosion over the grid between the January 10th and March 13th surveys that extended beyond the scour pit itself. The long cross-section (profile C-D) was approximately 6.5 meters long and -0.35 meters at its deepest point. The short cross-section (profile A-B) was approximately 2.6 meters long and -0.12 meters at its deepest point.

Scour around the A3 mine was complicated by the presence of the two quadpods and one spider deployed in the same area. Scour formed around all the equipment and merged into one. The most pronounced scour was around the A3 mine, and formed a pit with an approximate surface area of 8.60 meters^2 and a total volume of 1.64 meters^3 (Figs. 96 & 97). The pit was divided into 3 contour intervals, ranging in depth from -0.16 meters to -0.36 meters. The long cross-section (profile C-D) was approximately 3.75 meters long with a maximum depth of 0.46 meters. The short cross-section (profile A-B) was roughly 2.4 meters long and reached a depth of -0.35 meters.

The A4 mine formed a scour pit of approximately 11.80 meters^2 in surface area and 1.54 meters^3 in total volume (Figs. 98 & 99). Three contours divided the pit, ranging in depth from -0.10 meters to -0.30 meters. The long cross-section (profile C-D) was

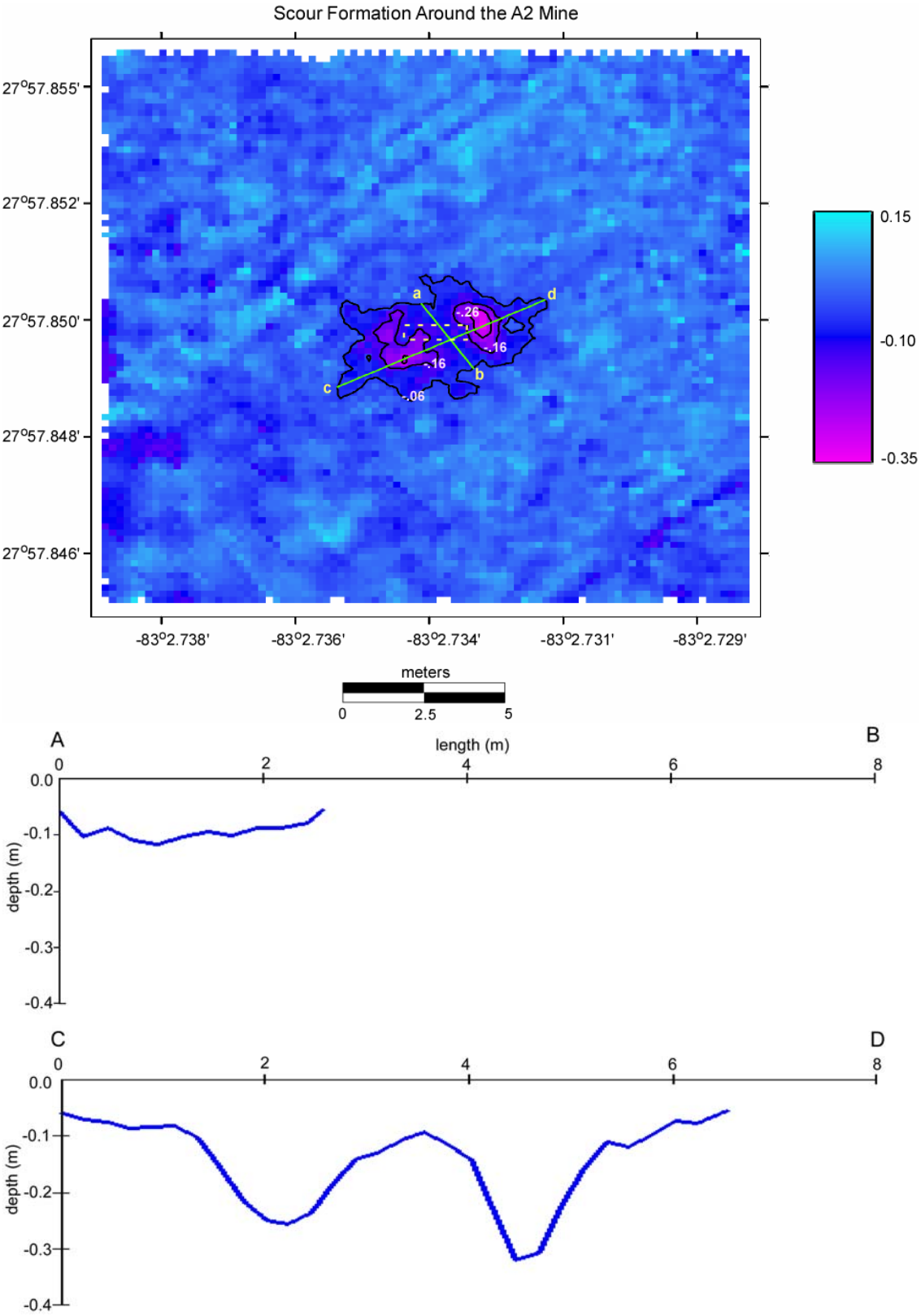

Figure 94. A2 scour pit. Contours are in 10-cm increments. Yellow outline denotes last position of mine as observed in the March 13th survey.

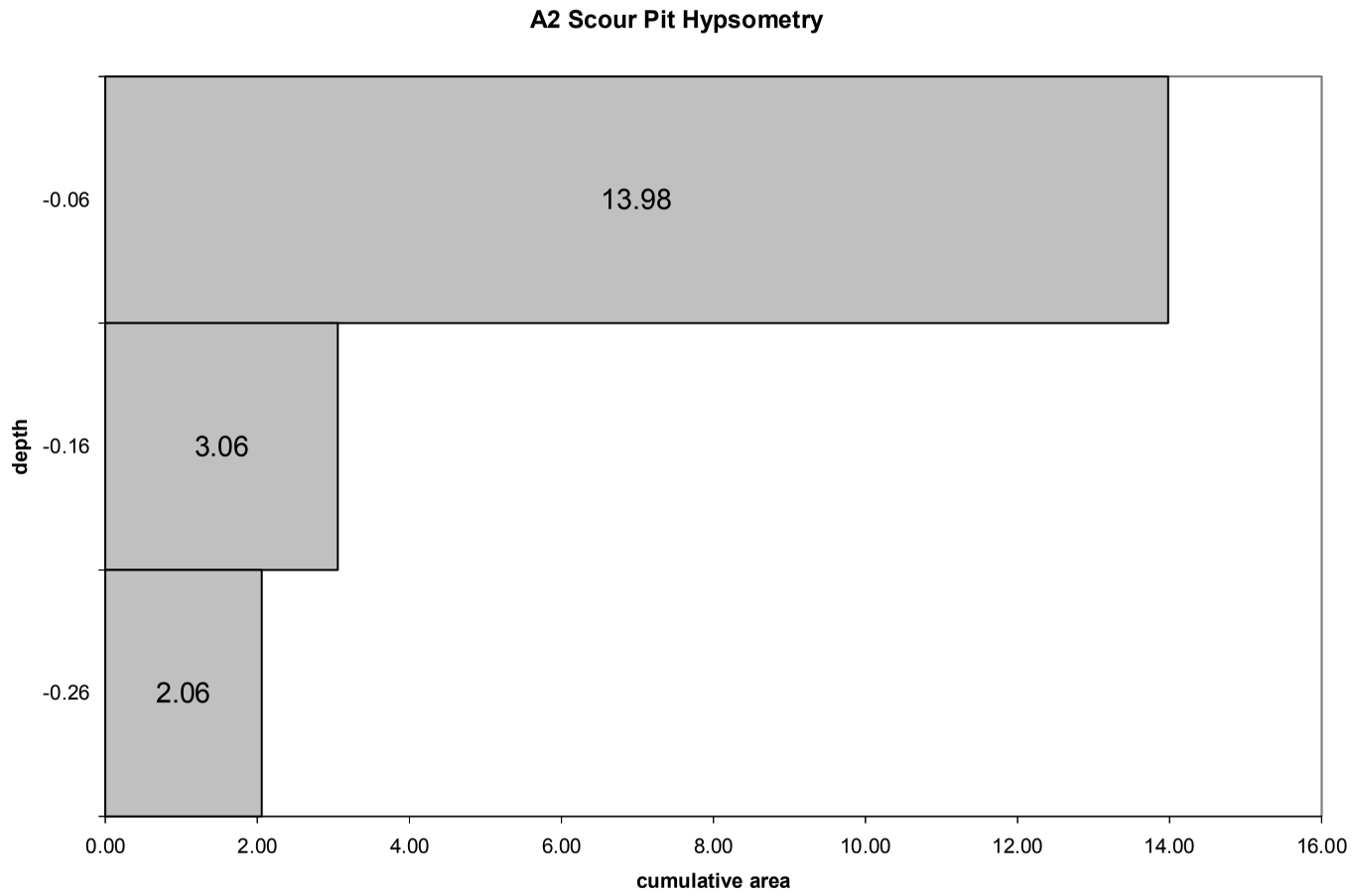

Figure 95. A2 scour pit hypsometry.

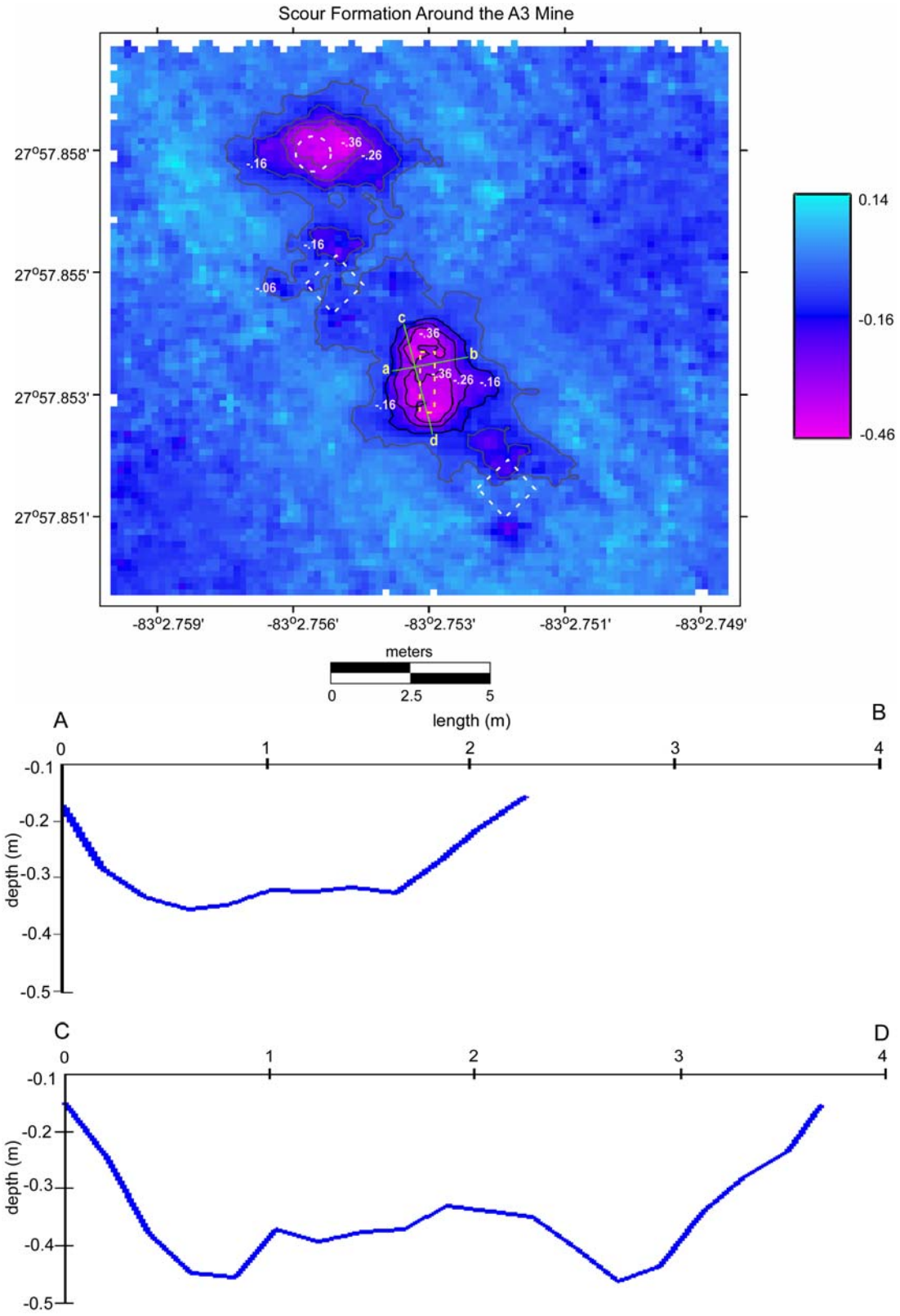

Figure 96. A3 scour pit. Contours are in 10-cm increments. Yellow outline denotes last position of mine as observed in the March 13th survey.

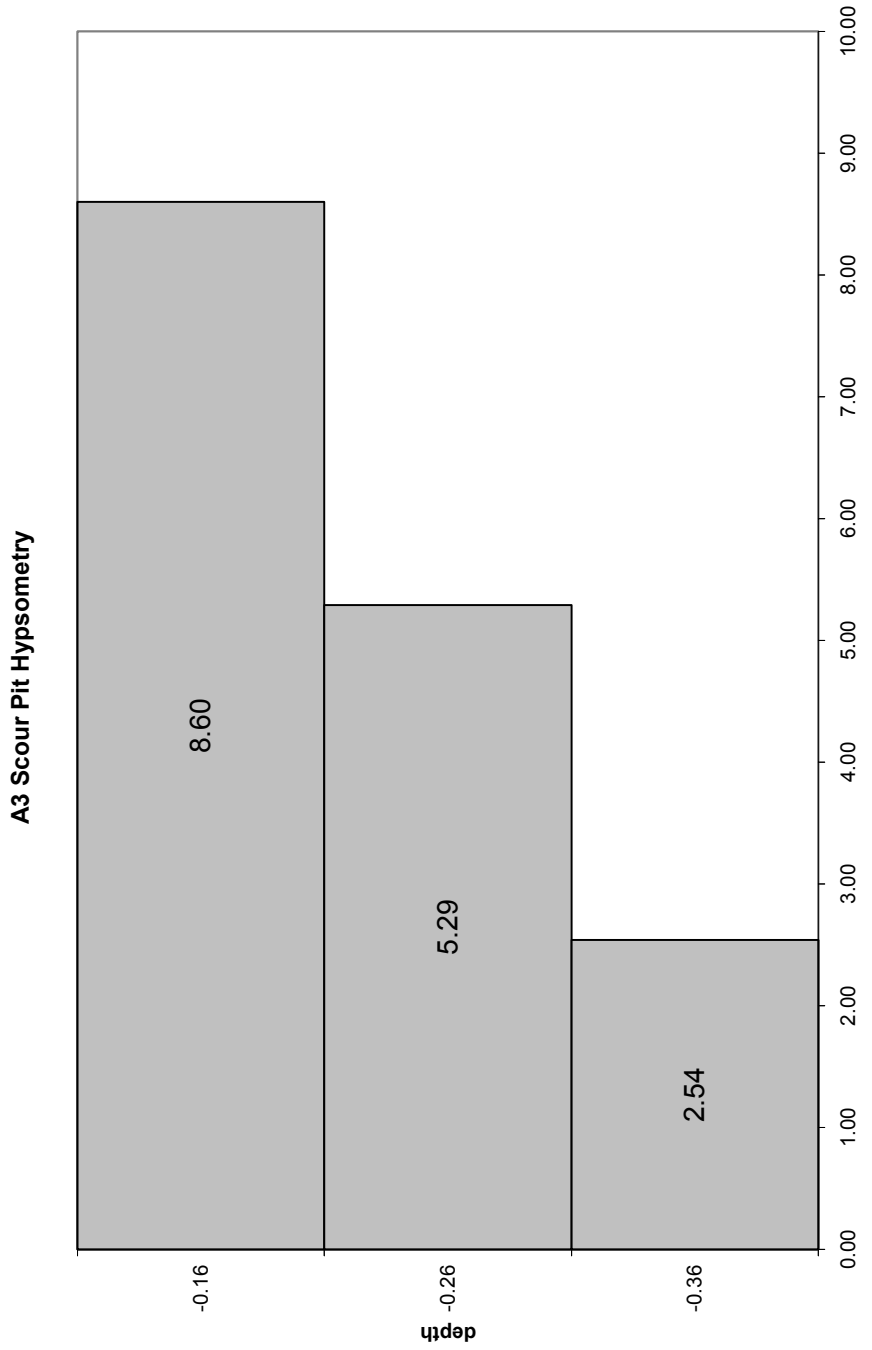

Figure 97. A3 scour pit hypsometry.

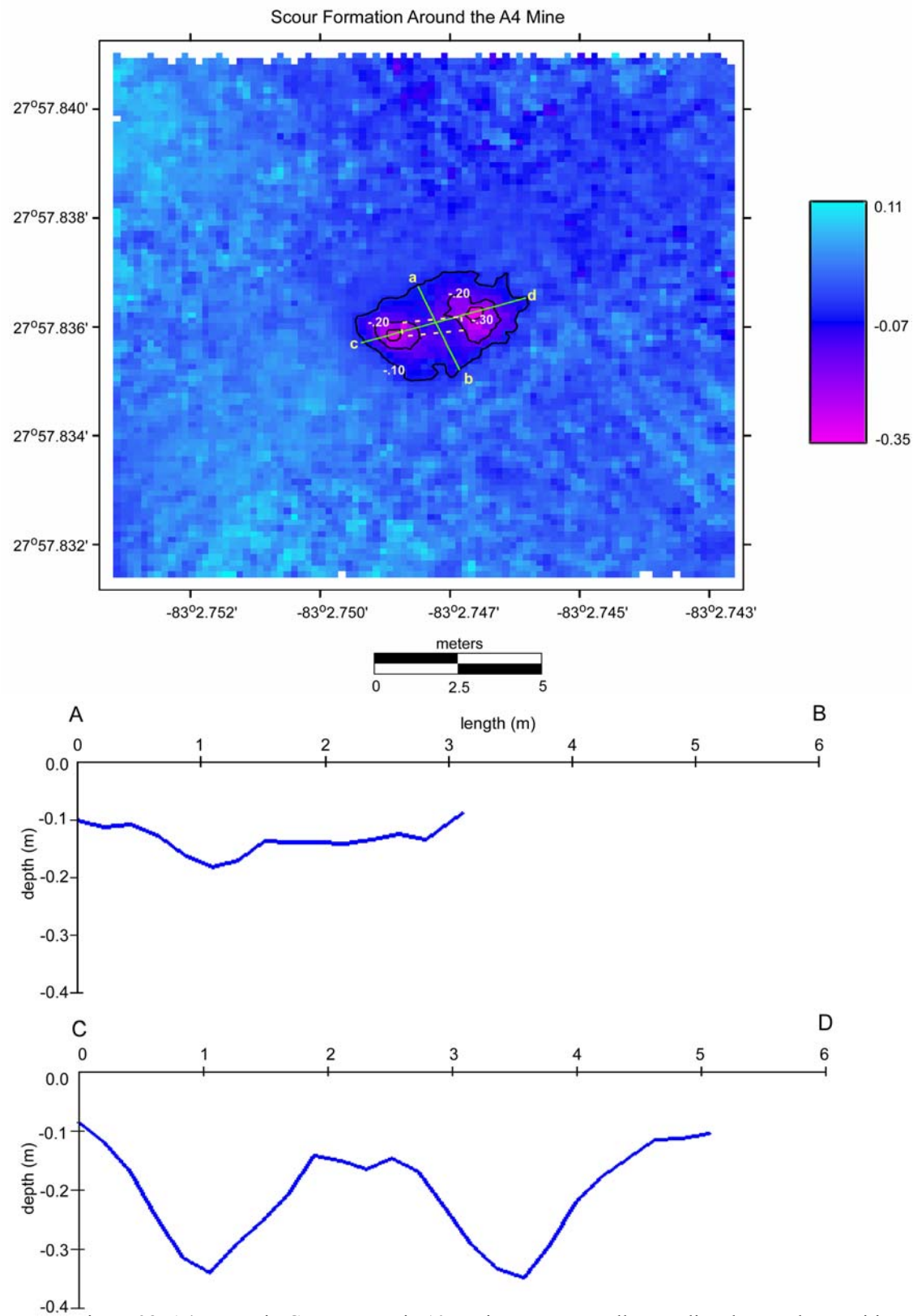

Figure 98. A4 scour pit. Contours are in 10-cm increments. Yellow outline denotes last position of mine as observed in the March 13th survey.

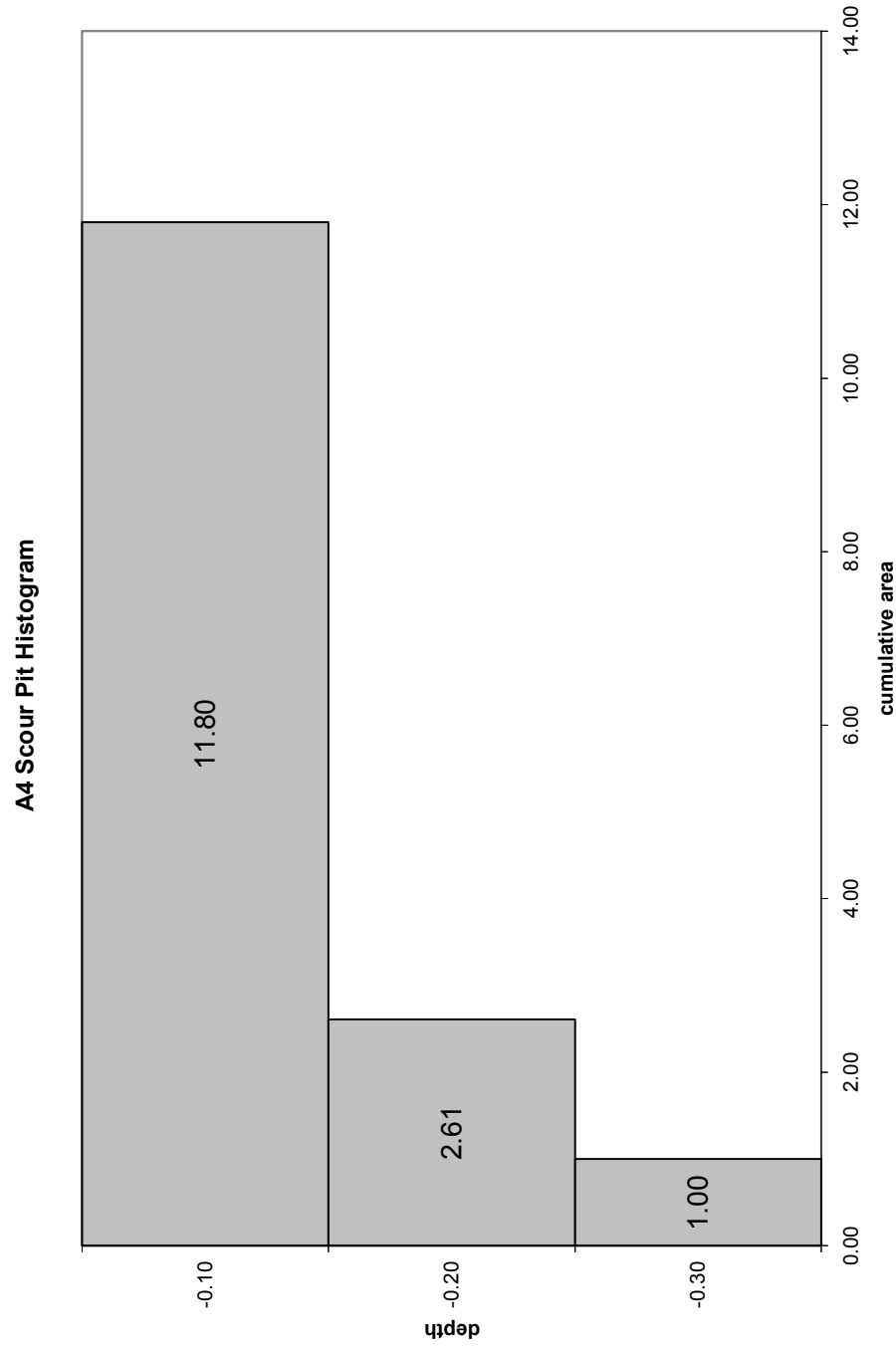

Figure 99. A4 scour pit hypsometry.

roughly 5.1 meters long with a maximum depth of -0.35 meters. The short cross-section (profile A-B) was approximately 3.0 meters long and reached a maximum depth of -0.17 meters.

The F5 and F6 mines were deployed along with the acoustic mines in the shallow fine sand. They had a length of 1.499 meters and a diameter of 0.47 meters. The first survey over these mines was on January 13th, and the final survey was March 13th. The scour around the F5 mine formed a pit with a surface area of approximately 12.53 meters^2 and a volume of 2.04 meters^3 (Figs. 100 & 101). The pit was divided into 3 contours, ranging in depth from -0.01 meters to -0.21 meters. The long cross-section (profile C-D) was roughly 4.2 meters long and reached a maximum depth of -0.30 meters. The short cross-section (profile A-B) was approximately 3.3 meters long and reached a depth of -0.21 meters.

Scour around the F6 mine formed a pit with an approximate surface area of 10.60 meters^2 and a volume of 1.84 meters^3 (Figs. 102 & 103). Seven counters divided the pit, ranging in depth from 0.10 to -0.50 meters. The first contour was positive, indicating that there was a deposition of sediment between the January 13th and March 13th surveys around the mine. For the F6 mine, the short cross-section (profile A-B) passed through the deepest point in the pit. Profile A-B was approximately 3.20 meters long and reached a depth of -0.58 meters. The long cross-section (profile C-D) was roughly 3.40 meters long and had a maximum depth of -0.35 meters.

The F9 and F10 mines were deployed in the deep fine sand site during the IRB experiment (Figs. 104 &105). For both mines, the first survey was on January 13th. The

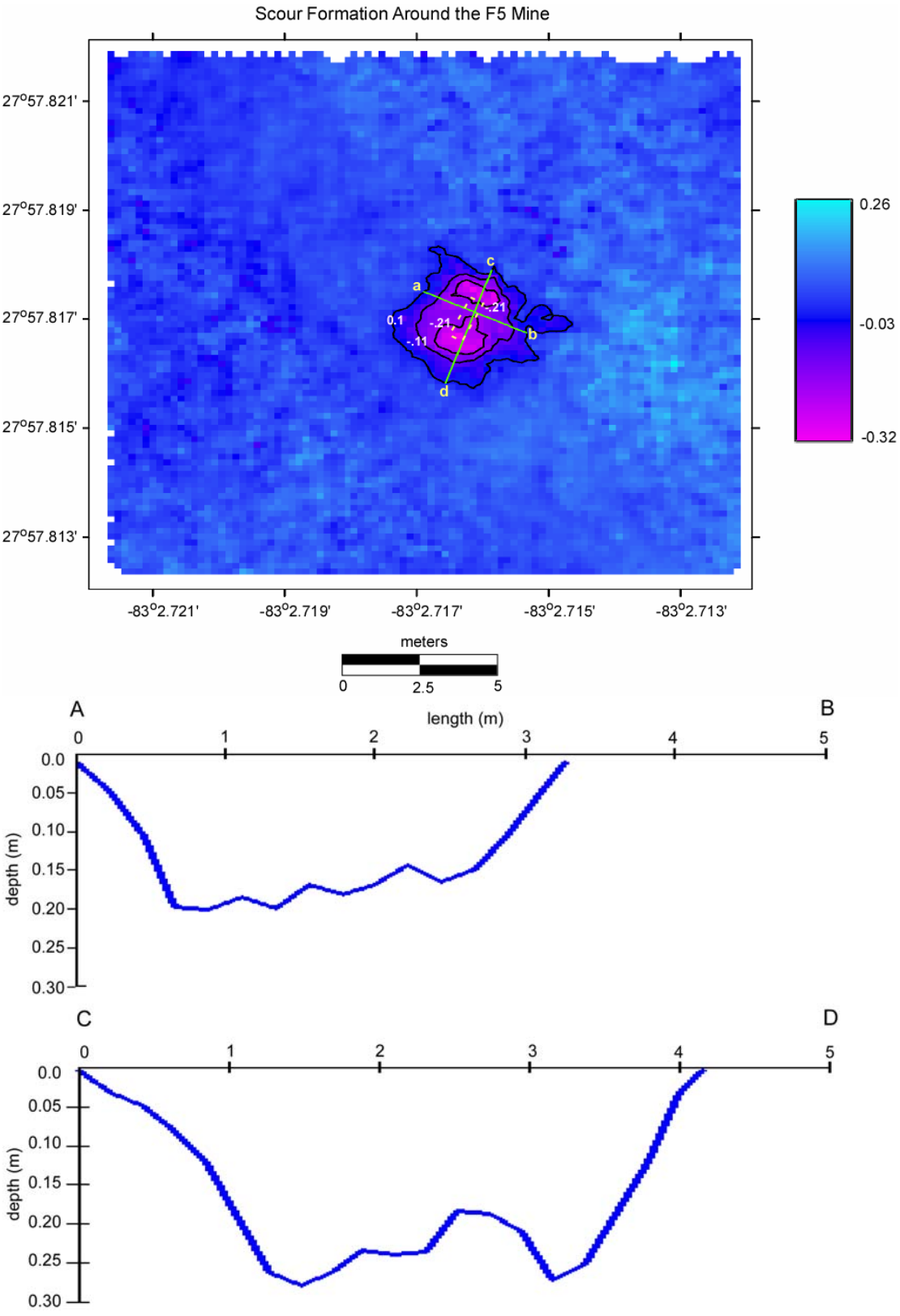

Figure 100. F5 scour pit. Contours are in 10-cm increments. Yellow outline denotes last position of mine as observed in the March 13th survey.

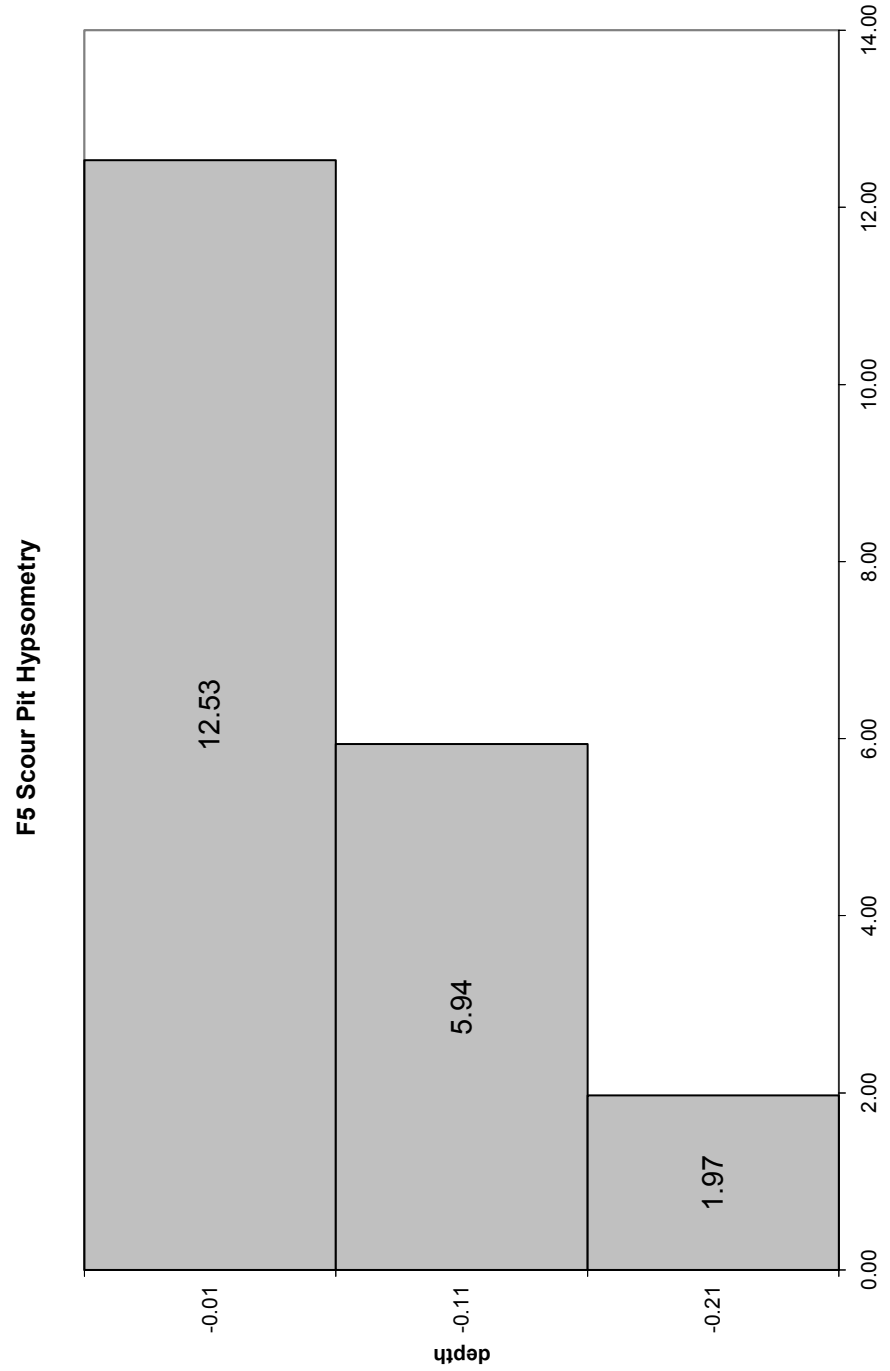

Figure 101. F5 scour pit hypsometry.

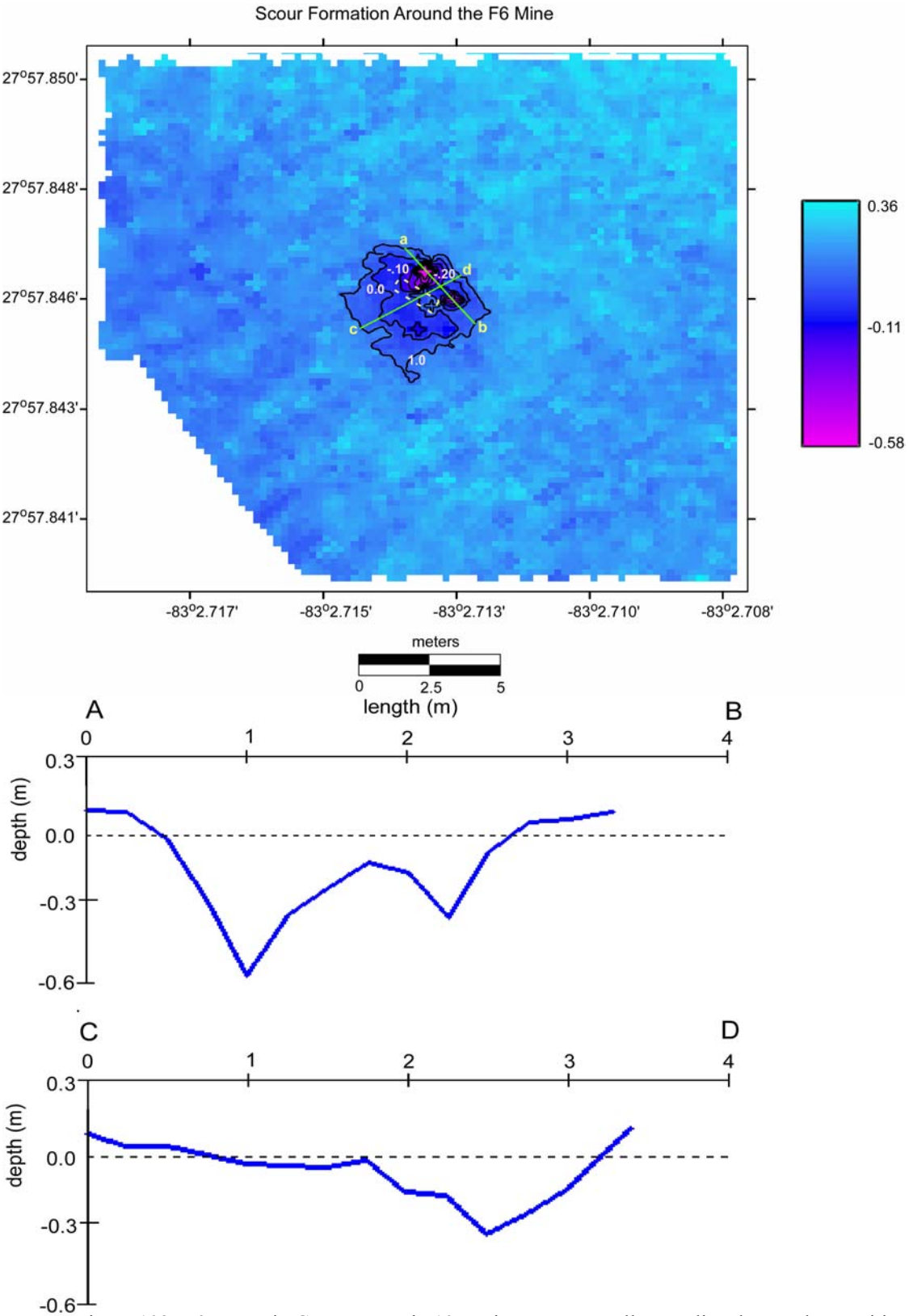

Figure 102. F6 scour pit. Contours are in 10-cm increments. Yellow outline denotes last position of mine as observed in the March 13th survey.

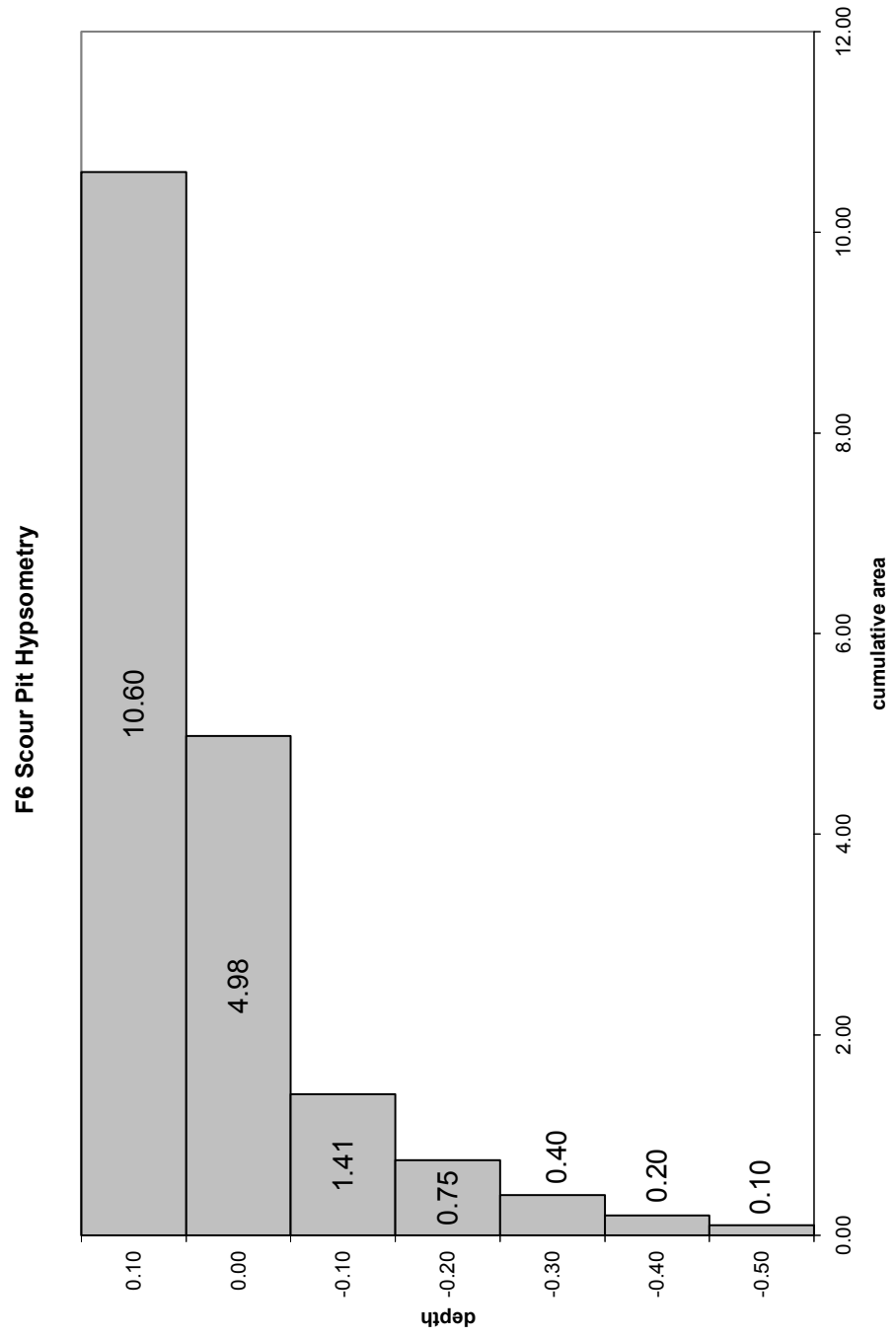

Figure 103. F6 scour pit hypsometry.

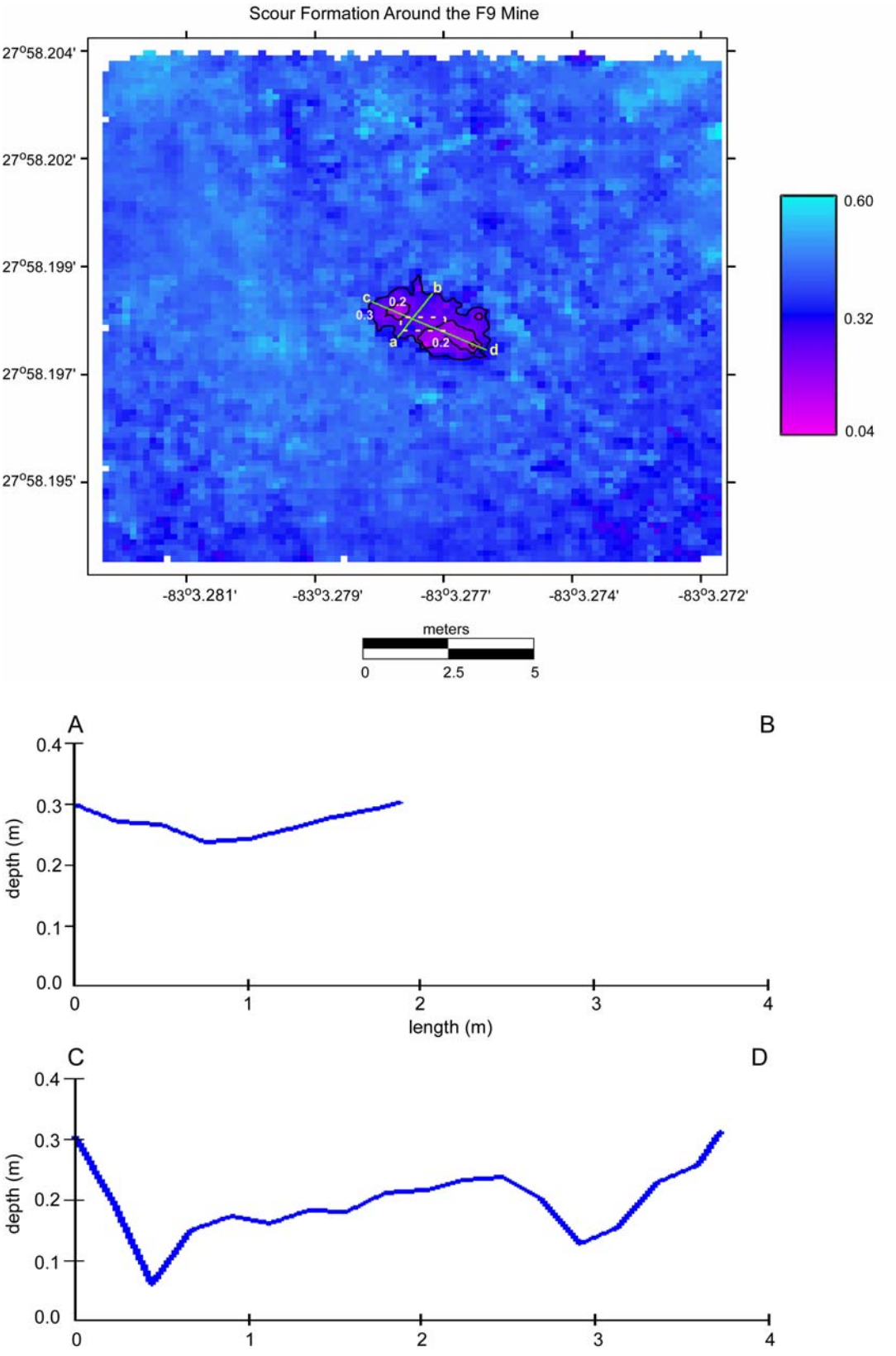

Figure 104. F9 scour pit. Contours are in 10-cm increments. Yellow outline denotes last position of mine as observed in the March 13th survey.

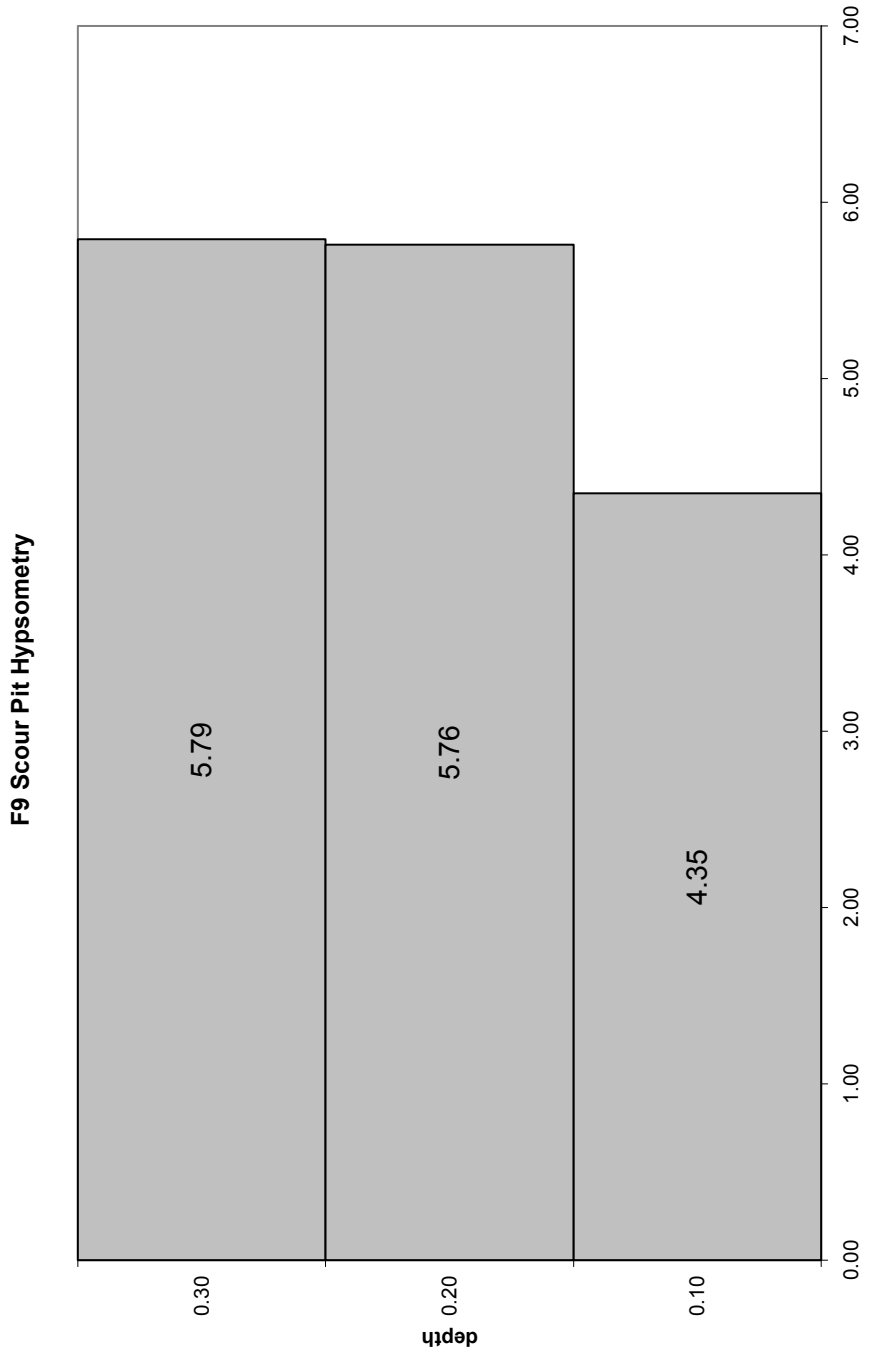

Figure 105. F9 scour pit hypsometry.

scour around the F9 mine formed a pit roughly 5.79 meters^2 in surface area and 1.59 meters^3 in volume. The pit was divided into 3 contour intervals, ranging in depth from 0.30 meters to 0.10 meters. The contours all had positive values, indicating that deposition occurred over the area before the pit started to form. The maximum depth within the pit should have been zero, since the seafloor cannot accrete underneath the mine. The actual maximum depth measured within the pit was 0.03 meters, well within the 20-centimeter accuracy of the grid. The long cross-section (profile C-D) was roughly 3.8 meters long and reached the maximum depth of 0.03 meters. The short cross-section (profile A-B) was approximately 2.0 meters long and had a depth of 0.22 meters.

The survey of March 13th did not capture the F10 mine, so the February 6th survey grid was used along with the January 13th grid for the finite difference. The scour around the F10 mine formed a pit with an approximate surface area of 6.53 meters^2 and a volume of 1.06 meters^3 (Figs. 106 & 107). Three contours divided the pit, ranging in depth from 0.15 meters to -0.05 meters. The long cross-section (profile C-D) was approximately 3.5 meters long and -0.10 meters deep. The short cross-section (profile A-B) was roughly 2.4 meters long and about 0.01 meters deep.

Summary of Analysis

With the exception of A1 and F6, the scour around the mines formed pits roughly 0.30 meters deep contained around the mine. The A1 pit was approximately .80 meters at its deepest point; however, 99% of the pit was contained within the first 0.40 meters. The F6 scour formed a pit approximately 0.58 meters deep, with ~ 98% of the pit contained within the first 0.40 meters. The deepest scour occurred along the flat ends of the mines,

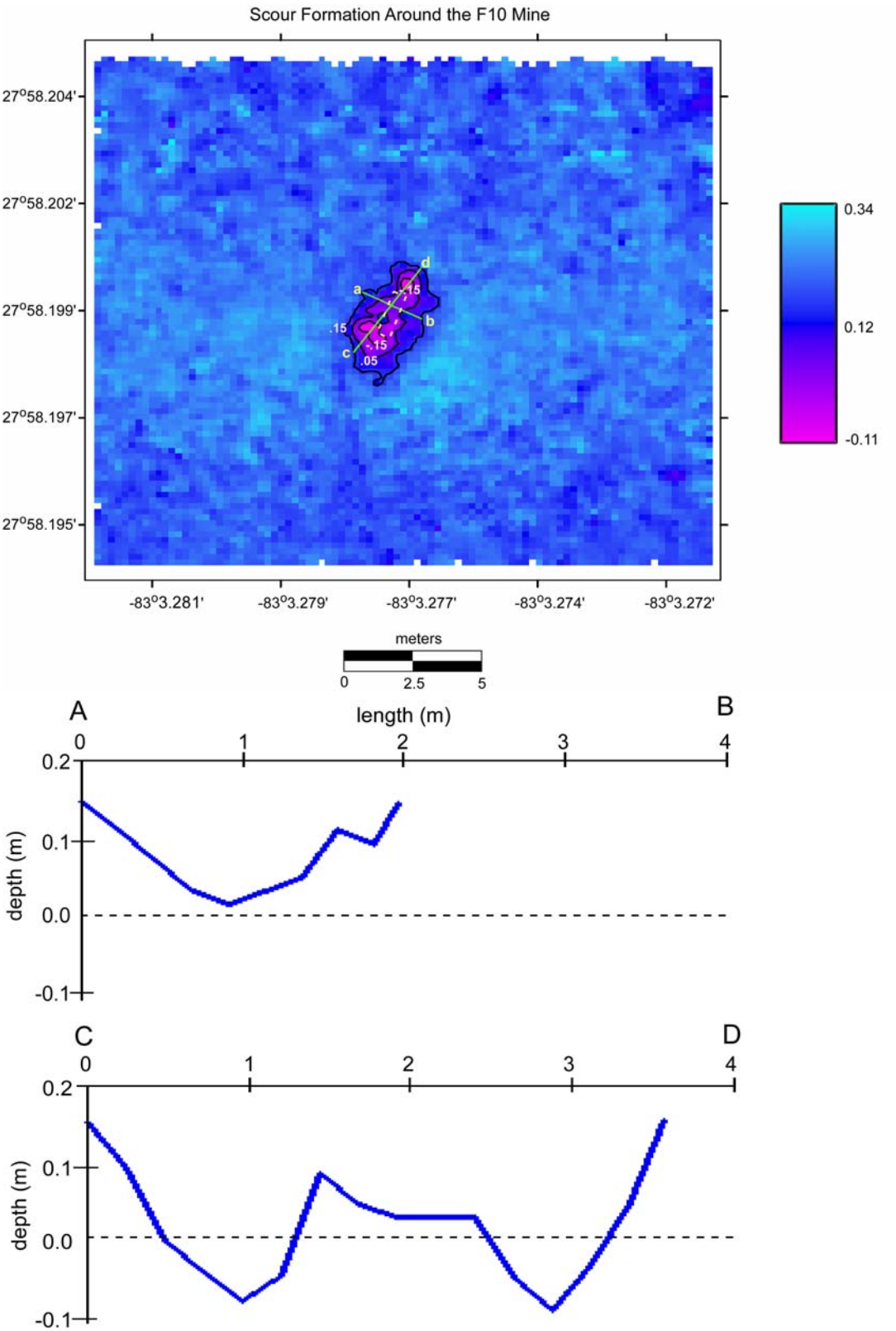

Figure 106. F10 scour pit. Contours are in 10-cm increments. Yellow outline denotes last position of mine as observed in the February 6th survey.

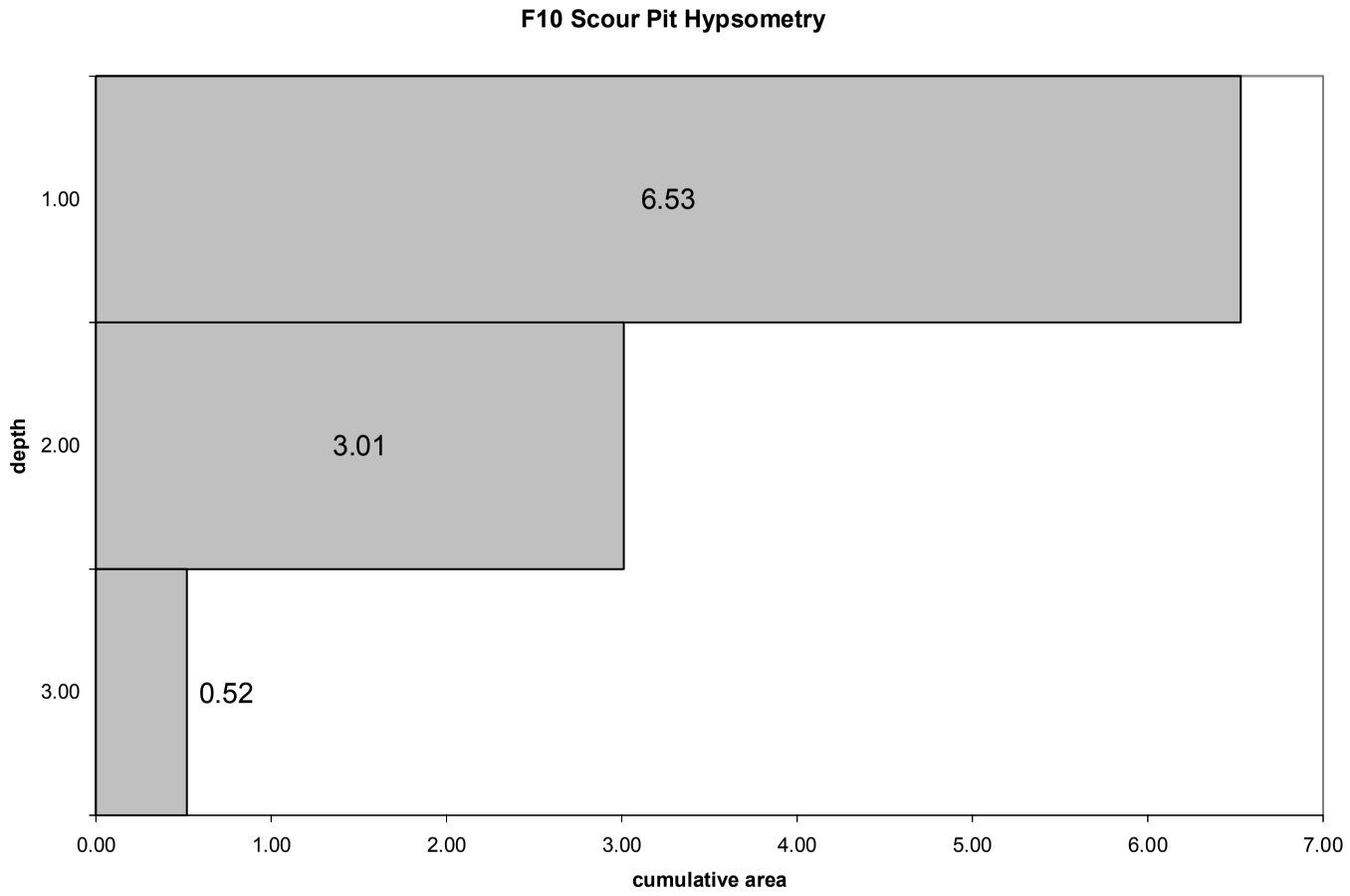

Figure 107. F10 scour pit hypsometry.

while the shallowest scour tended to occur along the sides. In general, scour around the acoustic mine formed the largest pits, with an average length of 5.5 meters and an average width of 3.1 meters. The scour around the optical mines formed pits with an average length of 3.9 meters and an average width of 2.8 meters. The largest scour pit formed around the A1 mine and had a surface area of 20.03 meters^2 and a volume of 3.67 meters^3. The smallest scour pit formed around the F9 mine and had a surface area of 5.79 meters^2 and a volume of 1.59 meters^3.

Chapter 5

Discussion

Over the course of the two month experiment, the 8 mines deployed in both shallow and deep fine sand showed a substantial observed burial, upwards of 74.5% (Figs. 108 & 109). Four of these mines had an observed burial of 96.2% or greater. Mines deployed in the coarse sand site showed significantly less burial, and appeared to scour into the bed until they presented approximately the same relief as the surrounding rippled bedforms (Fig. 110). These results are similar to those observed at Martha's Vineyard during the winter 2003 to spring 2004 MVCO mine burial experiment. The final multibeam survey over the MVCO site occurred approximately 7 months after deployment. The mines deployed in the fine sand sites completely buried with no traces of them were evident in the multibeam data. The mines deployed in the coarse sand site buried until they presented the same hydrodynamic roughness as the wave-orbital ripples (Mayer et al., 2005; Traykovski et al., 2005).

In a laboratory study by Voropayez et al. (2002), scour of cylindrical objects was depressed by the presence of ripples and burial did not occur. Periodic burial of the cylinders was observed when the ripple crest overtook the cylinder; however, this only occurred when the ripple heights were comparable or greater than the cylinder diameter. In the case of the MVCO and IRB experiments, observed ripple heights were significantly less than the mine diameter.

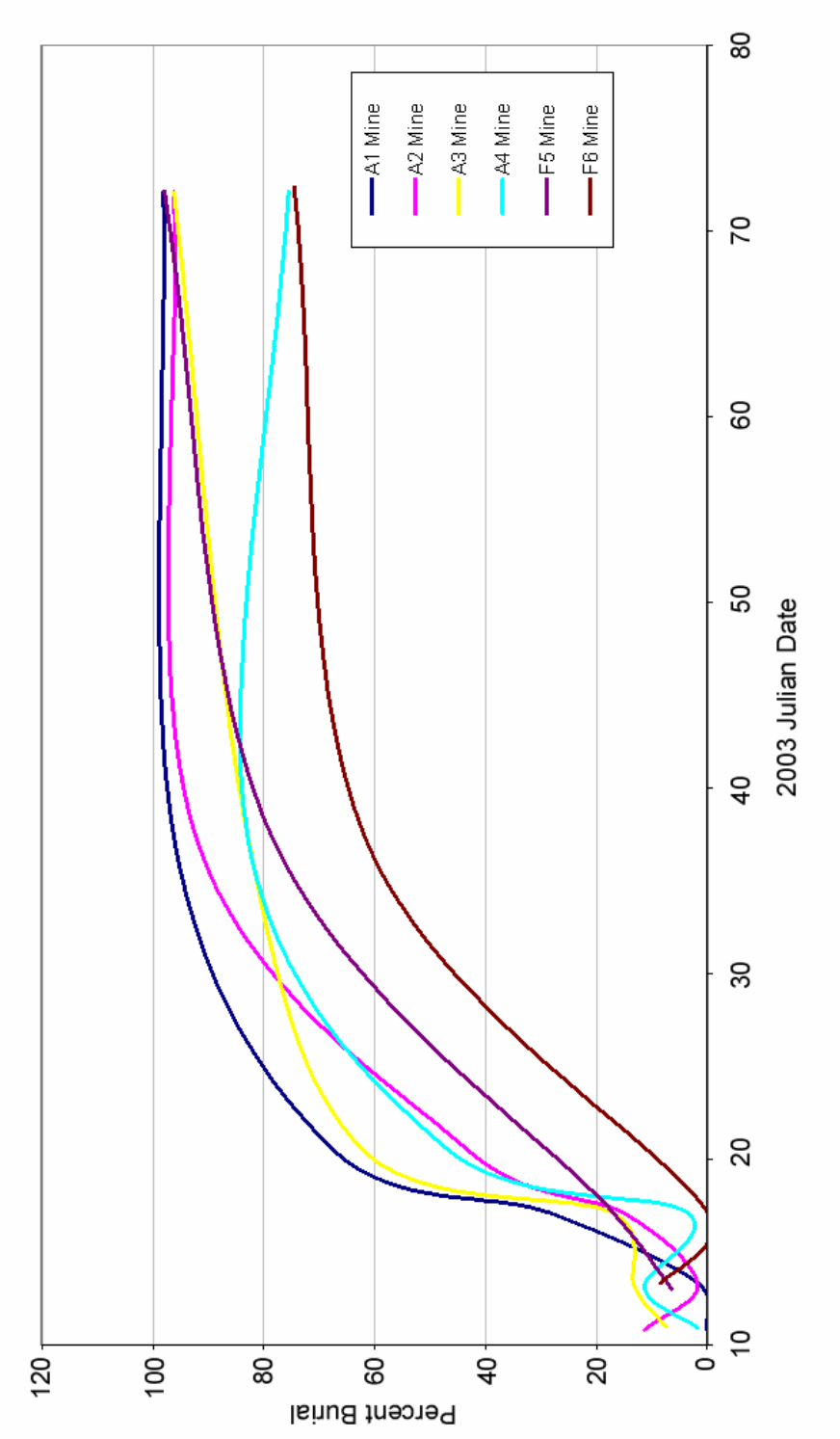

Figure 108. Comparison of burial rates for mines in the shallow fine site.

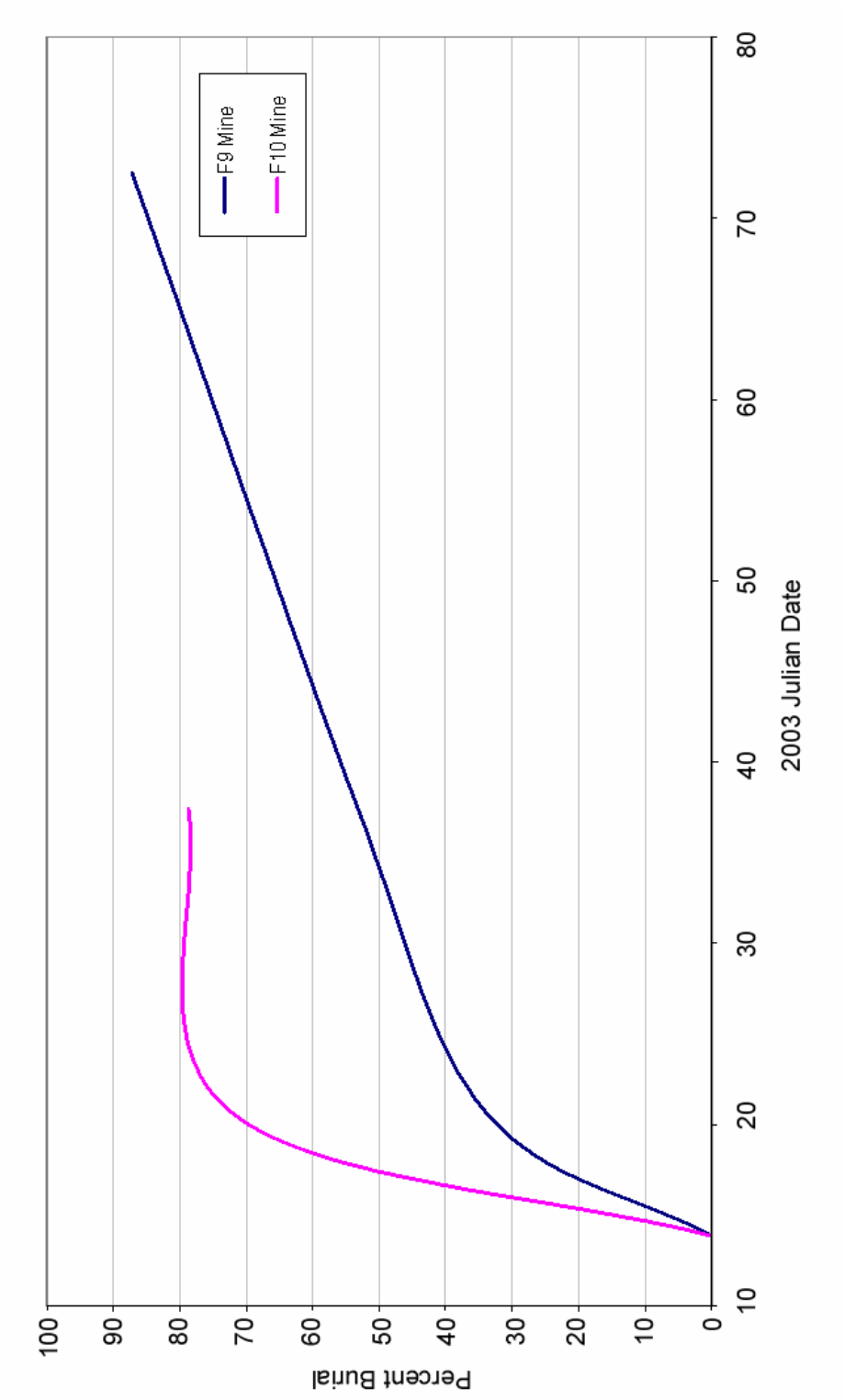

Figure 109. Comparison of burial rates for mines in the deep fine site.

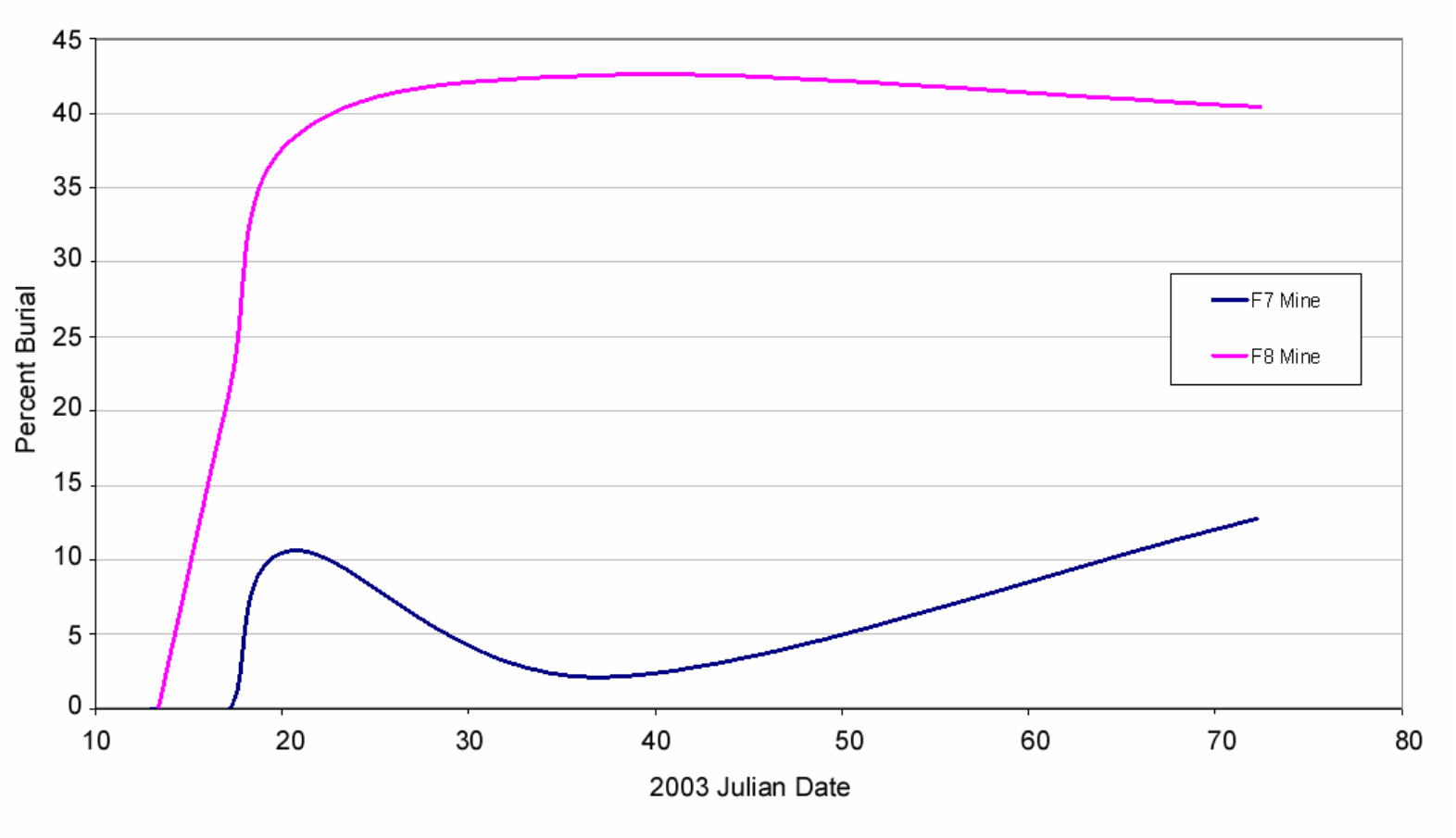

Figure 110. Comparison of burial rates for mines in the coarse site.

Despite the significant amount of burial seen at the two fine sand sites during this experiment, there was very little observed infilling of the scour pits and the mines remained relatively uncovered by sediment. This is in contrast to what was seen at the MVCO fine sand sites, where higher energy environments and a greater supply of muds resulted in scour pit infilling within two months, and complete burial and cover of the mines in seven months (Traykovski et al., 2005). Sediment infilling of scour pits is quite important, as it can signify the difference between mines that can and cannot be readily detected by side-scan sonar. The mines deployed in the fine sand sites off Indian Rocks Beach became more visible in the side-scan imagery over time as a result of the surrounding scour pits, which served to form greater targets. In the case of the MVCO fine sand sites, the mines became completely covered with sediment within seven months and no traces of them were evident in rotary side-scan images (Traykovski et al., 2005). It should be noted; however, that while the MVCO experiment lasted seven months, the experiment off Indian Rocks Beach only lasted two.

Four of the 10 mines deployed during the IRB experiment (A1, A4, F6, and F8) showed an anomalous shallowing between the February 6th and March 13th surveys. The exact cause of this shallowing is not known; however, there are several possible explanations. When comparing the depth of the mine between two surveys, it is important to note that the vertical uncertainty of the multibeam becomes combined. Therefore, the mine depth from one survey can fall within a ± 10-centimeter range of the mine depth from another survey, even if the mine itself does not move. It is also possible that the shallowing may be related to some unknown source of error related to multibeam system parameters or sound velocity profile used by the multibeam system to calculate depth

during the survey. Incorrect heave settings for the POS MV, the positioning and attitude system used during the surveys, may also be responsible for this shallowing.

Often, errors in observed depth in multibeam bathymetry are associated with errors in the tide record used to reference the data to a water level datum. A constant error over the whole tide record would result in errors over the whole multibeam survey. This is not seen in the data from Indian Rocks Beach. Although there are 7 instances of mine shallowing seen over the course of the experiment, there is no set pattern between them. Four of these shallowing events (mines F8, A1, A4, and F6) occurred between the February 6th and March 13th surveys. Mines A1, A4, and F6 were deployed in the shallow fine sand site. A1 and A4 were deployed adjacent, approximately 23 meters apart (Fig. 2). For these two mines, the amount of shallowing of the mine was approximately the same amount of shallowing observed in the ambient seafloor depth (See Tables 3 and 5). This may indicate an error in the tide record confined to the period that the survey passed over these two mines. The F6 mine was located farther north from A1 and A4, resting approximately 39 meters east of A2 (Fig. 2). There was no observed shallowing of the A2 mine, nor the A3 or F5 mines, during the March 13th survey; furthermore, the amount of shallowing observed for the F6 mine was roughly half that observed for the ambient seabed around the mine (Table 7). This indicates that the error most likely is not associated with the tide record; however, it is possible that tide errors affecting the ambient seafloor depth are masked by actual localized accretion around the mine.

The F8 mine showed the greatest amount of shallowing between the February 6th and March 13th surveys, 12 centimeters, that was closely matched by the observed 11-centimeter shallowing of the ambient seafloor depth. The F7 mine; however, also

deployed in the coarse sand site roughly 50 meters away did not show any shallowing of the mine during this survey. This would indicate that if an error in the tide record was responsible, it would have to have been confined to the time after the survey passed over the F7 mine, sometime after 0500 on March 13th, 2003 (GMT). A 7-centimeter shallowing of the F7 mine did occur between the January 13th and January 17th surveys; however, during this period there was an observed deepening of the ambient seafloor depth around the mine by 4 centimeters. In short, while an error in the tide record is a possible source of error, the mine shallowing events are more likely a result of other factors, such as vertical uncertainty in the multibeam system itself.

It should be noted that the ± 5-centimeter vertical uncertainty of the multibeam system assumed in this study was an estimate. Kongsberg Simrad lists the EM 3000's vertical uncertainty as 5 to 10 centimeters (RMS error) dependant on depth. The average depth of the Indian Rocks Beach study site is ~13 meters, which falls into the shallow water range. Furthermore, vessel positioning was handled by a TSS POS/MV 320 system with real time kinematics (RTK) using the Clearwater Beach Adams Mark Hotel as a base station. This combined system provides positioning accuracy on the order of ± 10 centimeters, and roll, pitch, a yaw measurements accurate to 0.02°. The positioning accuracy is extended to ± 1-meter based on other installation parameters and water column properties. The POS/MV system with RTK capabilities also provides real-time heave correction with a measurement accuracy of 5 centimeters or 5% of the heave amplitude (whichever is greater) for periods up to 20 seconds. As a result of this, and in an attempt to not mask the entire multibeam signal in noise, a vertical uncertainty of ± 5 centimeters was used. The anomalous shallowing of some of the mines suggests that this

estimate may be overly optimistic and that a more realistic uncertainty is closer to ± 10 centimeters. In addition, this error estimate does not include error propagation from the pressure sensor used to measure tides, or the NOAA station used in obtaining the tide record. Work is in progress to better determine the vertical uncertainty by completing a full propagation of all system component errors (Wolfson et al., manuscript in preparation).

One other issue with the multibeam data was the blurriness of some of the images, despite the target detection mode being turned off. Many of the initial surveys over the mine were blurred, due to the beam mode being set to target detection. Target detection causes a widening of the beams from 1.5° by 1.5° to 4.0° by 4.0°, allowing for greater detection capabilities; however, it can also cause a distortion of the target itself, a factor not discovered until the data was processed. The target detection mode was turned off for the survey of January 17th 2003 (with the exception of the A2 mine), and remained off for all subsequent surveys. Despite this, 3 of the 8 mines imaged on January 17th (the survey did not cover the coarse sand site) appeared blurry and distorted. The reason for this is not clear and may be related to bubble sweeps under the sonar or other material in the water distorting the acoustic beam. Additional potential causes for distortion follow.

It became apparent during processing that gridding the multibeam data at a resolution of 20 centimeters was pushing the capabilities of sonar. The EM 3000 multibeam has a beam width of 1.5° at nadir, giving it an effective footprint of ~28 centimeters in 13 meters of water depth (the sonar is mounted ~2 meters below the water surface). The across track beam spacing is 0.9° at nadir, giving an overlap of 0.6°, which equates to ~11 centimeters in ~13 meters of water depth. Therefore, a horizontal gridding

resolution of 20 centimeters should be reasonable for this study. Beam width and spacing; however, increase as the beam pointing angle (angle of the beam with respect to the sonar head) increases (Table 11). Therefore, there is a wider separation of the beams in the outer part of the swath and a gridding resolution of 20 centimeters may be too tight to properly image objects that fall within this area.

In some cases, the multibeam images depicted fairly accurate dimensions for the mines. In others; however, the mines did not image clearly at all. This is in contrast to the results from the MVCO experiment, where multibeam data not only showed correct dimensions of the mines but could also depict the tapered end of the FWG optical mines. Multibeam surveys for the MVCO study were completed using a Reson 8125 sonar. The sonar operates at a frequency of 455 kHz with a sub-decimeter resolution. In his article submitted for publication to the Journal of Ocean Engineering, Mayer et el. (2005) states that distortion of true mine diameter by the multibeam sonar may be due to the influence of neighboring cells on small targets during the gridding process. It is possible, therefore, that this is the case with the IRB data as well, and may explain some of distortion seen in the images, especially considering the lower 300 kHz frequency used at the IRB site.

The Simrad EM 3000 multibeam sonar has a maximum ping rate of 20 Hz in very shallow water. Average vessel speeds during the IRB surveys ranged from ~ 2.5 – 9.5 knots. It is possible that at a depth of ~ 13 meters, the observed ping rate of 10 Hz (limited by the two-way travel time from the sonar to the furthest point imaged) is not sufficient to detect the mines at boat speeds of up to 9.5 knots. Indeed, the surveys that imaged the mines most clearly were conducted at vessel speeds of about 6 knots or less. Vessel speed affects the along track distance between consecutive pings (Table 12). At an

water depth	vertical (0 degrees) 1.5° beam width 0.9° beam spacing	45 degrees 2.1° beam width 1.3° beam spacing	60 degrees 3.0° beam width 1.8° beam spacing
10 meters	0.21 0.13	0.83 0.36	1.68 1.0
13 meters	0.28 0.17	1.14 0.50	2.31 1.38
20 meters	0.47 0.28	1.87 0.82	3.77 2.26

Table 11. Beam footprint and beam spacing along the seafloor for various depths and beam pointing angles. Beam pointing angle is with respect to the sonar head. Top number is the beam footprint (width) in meters, bottom number is the beam spacing in meters. These numbers assume a flat seabed. Water depth is depth of the seafloor below the water surface. Calculations are based on the fact that the sonar was pole mounted to the vessel during surveys, and thus was approximately 2 meters below the actual water surface. Refer to Appendix B for a description of the equations used.

vessel speed (knots)	along track beam spacing (at 10 Hz)
2.5	0.13
3.5	0.18
4.5	0.23
** **5.5**	0.28
6.5	0.33
7.5	0.38
8.5	0.43
9.5	0.48

Table 12. Along track beam spacing for various vessel speeds. All numbers are in meters. All calculations are based on a ping rate of 10 Hz. At vessel speeds of 5.5 knots or greater, the along track beam spacing becomes greater than the beam footprint in 13 meters of water depth. Refer to Appendix B for a description of the equations used.

average vessel speed of 9.5 knots and a ping rate of 10 Hz, there is an along track distance of approximately 0.48 meters between pings. For an FWG optical mine oriented parallel to the survey track, this would result in a maximum of 3 pings on the mine surface. In ~ 13 meters of water depth, the beam footprint is ~ 28 centimeters (assuming a flat bottom). In a water depth of 13 meters at vessels speeds of 5.5 knots and greater, the along track beam spacing is greater than the beam footprint (0.28 meters), indicating that ground coverage is not 100 percent. This may help explain why the mine did not image during the January 20th 2003 survey over the F5 and F6 mine, where average vessel speed during the survey was approximately 6 knots (corresponding to a ping spacing of 0.3 meters at 10 Hz). Furthermore, the EM3000 beam spacing is controlled by fast Fourier transform (FFT) beam forming, causing the angular spacing of the beams to increase with distance from nadir. At nadir the beam spacing is approximately 0.9° apart; however, this grows to 1.8° at 60° from nadir. As a result, target detection capabilities of the sonar degrade with as the angle of incidence increases, which may help to explain the distortion of some of the images (Table 11).

The multibeam data from the IRB experiment were used to test the VIMS 2D mine burial model. The results mirrored those seen in the comparison of the MVCO data with the model (Trembanis et al., 2005; Mayer et al., 2005). In the case of mines located in fine sand, the model sufficiently predicts percent burial over the course of the experiment. In the case of mines deployed in coarse sand; however, the model greatly over-predicts the amount of burial. In coarse sands, it has been shown that the mines bury until they present approximately the same hydrodynamic roughness as the surrounding orbital ripples (Mayer et al., 2005; Traykovski et al., 2005). The current model does not

address bedform evolution and migration, which appears to be the cause of the model's poor performance in coarse sand. Another possible source of error involves how the model handles ambient seafloor depth. The model assumes that the local seafloor depth around the mine remains constant throughout the model run; however, multibeam data show localized erosion and deposition over the course of the experiment.

Scour analyses were performed for each of the mines deployed in fine sands, in order to better understand how the scour formed. The mine was carefully edited out of the data, and a difference grid was created using the first and last survey. This allowed for a better understanding of how scour formed around the mines over the course of the experiment. The greatest amount of scour occurred along the ends of the mines, while the shallowest scour tended to occur along the sides. On average, scour around the mines formed pits ~ 0.30 meters deep. Little to no infilling of the scour pits was observed over the course of the experiment. This is in contrast to the results seen at MVCO, where infilling was observed to occur in response to increased wave events (Traykovski et al., 2005). A recommendation for future work would be to create difference grids for each survey, which would allow for a more detailed examination of the scour. Another method would be to use IVS Fledermaus to explore 3D images of the scour, as described in Mayer et al. (2005).

This study shows that a Kongsberg Simrad EM 3000 can adequately image inert and instrumented mine-like cylinders near NADIR at a depth of ~ 13 meters at slow ship speeds. These data provide in situ observations of scour and burial around the mines and are useful in testing the VIMS 2D model. While the model behaves well for mines in fine sand, it cannot sufficiently predict burial in coarse sand in the presence of rippled

bedforms. This indicates that wave-orbital bedform evolution cannot be ignored in mine burial models – an issue currently being addressed by modelers. Further tests of the Kongsberg Simrad EM 3000 multibeam system for shallow water target detection is recommended in order to attempt to determine the cause for both the blurriness of some of the images and the anomalous shallowing of some of the mines, by using independent fixed elevation markers hammered through ~ 3 meters of sediment and into the seafloor limestone to serve as a ground truth elevation datum.

Chapter 6

Summary

Sea mines have been used in nearly every conflict since the American Revolutionary War. They are fairly simple to build and deploy, but require more advanced equipment, significant cost, and considerable risk to locate and counter (Griffen et al., 2003). One of the biggest issues in mine countermeasures today is the ability to detect buried mines on the seabed, an issue currently being address by the ONR Program in Mine Burial Prediction. One of the main objectives of this program is to better understand the temporal and spatial scales of mine burial and scour. Another objective is to develop predictive models of mine burial that can be used to determine whether areas should be hunted, swept, or avoided altogether. This study helps to address these objectives by using repeat high-resolution multibeam bathymetry data to monitor in situ scour and burial of inert and instrumented mines deployed off Clearwater, Florida. The multibeam data are used to test the VIMS 2D burial model. In addition, a method for extracting a vertical reference datum from pressure sensor data is presented.

The multibeam data show that for cylindrical mines deployed in fine sands (mean grain size 0.18 mm) the amount of burial was at least 74.5% two months after deployment, with half of the mines showing a burial of 96% or greater. For the two mines deployed in coarse sand, the maximum amount of burial reached 40.4% within two months of deployment. In general, it appears that mines in coarse sand scour until they present the same hydrodynamic roughness as surrounding rippled bedforms. Despite the

significant amount of burial seen at the two fine sand sites during this experiment, there was very little observed infilling of the scour pits and the mines remained relatively uncovered by sediment.

The VIMS 2D burial model is tested using the multibeam surveys of the mines. The model performs well for the mines deployed in the fine sand sites, with the exception of the A4 and F6 mines. These two mines show an anomalous shallowing that can not be accounted for by the vertical uncertainty of the multibeam. This shallowing is not understood and the cause is not clear. Additional testing of the target detection capabilities of the multibeam sonar are needed to further explore this issue. Despite this, the performance of the mine with the remaining 6 mines illustrates that is sufficiently predicts burial in areas of fine sand.

The model did not perform well for the mines deployed in coarse sands, where rippled bedforms complicated the near bottom hydrodynamics. As described in the Martha's Vineyard publications (Mayer et al., 2005; Traykovski et al., 2005), mines in coarse sediment scour until they present roughly the same hydrodynamics as the surrounding rippled bedforms. Ripples directly affect the morphodynamics of the seafloor and can thus affect rates of mine burial. Existing mine burial models do not account for bedform evolution, an issue currently being addressed by modelers.

Scour around mines is the driving force behind mine burial at the Clearwater field site and is the basis of mine burial probability models being applied there. Scour analyses of the mines at Clearwater indicate the most prevalent scour occurs at the ends of the mines, while the shallowest scour occurred along the sides. In general, scour formed pits roughly 0.30 meters deep around the mines within two months of deployment at the fine

sand locations. Significant scour pits did not form around mines at coarse sand sites. Although infilling of the scour pits was observed during the Martha's Vineyard experiment (Mayer et al., 2005; Traykovski et al., 2005), there is no evidence of infilling at the Indian Rocks Beach site.

Overall, the results of this study show the mines are clearly distinguishable in the multibeam data, allowing for observed amount of scour and burial to be obtained. Furthermore, these data show the VIMS 2D burial model can sufficiently predict burial for cylindrical mines in fine sand but that additional complexity is required to predict burial at the coarse site.

References

Collins, W.T., and Galloway J.L. (1998), Seabed classification with multibeam bathymetry. Sea Technology 39(9):45 – 49.

Collins, W.T., and Preston, J.M. (2002), Multibeam seabed classification. International Ocean Systems 6(4):12 – 15.

Gelfenbaum, G., and Guy, K. (2000), Bathymetry of west-central Florida: U.S. Geological Survey Open-File Report 99-417 (CD-ROM).

Griffen, S., Bradley, J., and Richardson, M.D. (2003), Improved subsequent burial instrumented mines. Sea Technology 44(11): 40 -44.

Hughes Clarke, J.E. (1998), Detecting small seabed targets using high-frequency multibeam sonar. Sea Technology 39(6):87 – 90.

Friedrichs, C. (2001), A review of the present knowledge of mine burial processes. Office of Naval Research, Award No. N00014-01-1-0169.

Gardner, J.V., Butman, P.B., Mayer, L.A., and Clarke, J.H. (1998), Mapping U.S. continental shelves. Sea Technology 39(9):10 – 17.

Locker, S.D., and Hine, A.C. (2003) ROV video survey on March 12, 2003 for the Winter 2003 ONR Mine Burial Experiment, Indian Rocks Beach, FL (Also including still images for February and March, 2003). [Digital Versatile Disk]

Locker, S.D., Hine, A.C., Wright, A.K., and Duncan, D.S. (2002), Sedimentary framework of an Inner continental shelf sand-ridge system, west-central Florida. AGU 83(47), Fall Meet. Suppl. Abstract: OS61A-0188

Mayer, L.A., Raymond, R., Glang, G., Richardson, M.D., Traykovski, P., and Trembanis, A. (2005), High-resolution mapping of mines and ripples at the Martha's Vineyard Coastal Observatory, submitted Journal of Ocean Engineering.

Naar D.F., and Donahue, B.T. (2002) High-resolution multibeam survey of ONR mine burial and scour study area near Clearwater, Florida. EOS, Transactions, AGU Volume 83, Number 47, F692.

Pohner, F. (1990), Processing of multibeam echosounder data. The Hydrographic Journal, 50: 10 p.

Richardson, M., Valent, P., Briggs, K., Bradley, J., and Griffin, S. (2001) NRL mine burial experiments. Proceedings of the Second Australian-American Joint Conference on Technology of Mine Countermeasures, Sydney Australia, 27-29 March..

Richardson, M.D., and Briggs, K.B., (2000), Seabed-Structure interactions in coastal sediments. Proceedings of the 4th International Symposium on Technology and the Mine Problem, Naval Postgraduate School, Monterey California, 13-16 March 2000.

Traykovski, P., Richardson, M.D., Mayer, L., and Irish, J.D. (2005), Mine burial experiments at the Martha's Vineyard Coastal Observatory, submitted to Journal of Ocean Engineering.

Trembanis, A.C., Friedrichs, C.T., Richardson, M.D., Traykovski, P.A., Howd, P.A., Elmore, P., and Wever, T. (2005), Predicting seabed burial of cylinders by scour: Application to the sandy inner shelf off Florida and Massachusetts. submitted to Journal of Ocean Engineering.

Voropayev, S.I., Testik, F.Y., Fernando, H.J.S., and Boyer, D.L. (2003), Burial and scour around short cylinder under progressive shoaling waves. Ocean Engineering 30: 1647-1667.

Wolfson, M.L., Naar, D.F., Howd, P.A., Locker, S.D., Donahue, B.T., Friedrichs, C.T., Trembanis, A.C., Richardson, M.D., Wever, T. (2005), Comparison of Multibeam Observations of Mine Scour Near Clearwater, Florida, to Predictions of Wave-Induced Burial. Submitted to Journal of Ocean Engineering.

Bibliography

Brissette, Lt(N) M.B., and Hughes Clarke, J.E. (1999), Side scan versus multibeam echosounder object detection: a comparative analysis. Proceedings of the U.S. Hydrographic Conference, Mobile, Alabama, April 26 – May 1 1999.

Du, Z., Wells, D., and Mayer, L. (1996), An approach to automatic detection of outliers in multibeam echo sounding data. The Hydrographic Journal (79): 19-23.

Geng, X., and Zielinski, A. (1999), Precise multibeam acoustic bathymetry. Marine Geodesy 22: 157-167.

Hughes Clarke, J.E., Mayer, L.A., and Wells, D.E. (1996), Shallow-water imaging multibeam sonars: a new tool for investigating seafloor processes in the coastal zone and on the continental shelf. Marine Geophysical Researches 18: 607-629.

Pratson, L.F., and Edwards, M.H. (1996), Introduction to advances in seafloor mapping using sidescan sonar and multibeam bathymetry data. Marine Geophysical Researches 18: 601-605.

Appendix A

Calculation of Ambient Seafloor Change

In order to determine if these changes in seafloor elevation were either a local or widespread regional change, five by five meter grids were taken from the northeast corner of each of the 18 by 18 meter grid. The seafloor depth was averaged over the 5-meter grid and was then compared to the seafloor depth observed around the mine. This analysis was performed for each mine deployed in both the shallow fine and deep fine sand site. The coarse sand site was not included due to the presence of rippled bedforms, which complicated the seafloor morphology.

For the A1 mine, the ambient seafloor changes seen around the mine during the six surveys were also seen in the 5-meter grids, ± a couple centimeters (Figs. 111 –116). The greatest discrepancy between the localized seafloor depth around the mine and the average seafloor depth seen within the 5-meter grid, 6 centimeters, occurred on January 20th. The seafloor around the mine had an average depth of 12.82 meters, while the average depth within the smaller grid was 12.88 meters. The greatest amount of seafloor change within the grid was seen between the January 13th and January 17th surveys, with an observed erosion of 16 centimeters.

The seafloor analysis for the A2 mine also showed an agreement between changes seen around the mine and those observed within the 5-meter grid (Figs. 117– 122). Again, the greatest discrepancy between the average seafloor depth seen around the mine and that seen within the 5-meter grid was 6 centimeters, observed on January 13th. The

greatest amount of seafloor change within the grid was an erosion of 9 centimeters, which occurred between the surveys of January 10th and January 13th.

The greatest discrepancy between the seafloor depth seen around the mine and that seen in the 5-meter grid for the A3 mine was only 3 centimeters, and occurred for both the January 20th and March 13th surveys (Figs. 123 – 128). As seen with the A2 mine, the greatest amount of seafloor change occurred between the January 10th and January 13th surveys, which showed an erosion of 9 centimeters.

For the A4 mine, the ambient seafloor changes seen around the mine during the six surveys agreed with those in the 5-meter grids, ± a couple of centimeters (Figs. 129 – 134). The greatest discrepancy between the ambient seafloor depth around the mine and the average seafloor depth seen within the 5-meter grid was 5 centimeters and occurred on March 13th. The greatest amount of seafloor change within the grid was seen between the January 10th and January 13th surveys, with an observed erosion of 12 centimeters.

The seafloor analysis for the F5 mine showed a fairly good agreement between changes observed around the mine and those in the 5-meter grid as well (Figs. 135 – 139). The January 20th, February 6th, and March 13th surveys showed an offset between the average seafloor depth of the 5-meter grid and that around the mine of 4 centimeters each, the greatest offset observed in the F5 analysis. Interestingly, despite the 4-centimeter discrepancy in the actual depth, both the seafloor around the mine and the seafloor in the 5-meter grid remained constant between the February 6th and March 13th surveys. The greatest amount of change within the grid, a sedimentation of 6 centimeters, occurred between the January 17th and January 20th surveys.

The greatest discrepancy between the average seafloor depth seen around the mine and that seen in the 5-meter grids for the F6 mine is only 4 centimeters, and occurred during the March 13th survey (Figs. 140 – 144). The greatest amount of seafloor change occurred between the February 6th and March 13th surveys, which showed a deposition of 12 centimeters.

The seafloor analyses for the mines in the deep fine site also showed a good correlation between the seabed elevation changes seen around the mines themselves and those seen in the 5-meter grids. Between February 6th and March 13th, there was an observed deposition of 20 centimeters around the F9 mine. During the same time, a 25-centimeter deposition was seen in the 5-meter grid, indicating that this change was not merely localized around the mine (Figs. 145 – 148). The greatest discrepancy between the ambient seafloor depth around the mine and the average seafloor depth of the 5-meter grid was 6 centimeters, and occurred on February 6th.

The last of the seafloor analyses were performed on surveys over the F10 mine. Interestingly, the greatest amount of seafloor elevation change within the 5-meter grid, a deposition of 20 centimeters, was seen between the January 13th and January 20th surveys (Figs. 149 –151). This agreed with the greatest amount of elevation change seen in the ambient seafloor around the mine itself, a deposition of 17 centimeters that occurred between the same surveys. Given F10's proximity to the F9 mine, the greatest amount of change would presumably have occurred during the same time. Due to the fact that F10 rested approximately due west of F9, it is possible that this difference represents a large bedform moving west to east through the area during that time period. The greatest discrepancy between the average depth of the seafloor within the 5-meter grid and the

ambient seafloor around the mine was 4 centimeters on February 6th, still within the multibeam depth uncertainty of 5 centimeters.

For all the mines deployed in both the fine and deep fine sand sites, the changes in ambient seafloor elevation around the mine were mirrored by the changes seen within the 5-meter grids, ± a few centimeters. This indicates that the seafloor elevation changes seen around the mines were actual changes occurring across the grid and not just a result of the mine's presence affecting local morphodynamics. Interestingly, about half of the histograms (20 out of a total of 41) are right-skewed, meaning that the distribution is not symmetric but leans towards deeper values of seafloor depth. The numbers of histograms with symmetric and left-skewed (shallow-biased) distributions are about equal, 10 and 11 respectively. The reason for this right-skewed trend in the histograms is not clear, but may indicate inappropriate parameter settings in the multibeam sonar causing a bias towards deeper depth values during calculation. Further testing of the multibeam sonar is needed to explore this possibility.

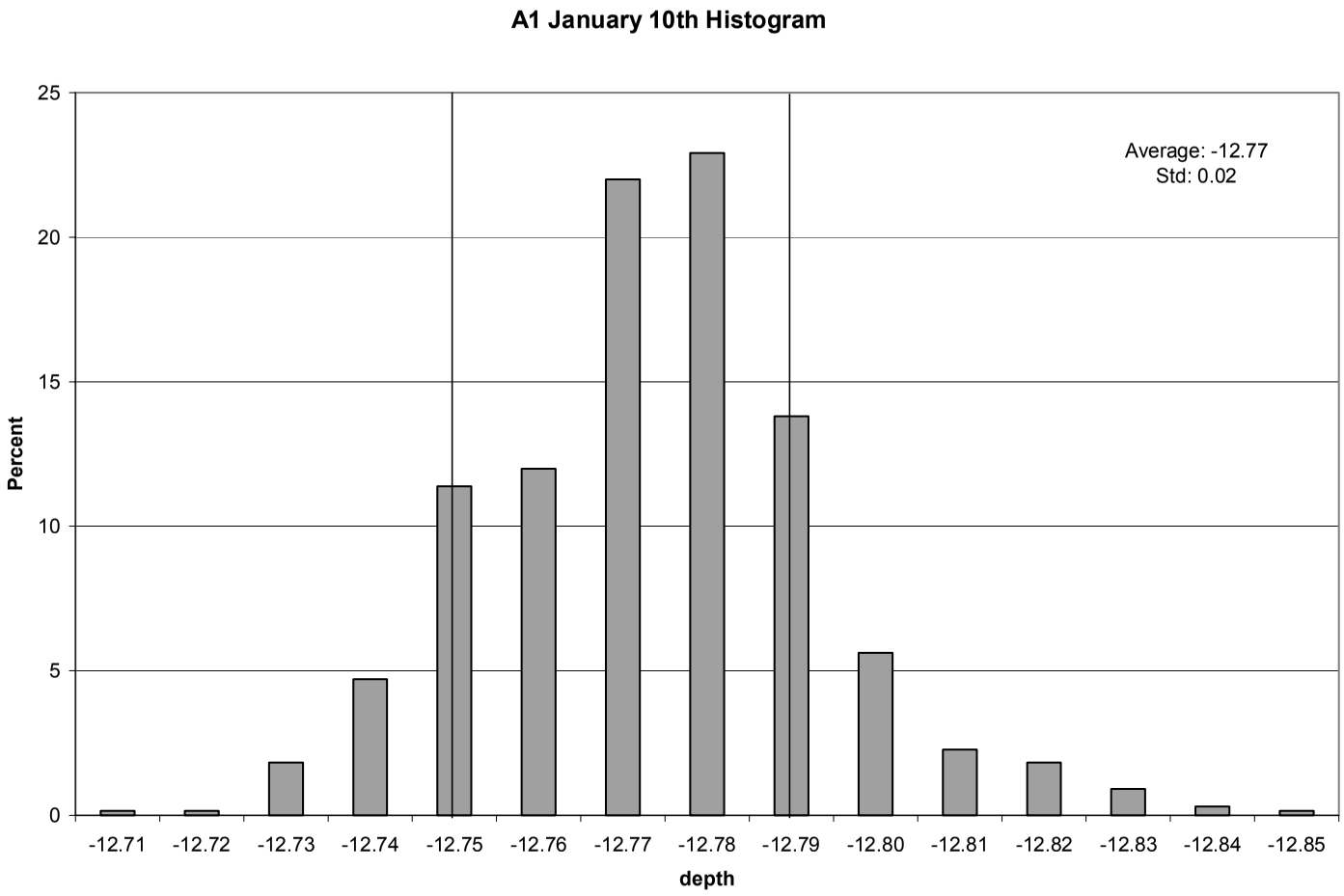

Figure 111. A1 January 10th histogram. Note that the distribution is right-skewed.

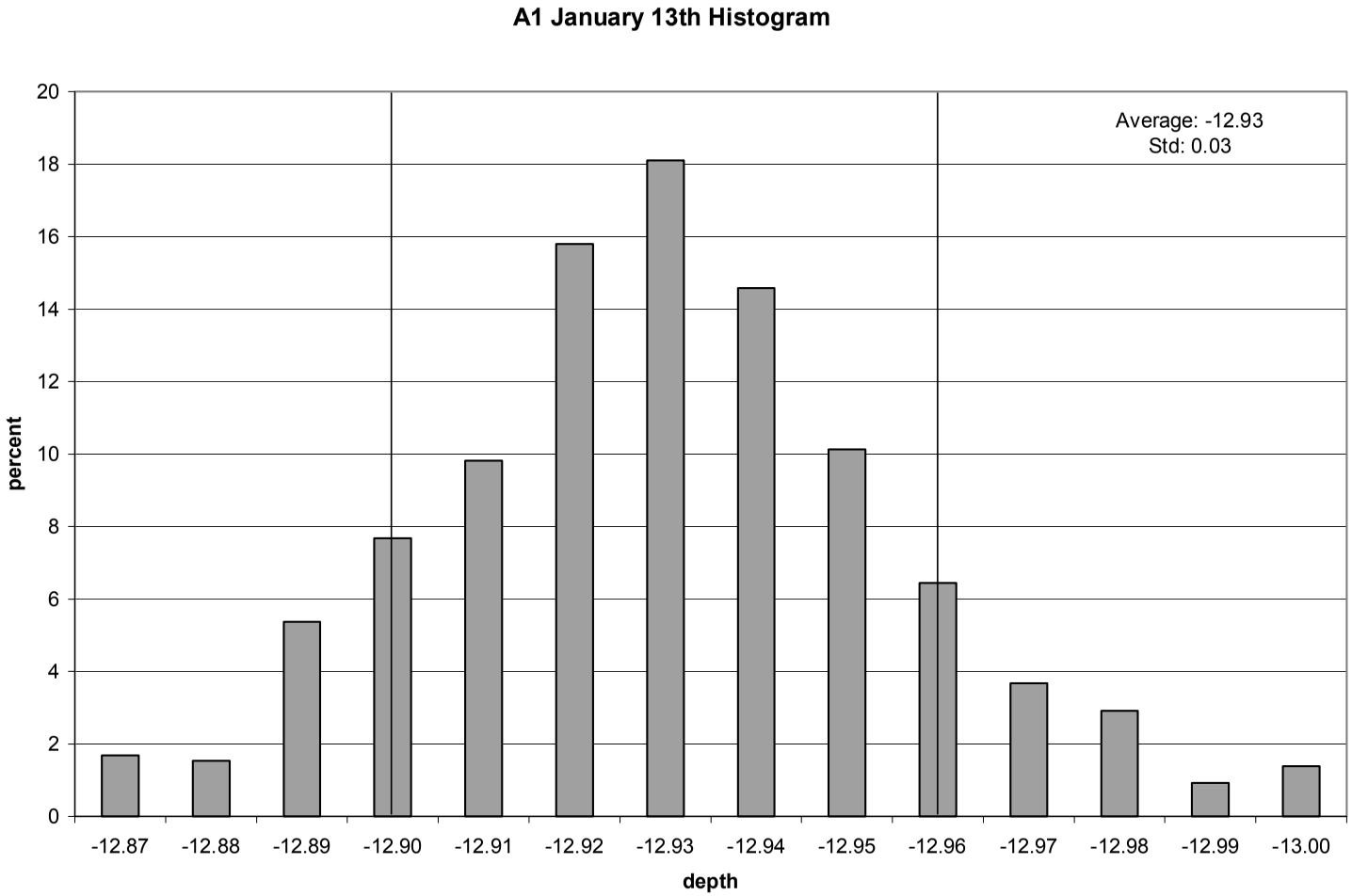

Figure 112. A1 January 13th histogram. Note that the distribution is right-skewed.

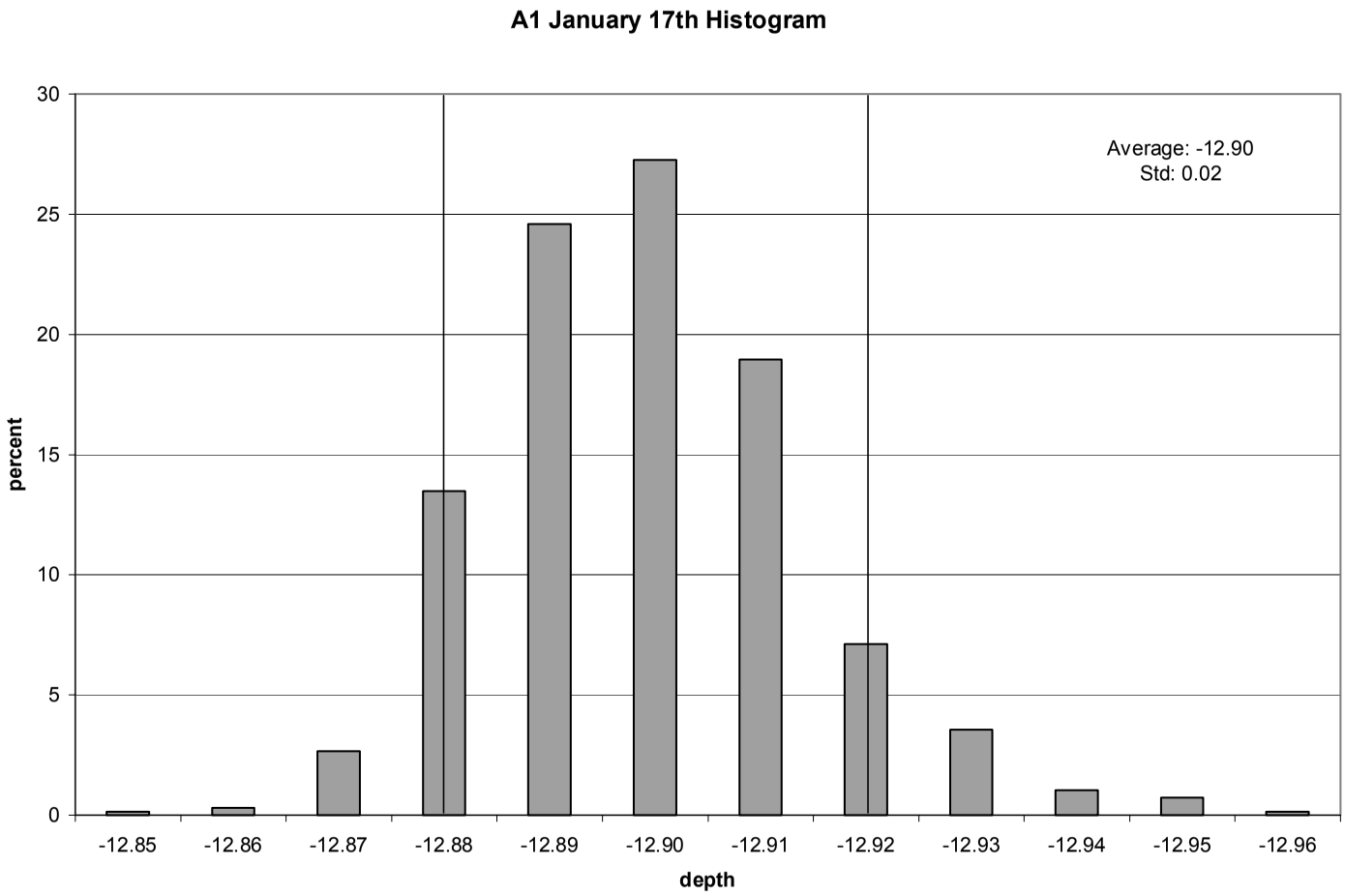

Figure 113. A1 January 17th histogram. Note that the distribution is right-skewed.

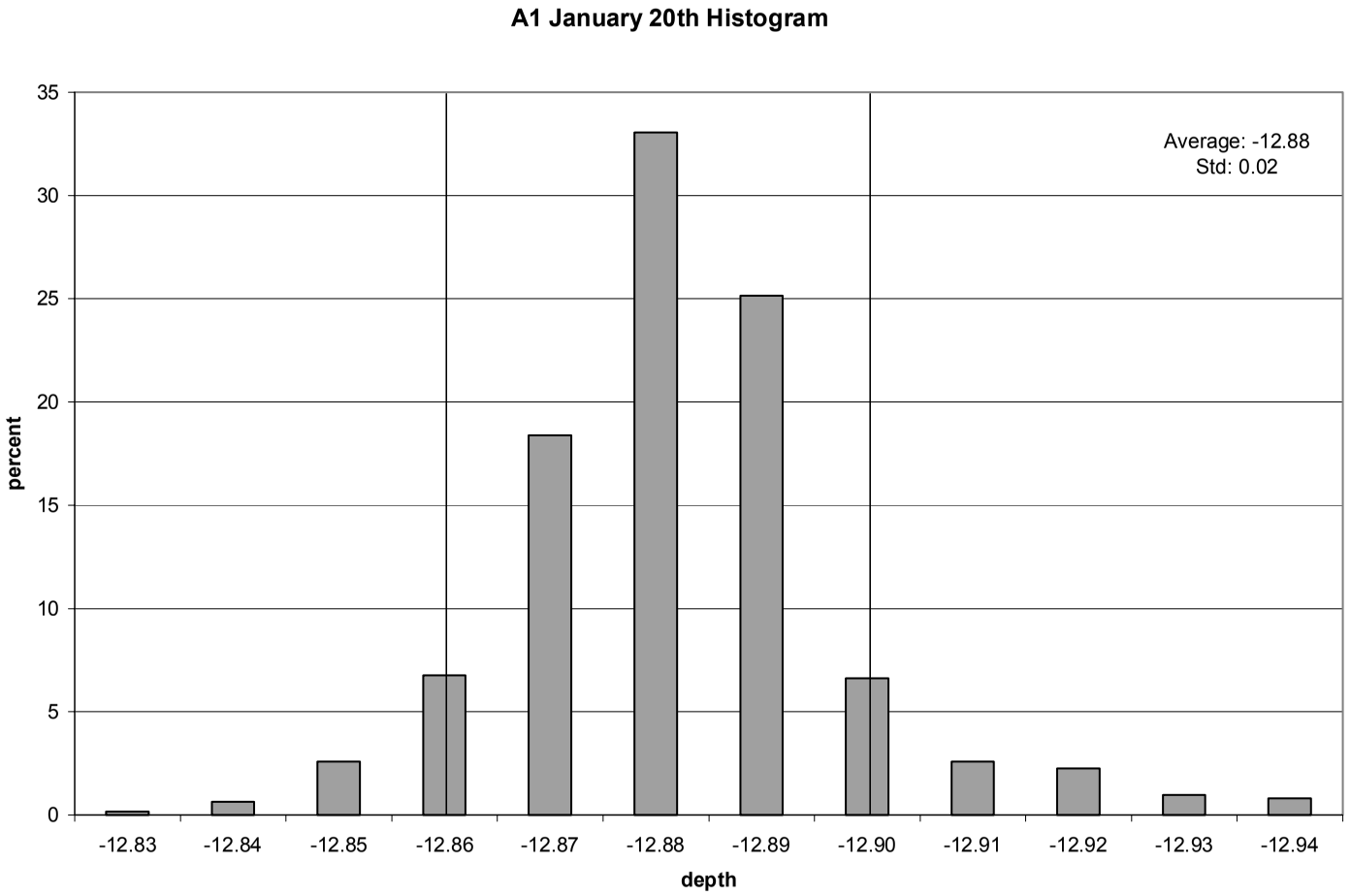

Figure 114. A1 January 20th histogram. Note that the distribution is right-skewed.

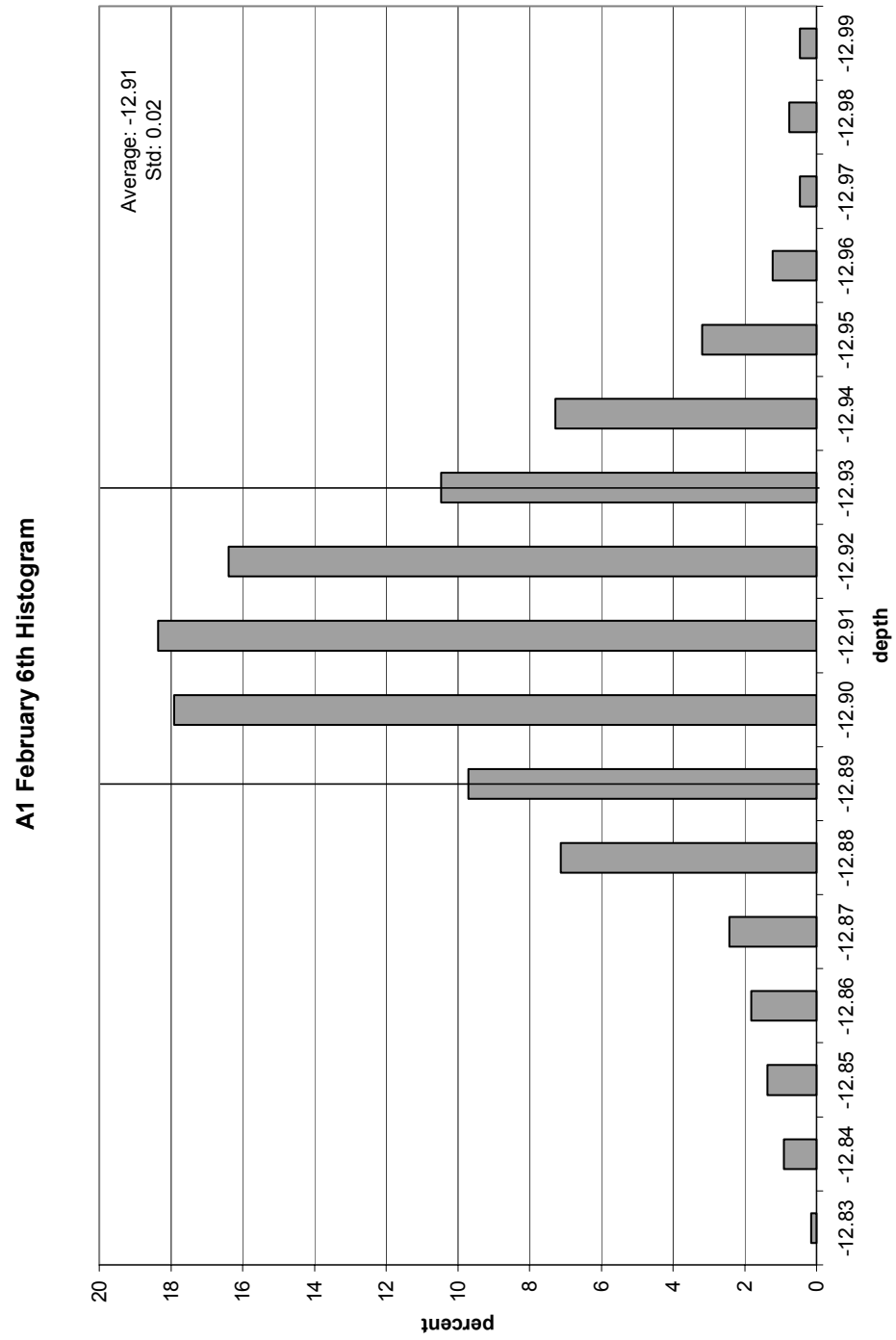

Figure 115. A1 February 6th histogram. Note that the distribution is normal.

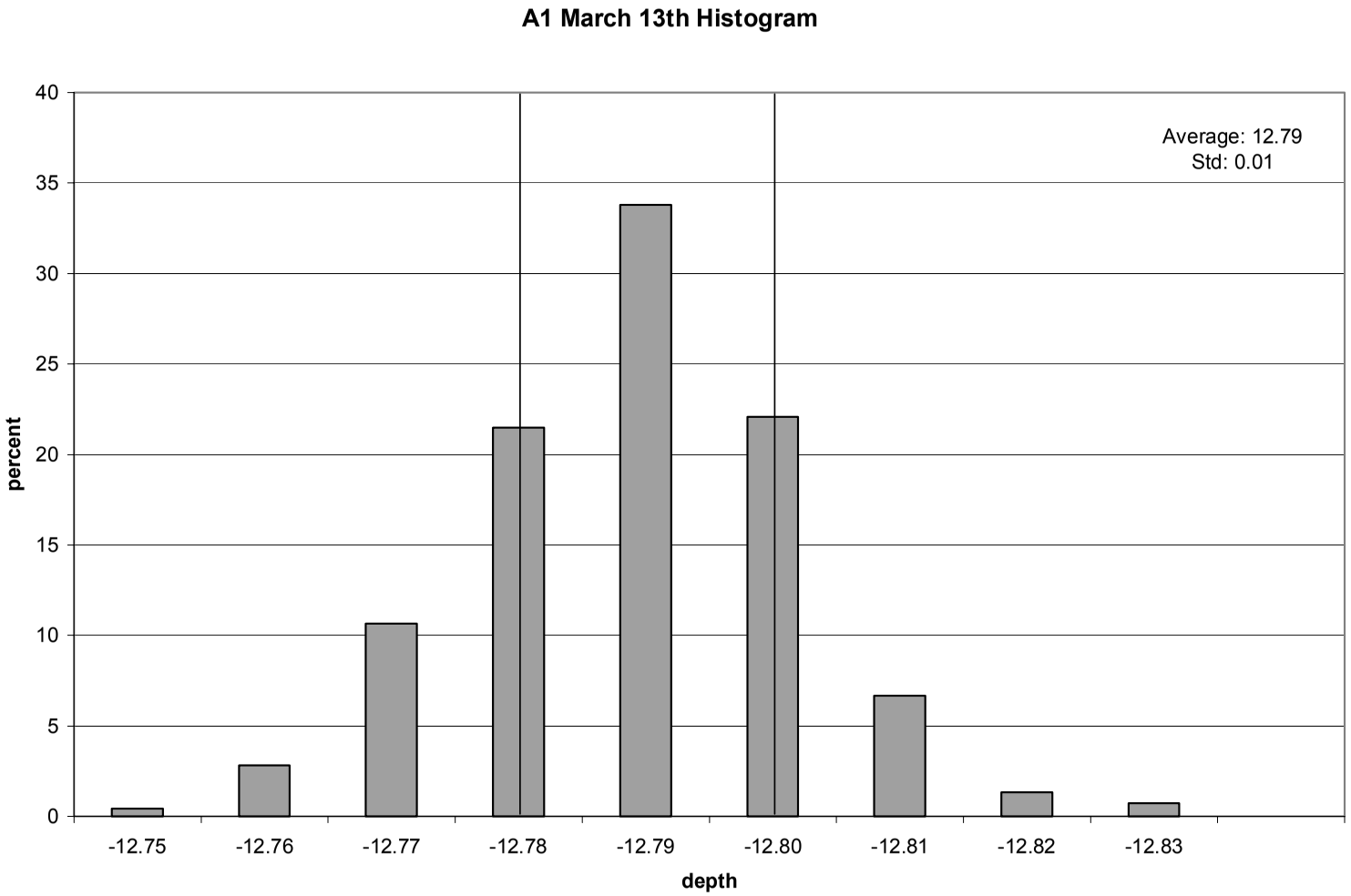

Figure 116. A1 March 13th histogram. Note that the distribution is normal.

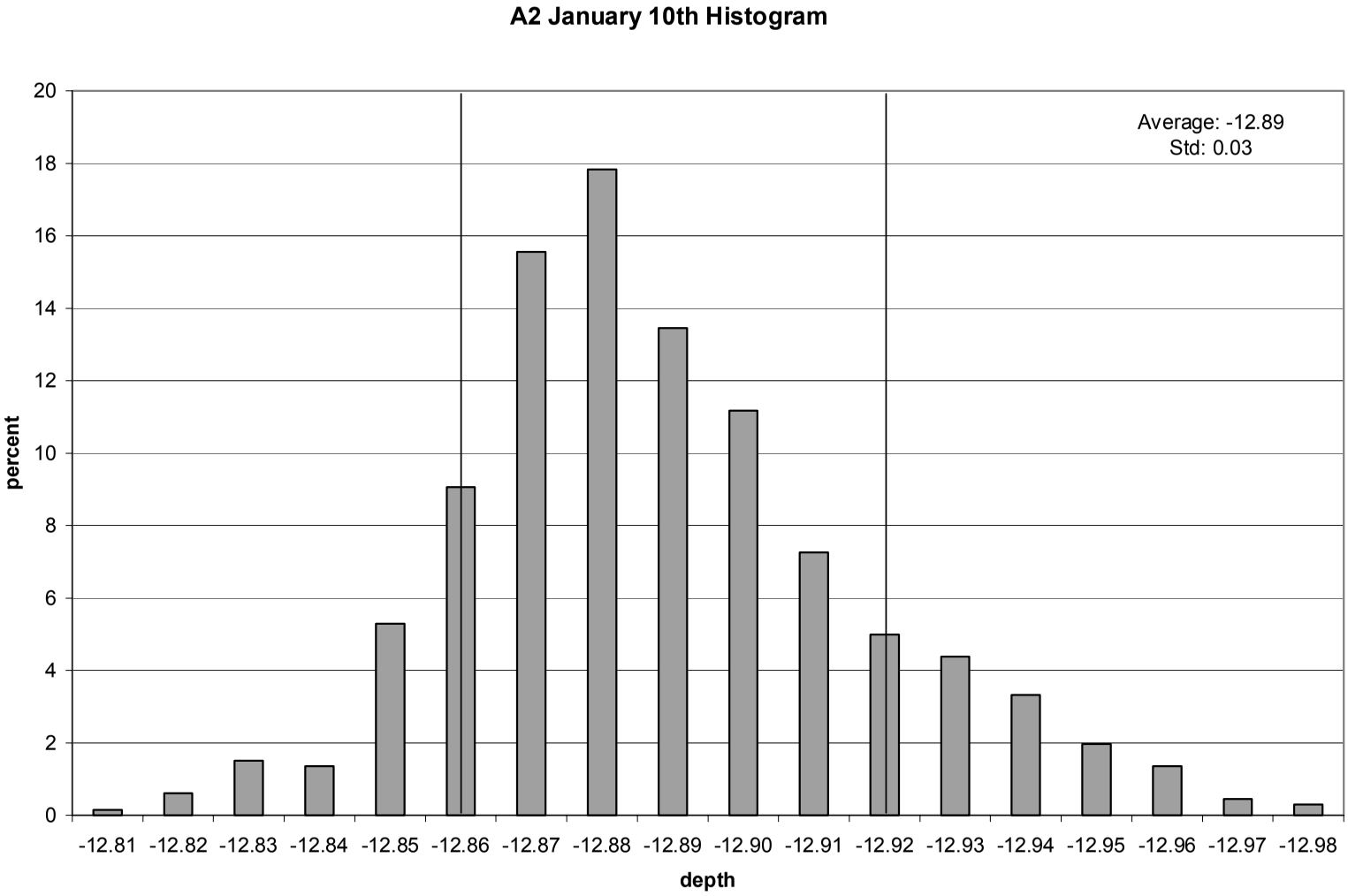

Figure 117. A2 January 10th histogram. Note that the distribution is right-skewed.

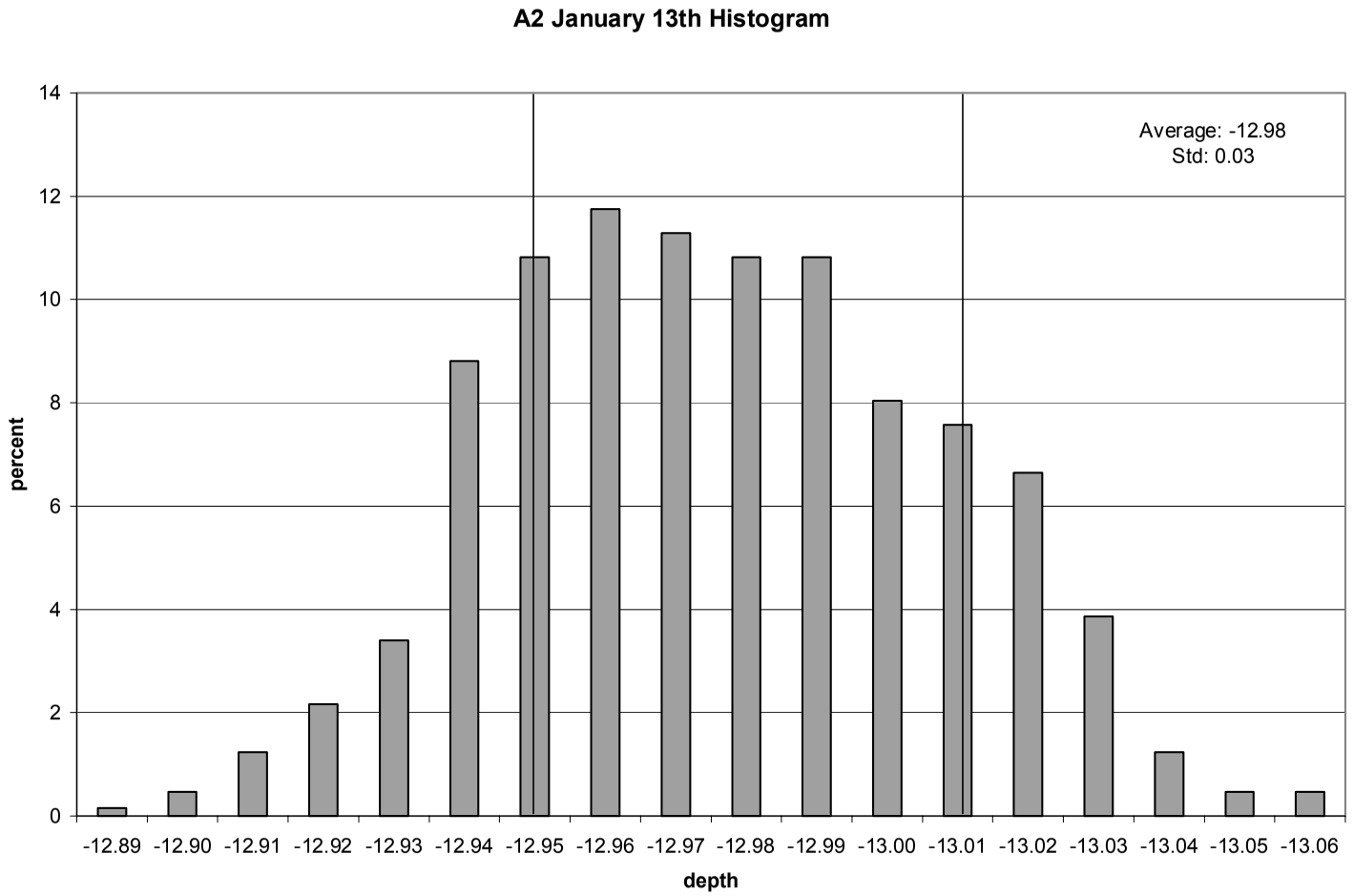

Figure 118. A2 January 13th histogram. Note that the distribution is left-skewed.

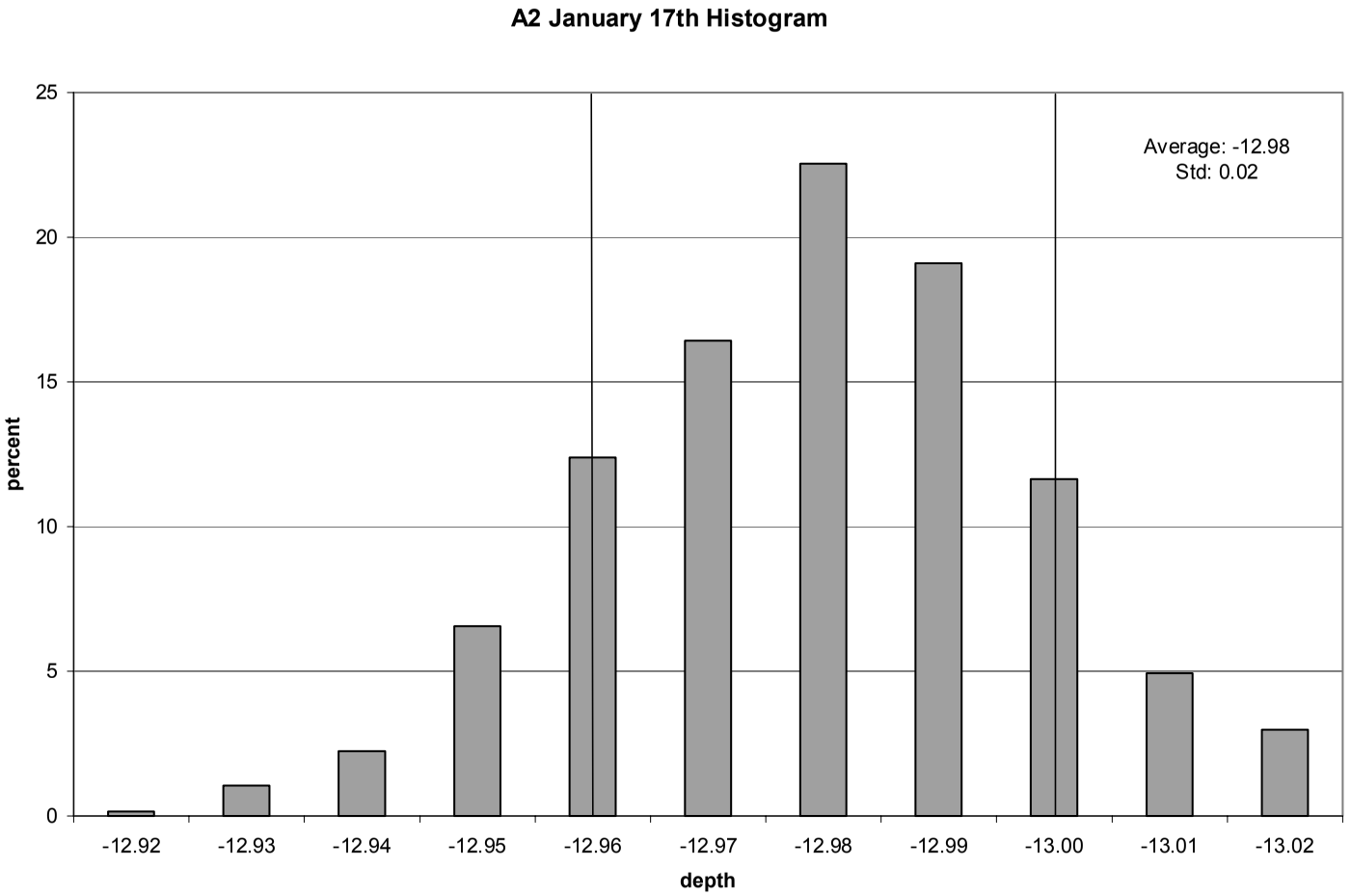

Figure 119. A2 January 17th histogram. Note that the distribution is left-skewed.

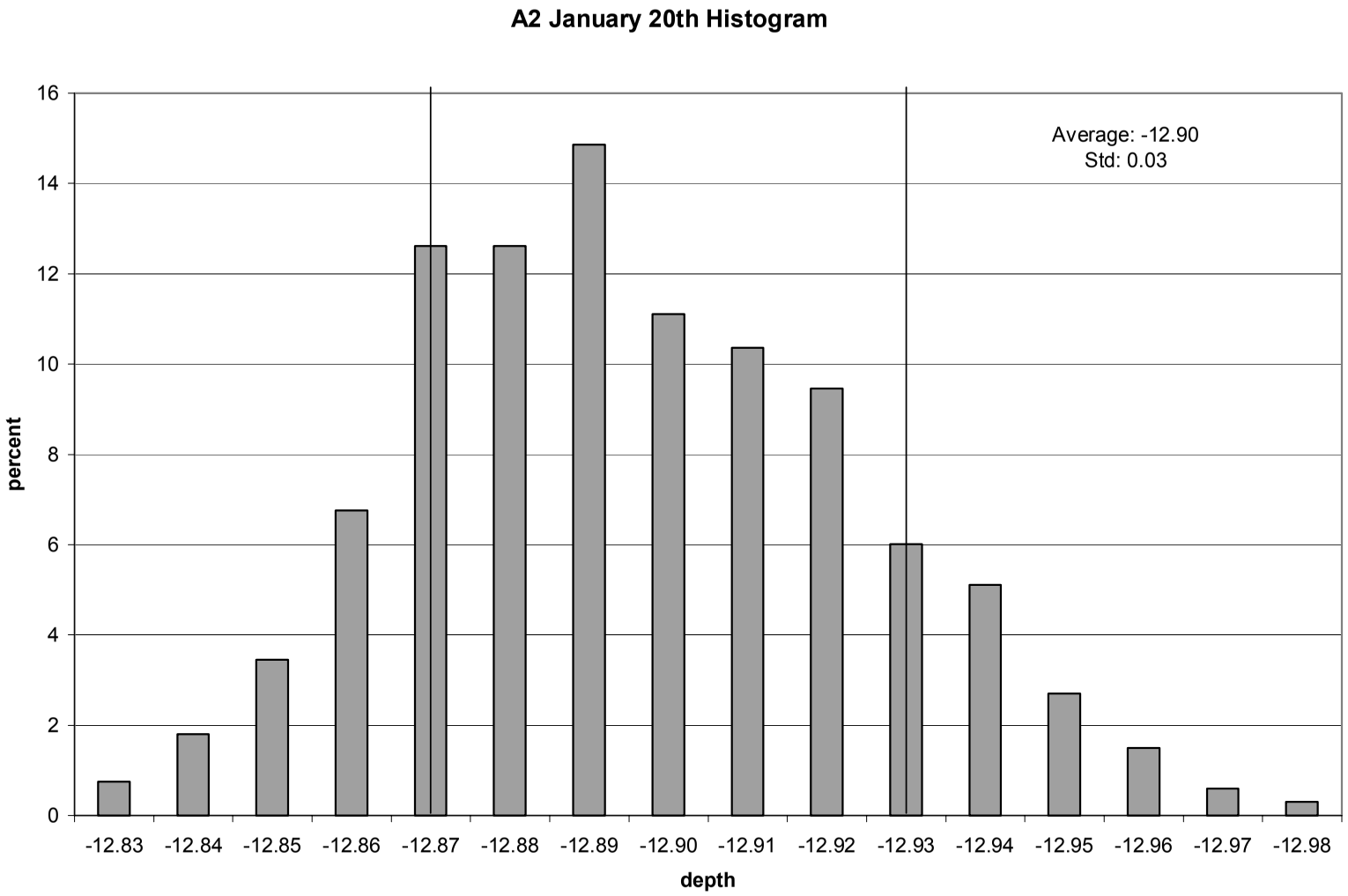

Figure 120. A2 January 20th histogram. Note that the distribution is right-skewed.

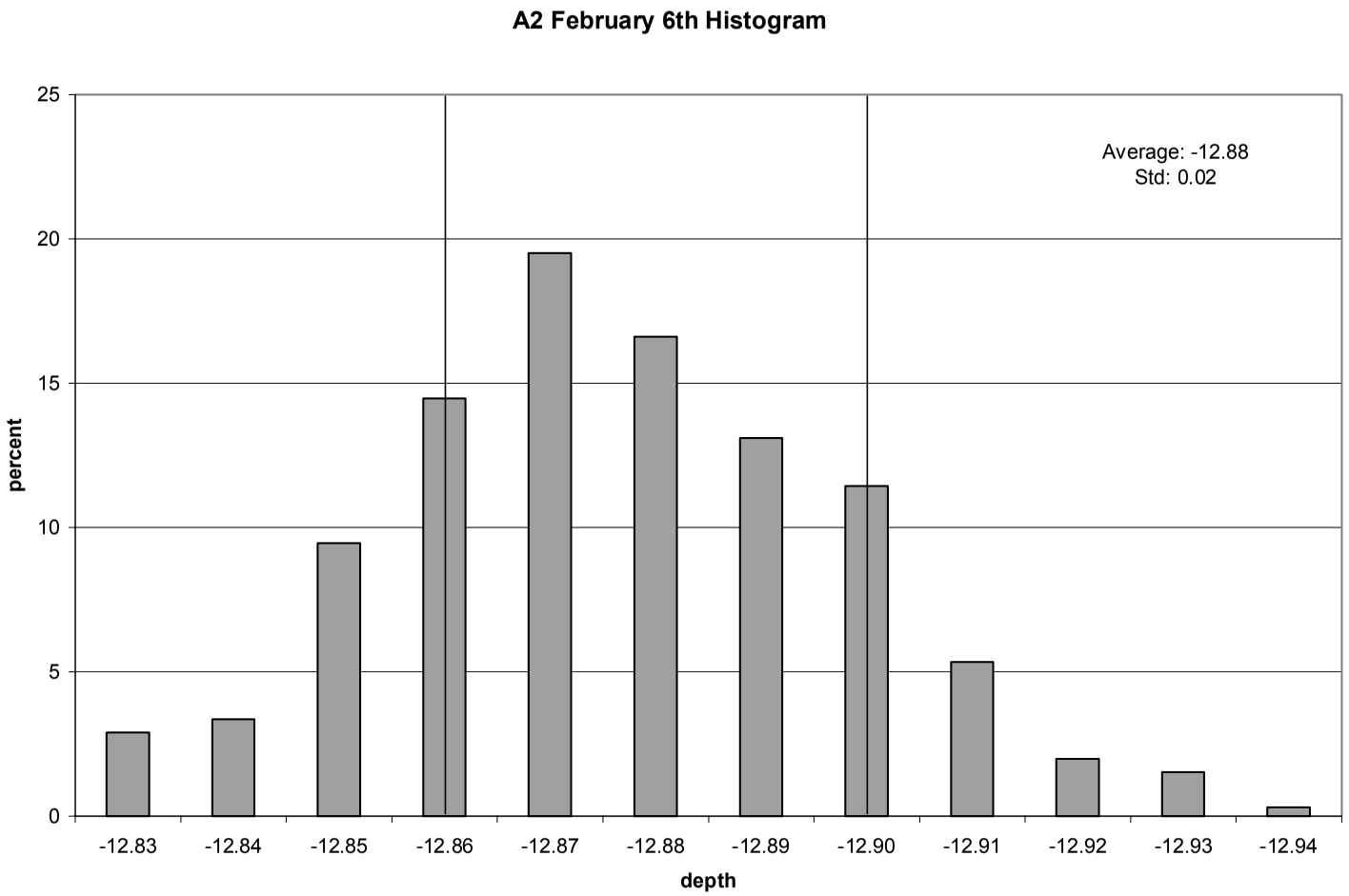

Figure 121. A2 February 6th histogram. Note that the distribution is right-skewed.

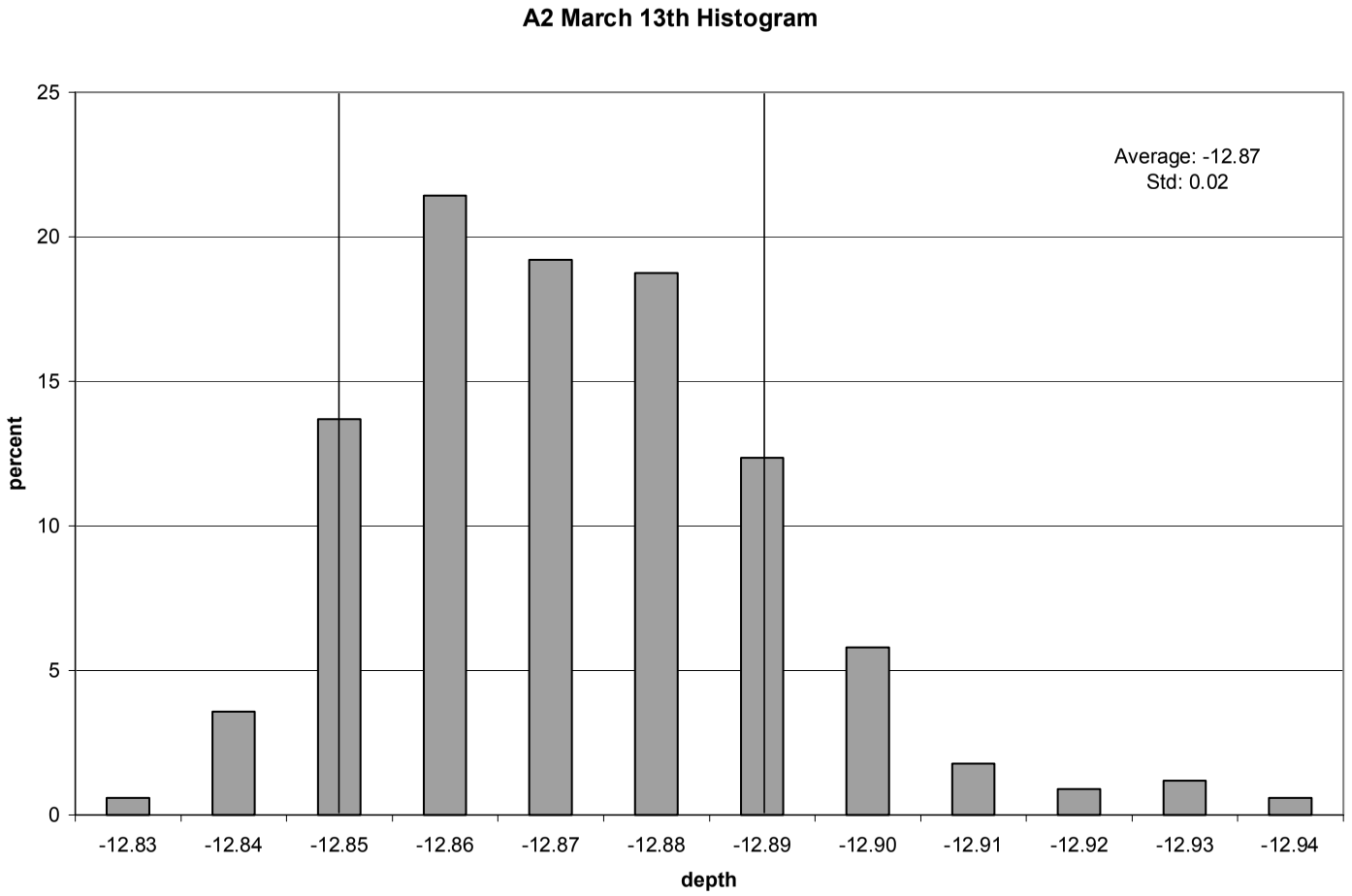

Figure 122. A2 March 13th histogram. Note that the distribution is right-skewed.

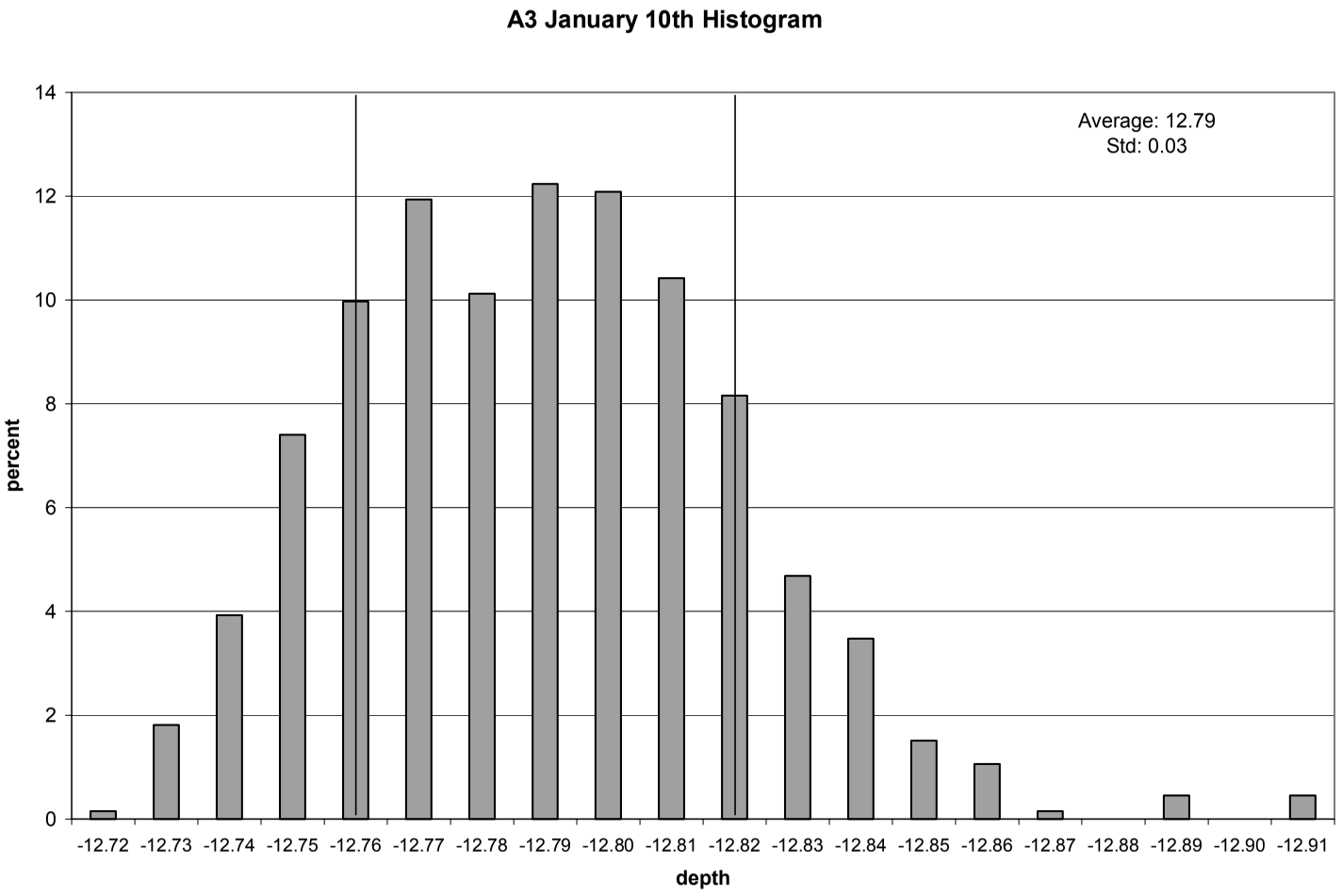

Figure 123. A3 January 10th histogram. Note that the distribution is right-skewed.

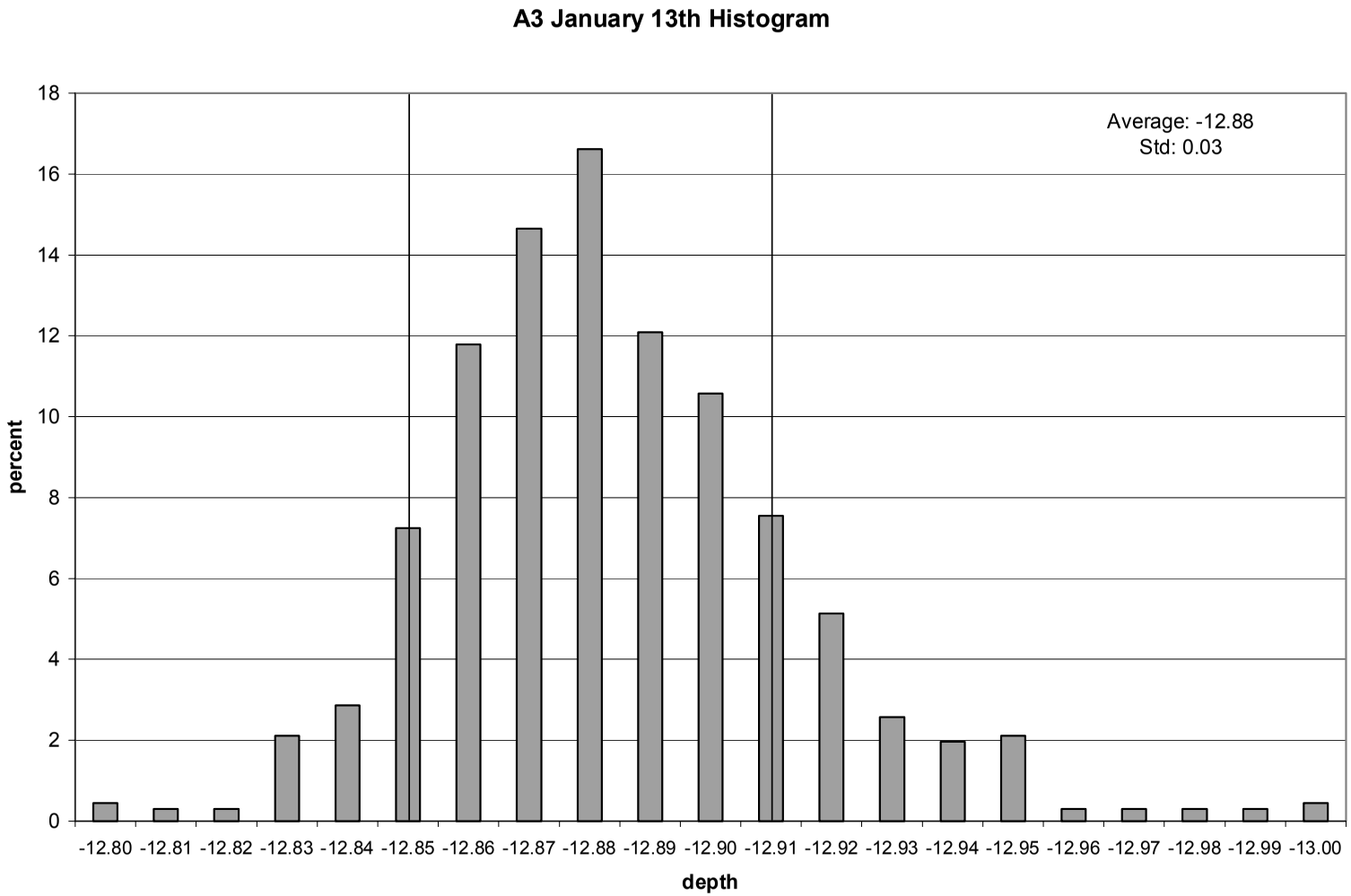

Figure 124. A3 January 13th histogram. Note that the distribution is right-skewed.

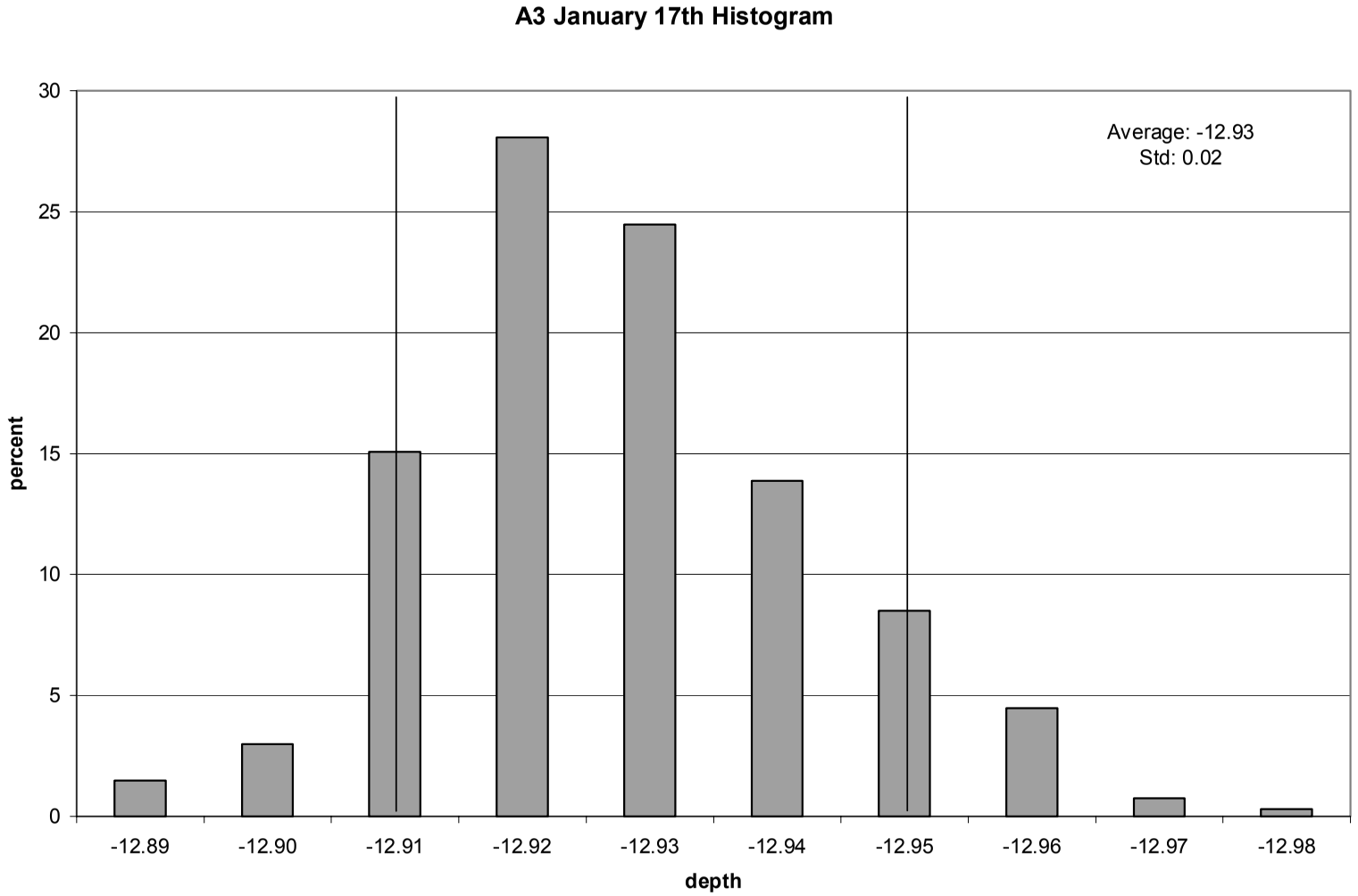

Figure 125. A3 January 17th histogram. Note that the distribution is right-skewed.

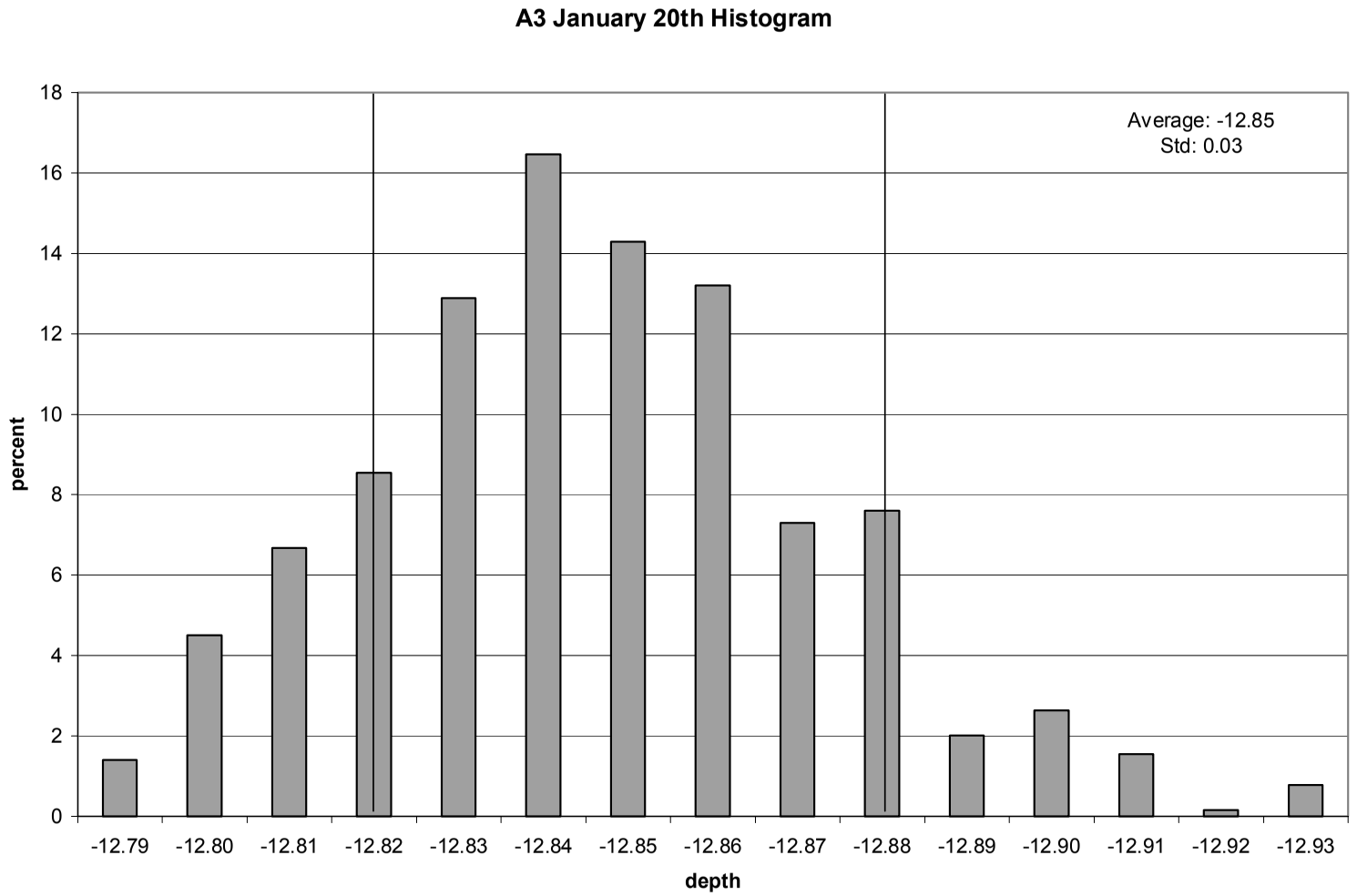

Figure 126. A3 January 20th histogram. Note that the distribution is right-skewed.

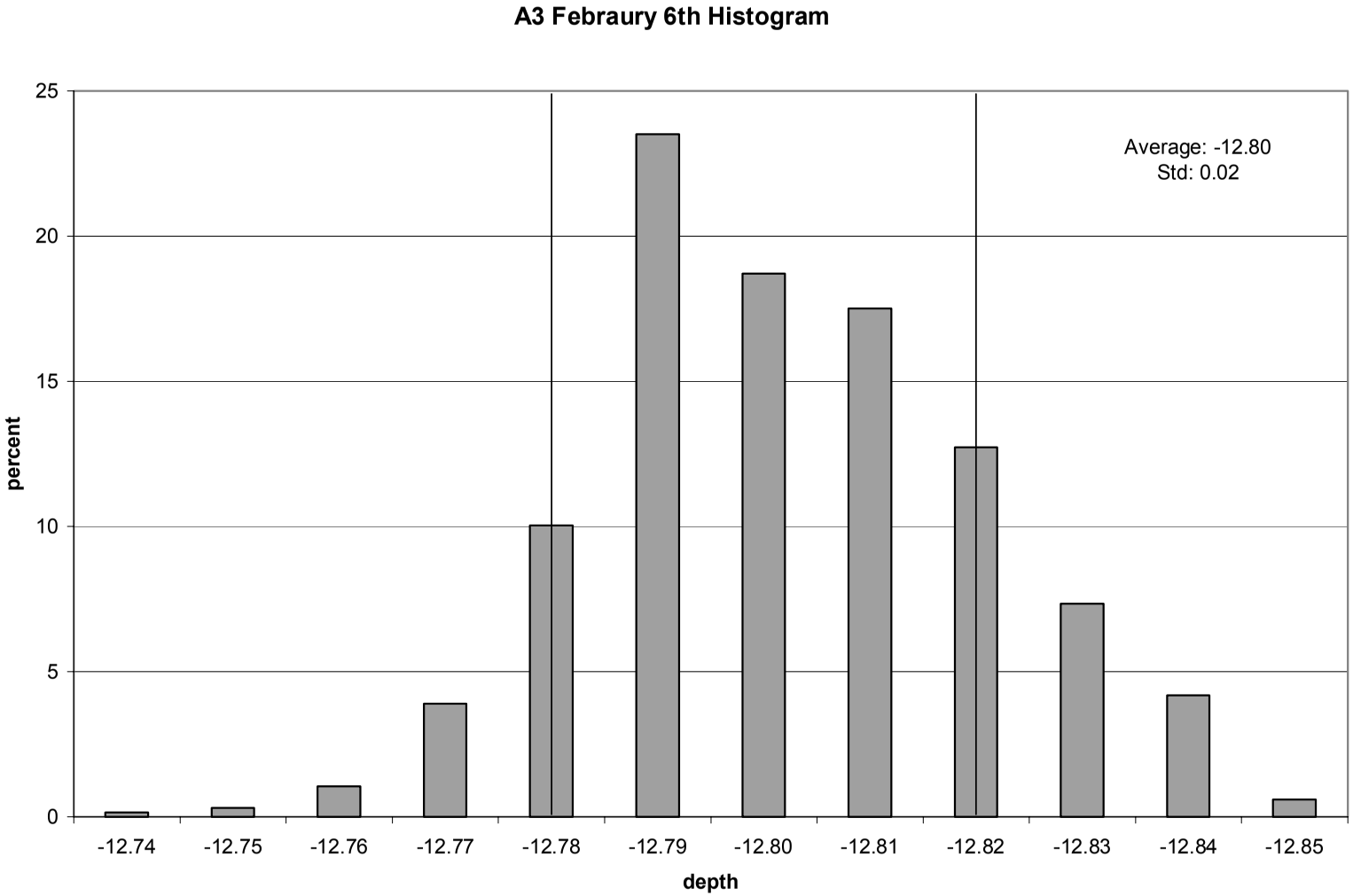

Figure 127. A3 February 6th histogram. Note that the distribution is left-skewed.

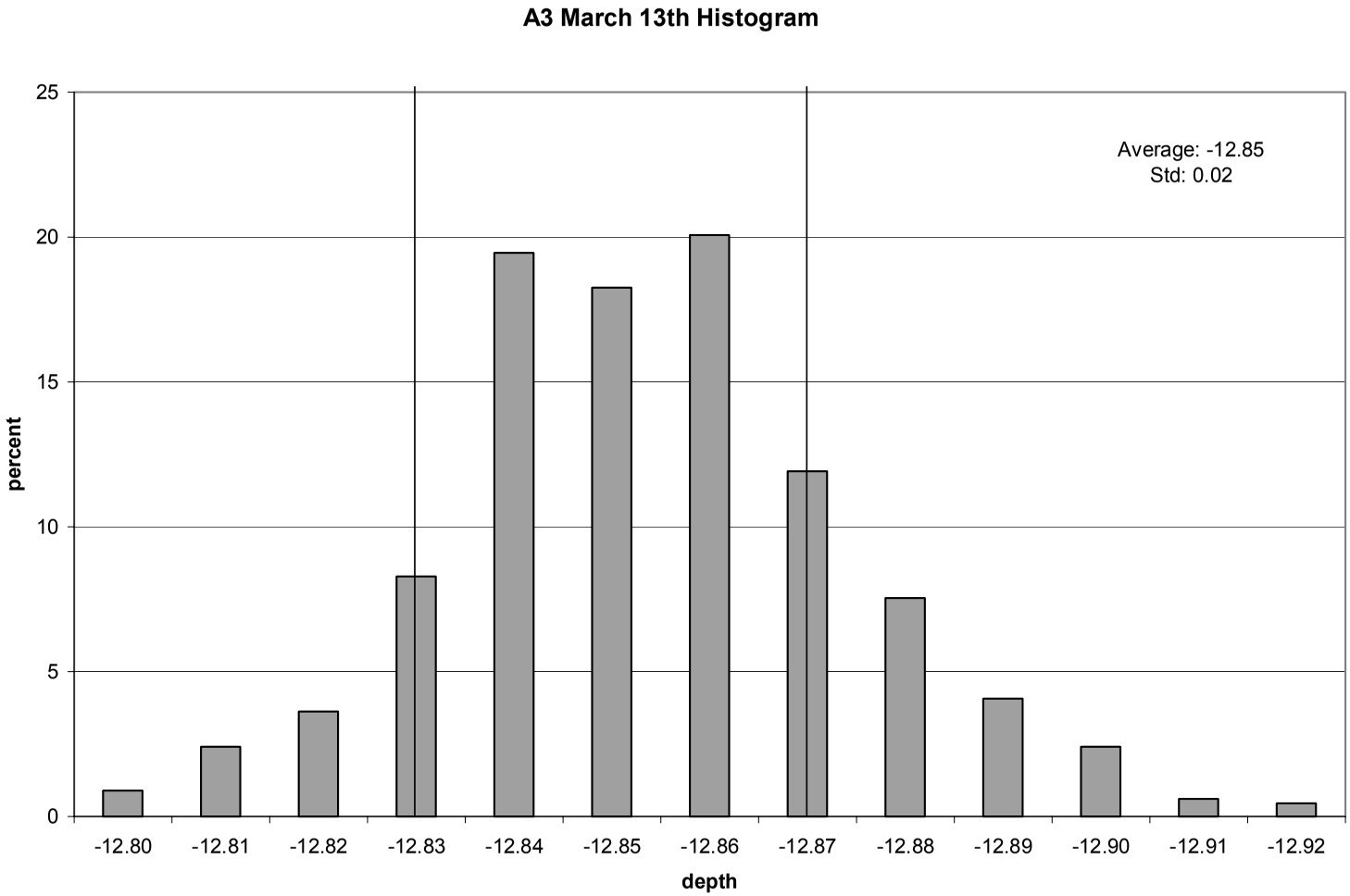

Figure 128. A3 March 13th histogram. Note that the distribution is right-skewed.

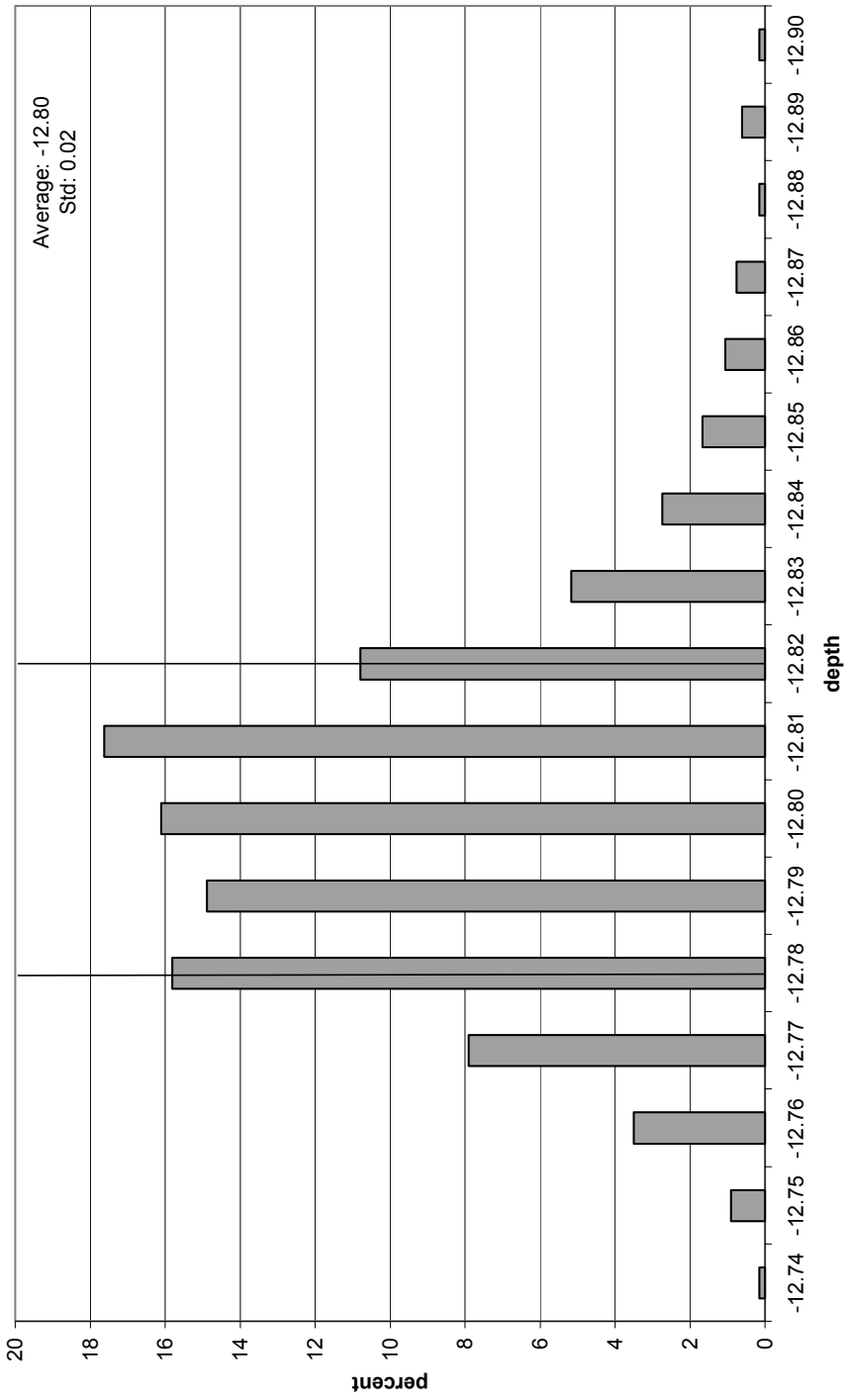

Figure 129. A4 January 10th histogram. Note that the distribution is right-skewed.

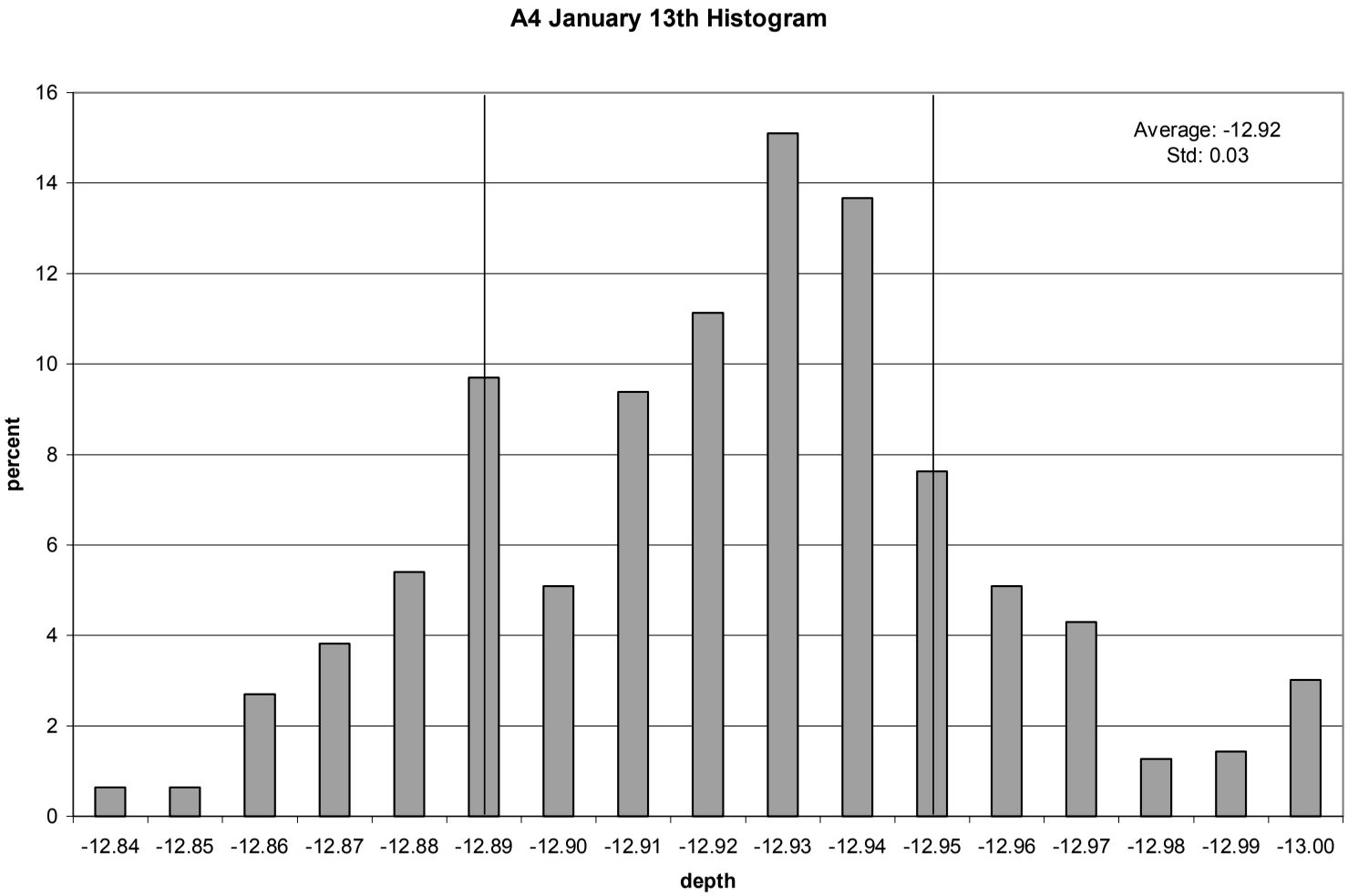

Figure 130. A4 January 13th histogram. Note that the distribution is normal.

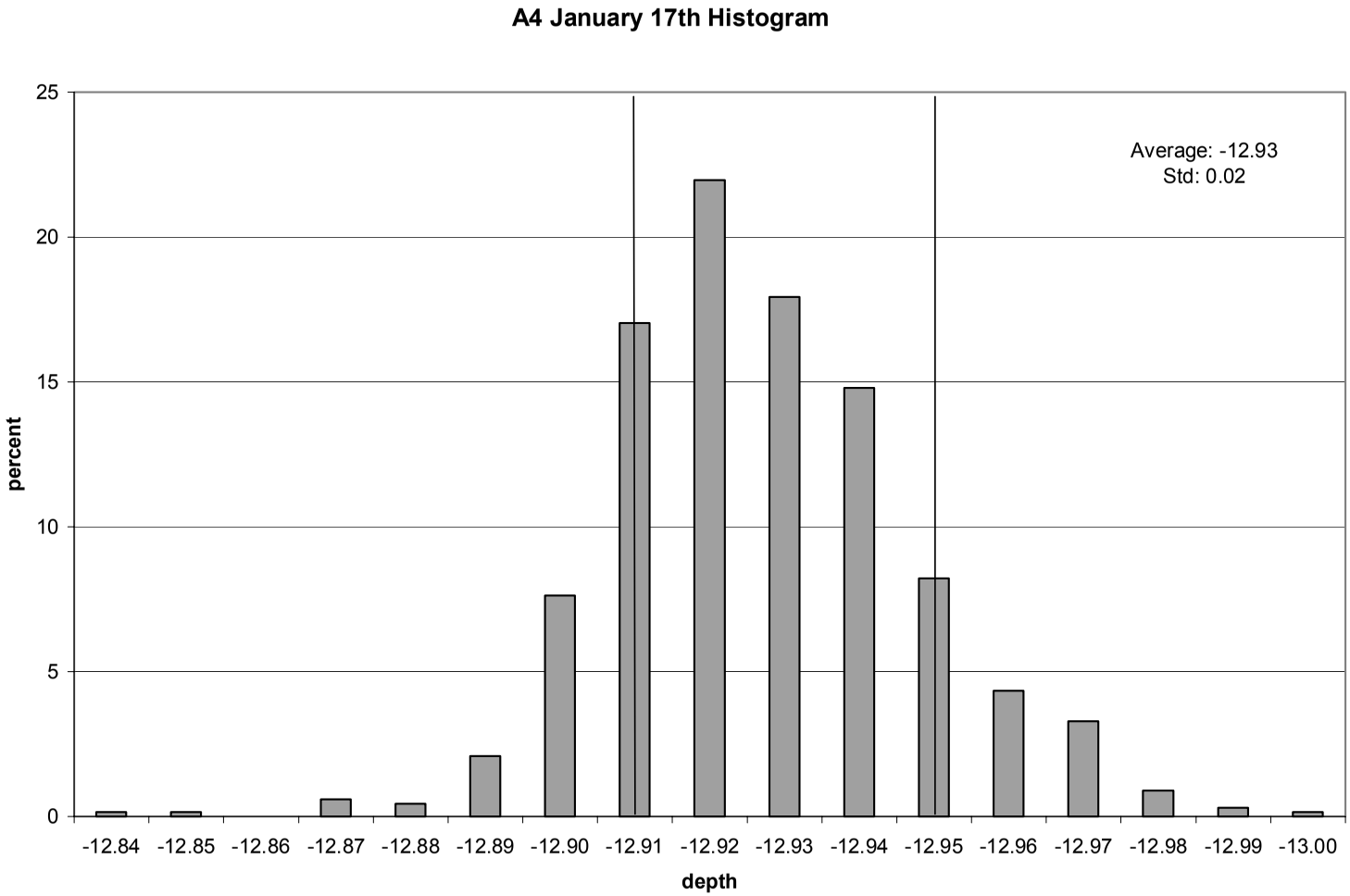

Figure 131. A4 January 17th histogram. Note that the distribution is left-skewed.

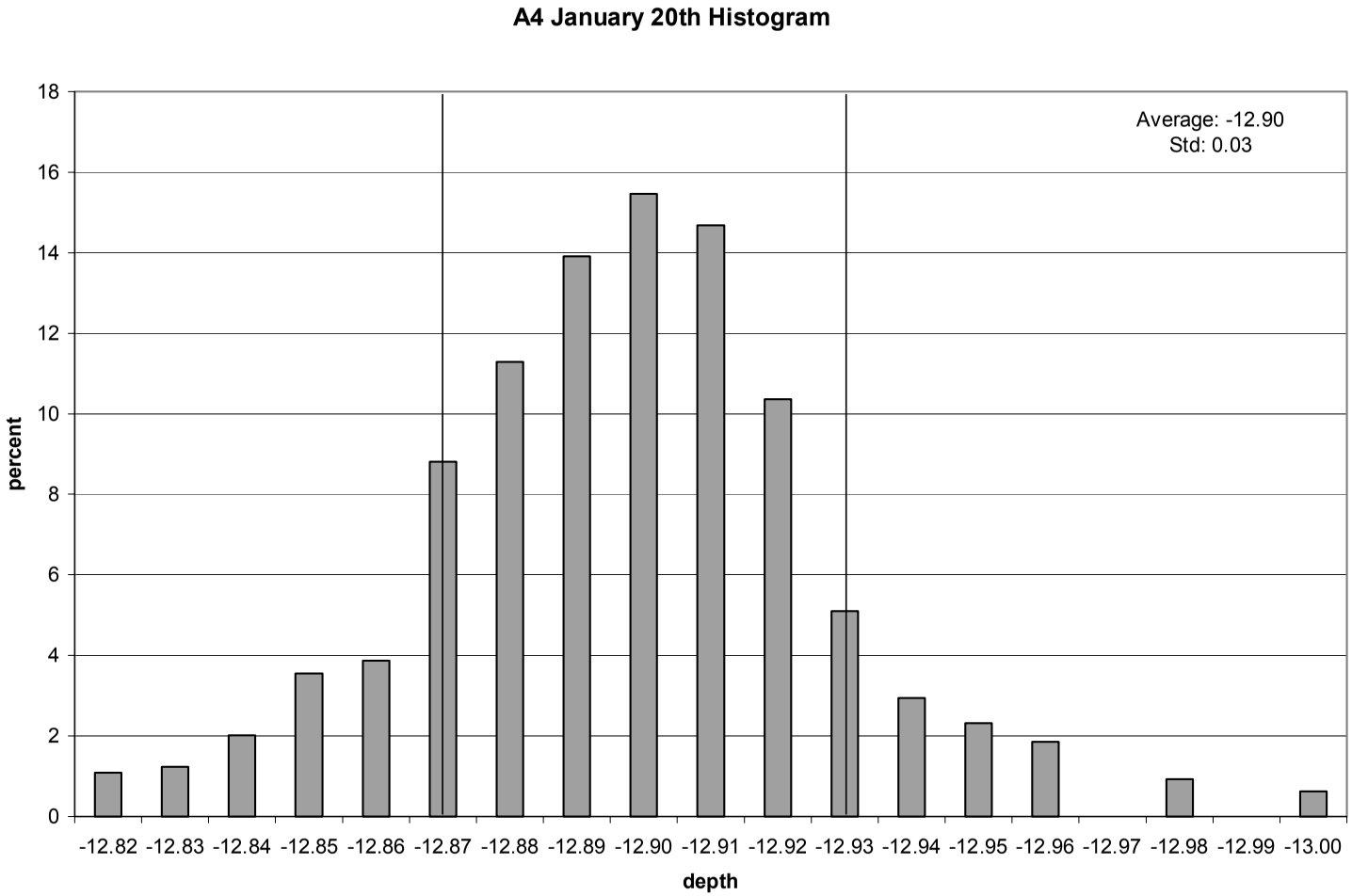

Figure 132. A4 January 20th histogram. Note that the distribution is right-skewed.

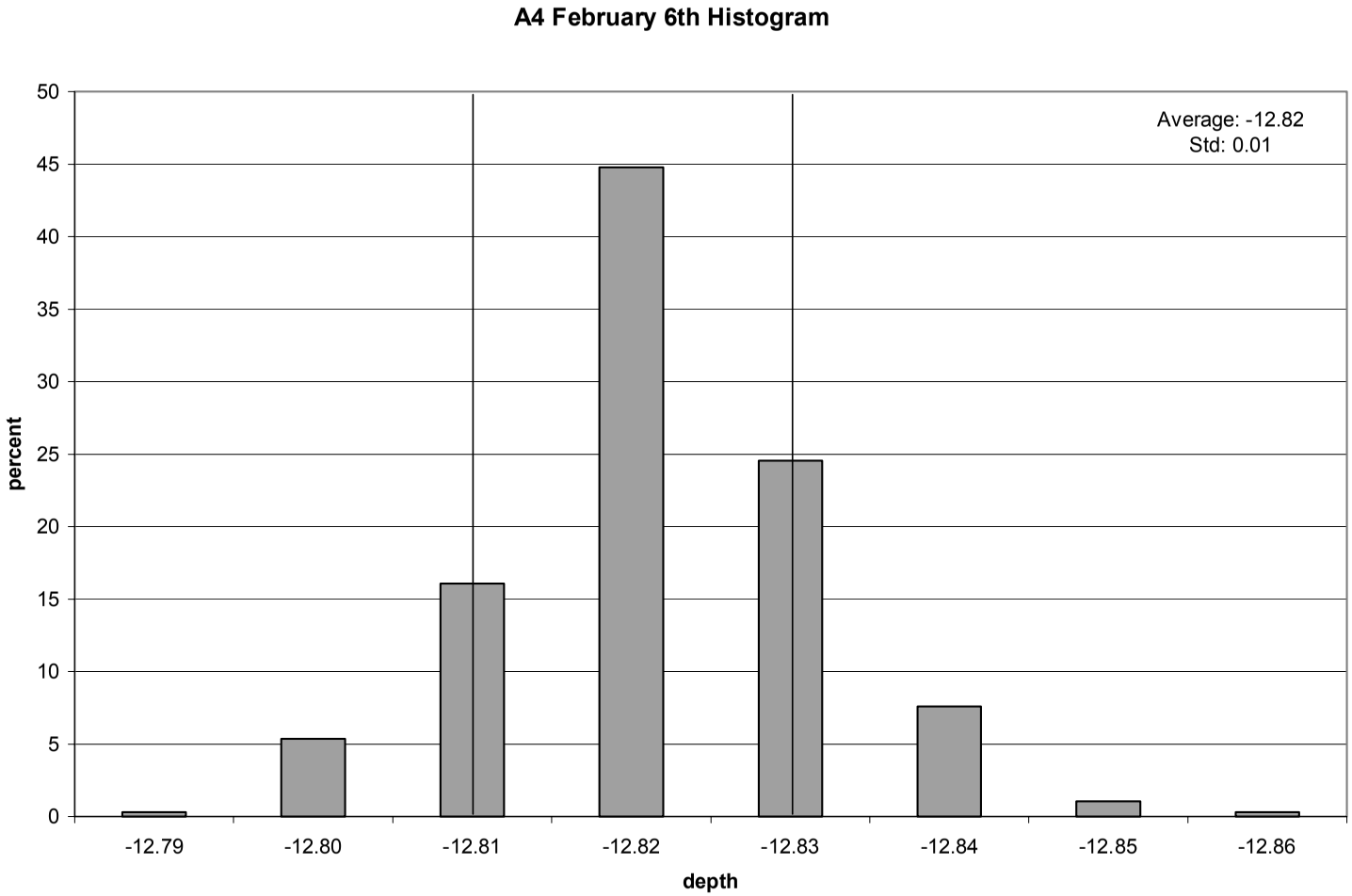

Figure 133. A4 February 6th histogram. Note that the distribution is right-skewed.

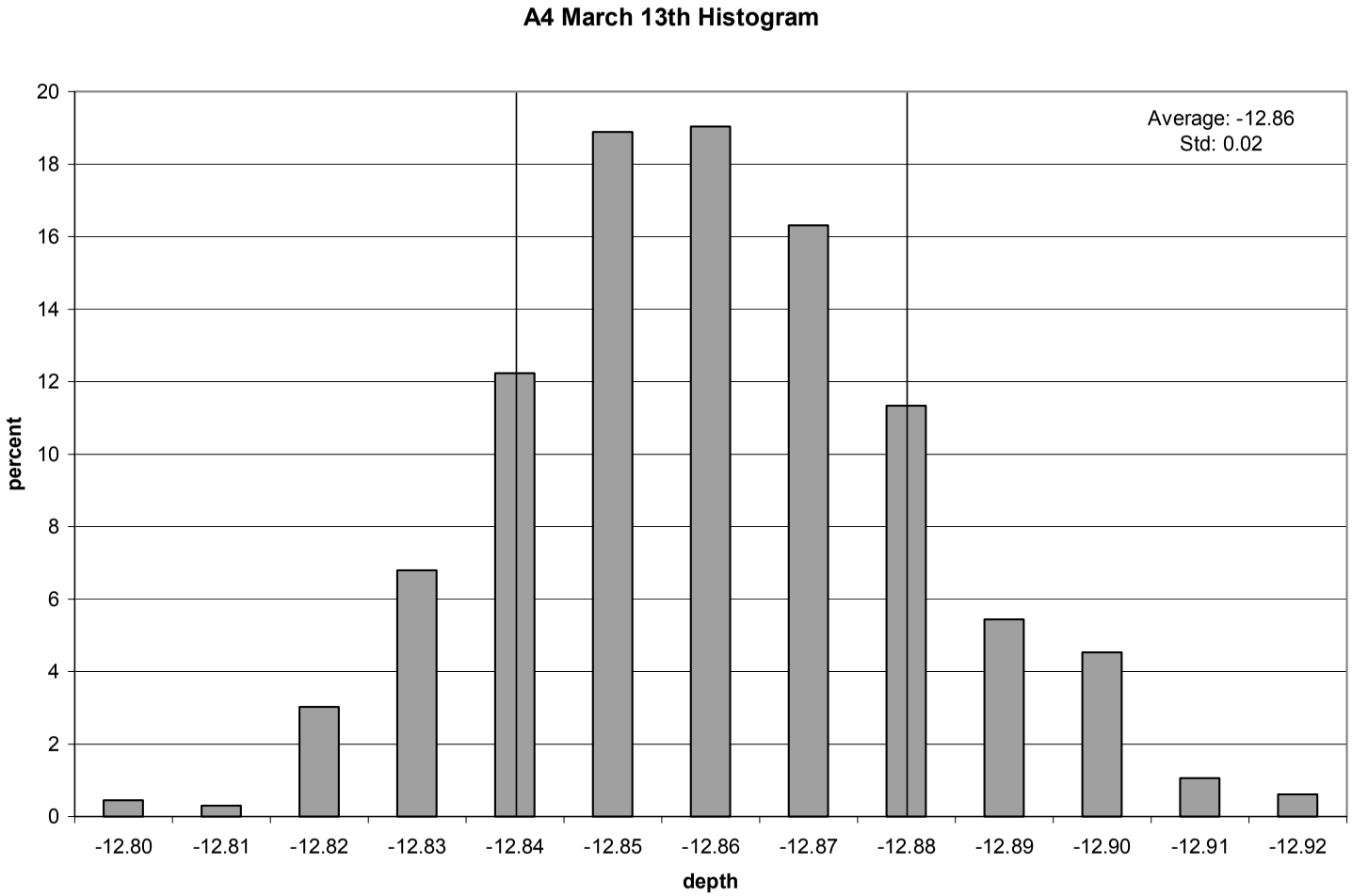

Figure 134. A4 March 13th histogram. Note that the distribution is normal.

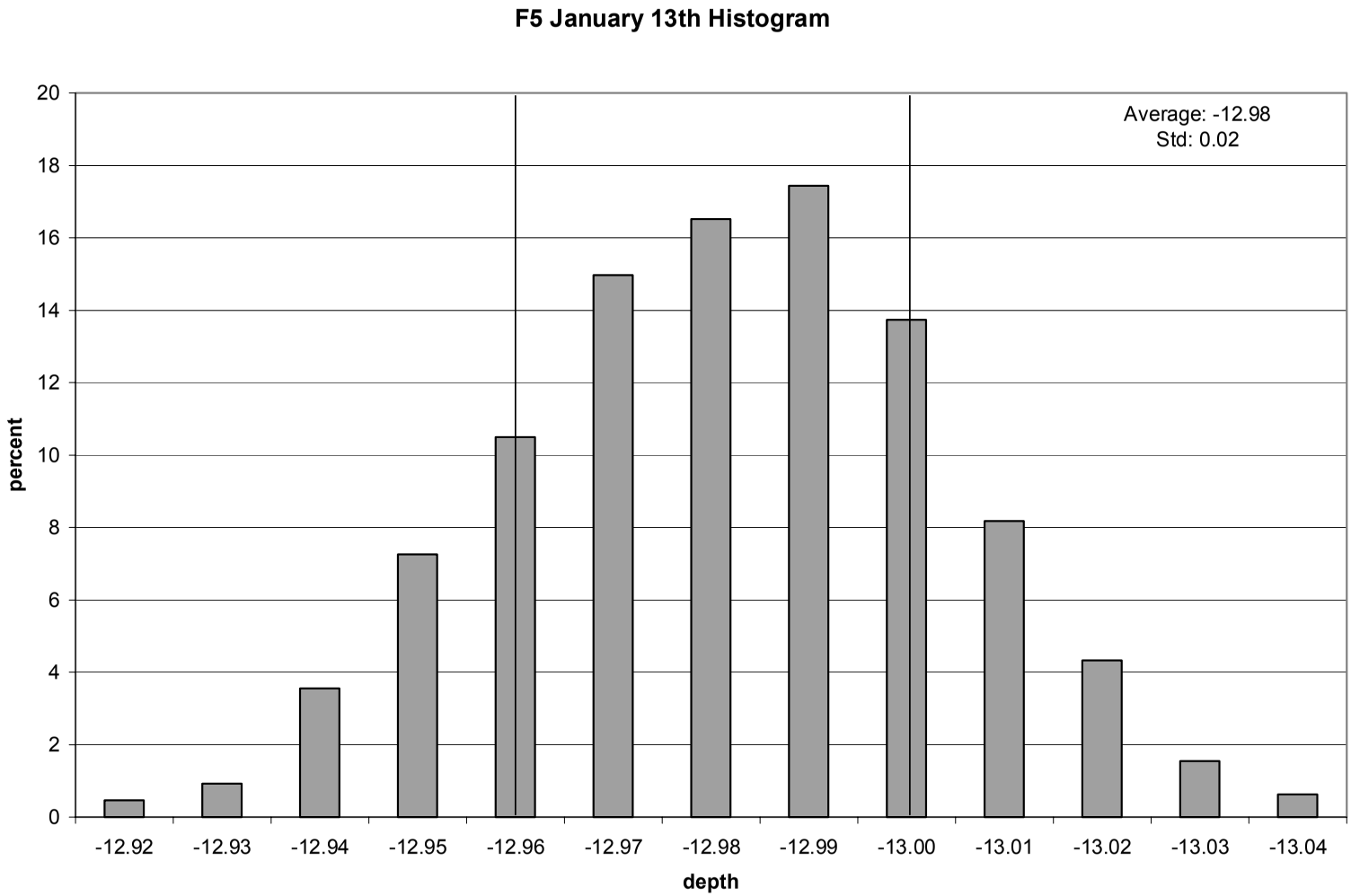

Figure 135. F5 January 13th histogram. Note that the distribution is normal.

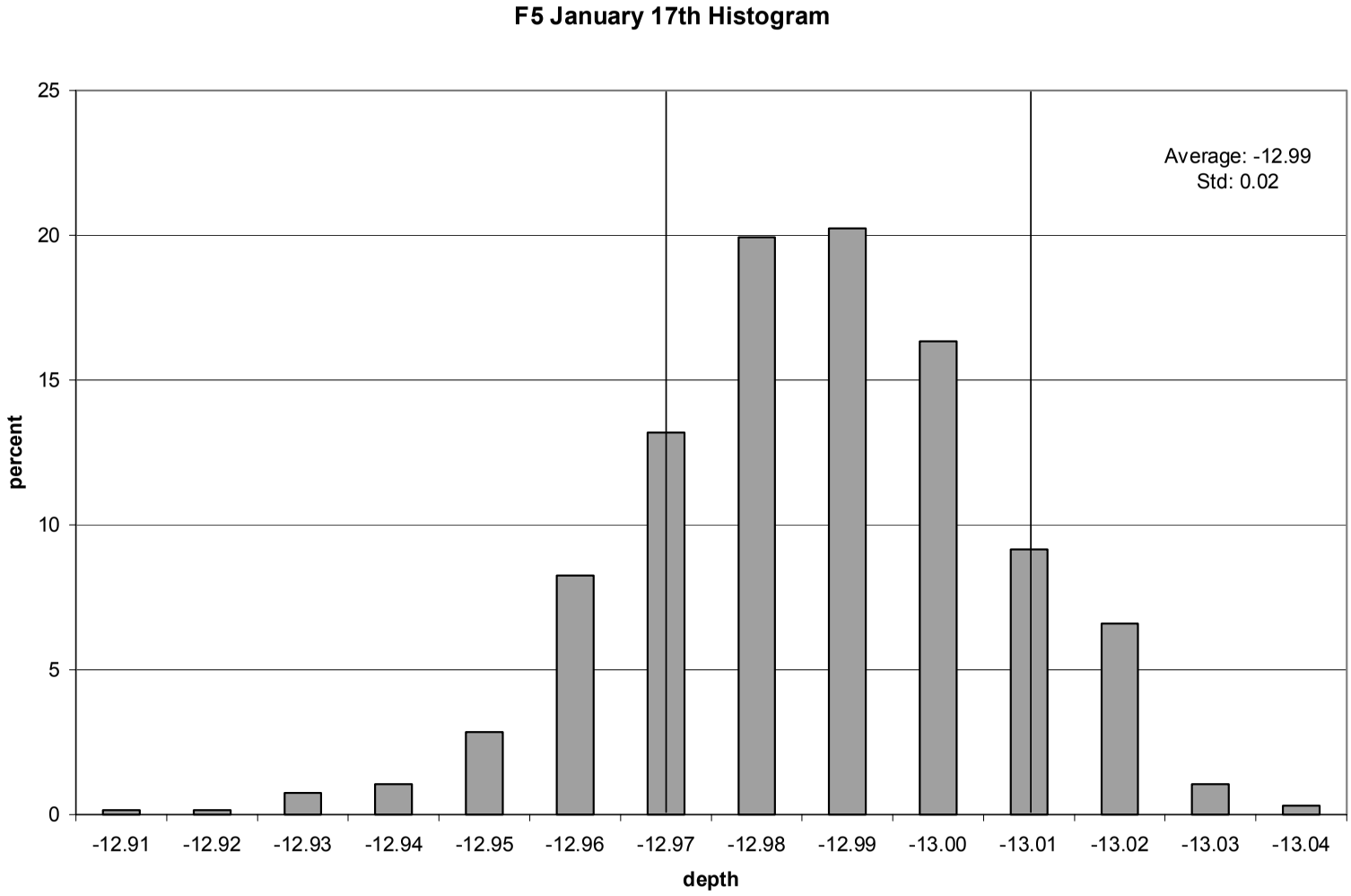

Figure 136. F5 January 17th histogram. Note that the distribution is left-skewed.

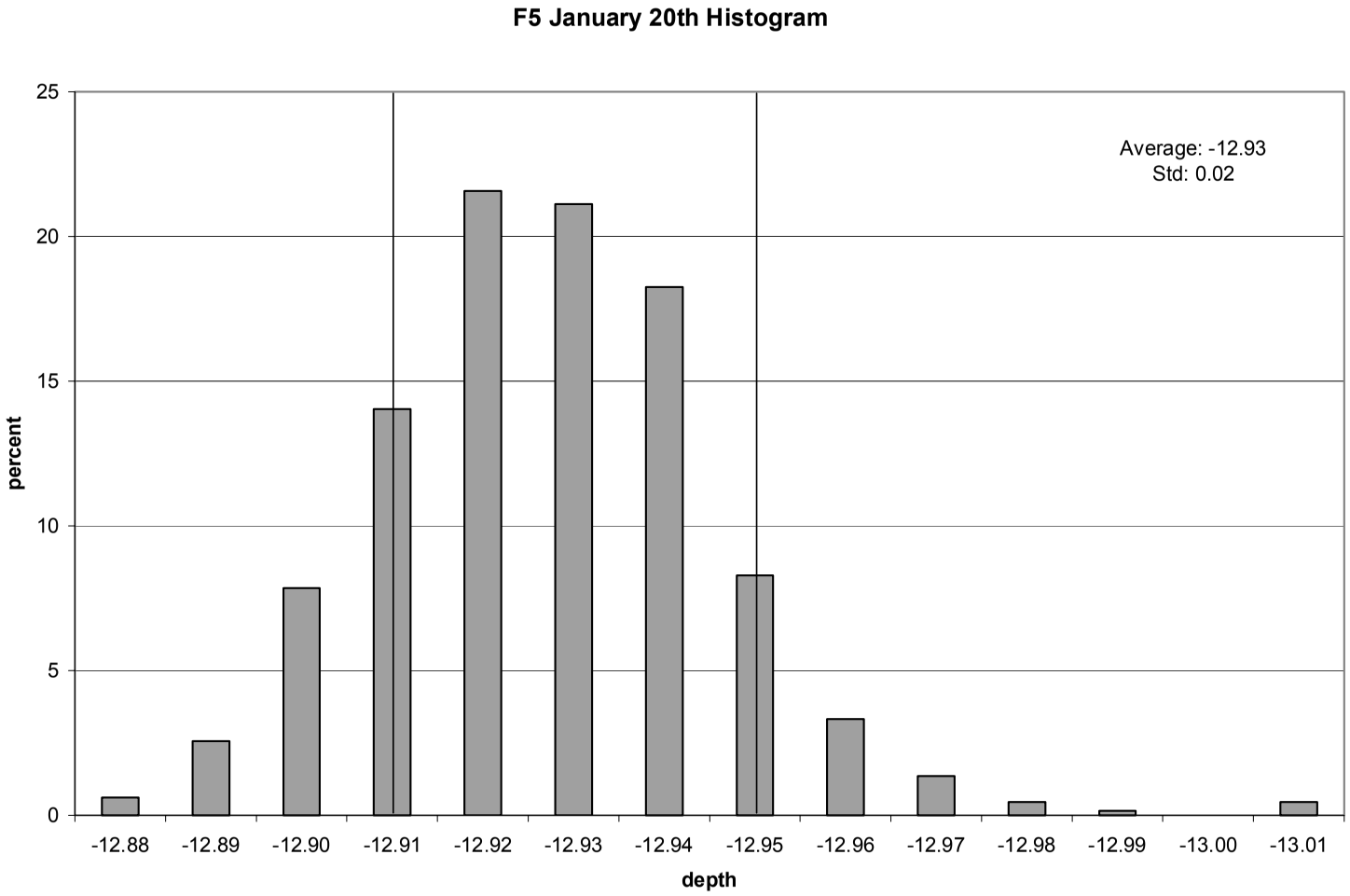

Figure 137. F5 January 20th histogram. Note that the distribution is right-skewed.

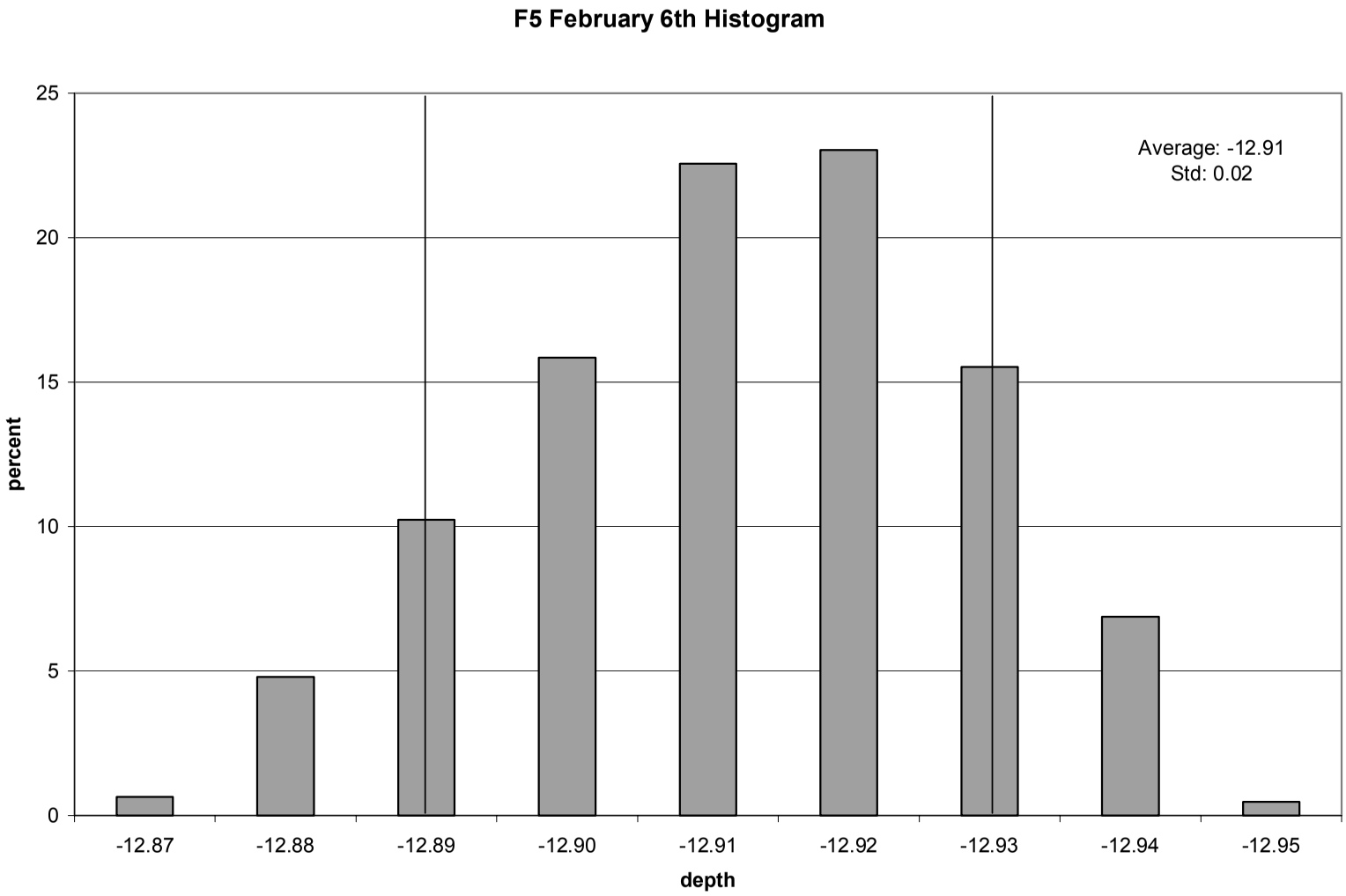

Figure 138. F5 February 6th histogram. Note that the distribution is normal.

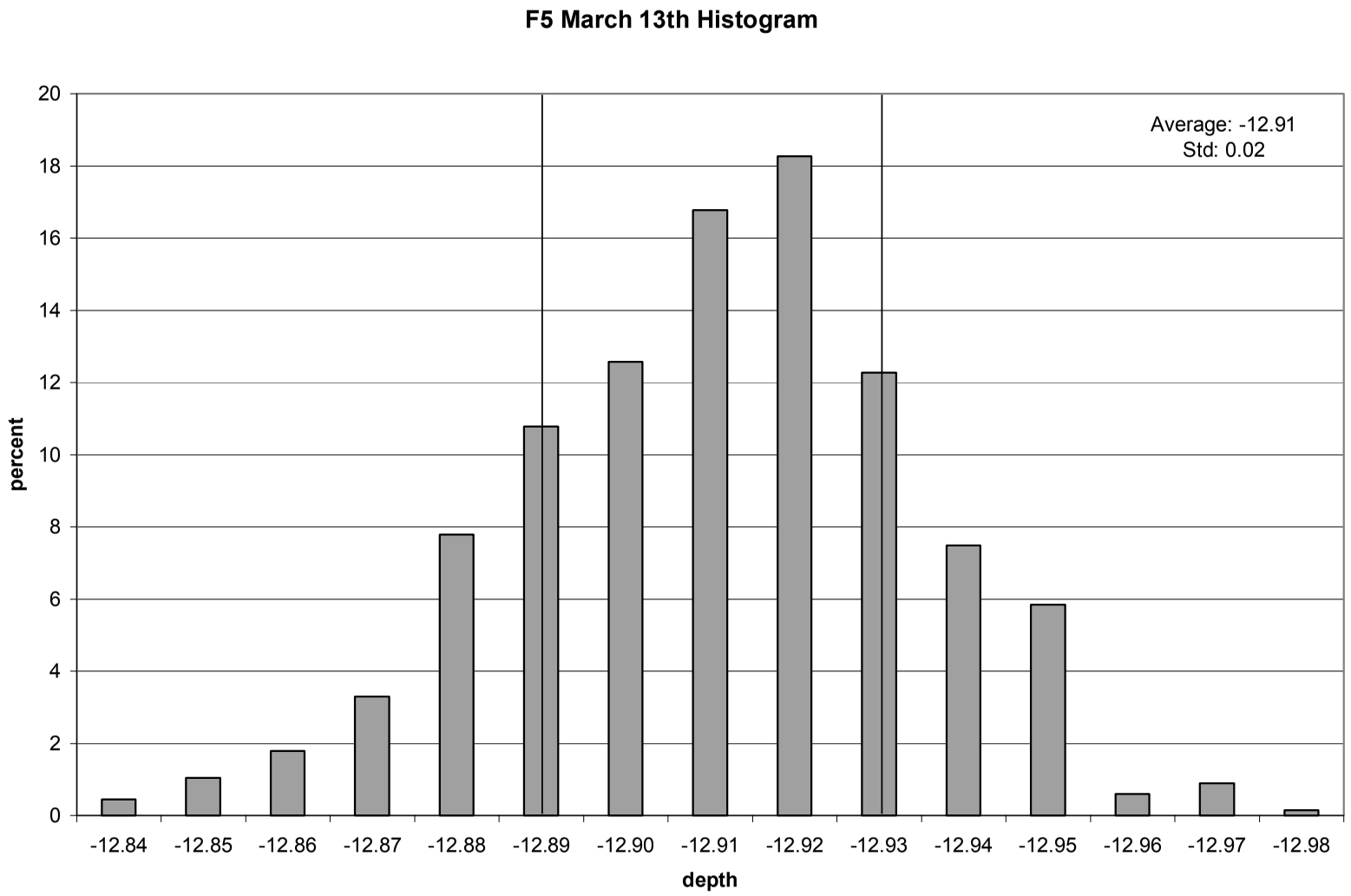

Figure 139. F5 March 13th histogram. Note that the distribution is normal.

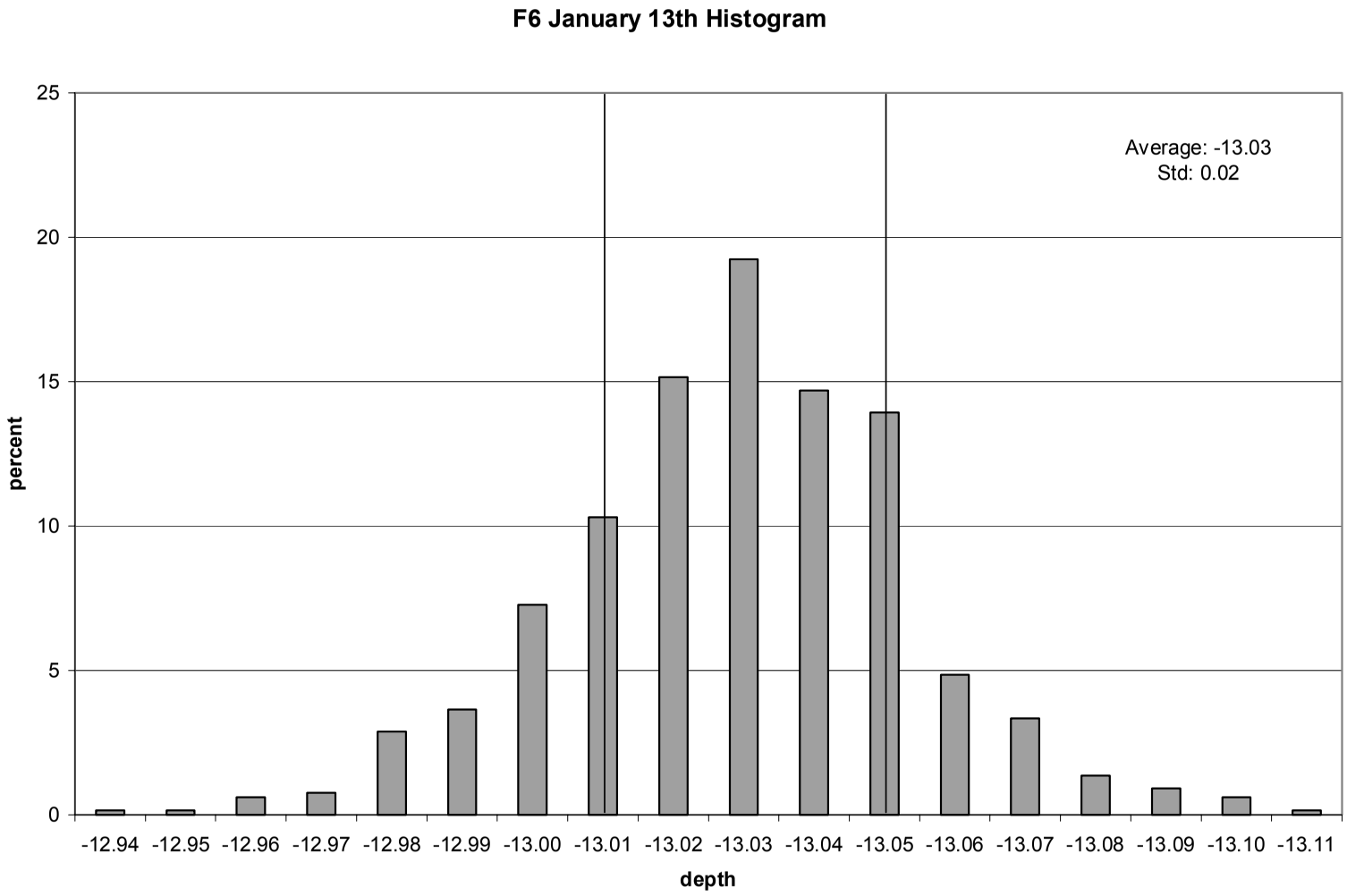

Figure 140. F6 January 13th histogram. Note that the distribution is left-skewed.

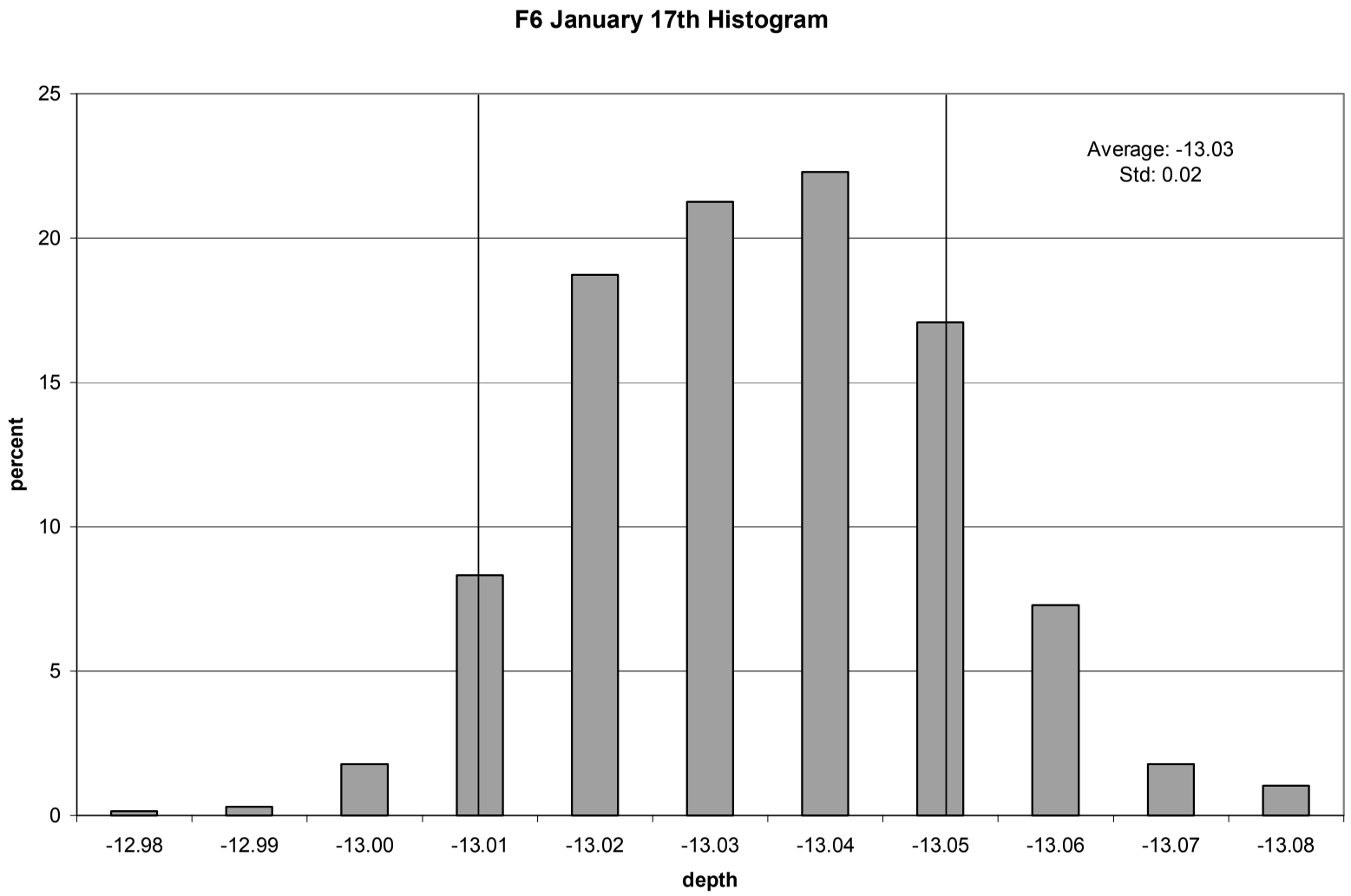

Figure 141. F6 January 17th histogram. Note that the distribution is normal.

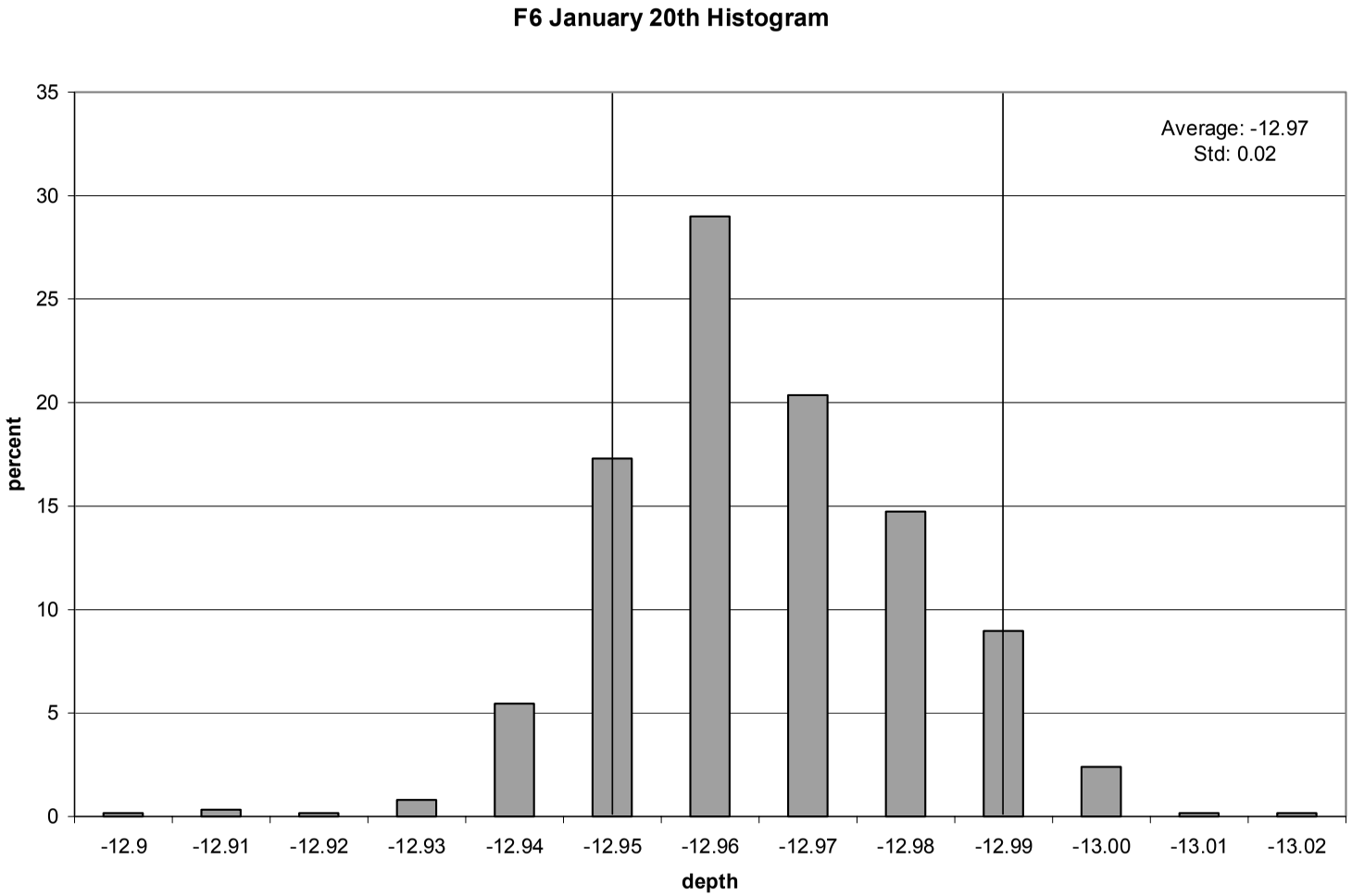

Figure 142. F6 January 20th histogram. Note that the distribution is left-skewed.

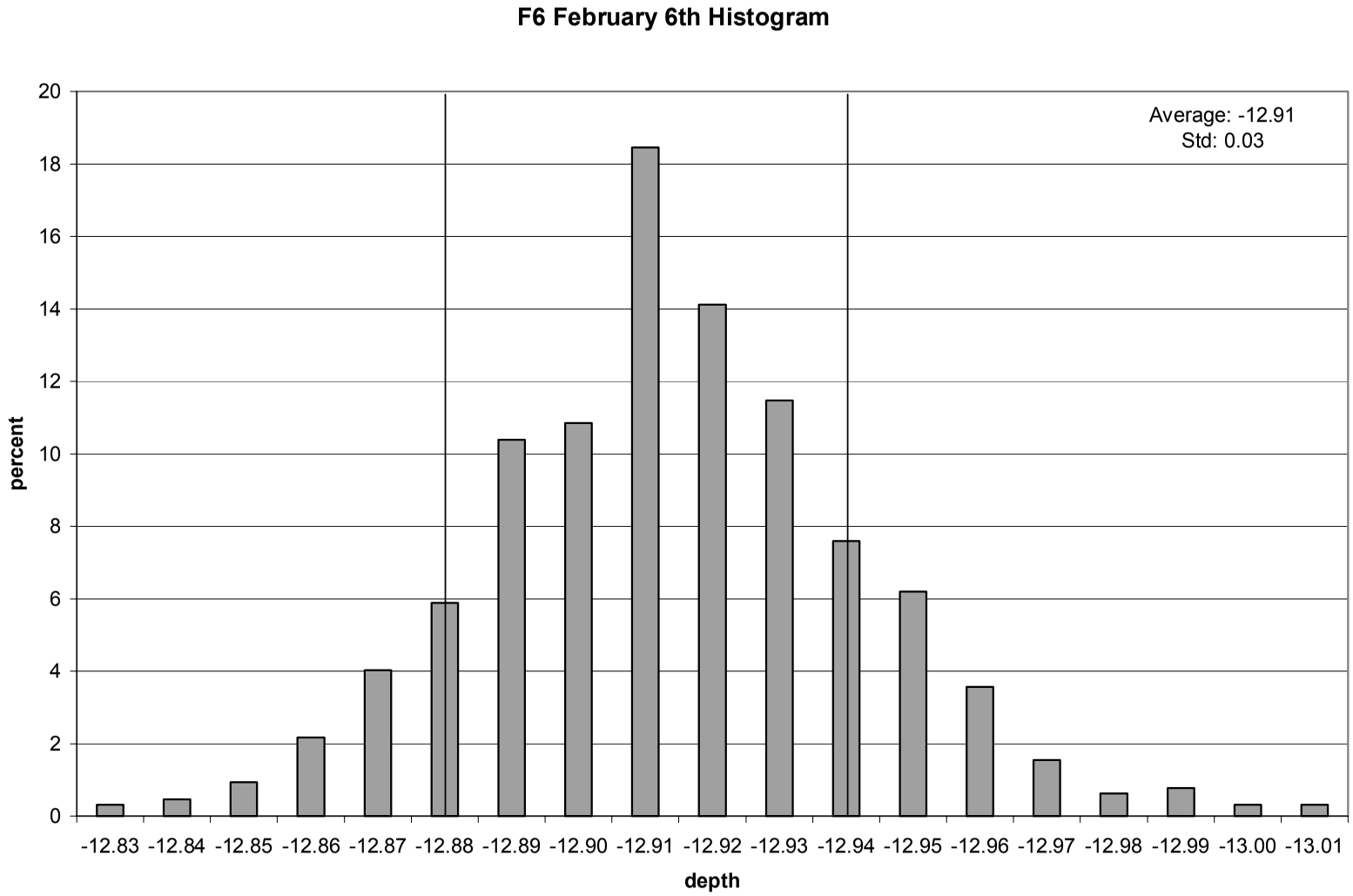

Figure 143. F6 February 6th histogram. Note that the distribution is right-skewed.

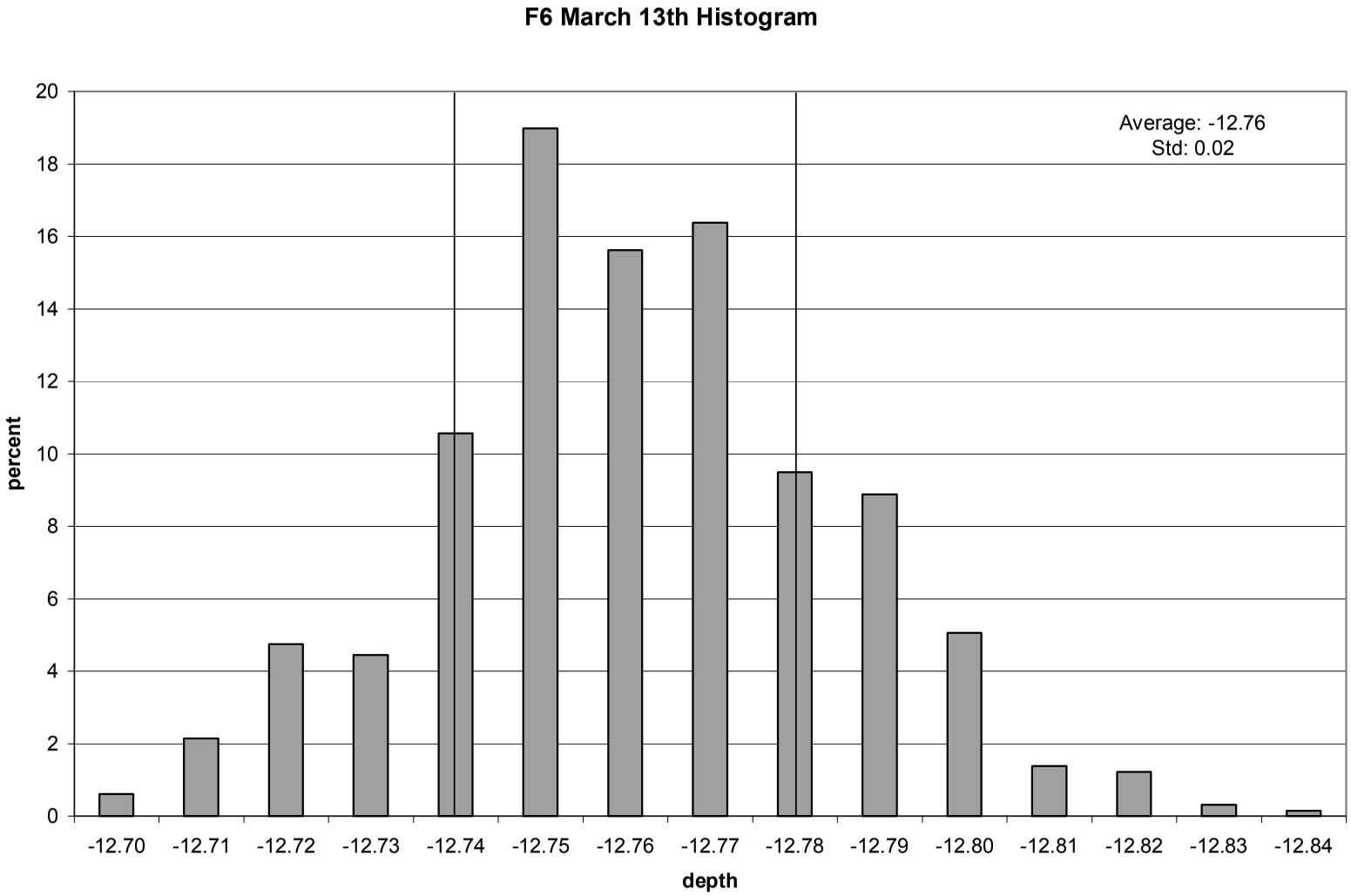

Figure 144. F6 March 13th histogram. Note that the distribution is right-skewed.

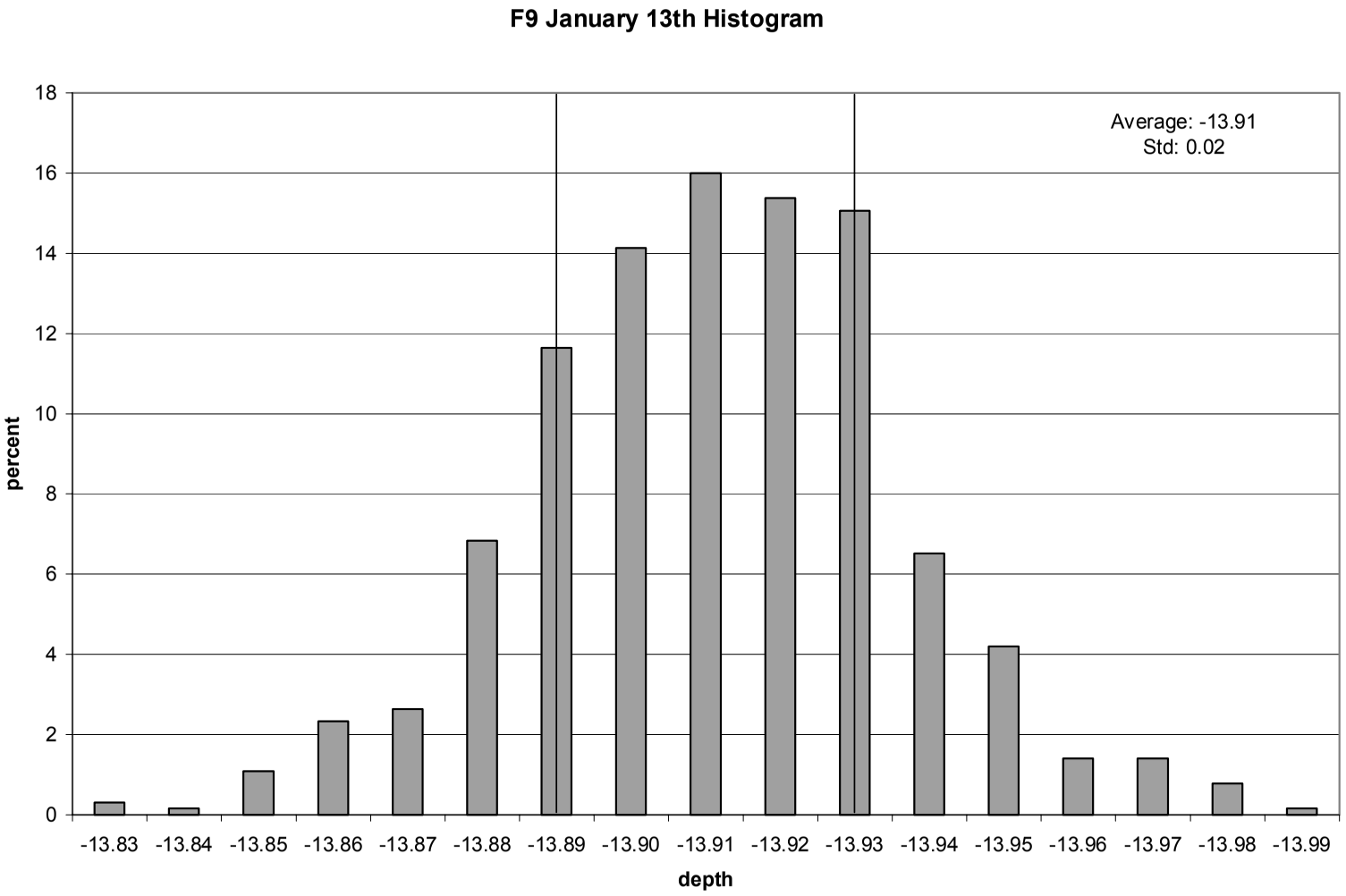

Figure 145. F9 January 13th histogram. Note that the distribution is normal.

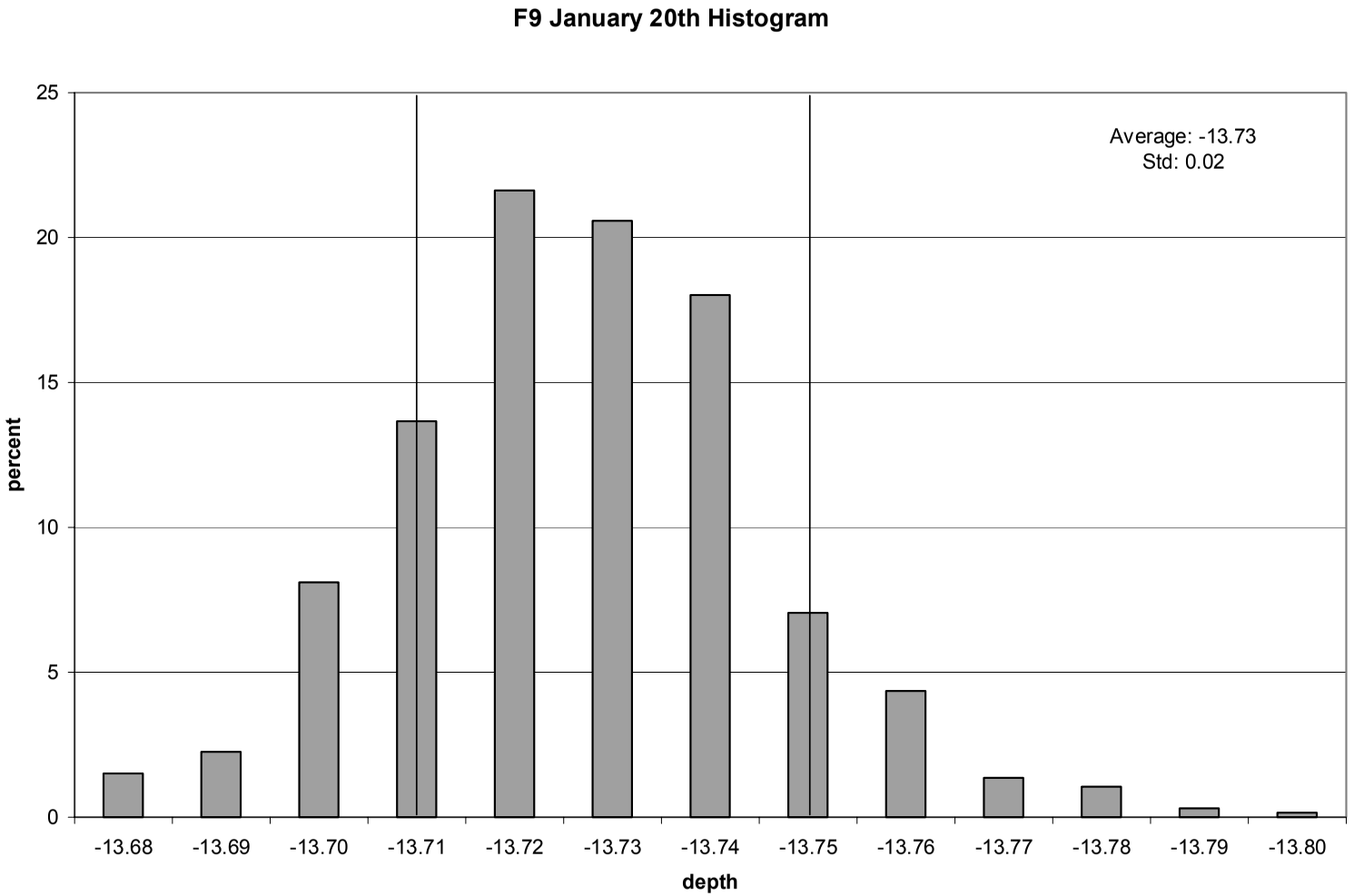

Figure 146. F9 January 20th histogram. Note that the distribution is right-skewed.

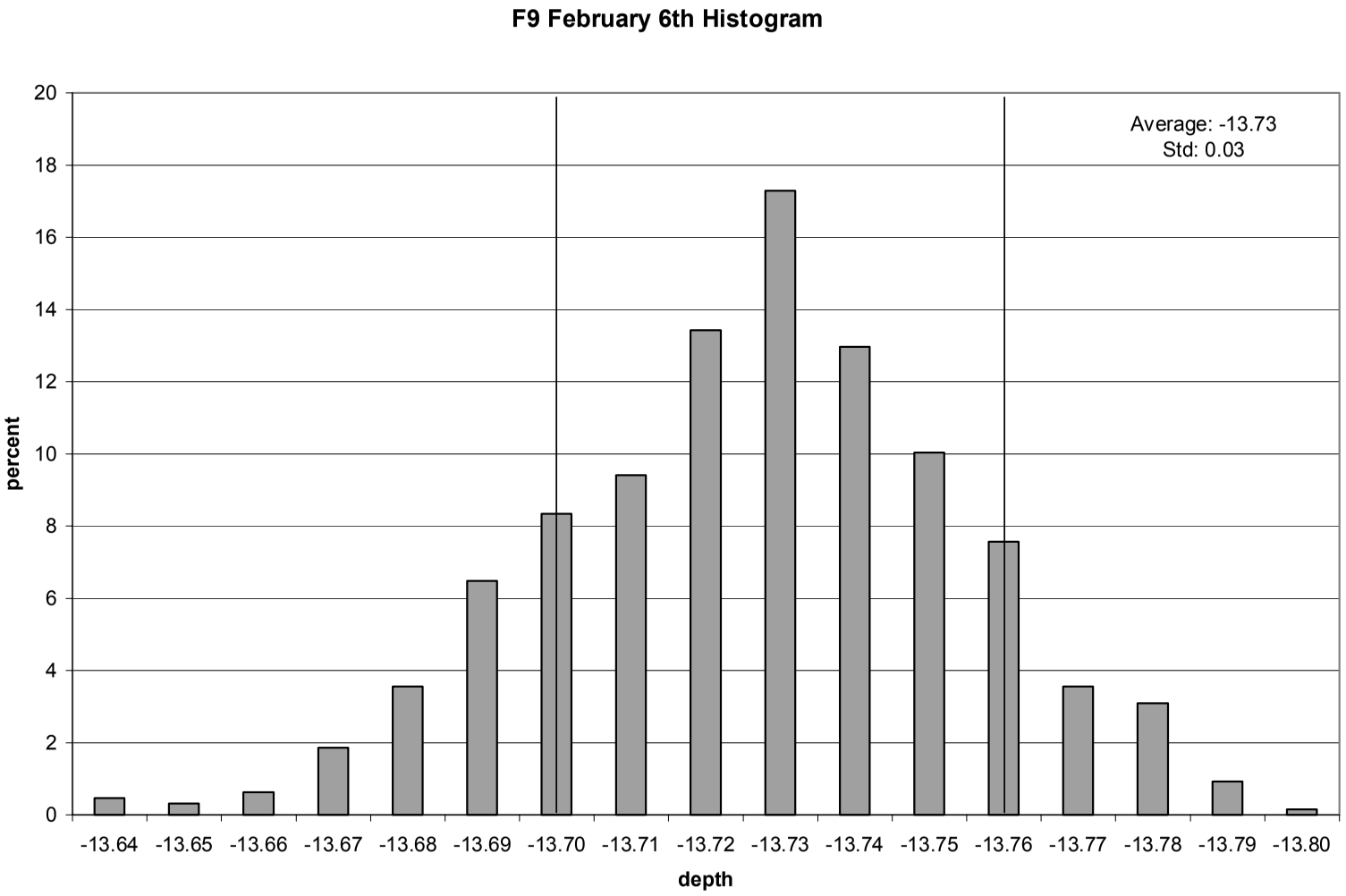

Figure 147. F9 February 6th histogram. Note that the distribution is left-skewed.

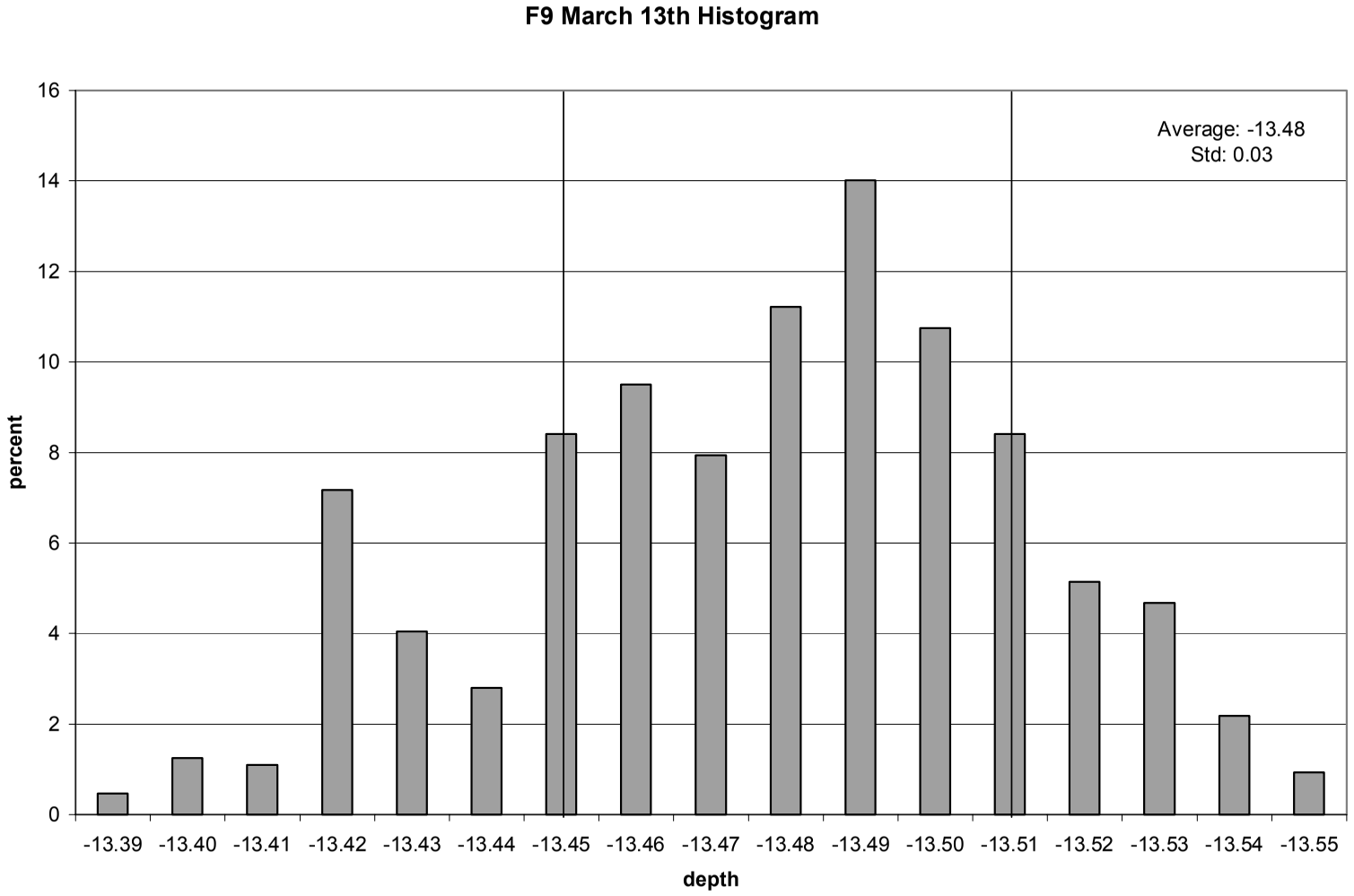

Figure 148. F9 March 13th histogram. Note that the distribution is left-skewed.

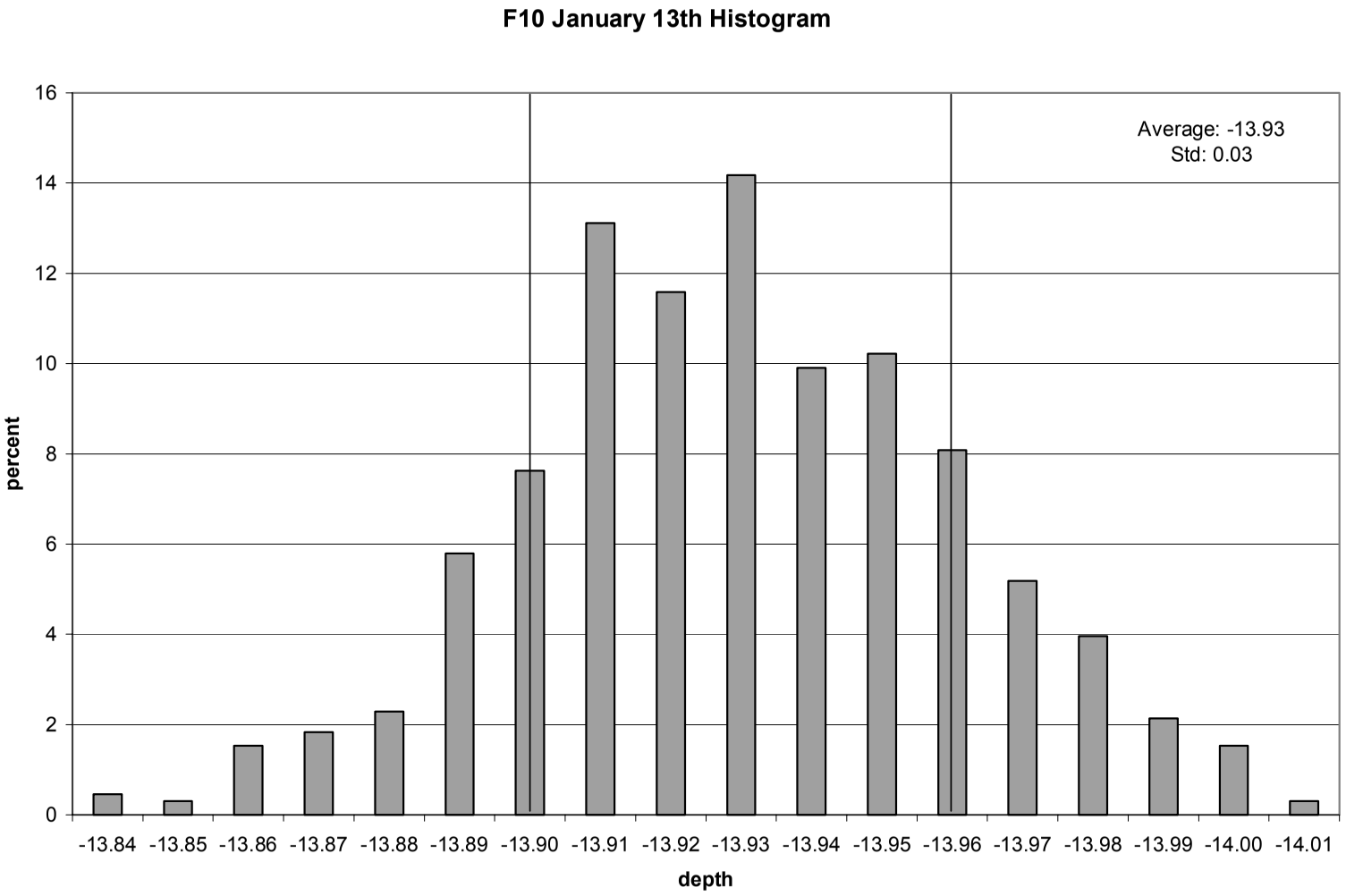

Figure 149. F10 January 13th histogram. Note that the distribution is left-skewed.

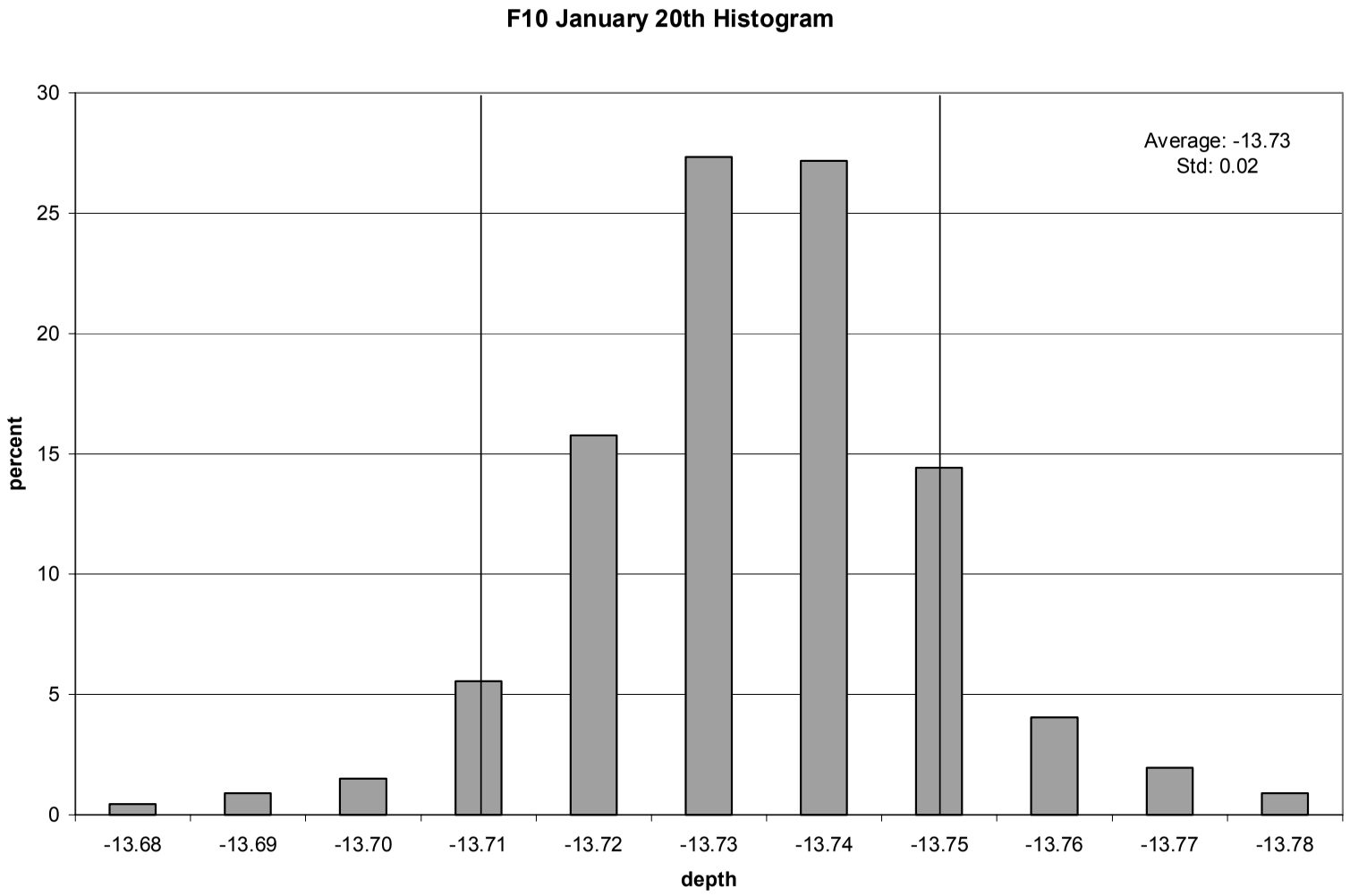

Figure 150. F10 January 20th histogram. Note that the distribution is normal.

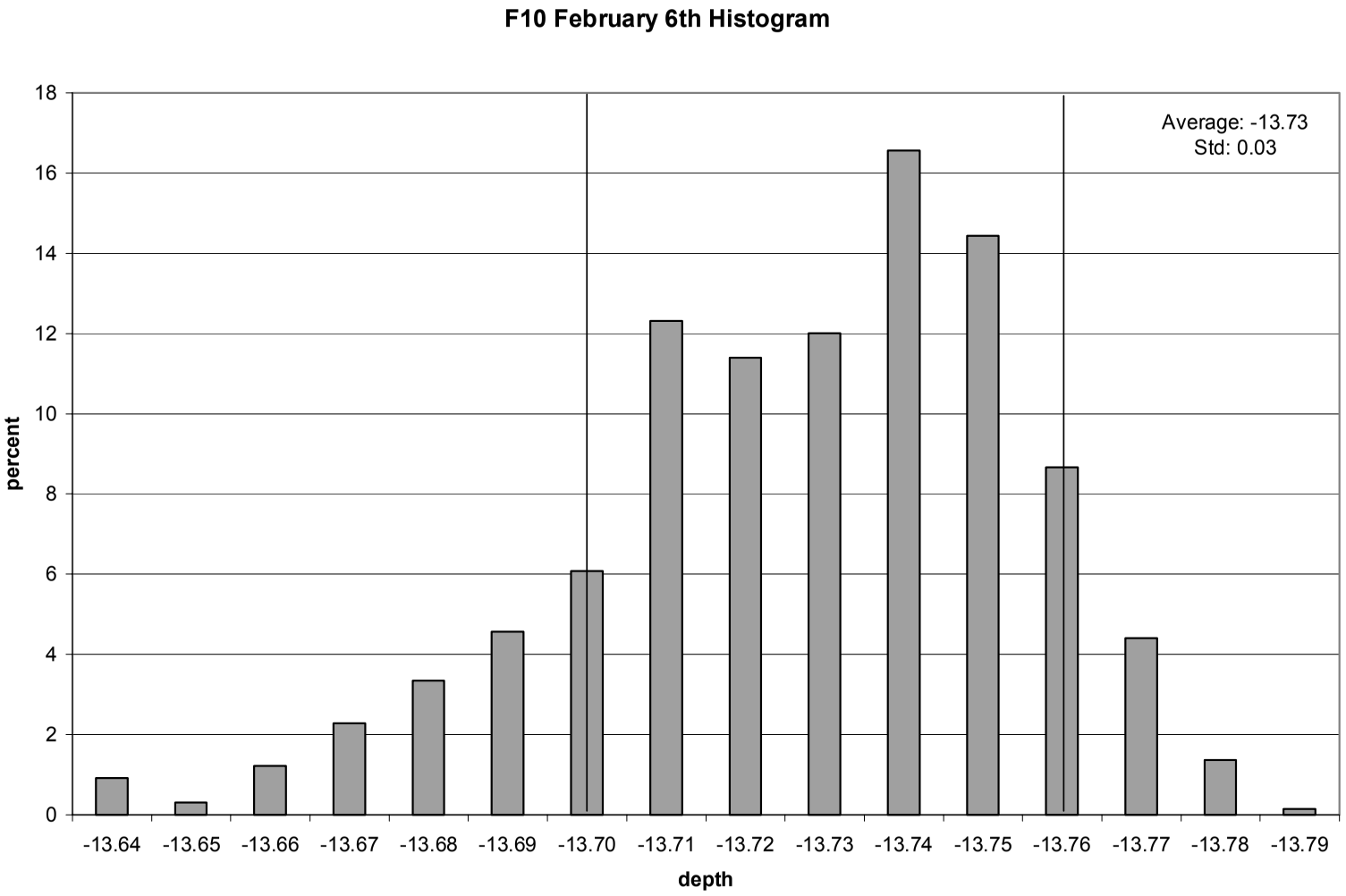

Figure 151. F10 February 6th histogram. Note that the distribution is left-skewed.

Appendix B

Description of Equations

Calculating the phase and amplitude offset between tides

The phase difference and amplitude offset between the tide record obtained from the pressure sensor data and the NOAA tide obtained from Clearwater Station 8726724 were calculated using an iterative equation in MATLAB, a powerful mathematics and statistical software package for data analysis (p. 14). The hourly NOAA tide record was interpolated in MATLAB in order to match the time series of the pressure sensor data. Next, the following iterative program was run:

```
p = []
STD = []            *standard deviation
AMP = []            *amplitude
PHASE = []          *phase

for A = 1:0.1:2
        for T = -1:0.1:1
            p = interp1(decimal_date,new_tide,decimal_date+T)
            m = nanstd(noaa_2hr – (A*p))
            STD = [STD;m];
            AMP = [AMP;A];
            PHASE = [PHASE; T];
         end
 end
```

Where:

decimal_date = time series for the pressure sensor tide record

new_tide = the tide record obtained from the pressure sensor

noaa_2hr = the interpolated 2-hour NOAA tide record

The code was run several times, changing the range and incremental value for T and A. After each run, the minimum value of STD was found along with its associated values for AMP and PHASE. The amplitude difference and phase offset between the two tide records were considered found once the values of AMP and PHASE remained unchanged between code runs. The final values of AMP and PHASE were found to be 1.06 and 0.003 respectively.

Calculating beam footprint and beam spacing for the multibeam sonar

The across track beam footprint and across track beam spacing (in meters) for the Kongsberg Simrad EM 3000 multibeam sonar were calculated for various water depths (p. 185). These calculations assume a flat seabed and are based on the sonar being pole mounted approximately 2 meters below the water surface.

Beam footprint:

$$2 \times \left[\left(\frac{d}{\cos(\phi)} \right) \times \left(\tan(b) \right) \right]$$

where: d = water depth (m) - 2
ϕ = beam pointing angle
b = beam width (degrees)

Beam spacing:

$$d \times \left[\left(\tan(\phi + \left(\frac{1}{2}(s) \right) \right) - \left(\tan(\phi - \left(\frac{1}{2}(s) \right) \right) \right]$$

where: d = water depth (m) - 2
ϕ = beam pointing angle
s = angular beam spacing (degrees)

The along track beam spacing (in meters) was also calculated for various vessel speeds for a ping rate of 10 Hertz (p. 185).

Along track beam spacing:

$$\frac{V_s \times 0.51}{p}$$

where: V_s = vessel speed (knots)
P = sonar ping rate (Hertz)